GIS-based Assessment of Debris Flow Susceptibility and Hazard in Mountainous Regions of Nepal

by

Bhuwani Prasad Paudel

Under the supervision of

Dr. M. Fall

and co-supervision of

Dr. B. Daneshfar

Thesis submitted to the

Faculty of Engineering

In partial fulfillment of the requirements

for the Doctorate in Philosophy degree in Civil Engineering

Abstract

Rainfall-induced landslides that change into debris flows and travel large distances are one of the treacherous natural calamities that can occur in mountainous areas, particularly in Nepal's mountains. Debris flow was the second highest cause of human death in Nepal after epidemics between 1971 and 2016. Because debris flow is common in mountainous regions, its prediction and remedial measures through land use plans are important factors to consider for saving lives and properties. The spatial distribution of the initial landslides that change into debris flow, on a watershed scale, is still an important area of study in this mountainous region to develop essential land use plan.

In this research, hydrologic, slope stability and Flow-R models are applied in GIS modeling to locate potential landslide and debris flow areas for a given threshold rainfall in a mountainous watershed-Kulekhani, Nepal. Soil samples from 73 locations within the watershed and a geotechnical investigation on one old landslide area were considered to determine the Soil Water Characteristics Curve (SWCC), friction angle, cohesion, and infiltration characteristics of the subsurface soils in the study area. This information is applied in an unsaturated slope stability model to find unstable locations in the study watershed in a GIS environment. The model is tested on a recorded 24-hour rainfall of 540 mm in the watershed, and potential landslide locations are obtained. The validation results show that there is a good agreement between the predicted and mapped landslides. For debris flow run out, Flow-R model, which has the capability to analyze debris flow inundation with limited input information, and the model software is readily available in the public domain, was chosen for further analysis. Two recent debris flow events and the study watershed are taken as case studies to identify the appropriate algorithms of Flow-R for runout analysis of the study areas.

Landslide-triggering threshold rainfall frequency is related to the frequency of landslides and the debris flow hazard in these mountains. The above validated models are applied in a GIS environment to locate potential debris flow areas in expected threshold rainfall. Rainfall records from 1980 to 2013 are computed for one- to seven-day cumulative annual maximum rainfall. The probable rainfalls for

1 in 10 to 1 in 200 years return periods are identified. The anticipated probable rainfalls are modeled in the GIS environment to identify the factor of safety of mountain slopes for landslide susceptibility in the study watershed. The Flow-R model with user-defined landslide-susceptible areas was chosen for debris flow runout analysis. A relation between the frequency of rainfall and landslide-induced debris flow hazard area is derived for return periods of 25, 50, 100, and 200 years. Also, the debris flow hazard results from the analysis are compared with a known event in the watershed and found to agree. This developed method can be applied to anticipated landslide and landslide-induced debris flow from the live rainfall record to warn hazard-prone communities for saving lives and regulating hazardous transportation corridors in these mountains. In addition to this, this methodology will be a useful tool to help policy makers create appropriate land use plans.

Acknowledgement

First of all, I would like to thank my supervisor, Dr. Mamadou Fall, for his enduring guidance, encouragement and support throughout the study period. Without his immense support I would not have had the strength and courage to accomplish this research. Another individual I am very grateful to is my co-supervisor, Dr. Bahram Daneshfar. His support and encouragement during my hard time with this research work are not only valued but also a lesson on how to be a good individual in some one's life. I would like to thank the employees of IT Services of my department, the Department of Civil Engineering and Central IT of University of Ottawa.

During this PhD study, I had ups and downs as various factors and obstructions came into my life. Thank you to everyone who gave me their time and support; there are too many to thank individually here. Many of you belong to the Department of Civil Engineering of both the University of Ottawa and Carleton University. I would like to thank my friends in these universities for their encouragement and support.

Comments received during proposal submission were valuable for me to learn various aspects of this research application. I thank the proposal examination committee for their valuable comments, which provided more insight and learning opportunities in some interesting areas, such as applicability of research on climate change condition. I would like to thank Dr. Jules Infante Sedano from the University of Ottawa, and Dr. Shawn Kenny from Carleton University.

I should mention three individuals who provided support for field investigations and data collection. I am grateful to Mr. Shiva Raj Adhikari, Department of Roads, Nepal, for his continued support for field work and data collection in Nepal. I want to thank Dr. Megh Raj Dhital, Professor, Tribhuvan University, Nepal, who provided previous research data and encouragement to focus in this area while we visited field sites together in different landslides in Nepal. Appreciation goes to Dr. Prabin Kayastha, Professor, Nepal Engineering College for providing valuable

Table of Contents

Chapter 4: Technical Paper 1 - GIS-based landslide (debris flow) susceptibility modeling in Kulekhani watershed, Nepal   53

Chapter 5: Technical Paper 2 - GIS-based assessment of debris flow runout in Kulekhani Watershed, Nepal   105

Chapter 6: Technical Paper 3 - GIS-based assessment of debris flow hazards in Kulekhani Watershed, Nepal   153

Chapter 7: Synthesis and integration of all the results   201

Chapter 8: Summary, application, conclusions, and recommendations   206

Appendix A   212

List of Figures

XIV

List of Tables

Chapter 1: Introduction

1.1   Problem statement

Debris flows are fast-moving landslides that occur in various types of environments throughout the world. Debris flows are highly hazardous natural calamities in mountainous regions. Rainfall is one of the prime triggering factors for the initiation of landslide, particularly debris flows.

Rainfall-induced landslides, which often change into debris flows, travel large distances on the sloped natural terrain in the Nepalese mountains. The Nepalese mountains are densely populated, and human life and property is vulnerable to wide-spreading debris flows. As debris flows are common in these mountainous regions, their prediction and remedial measures are important factors to consider for saving lives and property.

People reside in the middle of the mountains and low valleys of Nepal despite the vulnerability to debris flows and the high risk to lives and property. Every year, many people lose their lives and property due to such calamities. The record shows that rainfall-induced shallow landslides that turn into debris flows have taken, on average, 269 people's lives every year during the period of 1983 to 2016 (Figure 1.1) (Ministry of Home, Nepal 2015). A total of 9153 people lost their lives within this period (Ministry of Home, Nepal 2015). Landslides lead to flooding in the lower part of the mountains that have killed an average of 729 people per year between 1971 to 2016. Landslide and flooding destroyed about 5337 houses per year during the period from 1971 to 2014 (DWIDP 2017, Figure 1.2). Within the period of 2000 to 2009, 2042 people died from landslides and flooding (landslide alone, 1654) (K.C. 2013). A recent single landslide event in August 2014 killed 156 people in northern Nepal (Kantipur Online 2014).

It is obvious from the facts above that the prediction of the spatial distribution of debris flow hazards is important to save lives and property in Nepalese mountainous regions. In these regions, initially, landslides start with a small mass, entrain loose substrate and deposits along the flow path continuously until all

energy has been dissipated in the moderately- to mildly-sloped plain areas. Both the initiation locations and runout areas of debris flows are required for hazard analysis in these mountains, because people are developing these areas as their residences. Landslide initiation and debris flow inundation in hazard analysis has not been carried out in these mountains before.
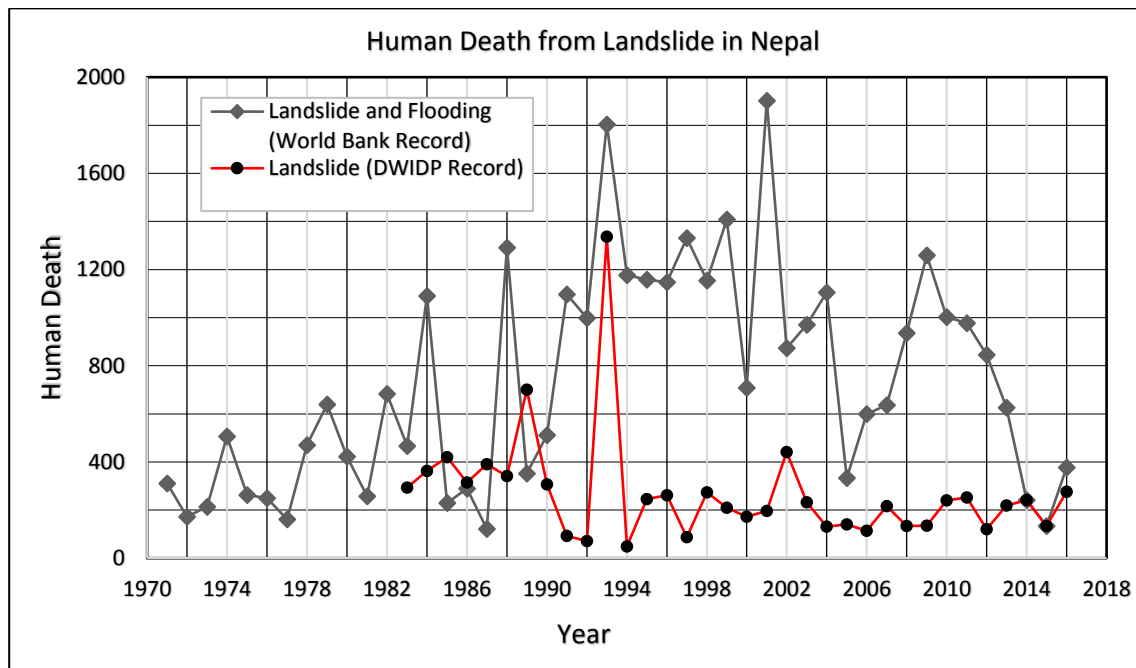
Figure 1.1: Death from rainfall induced landslide and flooding.
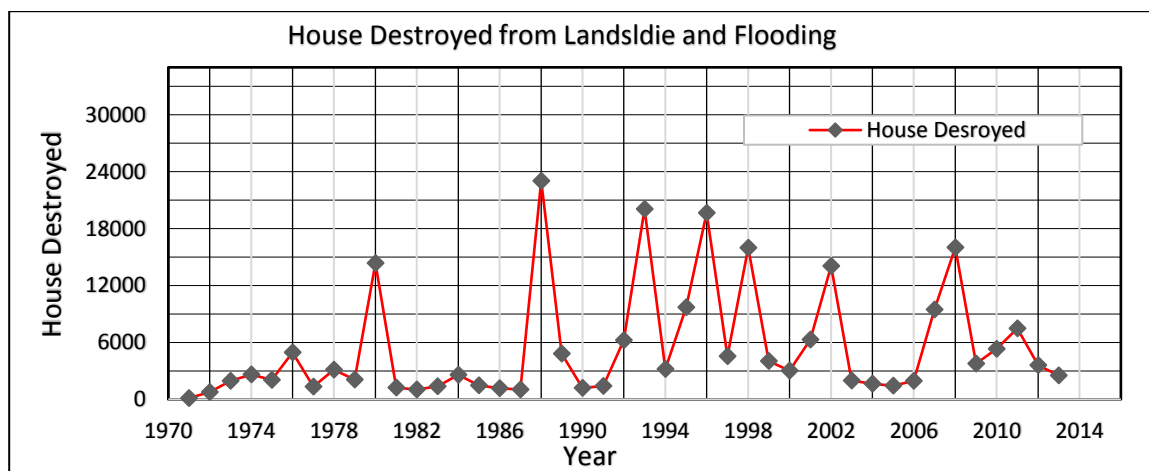
Figure 1.2: House destroyed from landslide and flooding in Nepal.

Landslide hazard assessment is also important for other regions of the world beyond the Nepalese mountains, and many studies have been conducted on the dangers of landslides and risks to people (Fall 2009, Fall et al. 2006, Van Westen et al. 2006, Caine 1980). However, these studies are largely dependent on many local factors, such as topography, geology, climate, and other site-specific information. Therefore, site-specific research is necessary to develop models for landslide danger and hazard assessments for specific locations on a watershed scale. Considering the physical parameters for landslide hazard assessments for the watershed scale in these mountains is still an important area of study for making developments in policy and saving lives and property.

Extensive research has been conducted recently in the Nepalese mountains on landslide dangers and the risk of living in mountainous areas by the following researchers: Devkota et al. (2013), Kayastha et al. (2010, 2012, 2013), Bhandary (2013), Bijukchhen et al. (2012), Dahal et al. (2012), Ghimire (2011), Pantha et al. (2010), Poudyal et al. (2010), Ray and De Smedt (2009), Kayastha and Smedt (2009), Dahal and Hasegawa (2008), Dahal et al. (2008), Sharma and Shakya (2008), Acharya et al. (2006), Dahal et al. (2006), Gabet et al. (2004), Chalise and Khanal (2001), Yagi (2001), Gerrard and Gardner (2000), Thapa and Dhital (2000), Dhital (2000), Dhakal et al. (1999), Wagner (1997), Upreti and Dhital (1996), Yagi and Nakamura (1995), Dhital et al. (1993), Dangol et al. (1993), and Deoja et al. (1991). However, debris flow runout from the initial landslide, and its hazard assessment on a watershed scale have not yet been studied. These studies are either for an individual landslide specific to anthropogenic interference in nature, such as a road corridor, or in relation to rainfall intensity and duration alone without any model for future expected spatial distribution of debris flow. Therefore, to date, research in this area is not sufficient to assess landslide (debris flow) hazard in these mountains for use in policy-making for specific developments in the region.

The landslide studies carried out to date should help policy makers to develop proper land use plans, educate people in appropriate land use for their livelihood, and to cope with this problem either for relocation of settlements to safer places or improve safety of lives and property. However, sufficient and interpretable

information of mountainous land for appropriate use has not been developed to an applicable stage. This study will be a step forward in understanding physical changes in mountainous slopes during monsoon rainfall leading to instability and landslide initiation, and towards the development of land use plans for appropriate practices in mountains, and resettlement strategies for policy makers on a watershed scale.

Rainfall intensity and duration periodically return, but landslide events and locations do not remain the same. In other words, landslides do not necessarily occur in the same places where they occurred previously. The relation of rainfall and landslides for a particular location of watershed depends on the physical changes to a slope during rainfall. The relation between rainfall and unstable locations is still to be understood in these mountains. Some locations in the mountains are very steep but still remain stable even when the soil is overburdened. The application of unsaturated soil technology and Geographic Information System (GIS)-based modeling tools can be used to understand their stability during rainfall. The outcome of this research is to identify the phenomenon that makes a particular hill slope severely unstable for a given rainfall intensity and duration that will be applicable for use in landslide hazard analysis.

The annual average rainfall distribution and rainfall intensity are higher in eastern and central Nepal, and gradually reduce towards the west. The landslide events observed by Dahal and Hasegawa (2008) also show more landslide events in the eastern and central part of the country. This shows that the rainfall threshold has a significant role in initiating landslides. However, the location of unstable slopes can only be identified with the study of subsurface physical changes on the mountain slope. The rainfall threshold influences the triggering of a landslide in a specific location of the slope, but this does not apply to all mountain slopes, and the prediction of stable and unstable areas is important for a given rainfall return.

Most of the models for hazard assessments are GIS-based statistical methods, which use previous landslide events as a base factor for the identification of potential landslides in the future (Jaisawal 2011, Remondo 2008). However, when a landslide occurs, the topography of the area changes and a similar rainfall

4

intensity and duration may no longer be the rainfall threshold, even though its recurrence period is the same. When one landslide event occurs, new analysis is required to consider the associated morphological change. A model that can consider physical features of the watershed during landslide-triggering rainfall threshold is necessary for finding potential landslide locations independently of previous events. This study will identify rainfall-event-related landslide-susceptible areas, debris flow inundation and debris flow hazards in a GIS environment.

1.2   Objectives of the thesis

The overall objective of this research is to develop models for debris flow hazard assessment for Nepal's mountains. To achieve this objective, the following sub-objectives or steps are considered in a GIS environment:

- Find the rainfall threshold intensity and duration for landslide initiation;
- Develop a model for the rainfall return period and spatial distribution of landslide events;
- Model the debris flow runouts on the study watershed to delineate areas that can be potentially affected by debris flows
- Develop debris flow hazards model for the study watershed with rainfall return period.

1.3   Research methodology and approach

The methodology developed for this research is shown as a flowchart in Figure 1.3. This figure also shows the relationship between the different work steps of the research performed. The methodology includes four main stages or parts.

The first stage dealt with acquisition of data and information about the study area. These data and information include geotechnical, geological, hydrogeological, topographical and rainfall details/information. A data list was developed and a visit to Nepal was made to acquire them. Initially, research was planned based on available existing information from the published literature and

government reports. However, after correspondence with various government agencies and a visit to Nepal to gather information, it was realized that the existing information was insufficient to conduct this research. No research was found on debris flow in the study area because of lack of funding and researchers' interest. There was a very poor recording system of previous research, which was another problem when gathering information or retrieving what was available. The developed data list required for conducting the research was sorted out by their availability from existing literature, and how necessary they were to conduct field and laboratory work. The initial table developed was modified, as shown in Table 1.1, for the required information and identified resources to obtain these data or conduct field or laboratory testing. Table 1.1 provides a summary of the data obtained from the published literature and/or government reports as well as of those obtained by conducting laboratory and/or field tests.
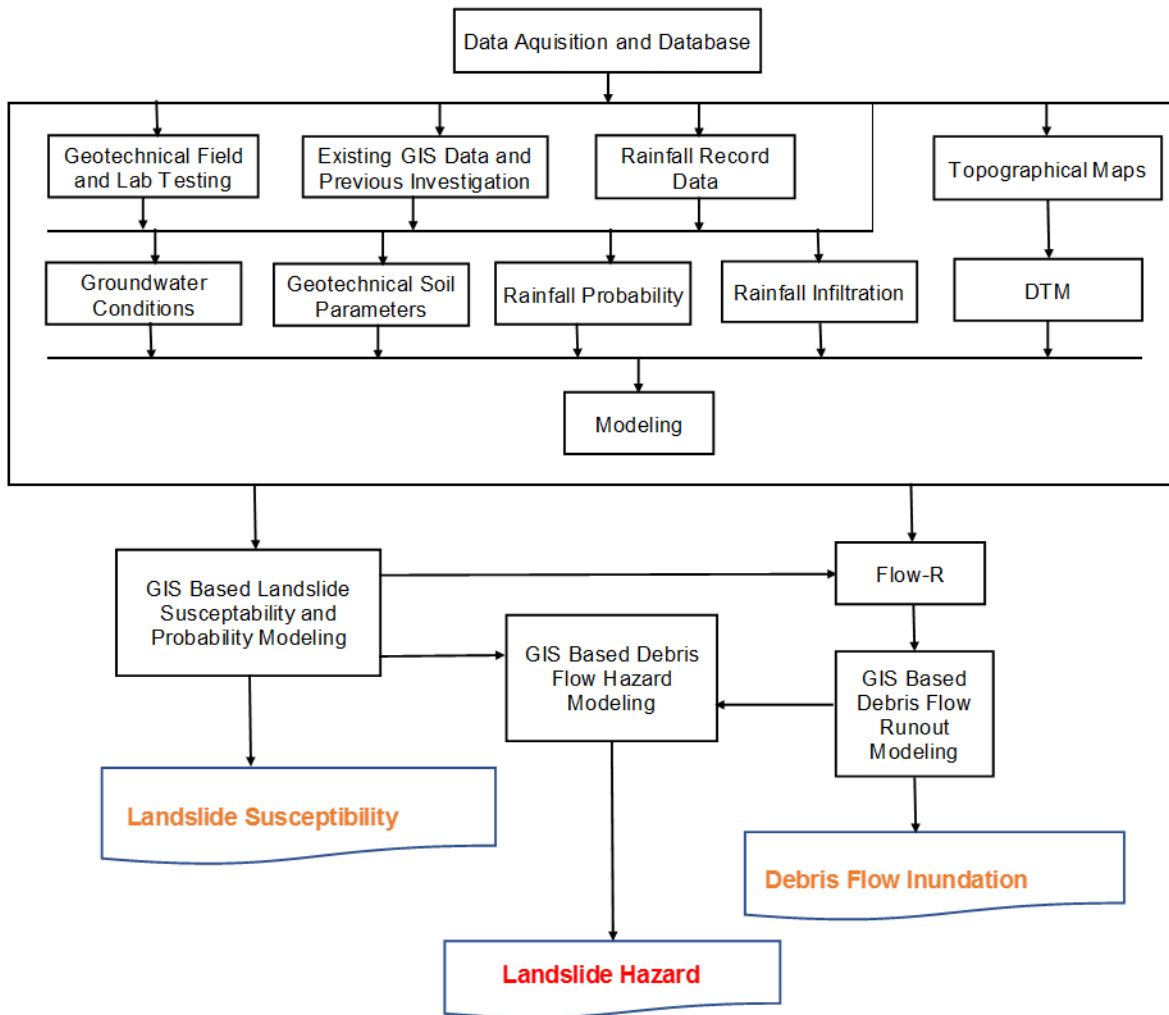
Figure 1.3: Methodology for the debris flow (landslides) hazard analysis and modeling.

Geotechnical laboratory and field tests were conducted according to Indian standard (IS) to determine most of the geotechnical characteristics of the study area. An old landslide site (27° 37' 19.2", 85° 8' 56.4"), Figure 1.4, within the watershed was considered for conducting in situ geotechnical investigation and collecting samples for laboratory testing. Soil strength parameters, such as cohesion, friction angle, and soil permeability results from the laboratory and in situ testing are considered in the analysis. The representative Soil Water Characteristics Curve (SWCC) was developed based on the Fredlund and Xing (1994) and Torres (2011) methods from grain size distribution. A total of 73

locations (Lamichhanne 2000) from a study watershed (Figure 1.4) were considered for SWCC development. Rainfall records from four rain gauge stations
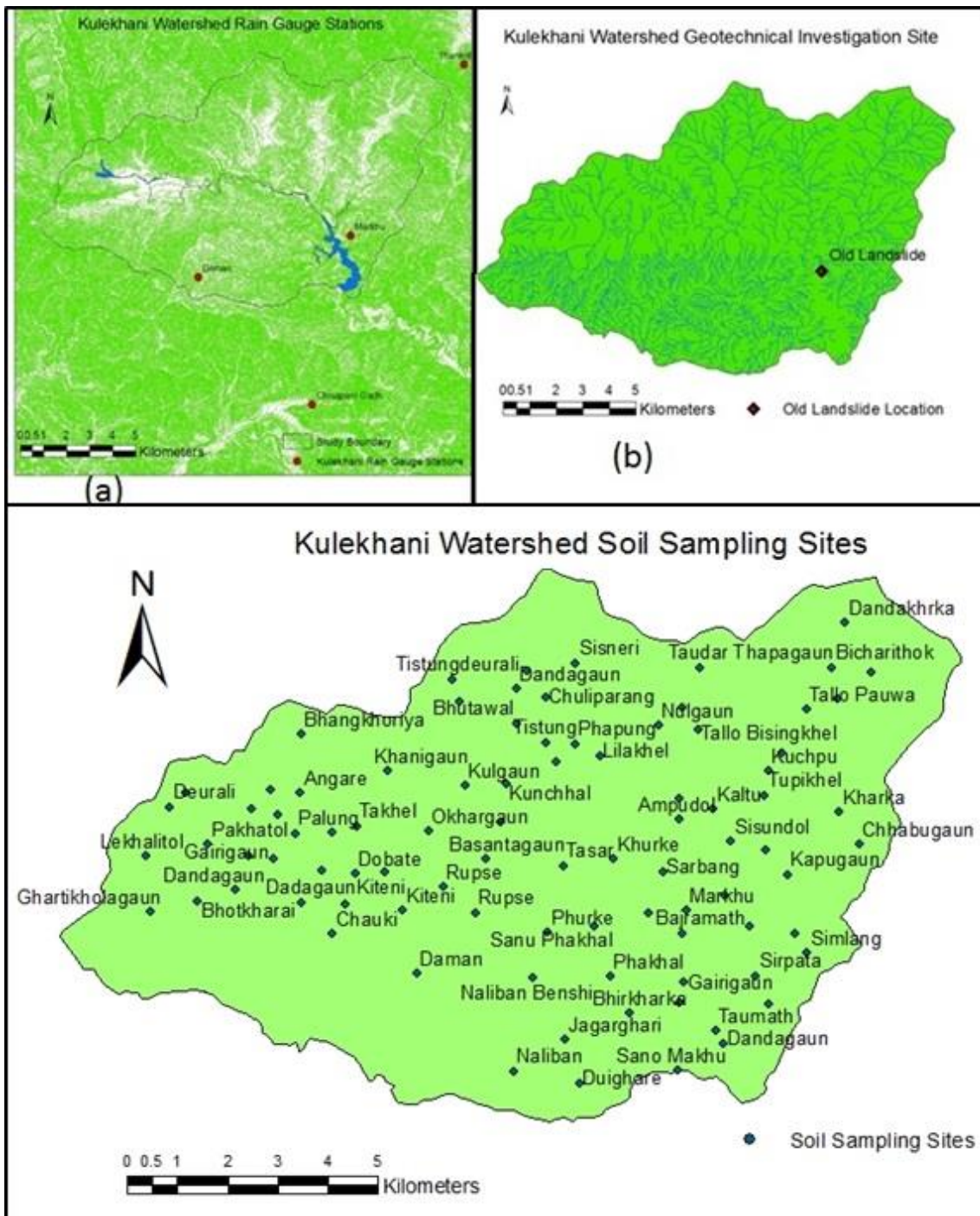
Figure 1.4: Kulekhani Watershed (a) Rain gauge stations for rainfall data, (b) Geotechnical field investigation at an old landslide area, and (c) Soil sampled from 73 locations from previous research (Lamichhanne 2000) used for SWCC.

(Figure 1.4) for 1980 to 2014 were used for the development of duration and intensity of rainfall data for infiltration depth computation. These records were also utilized for rainfall frequency, duration and intensity computation. Rainfall was recorded every 24 hours. Infiltration depths were computed using suction from SWCC and a combination of rainfall intensity and duration. A Digital Elevation Model (DEM), (Figure 1.5) was used for developing slope maps. Maps of all parameters were developed in the GIS environment. These maps were interpolated using Inverse Distance Weighted (IDW) methods to convert them to raster maps. Maps were converted in the same way for raster calculation.
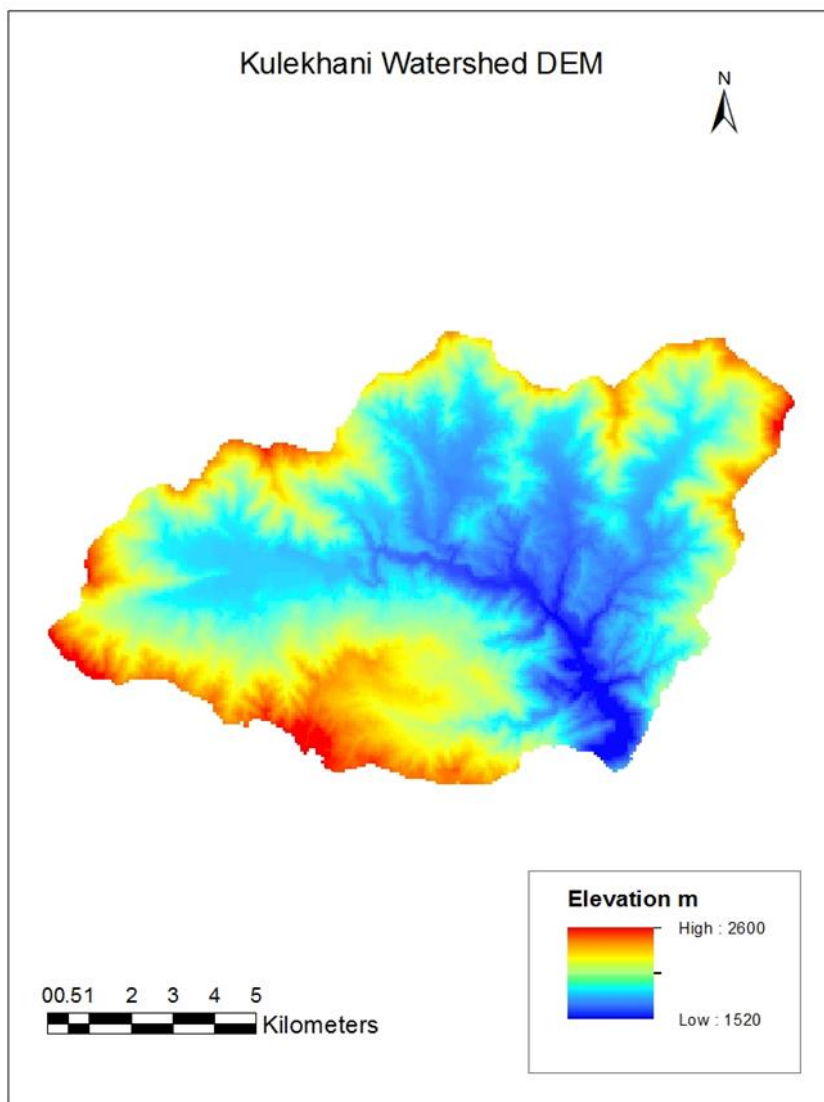
Figure 1.5: Kulekhani Watershed Digital Elevation Model.

Table 1.1 Data collected for the research.

Data Type	Methods and Sources	Available/ Tests conducted
Rainfall record in the study area	Existing literature, previous study area, rain gauge data from Department of Hydrology and Meteorology Nepal, data from other sources, if any.	Available
Topographical map of the study area	Existing literature, previous study area, Departments of Nepal, DWIDP, DOLIDAR, Hydrology and Meteorology, data from other sources, if any.	Available
SWCC (Soil Water Characteristic Curve)	From one or some of these sources of information: Moisture content test, suction test, hydraulic conductivity test with grain size distribution, Atterberg limits.	Tests conducted (IS 2720-2, IS 2720-25, IS 2720-39, IS 5529-1
Initial moisture content	Moisture from in situ soil.	Tests conducted
Saturated moisture content	Saturated moisture content, if possible during rainfall threshold.	Tests conducted for the determination of porosity (void ratio) (IS 2720-2, 1974)
Residual moisture content	Analysis from soil suction and volumetric water content.	Available / derived
Atterberg limits	In laboratory.	Tests conducted (IS 9252, 1985)
Specific gravity	In laboratory.	Tests conducted (IS 2720, 1980)
Void ratio	In laboratory from dry weight.	Analysis
Grain size distribution	In laboratory.	Tests conducted (IS 2720, 1985)
Cohesion	Unconfined compression test for clay, and direct shear test for sandy soil.	Tests conducted (2720-39-1, 1977)
Friction angle	In situ penetration test for sandy soil and direct shear test.	Tests conducted (2720-39-1, 1977)
Digital elevation model (DEM)	Department of Topography/previous literature.	Available

Hydro-meteorological data	Department of Meteorology, previous Report.	Available/required processing
Groundwater condition	Previous study or testing.	Literature and test conducted

DWIDP: Department of Water Induced Disaster Prevention, DOLIDAR: Department of Local Infrastructure Development and Agricultural Roads, IS=Indian Standard on Soil Engineering Practice.

In the second stage of this research, hydrologic and slope stability models are applied in GIS models to locate potential landslide areas (landslide initiation) for a given threshold rainfall in the study area. Rainfall intensity and subsurface soil infiltration capacity are used to identify the wetting front during threshold rainfall. This information is applied in the unsaturated slope stability model (Equation 1.1) to find areas in the study watershed that are susceptible to rainfall induced landslides, in other words, to develop landslide susceptibility (landslide initiation location) maps of the study area.

$$F_s = \left[\frac{\left((c' + (u_a - u_w)tan\phi^b) + ((\sigma_n - u_a)tan\phi') \right)}{(\gamma_t H sin\beta cos\beta)} \right][1.1]$$

where, F_s factor of safety, c' effective cohesion, ϕ' effective friction angle, σ_n normal stress, H wetting front depth, β slope angle, γ_t unit weight of soil, u_a pore air pressure, u_w pore water pressure, $(u_a - u_w)$ matrix suction, σ_n total normal stress, $\sigma_n - u_a$ effective normal stress on the slip surface, and ϕ' is the rate of increase in shear strength due to matrix suction.

The developed model was then validated using the recorded rainfall and observed landslides in the watershed.

In the third part of this work, debris flow runout modeling was performed to develop debris flow inundation maps for the study area. The modelling required the initial landslide location and spreading topography for the study watershed. The landslide susceptibility model developed in the first part is considered for the debris flow initiation location for runout modeling. The debris flow runout analysis can be carried out using empirical, semi-empirical, and dynamic methods. However, empirical methods are better options, if the modeling

11

work needs to be conducted with limited information (Horton at al. 2013, Carrara et al. 2008, Finlay et al. 1999, Rickenmann 1999, Costa 1984, Hungr et al. 1984, Johnson 1984), and are considered in this study. The empirical method, Flow-R model (Horton at al. 2013), and the susceptibility map of the landslide initiation location (source area) previously developed, are applied for debris flow modeling. Flow-R is an empirical model developed at the University of Lausanne. The model can be used for both susceptibility and runout analysis of debris flow. The Flow-R model has been applied in various regions of the world and found to have reasonable results. It is open source software, which is available freely. Also, in the Flow-R model, options for user-defined debris flow sources are available for runout-only simulation. In the Flow-R model, landslide source maps are converted into ASCII files from the GIS software, and applied in Flow-R for runout analysis. The final results from Flow-R are compiled with the watershed map back in GIS. The final map shows the landslide initiation and debris flow spreading in selected rainfall intensity and duration in the study watershed. This procedure is applied to other probable rainfall threshold durations and intensities for landslide initiation and debris flow inundation maps.

In the fourth part of this research, landslide (debris flow) hazard assessment was conducted. The modeling work for landslide hazards is associated with the above two procedures, landslide susceptibility and debris flow runout assessment. However, the landslide initiation locations were identified from the computed frequency of rainfall from one day to seven days for landslide initiation to debris flow inundation. Identified landslide locations are used as debris flow sources and the Flow-R model is applied for debris flow spreading. The debris flow inundation area is identified for a given probability. The identified source and debris flow inundation areas are enclosed by a 10-m setback distance and considered as a hazard area for a given rainfall return. Van Westen et al. (1999) suggested qualitative methodologies for such decision making, among three methodologies, qualitative methodologies, statistical methodologies, and geotechnical model-based methodologies for hazard area consideration such as setback distance. Also, rainfall-induced debris flows are shallow, and their

influence is approximated for this setback distance. The frequency of rainfall and hazard areas are presented in tables and maps.

1.4 Task and Organization of the Thesis

The thesis is organized into eight chapters as shown in Figure 1.5.

Chapter 1 provides the problem statement, thesis objectives, research methodology and approach, and task and organization of the thesis.

Chapter 2 contains technical and theoretical backgrounds with an introduction, background on GIS, the concepts of danger and hazards and a literature review of previous studies of landslide susceptibility in mountainous regions of Nepal.

Chapter 3 focuses on the characterization of the study area with its geographical and geomorphological characteristics, geological and geotechnical characteristics and climatic conditions.

Chapters 4 to 7 are structured into a paper-based thesis format, which comprises three technical papers.

Chapter 4 includes the Technical Paper 1, which deals with GIS-based modeling of landslide (debris flow) susceptibility in Kulekhani Watershed, Nepal.

Chapter 5 contains the Technical Paper 2, which focuses on GIS-based assessment of debris flow runout in Kulekhani Watershed, Nepal.

Chapter 6 presents the Technical Paper 3, which deals with GIS-based assessment of debris flow hazards in Kulekhani Watershed, Nepal.

The synthesis and integration of all the results for hazard assessment is presented in **Chapter 7**. The summary, conclusions, and recommendations are presented in **Chapter 8.**

It should be emphasized that since a paper-based thesis format is adopted, some of the contents in the thesis may be repeated because each paper is independently written and crafted according to manuscript instructions for the specified publication.
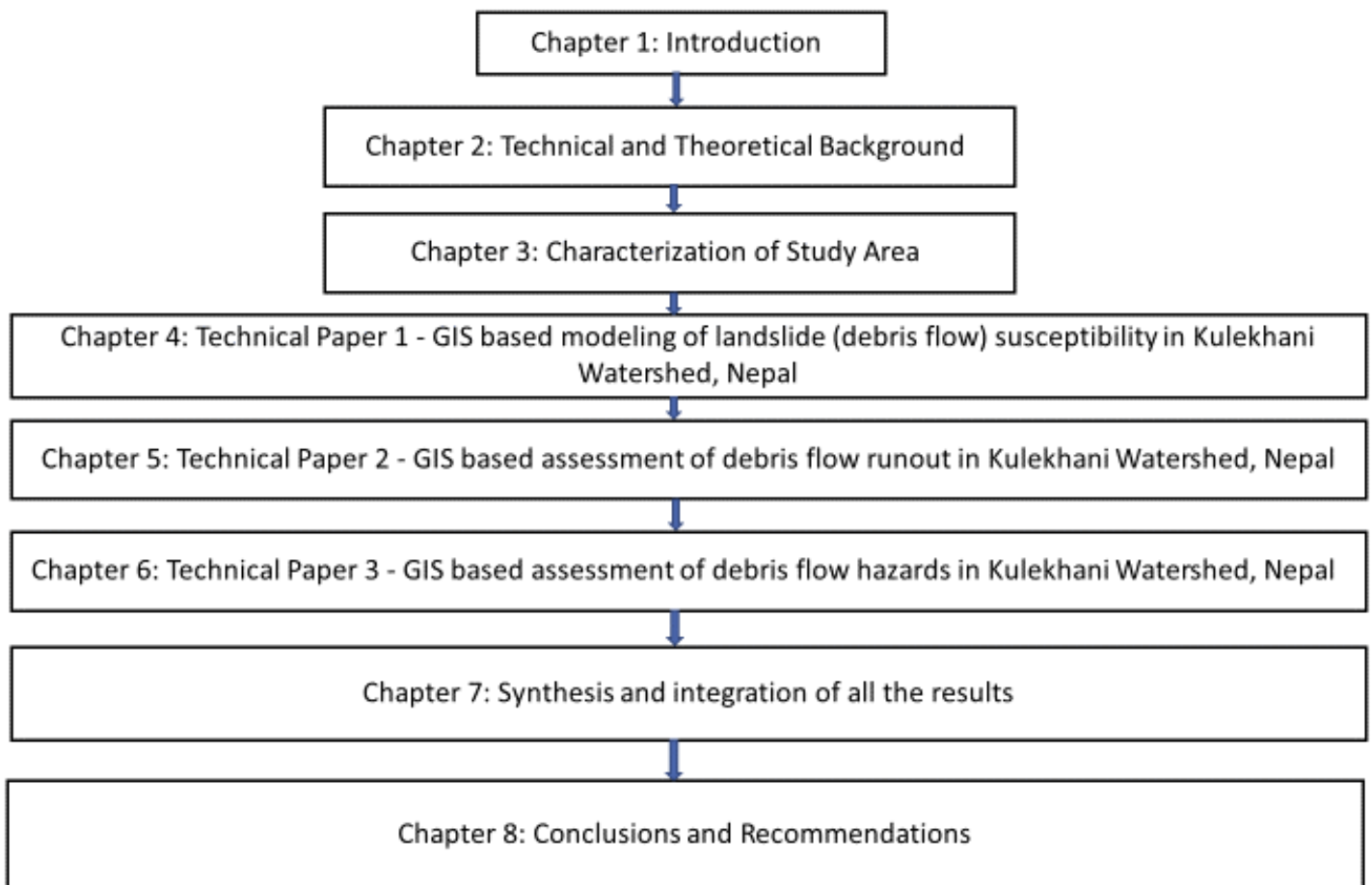
Figure 1.6: Thesis organization.

1.5   References

Acharya, G., De Smedt, F., Long, N.T. (2006), Assessing landslide hazard in GIS: a case study from Rasuwa, Nepal. *Bull Eng Geol Environ*, 65, (1), 99–107.

Bhandary, N.P., Yatabe, R., Dahal, R.K., Hasegawa, S., Inagaki, H. (2013), Areal distribution of large-scale landslides along highway corridors in central Nepal, Georisk: Assessment and Management of Risk for Engineered Systems and Geohazards, pp 31.

Bijukchhen, S.M., Kayastha, P., Dhital, M.R. (2012), A comparative evaluation of heuristic and bivariate statistical modelling for landslide susceptibility mappings in Ghurmi–Dhad Khola, East Nepal. Arab J Geosci.

Caine, N. (1980), The Rainfall Intensity: Duration Control of Shallow Landslides and Debris Flows Geografiska Annaler. Series A, Physical Geography, Vol. 62, No. 1/2 (1980), pp. 23-27.

Carrara, A., Crosta, G., Frattini, P. (2008), Comparing models of debris-flow susceptibility in the alpine environment, Geomorphology, 94, 353–378.

Chalise, S.R., Khanal, N.R. (2001), Rainfall and related natural disasters in Nepal. In: Tianchi, Li., Chalise S.R., Upreti, B.N. (eds), Landslide hazards, mitigation to the Hindukush-Himalayas. ICIMOD, Kathmandu, pp 63–70.

Costa, J.E. (1984), Physical geomorphology of debris flows. In Costa, J.e. and Fleisher, P.J. (Editors), Developments and Applications in Geomorphology: Springer Verlag, pp.268-317.

Dahal, R.K., Hasegawa, S. (2008), Representative rainfall thresholds for landslides in the Nepal Himalaya, Geomorphology Vol. 100, No.3-4, pp. 429-443.

Dahal, R.K., Hasegawa, S., Nonomura, A., Yamanaka, M., Dhakal, S., Paudyal, P. (2008), Predictive modelling of rainfall-induced landslide hazard in the Lesser Himalaya of Nepal based on weights-of-evidence. Geomorphology, 102, (3–4): 496–510.

Dahal, R.K., Hasegawa S., Masuda T., Yamanaka M. (2006), Roadside Slope Failures in Nepal during Torrential Rainfall and their Mitigation. Universal Academy Press, Inc. / Tokyo, Japan, 503–514.

Dahal, R.J., Hasegawa, S., Bhandary, N.P., Poudel, P.P., Nonomura, A., Yatabe, R. (2012), A replication of landslide hazard mapping at catchment scale, Geomatics, Natural Hazards and Risk Vol. 3, No.2, 161-192.

Dangol, V., Upreti, B.N., Dhital, M.R., Wagner, A., Bhattarai, T.N., Bhandari, A.N., Pant S.R., Sharma, M.P. (1993), Engineering geological study of a proposed road corridor in eastern Nepal. Bulletin of the Department of Geology, Tribhuvan University, Nepal, Special Issue, 3(1), 91-107.

Deoja, B.B., Dhital, M.R., Thapa, B., Wagner, A. (1991), Mountain risk engineering handbook, International Centre for Integrated Mountain Development (ICIMOD), Kathmandu, Nepal, pp 875.

Devkota, K.C., Regmi, A.D., Pourghasemi, H.R., Yoshida, K., Pradhan, B., Ryu, I.C., Dhital, M.R., Althuwaynee, O.F. (2013), Landslide susceptibility mapping using certainty factor, index of entropy and logistic regression model in GIS and their comparison at Mugling-Narayanghat road section in Nepal Himalaya, Nat Hazard 65: 135-165.

Dhakal, A.S., Amada, T., Aniya, M. (1999), Landslide hazard mapping and the application of GIS in the Kulekhani watershed Nepal. Mt Res Dev, 19(1): 3–16.

Dhital, M.R. (2005), Landslide investigation and mitigation in Himalayas: focus on Nepal. In: Proceedings of International Symposium Landslide Hazard in Orogenic Zone from the Himalaya to Island Arc in Asia, Kathmandu, Nepal, 1–1.

Dhital, M.R. (2003), Causes and consequences of the 1993 debris flows and landslides in the Kulekhani watershed, central Nepal, Debris-flow Hazards Mitigation: Mechanics, Prediction and assessment, Rickenmann &Chen (eds) pp 1931-1943.

Dhital, M.R. (2000), An overview of landslide hazard mapping and rating systems in Nepal. J Nepal Geol Soc, 22: 533–538.

Dhital, M.R., Khanal, N., Thapa, K.B. (1993), The role of extreme weather events, mass movements, and land use changes in increasing natural hazards, A Report of the preliminary field assessment and workshop on causes of recent damage incurred in southcentral Nepal, July 19-20, 1993. ICIMOD, Kathmandu, 123 pp.

DWIDP (Department of Water Induced Disaster Prevention) Nepal (2016), Annual disaster buliten, Kathmandu, Nepal.

Fall, M. (2009), A GIS-based mapping of historical coastal cliff recession. Bulletin of Engineering Geology and Environment 68(4): 473-482.

Fall, M., Azzam, R., Noubactep, C. (2006), A multi-method approach to study the stability of natural slopes and landslide susceptibility mapping, Engineering Geology 82 (2006) 241– 263.

Finaly, P.J., Mostyn, G.R., fell, R. (1999), Landslide risk assessment prediction of travel distance Canadian Geotechnical Journal 36, 556-562.

Fredlund, D.G., Xing, A.E. (1994), Equation for the soil-water characteristic curve, Can. Geotech. J 31:521-532.

Gabet, E.J., Burbank, D., Putkonen, J.K., Pratt-Sitaula, B.A., Ojha, T. (2004), Rainfall thresholds for landsliding in the Himalayas of Nepal Geomorphology 63,131 – 143.

Gerrard, J., Gardner, R.A.M. (2000), Relationships between rainfall and landsliding in the Middle Hills, Nepal. Norsk geogr. Tidsskr. 54, 74–81.

Ghimire, M. (2011), Landslide occurrence and its relations with terrain factors in the Siwalik Hills, Nepal: case study of susceptibility assessment in three basins. Nat Hazards, 56(1): 299–320.

Horton, P., Jaboyedoff, M., Rudaz, B., Zimmermann, M. (2013), Flow-R, a model for susceptibility mapping of debris flows and other gravitational hazards at a regional scale, Nat. Hazards Earth Syst. Sci., 13, pp 869–885.

Hungr, O., Morgenstern, N. R. (1984), Experiments on the flow behavior of granular materials at high velocity in an open channel, Geotechnique, 34, 3 405-413.

Johnson, A. M., Rodine, J. R. (1984), Debris Flow, Brundsden, D., and Prior, D.B., eds., Slope Instability, John Wiley & Sons. p. 257-361.

Kayastha, P., De Smedt, F. (2009), Regional slope instability zonation using GIS technique in Dhading, Central Nepal. In: Malet J P, Remaître A, Boggard T, eds. Landslide Processes: From Geomorphologic Mapping to Dynamic Modelling, CERG, France, 303–309.

Kayastha, P., Dhital, M.R., Smedt, F.D. (2013), Evaluation and comparison of GIS based Landslide Susceptibility Mapping Procedures in Kulekhani Watershhed, Nepal. Jurnal of Gelogical Society of India, v 81, 219-231.

Kayastha, P., Dhital, M.R., Smedt, F.D. (2012), Landslide Susceptibility mapping using the weight of evidence method in the Tinau Watershed, Nepal. Nat Hazards 63:479-498.

Kayastha, P., De Smedt, F., Dhital, M.R. (2010), GIS based landslide susceptibility assessment in Nepal Himalaya: a comparison of heuristic and statistical bivariate analysis. In: Malet J P, Glade T, Casagli N, eds. Mountain Risks: Bringing Science to Society. CERG Editions, 121–128.

K.C., S. (2013), Community vulnerability to floods and landslides in Nepal ecology and society 18(1): 8. (http://dx.doi.org/10.5751/ES-05095-180108.).

Ministry of Home, Nepal Disaster Report (2015) public web resource: http://neoc.gov.np/en/publication/.

Pantha, B.R., Yatabe, R., Bhandary, N.P. (2010), GIS-based highway maintenance prioritization model: an integrated approach for highway maintenance in Nepal Mountains. J Transp Geogr, 18(3): 426–433.

Poudyal, C.P., Chang, C., Oh, H., Lee, S. (2010), Landslide susceptibility maps comparing frequency ratio and artificial neural networks: a case study from the Nepal Himalaya. Environ Earth Sci, 61(5), 1049–1064.

Ray, R.L, Smedt De, F. (2009), Slope stability analysis on a regional scale using GIS: a case study from Dhading, Nepal. Environ Geol, 57(7): 1603–1611.

Remondo, J., Bonachea, J., Cendrero, A. (2008), A statistical approach to landslide risk modelling at basin scale; from landslide sus-ceptibility to quantitative risk assessment, Geomorphology 94 (2008) 496–507.

Rickenmann, D. (1999), Empirical Relationships for Debris Flows, Natural Hazards 19: 47–77, 1999.

Sharma, R.H., Shakya, N.M. (2008), Rain induced shallow landslide hazard assessment for ungauged catchments, Hydrogeol J, 16(5):871–877.

Thapa, P.B., Dhital, M.R. (2000), Landslide and debris flows of 19–21 July 1993 in the Agra Khola watershed of central Nepal. J Nepal Geol Soc, 21: 5–20.

Torres, G.H. (2011), Estimating the soil-water characteristics curve using grain-size analysis and plasticity index, M.Sc., Thesis, Arizona State University, Tempe, AZ.

Upreti, B.N., Dhital, M.R. (1996), Landslide studies and management in Nepal, International Centre for Integrated Mountain Development (ICIMOD), Kathmandu, Nepal, pp 87.

Van Westen, C.J. Seijmonsbergen, C., Mantovan, F. (1999), Comparing Landslide Hazard Maps 20: 137-158.

Van Westen, C.J., Van Asch, T.W.J., Soeters, R. (2006), Landslide hazard and risk zonation; why is it still so difficult? Bulletin of Engineering geology and the Environment 65 (2), 167–184.

Van Westen, C.J., Castellanos, E, Kuriakose. S. L. (2008), Spatial data for landslide susceptibility, hazard and vulnerability assessment: An overview. Engineering geology, 102: 112:131.

Wagner, A. (1997), Hazard mapping and geophysics applied to landslide study in the Himalayas and Hindukush, an unpublished brochure submitted to ITECO Nepal.

Yagi, H. (2001), Landslide study using aerial photographs, Landslide Hazard Mitigation in the Hindu Kush-Himalayas. In: Tianchi L, Chalise SR, and Upreti BN (eds) Landslide hazard mitigation in the Hindu-Kush Himalayas, ICIMOD, Nepal, 79.

Yagi, H., Nakamura, S. (1995), Hazard mapping on large scale landslides in the lower Nepal Himalayas. In: Proceedings of international seminar on water induced disasters (ISWID-1995), DPTC-JICA, Kathmandu, Nepal, 162-168.

Chapter 2: Technical and Theoretical Background

2.1   Introduction

The research deals with modeling of landslide initiation, debris flow inundation and hazard assessment in the study area. The main modeling tools used include GIS and the Flow-R model. To facilitate the understanding of the main results presented in this thesis, theoretical and technical background on GIS and Flow-R are provided in this chapter. Moreover, since the terms hazard, and risks danger are used or discussed in procedures of modeling debris flow susceptibility and hazard, background on the concepts of danger, hazard and risk is also given in this chapter. Furthermore, a literature review on previous studies that dealt with landslides susceptibility in mountainous regions of Nepal is also presented in this chapter to underline the uniqueness or novelty of the results presented in this thesis.

2.2   Background on GIS

Geographical Information System (GIS) is a tool used to develop, store, edit, analyze, and populate data in spatial reference. There are two types of data systems in GIS: vector and raster.

Vector data represents points, lines, and polygons with geographical references. A vector data system is useful for representing features which have a boundary, such as different land use in the watershed, geology, rainfall variation with contours, topography, and river networks. The software used in this research is ESRI's ArcGIS 10.2, which has the capability to format these data, which can then be used later in other GIS software as vector data. Vector files saved in shape files (extension .shp), together with two other extensions (.shx and .dbf). In addition to this, there will be other extension (.proj and .lyr) files for storing data and retrieving and executing later on in the same software or other GIS software.

There is a separate folder, together with Arc GIS Icon, Geodatabase, which is for storing data for raster, vector, and tabular data in three different file folders: file,

personal, and ArcSDE. Raster data is represented by pixels in a raster model. Raster data has a grid system with the size of the cell and associated data, such as coordinates, factor of safety and geological and geotechnical characteristics. Raster data does not have any boundary like vector files. Raster data smoothly change from one cell to another. Data such as digital elevation models, landslide susceptibility, hazards, and risk of watershed are best suited to a raster data system. For modeling landslide initiation, debris flow area and hazard area, input features are required in raster format. In raster format, GIS can analyze by adding, substracting, multiplying, sorting, and more mathematical and statistical operations through its map algebra among associated assigned cells. Raster data are saved in separate folders with separate extensions (.adf, .dat, or.nit). Image files stored in extensions, such as .tif, provide the geographical reference and data characteristics. GIS software should be capable of synthesizing data as required for modeling and mapping through various tools. In this research, ESRI product ArcGIS is used for analysis, and has the capability to model and develop landslide initiation, debris flow inundation, hazard, and risk analysis and mapping.

The initial topographical features of the study watershed area are available in contour maps. The topographical map is a series of line vectors modeled to Triangulated Irregular Network (TIN) to develop DEM, a raster map. The watershed is one of the most popular destinations for vegetable cultivation, tourism, residential divisions, forest/barren, and a reservoir (water body). These features are available in vector maps and converted into raster for further use for developing slope stability maps. Maps of all parameters are developed into raster format in the GIS environment. The samples recovered from 73 locations (Lamichhanne 2000) in the study watershed have point information in vector format. Initially this information is developed in a spread sheet with spatial locations. There are various interpolation methods available in GIS environment, such as Kriging, Natural Neighbor, Inverse Distance Weighted (IDW). In this research Inverse Distance Weighted (IDW) is selected because, for limited number of interpolating data, this method provides better result than other methods. All these data are populated in GIS and interpolated with (IDW) methods to create continuous raster maps for the whole watershed. The extent of these

maps and their cell numbers are sized to the same scale for raster analysis. Map algebra is used for analysis of the susceptibility and hazard maps.

2.3   Background on the concepts of danger, hazard and risks

Danger and hazard are related terms, but they have different meanings in safety perspectives. Danger is a situation with the potential to generate unsafe or injurious conditions for human life or the environment (Fall 2009). Danger itself does not define how much probability a particular event or situation has to cause what degree of damage. For example, it is more dangerous to travel by airplane than car from one place to another (Fall 2009) if we compare these transport means. A situation may be dangerous for any natural or anthropogenic reasons, but whether that situation causes any harm cannot be evaluated through danger alone, and requires hazard analysis. Hazard provides the probability of harm from a potentially dangerous situation. Landslide-induced debris flows are dangerous to life, property, and the environment. Debris flows are dangerous, but the probability of damage from this event can be evaluated through hazard analysis.

Hazard is defined by Varnes et al. (1984) (IAEG Commission, 1984) as "*a probability of occurrence of a potentially damaging event in a given area and period of time*". After 15 years of Varnes et al.'s definition, Guzzetti et al. (1999) further defined landslide hazard and added "magnitude" and redefined "probability of occurrence of a given magnitude of landslide in a given duration and location". Therefore, it is important to consider three components: probability of occurrence of a landside, its location, and its size when one conducts landslide hazard assessment. Fall (2009) further clarified the term, stating that landslide hazard is characterized by "its location, intensity (magnitude), frequency and probability". Probability of the landside initiation, debris flow inundation, and magnitude of the event for vulnerability to the element at risk are important factors for landslide hazard assessment.

Furthermore, damage from landslides hazard is required to evaluate in a measurable unit and another term involves "risk assessment". Together with the danger and hazard term, risk needs to be understood. The probability of landside

initiation, debris flow inundation, and the magnitude of events for vulnerability to the element at risk are important factors for landslide risk assessment. The definition from UNISDR (2016) for risk is "the combination of the probability of an event and its negative consequences". For landslides, Varnes and the IAEG (1984) proposed a definition of risk, (RS) as an expected degree of loss due to a landslide". Later, this was adopted by UNDRO (Office of the United Nations Disaster Relief Co-Ordinator 1991). Furthermore, Corominas et al. (2014) and Fall (2009) defined risk as a product of hazard, vulnerability, and element at risk (amount). The items required for risk assessment can be obtained qualitatively or quantitatively (Dai et al. 2002, Van Westen et al. 2006, Li et al. 2010). Risk assessment can include these four components: physical, economic, societal, and environmental (Fell et al. 2005, Van Asch et al. 2014). Risks to environment, economy, and physical infrastructures are more tangible and measurable than the societal risk (Fell 1994, Phoon 2004, Fell et al. 2005, Hufschmidt et al. 2005, Van der Geest and Schindler 2016, Bogard 1989). Although landslide risk is very simple as defined by Varnes (1984), the quantitative estimation of risk remains a difficult task due to problems in quantifying the individual components of the risk equation (Fell et al. 2005, Van Westen et al. 2006), such as a complex term "hazard".

For the understanding of landslide hazard and the definition of risk, vulnerability and the element at risk is equally important. The term "vulnerability" is a degree of damage or potential maximum losses due to potential external events in a given duration of time (Liu et al. 2002). Vulnerability is a predisposition to suffer damage due to external events (Fall 2011). Vulnerability values ranges from 0 to 1 (UNDP 2004, Liu and Lei 2003, Liu et al. 2002, Fell and Hartford 1997, IUGS 1997, Panizza 1996, Alexander 1993, Liam Finn 1993, United Nations 1991). The term "element at risk" from a landslide encompasses the vulnerability of fixed assets, gross domestic product, land resources, population density, population age group and their education, and productivity. Procedures for quantitative vulnerability estimation are found in Uzielli (2008), Fell et al. (2005), Roberds (2005), Wong (2005), Bell and Glade (2004), Ko Ko et al. (2003), Wong et al. (1997), Roberds et al. (1997), Einstein (1997), and Fell and Hartford (1997).

2.4   Background on Flow-R

Flow-R model is adopted in this research for debris flow assessment. This is an empirical model developed in the University of Lausanne. The model can be used for identifying landslide susceptibility and debris flow runout (Horton et al. 2013). Flow-R means "*flow path assessment of gravitational hazards at a Regional scale*" (Horton et al. 2013, www.flow-r. org). This model is applied in various regions of the world beyond Alps with valid and reasonable results (Horton et al. 2013). Steps necessary to assess debris flow in this model are: Source identification, and propagation.

Debris flow modeling (both susceptibility location and runout) is a complex phenomenon because of influence by various local factors and uncertainty of modeling parameters. This model provides reasonable results from the limited information for a watershed scale. Debris source area can be identified by applying conditions on the defined grids with favorable, unfavorable or no data for selected parameters. These parameters may be slope, flow accumulation, curvature, geology, land use, lithology so on. Horton et al. (2008) found 0.01 km^2 threshold upslope area for debris flow susceptibility for central Alps considering only two parameters, slope and flow accumulations. However, this value varies for different locations (Fischer et al. (2012). Heinimann (1998), Rickenmann and Zimmermann (1993) and Horton et al. (2013) applied only these parameters (channel slopes and upslope area thresholds) for debris flow initiation for rare and extreme events in Alps region. They found Equation [2.1] and [2.2] for rare event and Equation [2.3] and [2.4] for extreme event.

$$\mathrm{Tan}B_{theres} = 0.32 S_{uca}^{-0.2} \qquad \text{if } S_{uca} < 2.5 km^2 \qquad\qquad [2.1]$$

$$TanB_{theres} = 0.26 \qquad \text{if } S_{uca} \geq 2.5 km^2 \qquad\qquad [2.2]$$

$$\mathrm{Tan}B_{theres} = 0.32 S_{uca}^{-0.15} \qquad \text{if } S_{uca} < 2.5 km^2 \qquad\qquad [2.3]$$

$$TanB_{theres} = 0.26 \qquad \text{if } S_{uca} \geq 2.5 km^2 \qquad\qquad [2.4]$$

where, TanB$_{thres}$ is the threshold slope, and S$_{uca}$ the surface of the upslope contributing area from the selected point. For this research, these relationships are

not applicable as is, and it requires customizing with site specific model results and field observations. This task includes parametric analysis and comparison with field observation with available DEM and other influencing factors. However, Flow-R has capability to simulate user defined source to model debris flow propagation in a given watershed. Once the source of debris flow is identified separately, the model can be used for debris flow propagation. The source of debris flow in this research is proposed to be identified through slope stability model.

Flow-R model interface is shown in Figure 2.1. In the top menu bar options, tools and help are available. Options menu provides the language of modeling, either in English or French. Tools bar contains Data Format, Batch Mode and Extensible Markup Language (XML) editor options. The study area maps required to change into ASCII for Flow-R model. Import menu can be used for importing files saved in computer folders in ASCII format. Within the imported menu the study area can be specified. These options are manual specified in the existing digital Elevation Model (DEM), by giving coordinates, based on a mask or select the whole DEM of the area. Other optional inputs are river selection and buffer areas. In this research, the whole study area is converted in ASCE II file format and imported in the model. Subsequently for the study area option in the model, whole DEM was selected for the study.

Creating working directories and location is required to specify for saving result files. The run defined option provides the selection of working file, choice of the river layer, and run name which later can be saved in the same folder and retrived and run again if necessary.
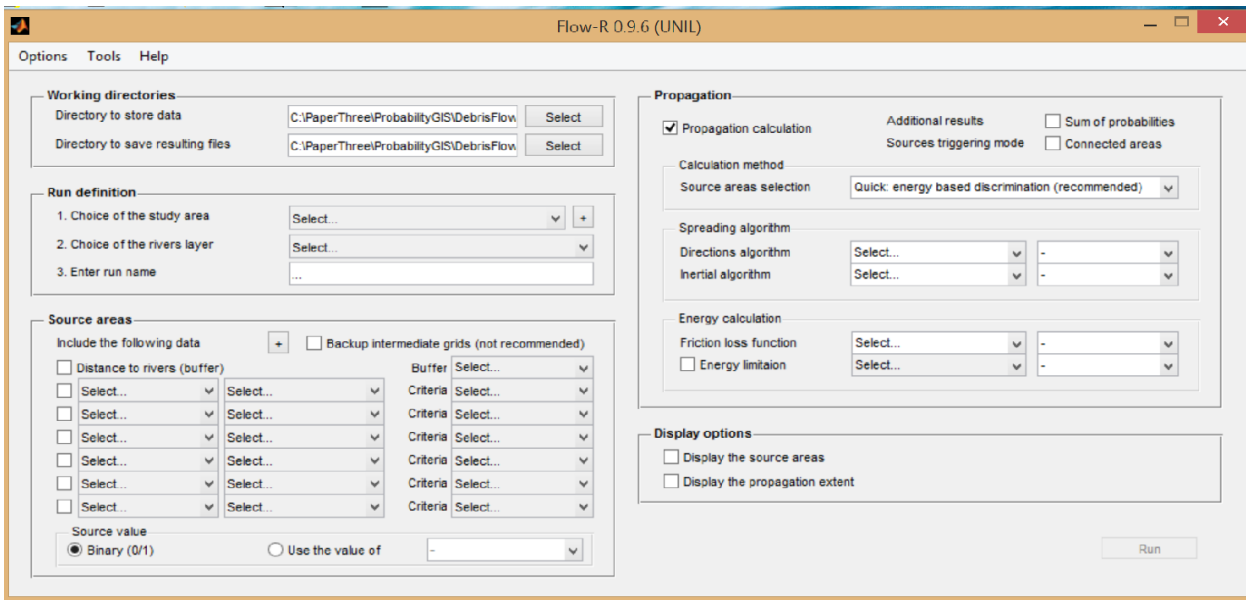
Figure 2.1: Flow-R model interface (Horton et al. 2013).

The remaining menus are divided in two categories, source and propagation. The input data options for source identification and propagation available for Flow-R format are shown in Table 2.1. For processing, the Input data required to prepare and saved in the same folder where results will be saved.

Table 2.1 Input and results from Flow-R source identification and propagation.

Description	Input Data (ASCII format)	Output Result (ASCII format)
Source Identification	DEM of the study area, Predefined source, Slope, Aspect, Flow accumulation, Total curvature, Profile curvature, Land use, Geology, Lithology, Custom known constrain or source	Landslide susceptible area within the study area
Debris Flow Propagation	Computed susceptible area, User defined susceptible area in DEM Whole study DEM	Area covered by debris flow source and run out in the study area

The input files and specific criteria can be specified for source identification. In this research, source is pre-identified within the whole DEM. The source map developed separately and changed into ASCII and provided the Boolean criteria: one (1) for the source and zero (0) for the rest of the area within the DEM.

In Flow-R model, models listed in Table 2.2 are available for debris propagation analysis. All options available in the model are applied and compared with the field observation to select appropriate model. Initial modeling shows that selecting any of the models for source identification and to define source areas does not make any difference on propagation. Both, Holmgren (1994) or modified Holmgren (1994) algorithms (Horton et al. 2013) are appropriate to use for spreading algorithms in this watershed. There are two options for initial algorithms, Weights and Direction Memory. Direction Memory does not show actual debris flow spreading but any under Weights; Default (proportional), Cosinus and Gamma 2000 algorithms provide appropriate runout results. For friction loss function and energy loss function, other algorithms are also available such as Perla et al. (1980), Simplified Friction Limited Model (SFLM) (Corominas 1996). However, lower travel angle and lower velocity are sufficient to model debris flow runout, which will be applied for further research.

Table 2.2 Available Algorithms in Flow-R Model for Debris Flow Propagation.

Source Area Selection	Spreading Algorithms				Energy Calculation			
	Direction Algorithm		Initial Algorithm		Friction Loss Function		Energy Limitation	
(Only Superior Sources (Debris-Flows only), Energy Base Discrimination, Complete Propagation of all source areas (long)	Holmgren (1994)	Exponent 1 to 50	Weights	Default, Cosinus, Gamma 2000	Travel angle	From 0.1 ° to 50 °	Velocity	1 mps to 50 mps
	Holmgren (1994) Modified	Dh from 0.25m to 70 Exponent 0.1 to 50	Direction memory	Len=005 to 100, Open 090 to 300				

Mps=meter per second

2.5   Literature review on previous studies of landslide susceptibility in mountainous regions of Nepal

The growing landslide hazard year after year, and the importance of remedial measures for saving lives and property was identified as early as the 1980s in Nepal (Caine and Mool 1982). However, due to a lack of accessibility and resources, and the complexity of the problem for research and implementation, the study of landslides did not proceed at a proper pace in Nepal. In the early 1990s, a severe debris flow occurred in central Nepal, and the importance of landslide research and hazard mitigation was realized by society and the government again. This led to the commissioning of research on landslide initiation and remedial measures. Numerous studies (e.g., Devkota et al. 2013, Kayastha et al. 2010, 2012, 2013, Bhandary et al. 2013, Bijukchhen et al. 2012, Dahal et al. 2012, Ghimire 2011, Pantha et al. 2010, Poudyal et al. 2010, Ray and De Smedt 2009, Kayastha and De Smedt 2009, Dahal and Hasegawa 2008, Dahal et al. 2008, Sharma and Shakya 2008, Acharya et al. 2006, Dahal et al. 2006, Gabet et al. 2004, Chalise and Khanal 2001, Yagi 2001, Gerrard and Gardner 2000, Thapa and Dhital, 2000, Dhital 2000, Dhakal et al. 1999, Wagner 1997, Upreti and Dhital 1996, Yagi and Nakamura 1995, Dhital et al. 1993, Dangol et al. 1993, and Deoja et al. 1991) have been conducted on landslide dangers and the risk of living in the Nepalese mountains. However, debris flow runout from the initial landslide, and its analysis on a watershed scale has not be addressed or studied. Key past studies on landslides in the Nepalese mountains are described and discussed below.

Ray and Smedt (2009) applied the slope stability equation in GIS and developed a landslide susceptibility map, which they validated against existing landslides in the Dhading area of Nepal. They applied pore pressure development with assumed groundwater flow from uphill areas, and accumulation of soil water from direct infiltration, for rainfall return periods of 2 to 50 years. Other influencing factors, such as topography and types of soils are also considered in the GIS environment for map integration to develop susceptibility maps. Factor of safety ranges are applied for the hazard zoning of the area. Computed factors of safety are used for the susceptibility and frequency of the landslide. In their analysis, only 29% of the

soil slopes smaller than 21° are unconditionally stable. This means that the area beyond 29% is unstable in one or another of the expected conditions. However, mountain slopes have not failed in that much extent and frequency as identified from their results.

Dahal et al. (2008) studied rainfall intensity and landslides events for 193 landslides in the Nepalese mountains, in a study similar to that conducted by Caine (1980). They collected data from all rain gauge stations and landslide events, and proposed rainfall threshold for landslide initiation for the entire Nepalese mountains. Their findings show that landslide events are proportionally distributed in the area according to annual average rainfall. It can be noted from their study that the annual average rainfall distribution and rainfall intensity are in agreement with the density of landslides from the east to west of Nepal. The number of landslides recorded in Nepal is higher in the eastern and central regions than the western region, and is similar to the annual average monsoon rainfall distribution from east to west. This shows that threshold rainfall plays a significant role in the initiation of landslides; however, the location of unstable slopes can only be identified with the study of subsurface physical changes on a mountain slope. The threshold rainfall triggers landslides only in a specific location of the mountain slope in a given rainfall event.

Dahal and Hasegawa (2008) recommended the following rainfall intensity and duration for landslide initiation (Equation [2.5]).

$$I = 73.90D^{-0.79}, \quad N_1 = 1.10D^{-0.59} \quad [2.5]$$

where, I is the hourly intensity in mm, D is the duration in hours, N_1 is the normalized rainfall intensity per hour—a ratio of critical rainfall to mean annual precipitation.

Their empirical equation provides a warning of the intensity and duration of rainfall related to landslides in previous events. However, it does not provide information on the location of the unstable areas or slopes. Using this equation, they reported that continuous rainfall of more than 12 mm per hour for 10 hours, 2 mm of rainfall

per hour for 100 hours, or daily rainfall in excess of about 144 mm, is required for landslide initiation. In these observations, all landslides are considered including deep-seated and shallow landslides. Also, the landslides considered in their study are not discriminated based on whether they were first initiated within the study period, or previously occurred and retroactive now. Physical parameters, such as subsurface soil characteristics and their influence on the density of landslides in a specific area of the country are not considered in their study. However, these records provide a good guide for how to proceed for further study of physical changes in slopes during threshold rainfall conditions.

The instability of a specific location depends on the geotechnical properties of subsurface soil, the groundwater profile, and rainfall threshold, so the aforementioned relation proposed by Dahal and Hasegawa (2008) is a baseline for further study in the region. Dahal and Hasegawa (2008) also indicated that landslides in the Nepalese Himalayas occur in as less as three times the required threshold rainfall for landslide initiation, in other worlds, which means that these mountains are more landslides susceptible and unstable. However, the landslide study focused only on initiation, and did not distinguish it from debris flow in the region, although Petley et al. (2007) observed 397 fatal landslides which were mostly debris flow. Dahal and Hasegawa (2008) identified 677 rainfall-induced landslides in the whole of Nepal, and they observed mostly debris flows in the natural terrain. Based on visual observations at the study site, as well as previous research (Dahal and Hasegawa 2008, Dahal et al. 2008, Dhital et al. 1993, Petley et al. 2007, Gabet et al. 2004, Ray and Smedt 2009, and Dhital 2003), the types of landslides in the proposed study region are mostly debris flows (Cruden and Varnes 1996). Consequently, the present study should consider relevant debris flow analysis in the watershed, as the types of landslides in the study area are predominantly debris flows.

Previous GIS-supported studies on landslides in Nepal were based on statistical approaches. These studies considered previous landslide events and spatial distribution as a base factor for the identification of future landslides in most of the

research in the region (Devkota et al. 2013, Kayastha et al. 2010, 2012, 2013, Bijukchhen et al. 2012, Pantha et al. 2010, Poudyal et al. 2010 and Kayastha and De Smedt 2009). Again, this method does not account for the changed physical features of the watershed with landslides, debris flow runout characteristics, which is many times more devastating than initial landslide. These issues should be addressed in the present thesis.

Landslide inventory was carried out by Kayastha et al. (2012), Dhital (2003) and, Deoja et al. (1991) after devastating rainfall in a watershed during 1993 (Figure 2.2). Landslides were observed in very-steep to moderately-steep mountain slopes at high altitude locations (Figure 2.2). Most of the landslides in the study area were changed into debris flows. Landslides were initiated on both natural slopes and anthropogenic disturbance locations, such as near roads and other infrastructure (Kayastha et al. 2012). Dhital (2003) studied these debris flows in detail, and found that the main triggering factor was 540 mm rainfall in one 24-hour period for the July 1993 landslide in the study watershed.
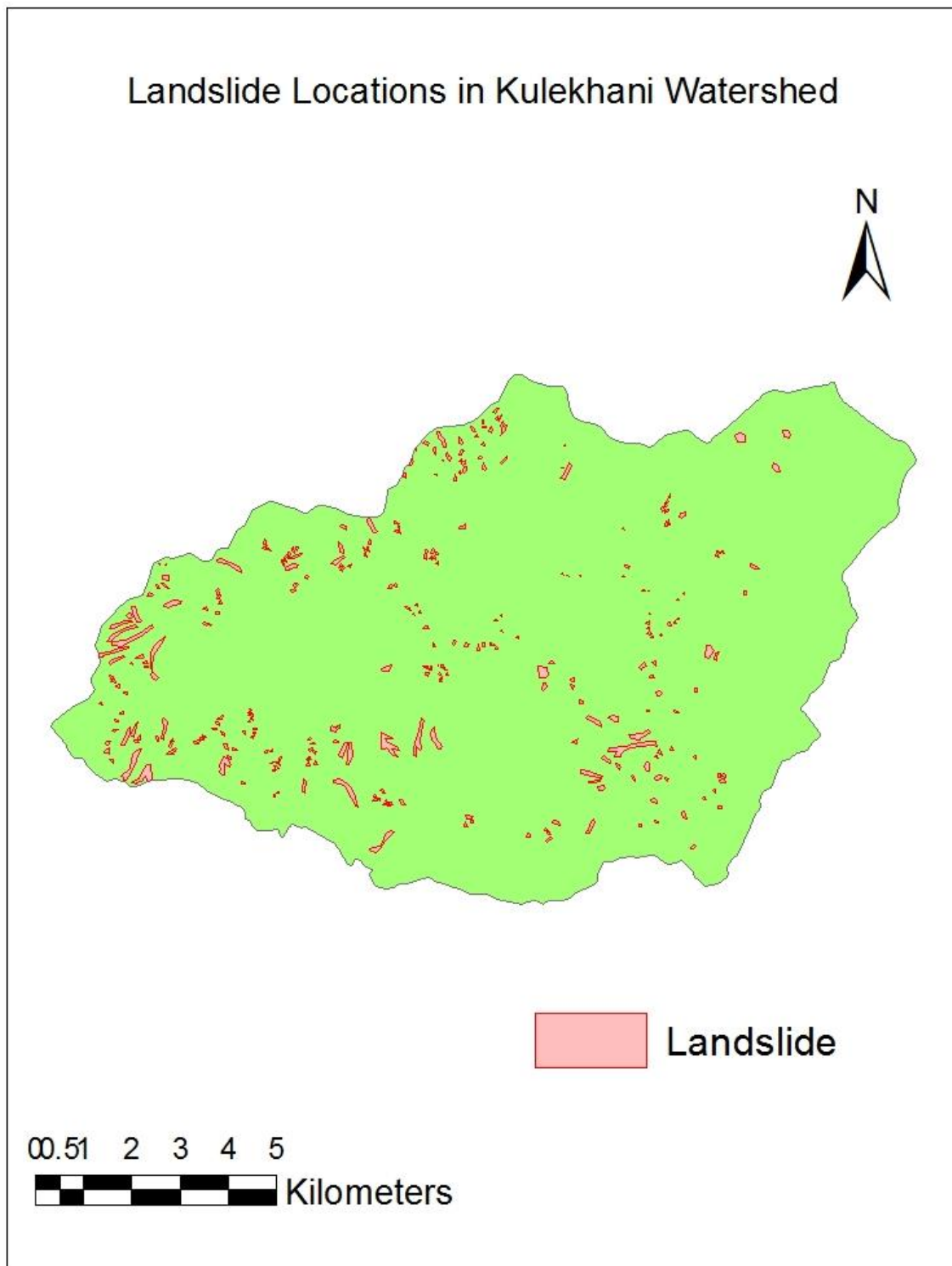
Figure 2.2: Observed landslide areas in the Kulekhani watershed after 540 mm rainfall in one 24-hour period (modified from Kayashta et al. 2013).

A debris flow of about 104,000 m^3 was initiated in northern Nepal nearly 109 km from Kathmandu, the capital city, on July 22, 1996 (Adhikari and Satoshi 2005). A

detailed study was conducted by Adhikari and Koshimizu (2005) into the causes of the debris flow, which damaged 18 houses and killed 56 people. The assumption was stream carried debris flow from the glacial lake which is within its watershed. However, the debris flow developed from an initial landslide about 500 m uphill not from outburst of glacial lake. A landslide originated after heavy rainfall, followed by low-intensity long-duration rainfall, and dammed the Bhairab Kunda stream, a tributary of the Bhotekoshi, which is one of the seven tributaries of the Saptakoshi, the largest river in Nepal. The rainfall intensity was not recorded close to the site, but a nearby station recorded 80 mm within a few hours. The debris flow material comprised boulders, cobbles, gravel, sand, silt, and clay, along with other unsorted materials. The debris flow study was completed, but future prediction of debris flow hazards using a model is still to be developed.

From the literature review presented above, it can be concluded that numerous studies on landslides in the mountainous regions of Nepal were conducted in the past years and decades. However, none of these studies dealt with GIS-based analysis of debris flow susceptibility, runout and hazards, in these regions of Nepal. This research gap and need will be addressed in this thesis.

2.6   Conclusions

Debris flows represent frequent and serious danger and hazards in mountainous Nepal. Rainfall is one of the primary triggering factors for the debris flows. Therefore, understanding and assessing debris flow danger and hazards in the mountainous regions of Nepal is critical for the safety of the population and property.

Previous landslide research in the Nepalese mountains was focused either on individual landslides or GIS-based statistical methods, and did not consider landslide initiation and debris flow together for hazard analysis. The rainfall threshold and landslide relation were derived for the region, but the spatial distribution of landslides generated by those rainfall durations and intensities is unknown. Thus, the development of a model capable of finding the spatial

31

distribution of landslide initiation for a given rainfall intensity and debris flow extent for hazard analysis is critical for saving lives and property in the region. This research gap and need will be addressed in this thesis using slope stability model with Flow-R in GIS environment.

2.7   References

Acharya, G., De Smedt, F., Long, N.T. (2006), Assessing landslide hazard in GIS: a case study from Rasuwa, Nepal. Bull Eng Geol Environ, 65, (1), 99–107.

Adhikari, D.P., Koshimizu, S. (2005), Debris flow disaster at Larcha upper Bhotekoshi Valley, central Nepal, The Island Arc (2005) 14, 410–423.

Alexander, D.E. (1993), Natural Disasters. UCL Press Limited, London, 632 pp.

Bell, R., Glade, T. (2004), Quantitative risk analysis for landslides – examples from Bildudalur, NW Iceland, Nat. Hazards Earth Syst. Sci., 4, 117–131.

Bhandary, N.P., Yatabe, R., Dahal, R.K., Hasegawa, S., Inagaki, H. (2013), Areal distribution of large-scale landslides along highway corridors in central Nepal, Georisk: Assessment and Management of Risk for Engineered Systems and Geohazards, pp 31.

Bijukchhen, S.M., Kayastha, P., Dhital, M.R. (2012), A comparative evaluation of heuristic and bivariate statistical modelling for landslide susceptibility mappings in Ghurmi–Dhad Khola, East Nepal. Arab J Geosci.

Bogard, W. (1989), Bringing social theory to hazards research: conditions and consequences of the mitigation of environmental hazards, Sociological Perspectives, 31, 147–168, 1989.

Caine, N., Mool P.K. (1982), Landslides in the Kolpu Khola drainage, Middle Mountains, Nepal. *Mt Res Dev* 2,157–173.

Catani, F., Casagli N., Ermini L., Righini G., Menduni, G. (2005), Landslide hazard and risk mapping at catchment scale, Arno River basin. Landslides 2(4):329–342.

Chalise, S.R., Khanal, N.R. (2001), Rainfall and related natural disasters in Nepal. In: Tianchi, Li., Chalise S.R., Upreti, B.N. (eds), Landslide hazards, mitigation to the Hindukush-Himalayas. ICIMOD, Kathmandu, pp 63–70.

Corominas, J., Van Westen, C., Frattini, P., Cascini, L. , Malet, J.-P., Fotopoulou, S., Catani F., Van Den Eeckhaut, M., Mavrouli, O., Agliardi, F., Pitilakis, K. • Winter M. G. Pastor M.• Ferlisi S., Tofani, V., Hervas J., Smith J.T. (2014), Recommendations for the quantitative analysis of landslide risk Bull Eng Geol Environ 73:209–263.

Corominas, J. (1996), The angle of reach as a mobility index for small and large landslides, Can. Geotech. J., 33, 260–271.

Dahal, R.K. and Hasegawa, S. (2008), Representative rainfall thresholds for landslides in the Nepal Himalaya, Geomorphology Vol. 100, No.3-4, pp. 429-443.

Dahal, R.J., Hasegawa, S., Bhandary, N.P., Poudel, P.P., Nonomura, A., Yatabe, R. (2012), A replication of landslide hazard mapping at catchment scale, Geomatics, Natural Hazards and Risk Vol. 3, No.2, 161-192.

Dahal, R.K., Hasegawa, S., Nonomura, A., Yamanaka, M., Dhakal, S., Paudyal, P. (2008), Predictive modelling of rainfall-induced landslide hazard in the Lesser Himalaya of Nepal based on weights-of-evidence. *Geomorphology*, 102, (3–4): 496–510.

Dahal, R.K., Hasegawa S., Masuda T., Yamanaka M. (2006), Roadside Slope Failures in Nepal during Torrential Rainfall and their Mitigation. Universal Academy Press, Inc. / Tokyo, Japan, 503–514.

Dai, F.C., Lee, C.F., Nagi. Y.Y. (2002), Landslide risk assessment and management: an overview. Engineering Geology, 64: 65-87.

Dangol, V., Upreti, B.N., Dhital, M.R., Wagner, A., Bhattarai, T.N., Bhandari, A.N., Pant

S.R., Sharma, M.P. (1993), Engineering geological study of a proposed road corridor in eastern Nepal. Bulletin of the Department of Geology, Tribhuvan University, Nepal, Special Issue, 3(1), 91-107.

Deoja, B.B., Dhital, M.R., Thapa, B., Wagner, A. (1991), Mountain risk engineering handbook, International Centre for Integrated Mountain development (ICIMOD), Kathmandu, Nepal, pp 875.

Devkota, K.C., Regmi, A.D., Pourghasemi, H.R., Yoshida, K., Pradhan, B., Ryu, I.C., Dhital, M.R., Althuwaynee, O.F. (2013), Landslide susceptibility mapping using certainty factor, index of entropy and logistic regression model in GIS and their comparison at Mugling-Narayanghat road section in Nepal Himalaya, Nat Hazard 65: 135-165.

Dhital, M.R., Khanal, N., Thapa, K.B. (1993), The role of extreme weather events, mass movements, and land use changes in increasing natural hazards, A Report of the preliminary field assessment and workshop on causes of recent damage incurred in southcentral Nepal, July 19-20 1993. ICIMOD, Kathmandu, 123 pp.

Dhital, M.R. (2000), An overview of landslide hazard mapping and rating systems in Nepal. J Nepal Geol Soc, 22: 533–538.

Einstein, H.H. (1997), Landslide risk systematic approaches to assessment and management. In: Cruden, D.M., Fell, R. (Eds.), Landslide risk assessment, Proceedings of the International Workshop on Landslide Risk Assessment, Honolulu, 19–21 February 1997. Balkema, Rotterdam, pp. 25–50.

Fall, M. (2009), Lecture notes hazard assessment, University of Ottawa, Ottawa, Canada.

Fall, M. (2009), A GIS-based mapping of historical coastal cliff recession. Bulletin of Engineering Geology and Environment 68(4): 473-482.

Fall, M., Azzam, R., Noubactep, C. (2006), A multi-method approach to study the stability of natural slopes and landslide susceptibility mapping, Engineering Geology 82 (2006) 241– 263.

Fell, R., Ho, K.K.S., Lacasse, S., Leroi, E. (2005), A framework for landslide risk assessment and management. In: Hungr, O., Fell, R., Couture, R., Eberhardt, E. (Eds.), Landslide Risk Management, Taylor and Francis, London, pp. 3–26.

Fell, R., Hartford, D. (1997), Landslide risk management. In: Cruden, D., Fell, R. (Eds.), Landslide Risk Assessment. Balkema, Rotterdam.

Fell, R. (1994), Landslide risk assessment and acceptable risk. Canadian Geotechnical Journal 31, 261–272.

Fischer, L., Rubensdotter, L., Sletten, K., Stalsberg, K., Horton, P., Jaboyedoff, M. (2012), Debris flow modeling for susceptibility mapping at regional to national scale in Norway. In Proceedings of the 11th International and 2nd North American Symposium on Landslides (pp. 723–729). Banff, Alberta, Canada.

Fuchs, S.H.K., Hubl, J. (2007), Towards an empirical vulnerability function for use in debris flow risk assessment. Natural hazard Earth System sciences, 7: 495-506.

Gabet, E.J., Burbank, D., Putkonen, J.K., Pratt-Sitaula, B.A., Ojha, T. (2004), Rainfall thresholds for landsliding in the Himalayas of Nepal Geomorphology 63,131 – 143.

Gabor, T., Griffith, T. (1980), The assessment of community vulnerability to acute hazardous materials incidents, Journal of Hazardous Materials, 8, 323–333.

Galli, M., Guzzetti, F. (2007), Landslide vulnerability criteria: Acase study from Umbria, Cental Italy. Environmental management, 40: 649-664.

Ghimire, M. (2011), Landslide occurrence and its relation with terrain factors in the Siwalik Hills, Nepal: case study of susceptibility assessment in three basins. Nat Hazards, 56(1): 299–320. Pantha, B. R., Yatabe, R., Bhandary, N.P. (2010), GIS-based highway maintenance prioritization model: an integrated approach for highway maintenance in Nepal Mountains. J Transp Geogr, 18(3): 426–433.

Gilard, O., Givone, P. (1997), Flood risk management: new concepts and methods for objective negotiations, edited by: Leavesley, G., Lins, H., Nobilis, F., Parker, R., Schneider, V. and van der Ven, F., Destructive water: water-caused natural disasters, their abatement and control, IAHS Press, Oxfordshire, 145–155.

Gerrard, J., Gardner, R.A.M. (2000), Relationships between rainfall and landsliding in the Middle Hills, Nepal. Norsk geogr. Tidsskr. 54, 74–81.

Guzzetti, F., Carrara, A., Cardinali, M., Reichenbach, P. (1999), Landslide hazard evaluation: an aid to a sustainable development. Geomorphology, 31: 181-216.

Guzzetti, F. (2005), Landslide Hazard and Risk Assessment. PhD Thesis, Mathematics-Scientific Faculty, University of Bonn, Bonn, Germany, 389 pp.

Guzzetti, F., Peruccacci, S., Rossi, M., Stark, C.P. (2008a), The rainfall intensity–duration control of shallow landslides and debris flows: an update Landslides, Volume 5, Issue 1, pp 3-17.

Guzzetti, F., Reichenbach, P., Ardizzone, F., Cardinali, M., Galli, M. (2006), Estimating the quality of landslide susceptibility models. Geomorphology 81, 166–184.

Guzzetti, F., Ardizzone, F., Cardinali, M., Galli, M., Reichenbach, P. (2008b), Distribution of landslides in the Upper Tiber River basin, central Italy. Geomorphology 96, 105–122.

Heinimann, H.R. (1998), Methoden zur Analyse und Bewertung von Naturgefahren, Bundesamt f¨ur Umwelt, Wald und Landschaft (BUWAL), 85, 247 pp.

Holmgren, P. (1994), Multiple flow direction algorithms for runoff modelling in grid based elevation models: An empirical evaluation, Hydrol. Process., 8, 327–334.

Horton, P., Jaboyedoff, M., Rudaz, B., Zimmermann, M. (2013), Flow-R, a model for susceptibility mapping of debris flows and other gravitational hazards at a regional scale, Nat. Hazards Earth Syst. Sci.,13, pp 869-885.

Horton, P., Jaboyedoff, M., Bardou, E. (2008), Debris flow susceptibility mapping at a regional scale, in: Proceedings of the 4th Canadian Conference on Geohazards, edited by: Locat, J., Perret, D., Turmel, D., Demers, D., and Leroueil, S., Qu´ebec, Canada, 20–24 May pp 339–406.

Hufschmidt, G., Crozier, M., Glade, T. (2005), Evolution of natural risk: research framework and perspectives, Natural Hazards and Earth System Sciences, 5, 375–387.

IUGS (International Union of Geological Sciences) (1997), Quantitative risk assessment for slopes and landslides – the state of the art, edited by Cruden, D. and Fell, R.: Landslide Risk Assessment., Proc. of the International Workshop on Landslide Risk Assessment – Honolulu, Hawaii, USA, 19–21 February 1997, Balkema, Rotterdam, 3–12.

Kates, R. (1985), The interaction of climate and society, edited by: Kates, R., Ausubel, J. and Berberian, M., Climate impact assessment, Wiley, New York, 3–36, 1985.

Kaynia, A.M., Papathoma-Kole, M., Neuhauser, B., Ratzinger, K., Wenzel, H., Medinacetina, Z. (2008), Probabilistic assessment of vulnerability to landslide: Application to the village of Lichtenstein, Baden-Württemberg, Germany. Engineering Geology, 101: 33-48.

Kayastha, P., De Smedt, F. (2009), Regional slope instability zonation using GIS technique in Dhading, Central Nepal. In: Malet J P, Remaître A, Boggard T, eds. Landslide Processes: From Geomorphologic Mapping to Dynamic Modelling, CERG, France, 303–309.

Kayastha, P., Dhital, M.R., Smedt, F.D. (2013), Evaluation and comparison of GIS based Landslide Susceptibility Mapping Procedures in Kulekhani Watershhed, Nepal. Jurnal of Gelogical Society of India, v 81, 219-231.

Kayastha, P., Dhital, M.R., Smedt, F.D. (2012), Landslide Susceptibility mapping using the weight of evidence method in the Tinau Watershed, Nepal. Nat Hazards 63:479-498.

Kayastha, P., De Smedt, F., Dhital, M.R. (2010), GIS based landslide susceptibility assessment in Nepal Himalaya: a comparison of heuristic and statistical bivariate analysis. In: Malet J P, Glade T, Casagli N, eds. Mountain Risks: Bringing Science to Society. CERG Editions, 121–128.

Ko Ko, C., Flentje, P., Chowdhury, R. (2003), Quantitative landslide hazard and risk assessment: a case study. Quarterly Journal of Engineering Geology and Hydrogeology 36, 261–272.

Leone, F., Asté, J.-P., Leroi, E. (1996), L'évaluation de la vulnérabilité aux mouvements du terrain: Pour une meilleure quantification du risque, Revue de Géographie Alpine, 84, 35–46.

Li, Z., Nadim, Farrokh., Huang, H. Uzielli, M., Lacasse, S. (2010), Quantitative vulnerability estimation for scenario-based landslide hazards Landslides 7: 125–134.

Liam Finn, W.D. (1993), Geotechnical aspects of the estimation and mitigation of earthquake risk. Pages 35–77 in B.E. Tucker, M. Erdik and C.N. Hwang (eds.) Issues in urban earthquake risk, Kluwer Academic Publishers, Dordrecht.

Liu, X., Lei, J. (2003), A method for assessing regional debris flow risk: an application in Zhaotong of Yunnan province (SW China). Geomorphology, 52: 181-191.

Liu, X., Yue, Z.Q., Tham, L.G., Lee, C.F. (2002), Empirical assessment of debries flow risk on a regional scale in Yunnan province, southwestern China. Environmental management, 30: 249-264.

Liverman, D. (1990), Vulnerability to global environmental change, edited by: Kasperson, R., Dow, K., Golding, D. and Kasperson, J., Understanding global environmental change: the contributions of risk analysis and management, Clark University, Worcester, 27–44.

Mitchell, J. (1989), Hazards research, edited by: Gaile, G. and Willmott, C., Geography in America, Merill, Colombus, 410–424, 1989.

Panizza, M. (1996), Environmental geomorphology. Elsevier, Amsterdam 267 p.

Pantha, B.R., Yatabe, R., Bhandary, N.P. (2010), GIS-based highway maintenance prioritization model: an integrated approach for highway maintenance in Nepal Mountains. J Transp Geogr, 18(3): 426–433.

Poudyal, C.P., Chang, C., Oh, H., Lee, S. (2010), Landslide susceptibility maps comparing frequency ratio and artificial neural networks: a case study from the Nepal Himalaya. Environ Earth Sci, 61(5), 1049–1064.

Perla, R., Cheng, T.T., McClung, D.M. (1980), A two-parameter model of snow-avalanche motion, J. Glaciol., 26, 197–207.

Petak, W., Atkisson, A. (1991), Natural hazard risk assessment and public policy, Springer, New York, 1982.

Petley, D., Hearn, GJ., Hart, A. (2007), Trends in landslide occurrence in Nepal. Natural Hazards, 43, 23-44.

Phoon, K.K. (2004), Risk and vulnerability for geohazards vulnerability in relation to risk management of natural hazards. ICG Report 2004-2-3, Oslo.

Pijawka, K., Radwan, A. (1985), The transportation of hazardous materials: risk assessment and hazard management, Dangerous Properties of Industrial Materials Report, September/October, 2–11.

Ray, R.L, Smedt De, F. (2009), Slope stability analysis on a regional scale using GIS: a case study from Dhading, Nepal. *Environ Geol*, 57(7): 1603–1611.

Rautela, P., Lakhera, R. (2000), Landslide risk analysis between Giri and Tons Rivers in Himachal Himalaya (India), International Journal of Applied Earth Observation and Geoinformation, 2, 153–160.

Reid, L.M, Page M.J. (2003), Magnitude and frequency of landsliding in a large New Zealand catchment Geomorphology Volume 49, Issues 1–2, 1 January 2003, Pages 71–88Rickenmann, D. (1999), Empirical relationships for debris flows, Nat. Hazards, 19, 47–77.

Rickenmann, D., Zimmermann, M. (1993), The 1987 debris flows in Switzerland: documentation and analysis, Geomorphology 8, 175–189.

Roberds, W. (2005), Estimating temporal and spatial variability and vulnerability. Landslide risk management. Edit by Hunger, Fell, Couture and Eberhardt. Taylor and Francis group, London. pp. 129-157.

Roberds, W.J., Ho, K., Leung, K.W. (1997), An integrated methodology for risk assessment and risk management for development below potential natural terrain landslides, In: Cruden, D.M., Fell, R. (Eds.), Landslide risk assessment, Proceedings of the International Workshop on Landslide Risk Assessment, Honolulu, 19–21 February 1997. Rotterdam, Balkema, pp. 333–346.

Smith, K. (2001), Environmental hazards, Routledge, London, 2001.

Sharma, R.H., Shakya, N.M. (2008), Rain induced shallow landslide hazard assessment for ungauged catchments, Hydrogeol J, 16(5):871–877.

Susman, P., O'Keefe, P., Wisner, B. (1983), Global disasters, a radical interpretation. In Interpretations of Calamity from the Viewpoint of Human Ecology, ed. K. Hewitt, 263-283. Boston, MA: Allen and Unwin.

Thapa, P.B., Dhital, M.R. (2000), Landslide and debris flows of 19–21 July 1993 in the Agra Khola watershed of central Nepal. J Nepal Geol Soc, 21: 5–20.

UNISDR (2016), the united nations office for disaster risk reduction, web resources, (http://www.unisdr.org/we/inform/terminology).

UNDP (2004), United Nations Development Program, A Human development report 2004. United Nations, New York, 299pp.

United Nations Disaster Relief Organization (UNDRO) (1991), Mitigating Natural Disasters: Phenomena, Effects and Options: A Manual for Policy makers and Planners. New York: United Nations.

UNDRO (1991), Mitigation, Natural Disasters: Phenomena, Effects and Options. UN New York. Cutter, S.L. (1993), Living with risk: The geography of Technological Hazard. New York: Edward Arnold.

UNDRO (1982), Natural disasters and vulnerability analysis, Office of the United Nations Disaster Relief Co-ordinator, Geneva.

Uzielli, M., Nadim, F., Lacasse, S., Kaynia, A.M. (2008), A conceptual framework for quantitative estimation of physical vulnerability to landslides Engineering Geology 102 (2008) 251–256.

Van Asch, T., Corominas, J., Greiving, S., Malet, J.-P., Sterlacchini, S. (2014), Mountain Risks: From Prediction to Management and Governance (http://www.springer.com/series/6362).

Van Westen, C.J., Van Asch, T.W.J., Soeters, R. (2005), Landslide hazard and risk zonation; why is it still so difficult? Bulletin of Engineering geology and the Environment 65 (2), 167–184.

Van der Geest, K., Schindler, M. (2016), loss and damage from a catastrophic landslide in Nepal, Nat. Hazards Earth syst. Sci. Brief communication. Recent landslides in Nepal Landslide Nat. Hazards Earth Syst. Sci. Discuss., Nat. Hazards Earth Syst. Sci.

Varnes, D.J, IAEG Commission on landsides and other Mass Movement (1984), Landslide hazard zonation: a review of principles and practice. The UNESCO Press, Paris, 63pp.

White, P., Pelling, M., Sen, K., Seddon, D., Russell, S., Few, R. (2005), Disaster risk reduction. A development concern, DFID.

Weichselgartner, J., Bertens, J. (2000), Natural disasters: acts of God, nature or society, edited by: Brebbia, C., Risk Analysis II, WIT Press, Southampton, 3–12.

Westen, C.J., Van Asch, T.W.J., Soeter, R. (2006), Landslide hazard and risk zonation why is still so difficult? Bulletin Engineering geology Environment, 65: 167-184.

Wisner, B., Blaikie, P., Cannon, T., Davis, I.: At risk, Routledge, London, 2004.

Wong, H.N. (2005), Landslide risk assessment for individual facilities. In: Hungr, O., Fell, R., Couture, R., Eberhardt, E. (Eds.), Landslide risk management, Proceedings of the International Conference on Landslide Risk Management, Vancouver, 31 May–3, June 2005. Taylor & Francis, London, pp. 237–296.

Wong, H.N., Ho K.K.S., Chan Y.C. (1997), Assessment of consequences of landslides. Cruden DM and Fell R (Eds.) Landslide risk assessment - Proceedings of the Workshop on Landslide Risk Assessment, Honolulu, Hawaii, USA, 19-21 February 1997. Rotterdam, A.A. Balkema:111-49.

Yagi, H. (2001), Landslide study using aerial photographs, Landslide Hazard Mitigation in the Hindu Kush-Himalayas. In: Tianchi L, Chalise SR, and Upreti BN (eds) Landslide hazard mitigation in the Hindu-Kush Himalayas, ICIMOD, Nepal, 79.

Yagi, H., Nakamura, S. (1995), Hazard mapping on large scale landslides in the lower Nepal Himalayas. In: Proceedings of international seminar on water induced disasters (ISWID-1995), DPTC-JICA, Kathmandu, Nepal, 162-168.

Zimmermann, M., Mani, P., Gamma, P. (1997), Murganggefahr und Klima¨anderung – ein GIS-basierter Ansatz, NFP 31 Schlussbericht, Hochschulverlag an der ETH, Z¨urich, 1997 (in German).

Chapter 3: Characterization of the study area

3.1   Introduction

The Mountainous region of Nepal was chosen as a study area for this research. The study watershed, as shown in Figure 3.1, is about centrally located and representative of the geographical and climatic region of Nepal's Mountains. The watershed is connected through the Tribhuvan Highway in the Makawanpur District of Nepal. The highway distance is about 57 km from Kathmandu, the capital city of Nepal. The altitude and mean temperature in these mountains increase from north to south, and the annual average rainfall reduces from east to west. The study area is a medium-sized watershed, which consists of approximately 124 km^2 drainage area (Figures, 3.1-3.2). The watershed is a sub-basin of the Bagmati River, which has an urban watershed including the entire Kathmandu valley. The study watershed is divided into eight Village Development Committees (VDC). A VDC is a small political unit similar to a county, in which field-level government offices are located.
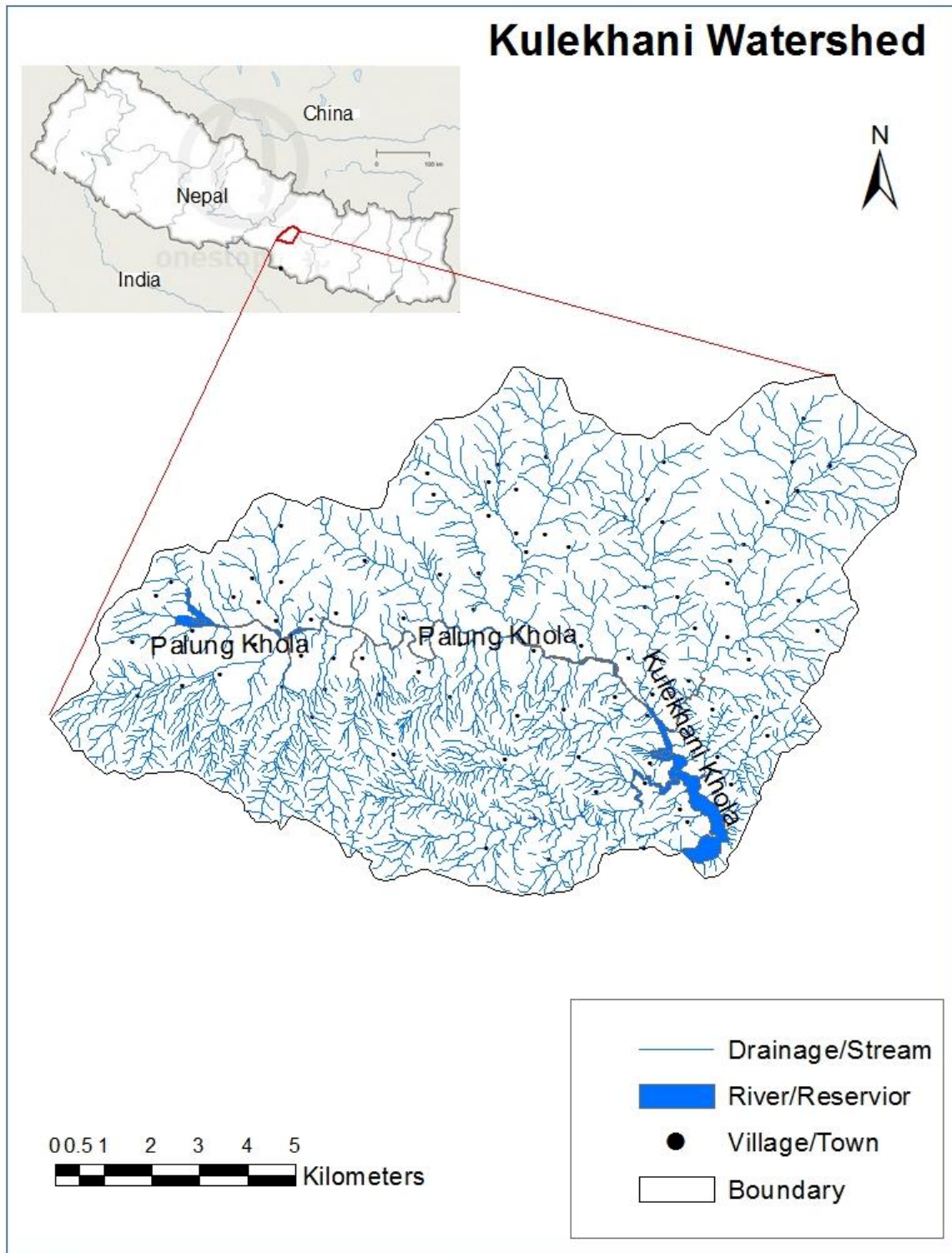
Figure 3.1: Location of the study watershed.

3.2   Geographical and geomorphological characteristics

The study watershed is located within the area bounded by latitude 27°35'04"N to 27°41'00"N and longitude 85°02'22" to 85°12'8"E. The elevation ranges from approximately 1520 to 2600 m (Regmi 2002, Dhital 2003) above mean sea level (msl) (Figure 3.2).
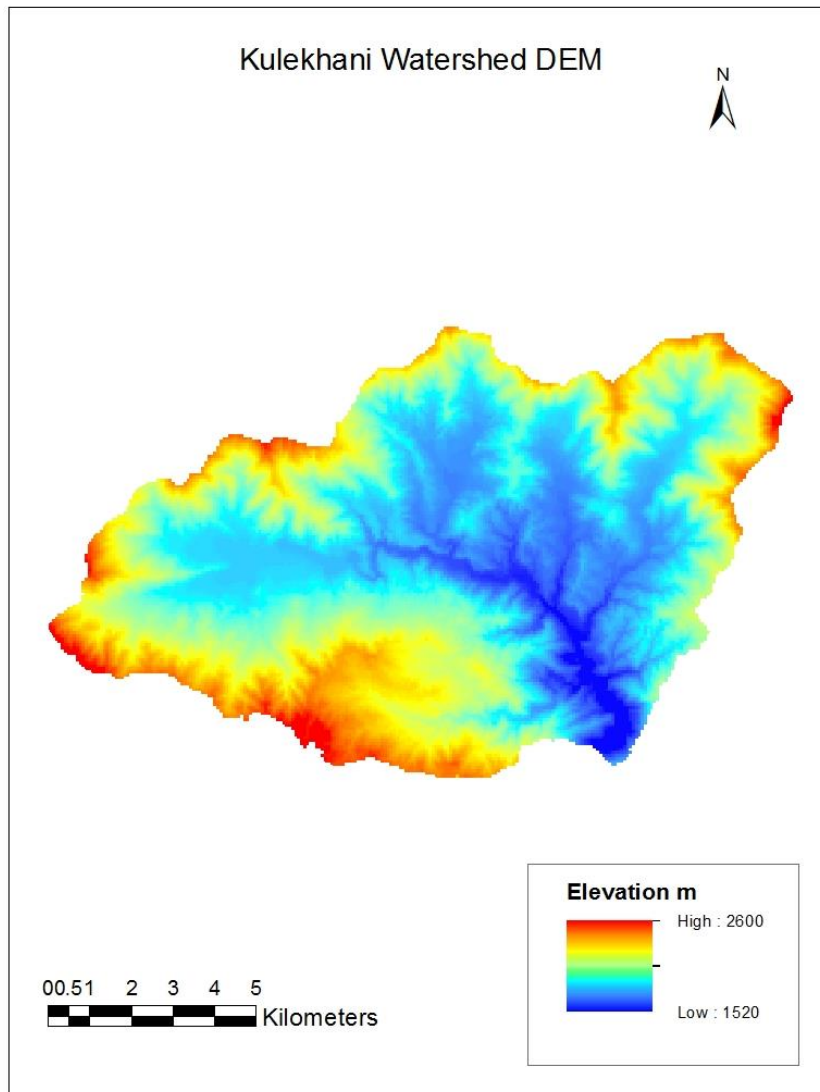
Figure 3.2: Digital Elevation Model (DEM) for the study watershed, Kulekhani.

The main river in the watershed is the Palung Khola, which merges to become the Kulekhani Khola further downstream (Figure 3.1). The major tributaries of the

Kulekhani watershed are Palung Khola (Khola means creek, brook, or stream in Nepali), Gharti Khola, Phedigaon Khola, Bhangkhoria Khola, Kitini Khola, Andheri Khola, Tistung Khola, Chitlang Khola, Chalkhu Khola, Bisingkhel Khola, Setikhani Khola, and Thado Khola.

3.3   Geological and geotechnical characteristics

Nepal has diverse geological and geomorphic landscapes in its south-to-north narrow, and east-to-west wide mountains stretches. Nepal's mountains are comparatively young and fragile, compared to other parts of the world (Upreti 2001). Most of the northern part of the country is covered by the high Himalayas, and the southern part with an alluvial plain. These mountains are rising every year from regional tectonic movements (Bettinelli et al. 2006). The movement of the Indian plate under the Tibetan plate is continuing, and its velocity is 1 to 5 cm per year (Bettinelli et al. 2006, Jackson and Bilhan 1994, Pandey et al. 1995, Bilham et al. 1997). This geological process continues lifting the Nepalese mountains by the same amount every year. The highest mountain, Mount Everest, is 8848 m high, and the low-lying plain near the mountain is only 69 m above msl. These two locations are within 200 km of each other. From south to north, Nepal is divided into five tectonic zones: the southern-most plain area, Siwalik Zone, Lesser Himalaya, Higher Himalayan and Tibetan-Tethys Himalayan, and the northern-most mountains (Dhital 2016, Gansser 1964, Hagen 1969). These zones are separated with faults, such as the Main Frontal Thrust for the Siwalik and plain area, the Main Boundary Thrust for the Siwalik and the Lesser Himalayan Zone, the Main Central Thrust for the Higher Himalayan Zone and Lesser Himalayan Zone. The South Tibetan Detachment System is between the Higher Himalayan Zone and the Tibetan-Tethys Himalayan Zone. The study watershed is in between the Main Central Thrust and the Main Boundary Thrust, within the Lesser Himalayas zone.

Hegen (1969) studied the geographical and geological features of Nepal mountains for many years in the 1950s and 1960s. He classified eight geomorphologic regions in Nepal: "1) Terai (the northern edge of the Indo-

Gangetic plain, southern outskirts of Nepal), 2) Siwalik (Churia) Range, 3) Dun Valleys, 4) Mahabharat Range, 5) Midlands, 6) Fore Himalaya, 7) Higher Himalaya, and 8) Inner and Trans Himalayan Valleys". The study watershed is located in the Mahabharat Range (Lesser Himalayas), between the Main Central Thrust north and Main Boundary Thrust south. The Mahabhart Range is made up of Phyllite, schist, slate, quartzite, limestone, granite, and gneiss ranging in age from the Paleozoic era to the Precambrian period (Upreti 1999, 2001, Dhital 2016).

The geology of the watershed is shown in Figure 3.3 (Dhital 2003, Kayastha et al. 2012, Regmi 2002, Lamichhanne 2000, Dhital 2015). The bed rocks in the study area are slate, phyllite, schist, quartzite, marble, and granite as they are located in the Mahabharat Range. The formation of bedrock in the watershed area mostly belongs to the Bhimphedi Group and Phulchauki Group of the Kathmandu Complex (Stocklin 1981). The Bhimphedi Group consists of Chisapani Quartzite (a fine-grained quartzite), Kulekhani formation (consists of bands of schist and quartzite), and Markhu formation (alternative layer of marbles and schist). The Phulchauki Group consists of Tistune Formation, Sopyang Formation, and Chandragiri limestone. The named Tistung formation is slate and phyllite; the Sopyang Formation is slate and limestone interbedded; and Chandragiri is a single unit of limestone bedrock. The outcrop granite is highly weathered, and changed into grey-colored residual soils in the southern part of the watershed.
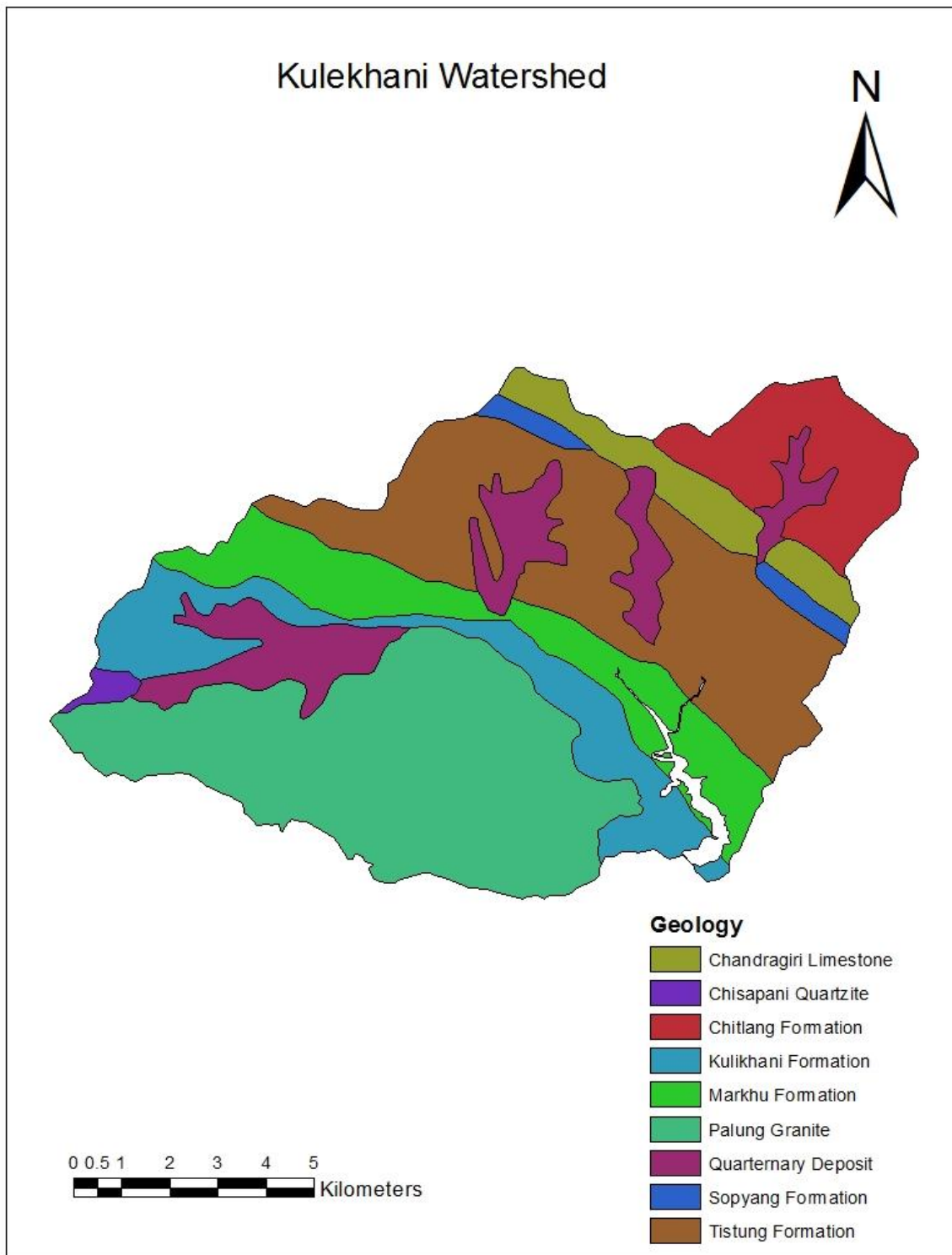
Figure 3.3: Geology of the study watershed (after Stöcklin and Bhattarai 1977, Stöcklin 1980, Regmi 2002 and Kayastha et al. 2013).

The surficial cover in the watershed is colluvial, residual, and alluvial soils. Kayastha et al. (2012), Dhital (2003), Regmi (2002), Lamichhanne (2000), and

Dhital (2016, 2003, 1993) studied details of the surface and subsurface profile in the study region. The main part of the watershed is covered with colluvium, which originates from erosion, wind drifting, and landslides of residual soils. Colluvium consists of an unsorted matrix of soil, rock fragments, and gravel. It is found in moderately-sloped mid-hills and foot-hills of mountains. Colluvium is observed up to 2500 m altitude in some locations. The residual soil is mainly from weathered granite. It is located at higher altitudes and in the southern part of the watershed where granite is underlain. The low-lying river valley area is mostly covered with alluvial, and sparsely with fluvial, deposits. Most valleys formed along the Palung Khola and its major tributaries Kiteni Khola, Bisingkhel Khola, and Thado Khola have alluvial deposits. Detailed information on soil types in the area is available in Lamichhanne (2000).

The steep slope consists of bedrock outcrops or compacted overburden soil, but comparatively loose deposits in mildly-sloping hills in the watershed. Hasegawa et al. (2009) studied geotechnical properties of the predominant soil types in the highway corridor in western Nepal, and found peak internal frictional angles of 22° to 36° and, residual angles of 22° to 34° for slip materials along the landslide.

One previous landslide location was chosen for the geotechnical investigations of this study site to obtain relevant geotechnical data (e.g., cohesion and friction angle, representing soil strength parameters). The cohesion and friction angles were obtained from direct shear testing (IS:2720-1985). On-site infiltration tests were conducted on two boreholes for infiltration capacity and permeability of in situ soils. The initial moisture content, saturated moisture content, saturated unit weight, dry unit weight, specific gravity, void ratio, grain size distribution, and cohesion and friction angle were obtained from collected samples. The tested results are shown in Tables 3.1, 3.2, and 3.3.

Table 3.1 Permeability of in situ soils.

Test Hole	Applied volume of water (cm³/sec)	Diameter (mm)	Constant head (cm)	Flow rate cm³/sec	Permeability cm/sec
1	4	101.6	400	75.76	0.00678
2	3	101.6	300	19.84	0.00237
3	3	101.6	300	36.23	0.004323
4	4	101.6	400	19.84	0.00177
				Average	0.00381

Table 3.2 Shear strength parameters of the soils tested.

Borehole	Depth (m)	Effective Cohesion (kPa)	Friction angle Ø' (degree)	Water content (%)	Classification	Bulk density (gm/cm³)	Specific gravity
BH 1	0–1.5	15	30	23.03	ML, gravelly silt with sand.	1.79	2.70
	1.5–3.0	13	29	20.49	SM, silty sand with gravel.	1.81	2.65
	3.0–4.0	17	24	21.53	ML, gravelly silt with sand.	1.80	2.67
BH 2	0–1.5	15	29	21.31	SM, silty sand with gravel.	1.83	2.68
	1.5–3.0	19	25	18.21	ML, sandy silt with gravel.	1.86	2.63
	3.0–4.0	17	27	21.50	GM, silty gravel with sand.	–	2.70
BH 3	0–1.5	10	25	23.58	ML, sandy silt with gravel.	1.82	2.65
	1.5–3.0	5	32	24.49	ML, gravelly silt with sand.	1.84	2.69
	3.0–4.0	11	30	19.58	GM, silty gravel with sand.	–	2.67
BH 4	0–1.5	15	27	22.75	GM, gravelly silt with sand.	1.85	2.65
	1.5–3.0	17	26	21.15	GM, gravelly silt with sand.	1.84	2.61
	3.0–4.0	11	30	22.63	SM, silty sand with gravel.	1.83	2.48

Table 3.3 Derived parameters of the soils tested (continued).

Borehole	Depth (m)	Void ratio,e	Porosity (n)	Volumetric water, Θ (%)	Degree of saturation (%)	Gravimetric water content	Dry density, ρd (gm/cm³)	Moisture content residual (%)
BH 1	0–1.5	0.86	0.46	23.03	72.63	0.32	1.45	4.00
	1.5–3.0	0.76	0.43	20.49	71.43	0.29	1.51	5.00
	3.0–4.0	0.81	0.45	21.53	71.07	0.30	1.48	5.00
BH 2	0–1.5	0.70	0.41	21.31	68.22	0.27	1.55	4.00
	1.5–3.0	0.76	0.43	18.21	76.00	0.28	1.53	2.00
BH 3	0–1.5	0.84	0.46	23.58	78.53	0.31	1.47	4.00
	1.5–3.0	0.74	0.42	24.49	70.99	0.28	1.54	4.00
BH 4	0–1.5	0.76	0.43	22.75	79.70	0.29	1.51	5.00
	1.5–3.0	0.72	0.42	21.15	77.02	0.27	1.52	4.00
	3.0–4.0	0.66	0.40	22.63	85.30	0.27	1.49	2.00

3.4   Climatic conditions

Monsoon wind is a major factor for weather patterns in the Nepalese mountains (Upreti 1999, 2001 Nelson 1980). Moist wind flows from the Indian Ocean in the south, to the north and northwest and develop monsoon rainfall. The distribution of annual average rainfall is higher in the eastern than the western region of the mountains. The study area, Kulikhani watershed, is located in the central region where the rainfall received yearly is representative of the annual average of the country. Rainfall data for this study are collected from previous studies (Kayastha et al. 2013) and the Department of Hydrology and Meteorology, Nepal. Rainfall recording stations, their locations, and maximum and average recorded rainfall are shown in Table 3.4. The Daman and Markhu rainfall gauge stations are located within the study watershed. One-day to seven-day maximum cumulative rainfalls are analyzed from 1980 to 2013 and are shown in Table 3.5. The recorded daily maximum rainfall at the station shows that the maximum daily recorded rainfall from 1980 to 2013 is 442.5 mm in Chisapani Ghadi. Similarly, in Daman, Markhu,

and Thankot stations, the daily maximum rainfall recorded 373.2, 385.6, and 300.1 mm, respectively.

Table 3.4 Rainfall record from four rain gauge stations near and within the Kulekhani watershed.

Station No.	Station Name	Altitude	Longitude	Latitude	Max. Daily Rainfall (mm)	Avg. Annual Rainfall (mm)
904	Chisapani Gadhi	1706	85° 7' 58.8"	27° 33' 0"	442	2227
905	Daman	2314	85° 4' 58.8"	27° 36' 0"	373	1725
915	Markhu	1530	85° 9' 0"	27° 36' 57.6"	385	1475
1015	Thankot	1630	85° 12' 0"	27° 40' 58.8"	300	1826

Table 3.5 shows one- to five-day cumulative maximum rainfall events for four gauge stations within the watershed, Chisapani Ghadi, Daman, Markhu, and Thankot. The maximum one-day rainfall was in July 20, 1993. However, the two-day cumulative maximum rainfall is highest on the same date in Markhu, but a different date in other stations. In Daman, the cumulative rainfall event other than the one-day rainfall is higher around July 22, 2002. The highest record of 5-days cumulative rainfall in Daman is 730.00 mm. Chisapani Ghadi gauge station recorded the maximum five-day cumulative rainfall of 891.1 mm, and about 40% of the annual average rainfall at the station from July 21 to 25, 2002 alone. Table 3.6 shows the estimated rainfall and duration combination of Chisapani Ghadi, which has the highest recorded rainfall. Rainfall is recorded once a day for 24 hours duration. The recorded rainfall within 24 hours may not be distributed equally over the entire period. The total 24 hours' rainfall may be fall in 7.02 hours and 48 hours' rainfall in 10.36 hours period immediately before and after the recorded point of time. Therefore, 7 days recorded cumulative rainfall of 909.4 mm may have probability to be in 144.06 hours period. This combination of estimated cumulative rainfall and duration from one to seven days' recorded rainfall is given in Table 3.6.

Table 3.5 Cumulative rainfall record for four rain gauge stations from 1980 to 2013 in Kulekhani watershed.

Max Rainfall	Chisapani Gadhi		Daman		Markhu		Thankot	
	Date	mm	Date	mm	Date	mm	Date	mm
One Day	July 23, 2002	442.5	July 20,1993	373.2	July 20,1993	381	July 25, 2002	300
Two Day	July 23, 24, 2002	652.6	July 22, 23, 2002	513	July 20,21, 1993	429	July 24, 25, 2002	388
Three Day	July 22, 23, 24, 2002	800.8	July 22, 23, 24, 2002	636	July 22, 23, 24, 2002	519	July 24, 25, 26, 2002	450
Four Day	July 22, 23, 24, 25, 2002	868.8	July 22, 23, 24, 25, 2002	715	July 22, 23, 24, 25, 2002	556	July 24, 25, 26, 27,2002	491
Five Day	July 21, 22, 23, 24, 25, 2002	891.1	July21, 22, 23, 24, 25, 2002	730	July 21, 22, 23, 24, 25, 2002	561	July 23, 24, 25, 26, 27,2002	520

Table 3.6 Estimated cumulative rainfall at Chisapani Ghadi rain gauge station.

Rainfall Recorded in Chisapani Gadhi					
Total Recorded Duration	Date	mm	Min assumed Duration (hours)	Daily Rainfall (mm)	Assumed, mm/hour
One Day	July 23, 2002	442.5	7.02	441	63
Two Day	July 23, 24, 2002	652.6	10.36	443 210	63
Three Day	July 22, 23, 24, 2002	800.8	29.68	148 443 210	27
Four Day	July 22, 23, 24, 25, 2002	868.8	51.43	148 443 210 68	17
Five Day	July 21, 22, 23, 24, 25, 2002	891.1	73.43	22 148 443 210 68	12
Six Day	July 20, 21, 22, 23, 24, 25, 2002	905.2	120.22	14 22 148 443 210 68	8
Seven Day	July 21, 22, 23, 24, 25, 26, 2002	909.4	144.06	14 22 148 443 210 68 4	6

Most of the rainfall gauge stations recorded 24 hours rainfall in the study watershed, however the effect of short-duration high-intensity rainfall needs to be understood. For rainfall intensity estimation of less than 24 hours' duration, Shakya (2002) proposed Equation [3.1]. From Equation [3.1], rainfall for any duration can be estimated from 24 hours' given rainfall, if a shorter duration of estimated rainfall is necessary for analysis.

$$\left| \frac{P_t}{P_{24}} \right| = \left[\frac{\sin \pi t}{48} \right]^{0.4727} \qquad [3.1]$$

where, P_t is rainfall in a specified time t (in hours), P_{24} is the total rainfall in 24 hours. Usually, rainfall data are available for a given 24-hour interval, and the amount of rainfall in t hours can be obtained using this model. This relation is used for finding rainfall for a few hours from a given 24-hour rainfall record.

3.5 Land use pattern

The land use pattern in the study watershed is shown in Figure 3.4. Table 3.7 shows types of land areas as compared to the total land areas in the watershed. The watershed is located in the Makawanpur district, which has 239,076 hectares (ha) of total lands includes 167,453 ha forest, 40,842 ha agricultural farm, 18,815 ha non-agricultural land, 3,136 ha pasture and 8,830 ha is used for other purposes. The study watershed is located in the Northern part of the Makawanpur district which is famous for different types of herbs. Almost 120 types of herbal plants can be found in this area. Also, Sisno, Lokta, Bamboo, Amliso etc. are the other important plant of this area (Pokharel 2015). The land cover, elevation zone, geography and ecological zone of Nepal mountains are given in Appendix A.

Table 3.7 Watershed land type.

S.N.	Type of Land	Area (m^2)	Percent of Total Watershed Area
1	Building area or developed land	11386.6	0.01
2	Forest Cutting for Cultivation	73862.8	0.06
3	Cultivation	60985000	49.08
4	Forest	51459500	41.42
5	Nursery	240191	0.19
6	Grass	109357	0.09
7	Bush	9267890	7.46
8	Swamp	586965	0.47
9	Barren	238751	0.19
10	Water body	1280040	1.03
	Total	124252943.4	100
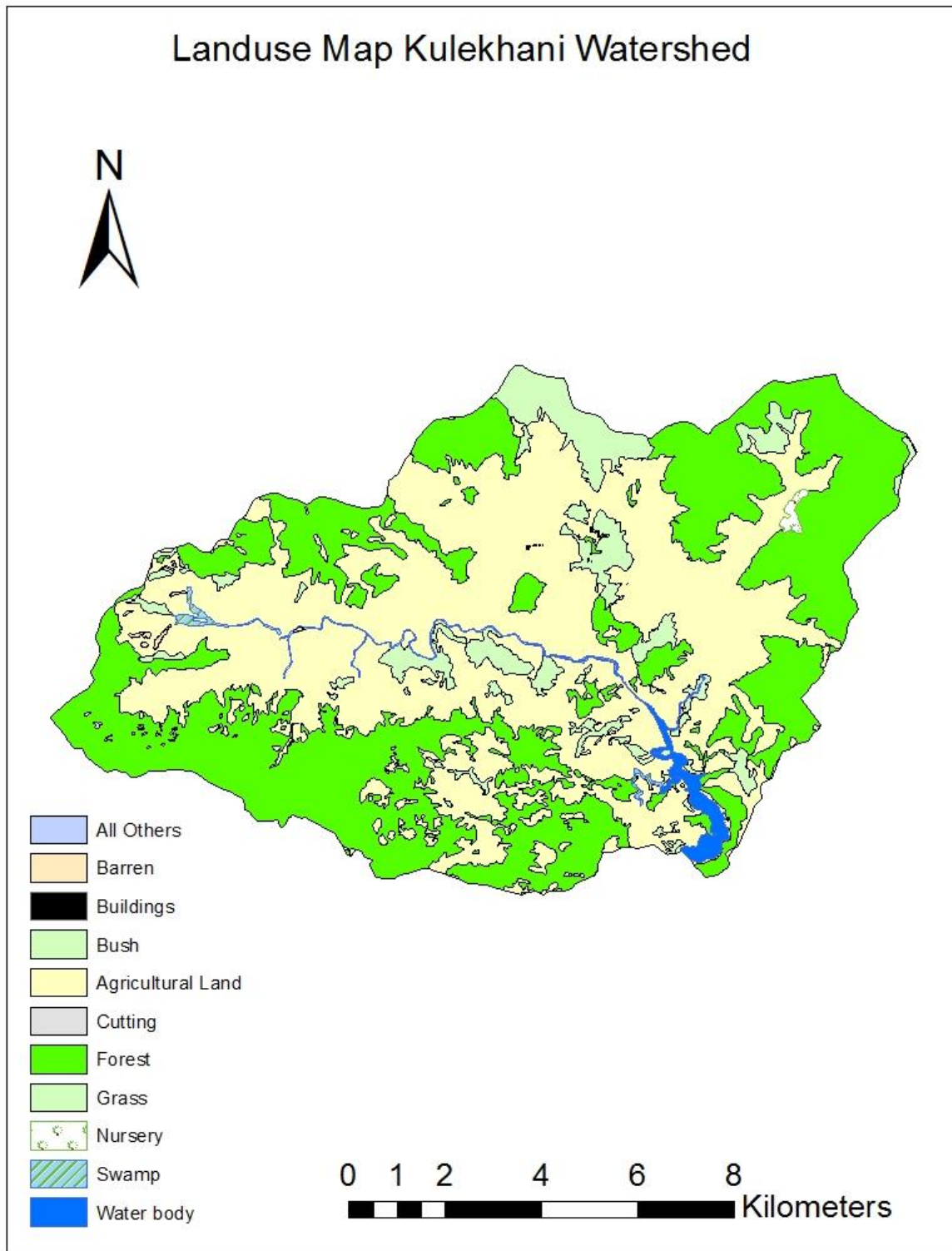
Figure 3.4: Land use patterns in the study watershed (Department of Topography, Nepal).

3.6   Conclusions

The study watershed is located in a mountainous region of Nepal covering a 124 km^2 drainage area at altitudes from 1500 to 2620 m above mean sea level. The bedrock in the area is slate, phyllite, limestone, granite marbles, schist, quartzite etc. The predominant overburden soil in the watershed is residual, colluvial, and alluvial. The watershed is located centrally in mountainous Nepal, and is representative of the average rainfall and landside events from east to west. The watershed was devastated by high-intensity rainfall—540 mm within 24 hours— and a massive debris flow was initiated. This debris flow took many lives, damaged properties in the watershed, and caused flooding downstream. Data for landslide initiation, debris flow inundation, and hazard analysis require topography, soil characteristics, lithology, and the rainfall record. This information was gathered from the literature and from field investigation for the study watershed for landslide hazard modeling.

3.7   References

Bettinelli, P., Avouac, J.-P., Flouzat, M., Jouanne, F., Bollinger, L., Willis, P., Chitrakar, G. (2006), Plate motion of India and Interseismic strain in the Nepal Himalaya from GPS and DORIS measurements, J. Geod., 80, 567–589, https://doi.org/10.1007/s00190-006-0030-3.

Bilham, R., Larson, K., Freymueller, J., Jouanne, F., LeFort, P., Leturmy, P., Mugnier, J.L., Gamond, J.F., Glot, J.P., Martinod, J., Chaudury, N.L., Chitrakar, G.R., Gautam, U.P., Koirala, B.P., Pandey, M.R., Ranabhat, R., Sapkota, S.N., Shrestha, P.L., Thakuri, M.C., Timilsina, U.R., Tiwari, D.R., Vidal, G., Vigny, C., Galy, A., deVoogd, B. (1997), GPS measurements of present day convergence across the Nepal Himalaya. Nature 386, 61–64.

Caine, N. (1980), The Rainfall Intensity: Duration Control of Shallow Landslides and Debris Flows Geografiska Annaler. Series A, Physical Geography, Vol. 62, No. 1/2 (1980), pp. 23-27.

Dhital, M. R. (2016), Geology of the Nepal Himalaya: Regional Perspective of the Classic Collided Orogen Springer, ISBN 10: 3319352059 ISBN 13: 9783319352053.

Dhital, M.R. (2003), Causes and consequences of the 1993 debris flows and landslides in the Kulekhani watershed, central Nepal, Debris-flow Hazards Mitigation: Mechanics, Prediction and assessment, Rickenmann &Chen (eds) pp 1931-1943.

Dhital, M.R., Khanal, N., Thapa, K.B. (1993), The role of extreme weather events, mass movements, and land use changes in increasing natural hazards, A Report of the preliminary field assessment and workshop on causes of recent damage incurred in southcentral Nepal, July 19-20 1993. ICIMOD, Kathmandu, 123 pp.

Gansser A. (1964), Geology of the Himalayas. Interscience, New York, 289 pp.

Hagen, T. (1969), Report on the geological survey of Nepal preliminary reconnaissance. *Zürich Mémoires de la soc. Helvétique des sci. naturelles*, pp185.

Hasegawa S., Dahal, R.K., Yamanaka, M. Bhandari, N.P. Yatabe, R, Inagaki, H. (2009) Causes of large landslides in the Lesser Himalaya of central Nepal. *Environ Geol* 57:1423-1434.

Jackson M., Bilham R. (1994), Constraints on Himalayan deformation inferred from vertical velocity fields in Nepal and Tibet. Journal of Geophysical Research 99 (B7) 13897-13912.

Kayastha, P., Dhital, M.R., Smedt, F.D. (2013), Evaluation and comparison of GIS based landslide susceptibility mapping procedures in Kulekhani watershhed, Nepal. Jurnal of Gelogical Society of India, v 81, 219-231.

Kayastha, P., Dhital, M.R., Smedt, F.D. (2012), Landslide Susceptibility mapping using the weight of evidence method in the Tinau Watershed, Nepal. *Nat Hazards* 63:479-498.

Lamichhanne, S.P. (2000), Engineering geological watershed management studies in the Kulekhani watershed, M.Sc. Thesis, Tribhuvan, University, Nepal.

Nelson, D. Laban, P., Shrestha, B.D., Kandel, G.P. (1980), a reconnaissance inventory of the major ecological land units and their watershed condition in Nepal, Integrted Watershed management project, Dept. of Sol Conservation and Watershed Management, Min. of forests, Kathmandu Working Paper No. 17, pp 292.

Pandey, M.R., Tandukar, R.P., Avouac, J.P., Lave, J., Massot, J.P. (1995), Interseismic strain accumulation on the Himalayan crustal ramp (Nepal). Geophys. Res. Lett. 22, 751–754.

Regmi, M.K. (2002), Geology of Kulekhani watershed in central Nepal with special reference to landslides and weathering, M.Sc. Thesis, Tribhuvan University, Nepal.

Shakya, B. (2002), A new approach within hydrometerological technique for the estimation of average depth of probable maximum precipitation (PMP) over Nepal. In: Wu et al. (Ed0, Flood Defence 2002, Science press, New York Ltd., pp 599-606.

Stocklin, J., Bhattrai K.D. (1981), Geology of Kathmandu area and Central Mahabharat Range, Nepal Himalaya, United Nations Mineral Exploration Technical Report, UNDP/Nepal, page 61.

Upreti, B.N. (1999), An overview of the stratigraphy and tectonics of the Nepal Himalaya. J Asian Earth Sci 17:577–606.

Upreti, B.N. (2001), The physiography and geology of Nepal and their bearing on the landslide problem. Tianchi L., Chalise S.R., and Upreti B.N. (eds) Landslide hazard mitigation in the Hindu-Kush Himalayas, ICIMOD, Nepal, 31-49.

Chapter 4: Technical Paper 1 - GIS-based landslide (debris flow) susceptibility modeling in Kulekhani watershed, Nepal

Bhuwani Prasad Paudel, Mamadou Fall, Bahram Daneshfar

Abstract

Rainfall-induced landslides that change into debris flows and travel large distances are one of the treacherous natural calamities in mountainous areas in Nepal. The spatial distribution of the initial landslides that change into debris flow, on a watershed scale, is still an important area of study in this mountainous region. In this research, hydrologic and slope stability models are applied in GIS modeling to locate potential landslide areas for a given threshold rainfall in a mountainous watershed—Kulekhani, Nepal. Soil information from 73 locations within the watershed and a geotechnical investigation on one old landslide area are taken to determine the Soil Water Characteristics Curve (SWCC), friction angle, cohesion, and infiltration characteristics of subsurface soil. Rainfall intensity and subsurface soil infiltration capacity are used to identify the wetting front during threshold rainfall. This information is applied in the unsaturated slope stability model to find unstable locations in the study watershed in a GIS environment. The model is tested on a recorded 24-hour rainfall of 540 mm in the watershed, and potential landslide locations are obtained. The validation results show that there is a good agreement between the predicted and mapped landslides. Previously recommended rainfall thresholds for the region, 2 mm rainfall per hour for 100 hours, 6 mm per hour for 24 hours, and 12 mm per hour for 10 hours are also applied in the model and used to obtain potential landslide locations in the watershed. Among these, the threshold of 12 mm rainfall per hour for 10 hours does not produce any unstable locations within the watershed. Also, the effect of short duration–high intensity and long duration–low intensity rainfall on potential landslide initiation is studied, and the worst conditions in the watershed were found for higher intensity rainfall up to 63 mm per hour. The longer the duration of rainfall of an intensity close to 63 mm per hour, the higher the landslide susceptibility.

4.1   Introduction

Landslides are a treacherous natural hazard in mountainous areas. They take many lives and damage property every year in rugged hills in Nepal. Having a unique steep topography that is composed of relatively new and fragile mountains, and synchronized torrential monsoon rainfall, loss of lives and property every year is a serious threat in this region. Meeting the livelihood demands of the majority of 27 million people, approximately 83% of the land is covered with mountains, and conventional land use practices for farming in hilly areas are one of the factors that contribute to severe damage from landslides year after year. The records show that rainfall-induced shallow landslides that turn into debris flows have taken, on an average, 269 people's lives every year during the period of 1983 to 2016. A total of 9153 people lost their lives within this period (Ministry of Home, Nepal 2016). Landslide leads to flooding in the lower part of the mountains that killed on an average 729 people per year between 1971 to 2016. A characteristic of this growing problem is infrastructure development without consideration of any geology or topography, and no proper land use plan. Excavation on slopes or vertical cutting without taking precautions against slope distress, knowingly or unknowingly degrading existing vegetation cover, and localized and severe torrential rainfall in recent years are other reasons for the increase in this dangerous occurrence. The importance of a proper land use plan, educating people in appropriate land use for their livelihoods, and relocation of settlements to safer places are important ways for policy makers to cope with this problem. However, sufficient and interpretable information regarding mountainous land for appropriate use has not yet been developed to an applicable stage. This study will be a step forward in understanding the effects of physical changes to mountainous slopes during monsoon rainfall on instability and landslide initiation, and a step towards the development of a land use plan for appropriate practices in mountains and a resettlement strategy for policy users.

The importance of landslide studies for early warnings and saving lives and property was identified as early as the 1980s in Nepal (Caine, 1980, Caine and Mool 1982). However, due to the complexity of the problem, and a lack of

accessibility and resources for research and implementation, landslide study work has not moved forward at an appropriate pace. In the early 1990s, a severe debris flow occurred in central Nepal, and the importance of research into, and mitigation of, this hazard was realized by the society and the government. Research and remedial measures were also initiated after this event. As mentioned above, on average, 269 people have lost their lives annually due to landslides, but the number of deaths and property loss has escalated in recent years. Landslide and flooding destroyed about 5337 houses per year during the period from 1971 to 2014 (DWIDP 2017). A total of 2042 people have died due to landslides, including 388 due to flooding, within the period of 2000 to 2009 (K. C. 2013). Recently, in August 2014, a single landslide event killed 156 people in northern Nepal. The consequence of torrential-rainfall-triggered landslides that change into debris flows is further devastating. These events disturb large areas, and lead to blocked streams and rivers, and inundate valuable low-lying land in mountain regions. This effect causes loss of life and property, starting on the mountain slope and continuing to its base, which is known as the Terai in Nepal. This loss of life and property is an ongoing continuous process that occurs during every torrential monsoon rainfall.

Once landslide initiation and its impact on society and infrastructure were recognized as an important issue to address in order to mitigate hazards, landslides in the region have been studied by several authors, such as Deoja et al. (1991), Dhital et al. (1991), Dangol et al. (1993), Yagi and Nakamura (1995), Upreti and Dhital (1996), Wagner (1997), Dhital (2000, 2005), Gerrard and Gardner (2000), Chalise and Khanal (2001), Upreti (2001), Yagi (2001), Gabet et al. (2004), Dahal et al. (2006), Dahal and Hasegawa (2008), Dahal et al. (2008a, 2008b), Poudyal et al. (2010), Ghimire (2011), Bijukchhen et al. (2012), and Bhandary (2013). Recently, GIS-based landslide mapping in the Nepalese mountains, including rainfall and other factors, has been adopted by Dhakal et al. (1999), Thapa and Dhital (2000), Neaupane and Piantanakulchai (2006), Acharya et al. (2006), Sharma and Shakya (2008), Ray and De Smedt (2009), Poudyal et al. (2010), Dahal et al. (2012), Devekota et al. (2013), Kayasta (2009), Pantha et al. (2010), Poudyal et al. (2010), Bijukchhen et al. (2012), and Kayastha et al.

(2010, 2012, 2013). However, physical changes in the subsurface of mountains slopes during rainfall, and their effect on landslide initiation has not be addressed, and thus is yet to be understood for mountainous Nepal. Initially, slopes are unsaturated and stable in mountainous regions, but rainfall causes physical changes in subsurface soil and severe instability develops in specific locations during rainfall of particular intensity. These physical changes, such as saturation of subsurface soil, loss of apparent cohesion related to suction, increase in disturbing forces, and reduction in overall soil resistance are more severe in some locations during particular rainfall events, which require to identification.

Rainfall effects on mountain slopes in other regions have been studied by many researchers, such as Hsu et al. (2002), Chen et al. (2005, 2006), Fall et al. (2006), Tsai and Yang (2006), Salciarini et al. (2008), Muntohar and Liao (2009), Meyer et al. (2012), Park et al. (2013), Chiang et al. (2012), Kim et al. (2010), Tsai and Chiang (2013), and Enrico and Antonello (2012), Horton et al. (2013). Casadel et al. (2003) suggested that using a rainfall threshold coupled with a simple model to predict areas of instability is more practical than using a complex model, after analyzing rainfall landslides in a watershed in California.

The study of a GIS-based statistical approach considered previous landslide events and their spatial distribution as a base factor for the identification of future landslides. Rainfall intensity and duration periodically return, but landslide events and locations do not remain the same. In other words, landslides not necessarily occur in the same place where they occurred in previous periods. The relation of rainfall and landslides for a particular location of watershed depends on the physical changes on slopes during rainfall. Identification of the relation between rainfall and unstable locations is still to be understood in these mountains. The spatial distribution of initiated landslides due to physical changes from rainfall in light of unsaturated soil mechanics and GIS-based mapping on a watershed scale is the main objective of this research. The outcome of this research is to identify the phenomenon that makes a particular hill slope severely unstable for a given rainfall intensity and duration of rainfall, that will be applicable to landslide hazard analysis.

4.2. Study Area

The study watershed is Kulekhani, located about 30 km south of Kathmandu (the capital city of Nepal). This watershed is one of many sites severely devastated by a landslide event in 1993 (Dhital 2003). The 1993 landslide event caused the deaths of 1138 people in a single incident in Nepal, including the study area—the Kulekhani watershed. This event opened eyes to the requirement for research on landslide and debris flow to save the lives and property of mountain people. The study of landslides in the Kulekhani watershed can be found in Lamichanne (2000), Dhital et al. (1993), Dhital (2003), Dhakal et al. (1997, 1999, 2000), and Kayastha et al. (2013). The watershed experienced extreme rainfall on July 19 and 20, 1993, which triggered more than 300 landslides, most of which changed into debris flows. The landslide event caused the total recorded deaths of more than 1500 people in the watershed region (Dhital 2003).

4.2.1 Geographical Description

The watershed is connected through the Tribhuvan Highway (about 57 km from Kathmandu) in the Makawanpur District of Nepal (Figure 4.1). The study area is in a medium-sized watershed, which consists of a drainage area of approximately 124 km^2 (Figure 4.1- 4.2). The watershed is a sub basin of the Bagmati River, which directly crosses the Indo-Nepal border without merging with other big river systems. The elevation of the study area ranges approximately from 1500 to 2620 m (Regmi 2002, Dhital 2003) above sea level (Figure 4.2). This watershed is located within latitudes 27°35'04"N to 27°41'00"N and longitudes 85°02'22"E to 85°12'8"E. The entire watershed is divided into eight Village Development Committees (VDC). A VDC is a small political unit similar to a County, in which field-level government offices are located.

The main river in the watershed is Palung Khola, which merges to become Kulekhani Khola further downstream. The major tributaries of the Kulekhani watershed are Palung Khola (Khola means creek, brook, or stream in Nepali), Gharti Khola, Phedigaon Khola, Bhangkhoria Khola, Kitini Khola, Andheri Khola,
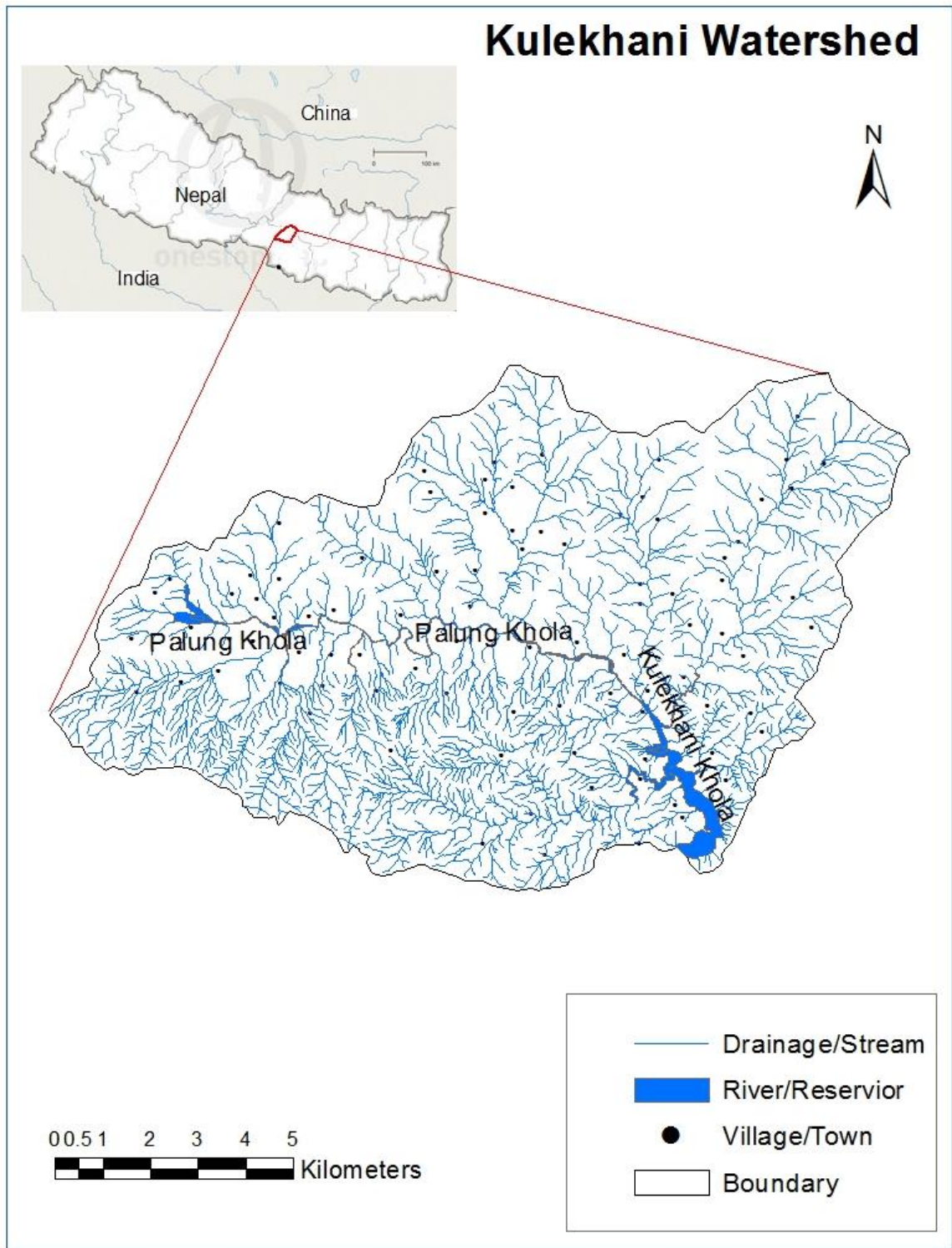
Figure 4.1: Location of the study area.

Tistung Khola, Chitlang Khola, Chalkhu Khola, Bisingkhel Khola, Setikhani Khola, and Thado Khola. The watershed is one of the most popular destinations for

vegetable cultivation, tourism, residential divisions, landscape of forest/barren, and a reservoir (water body).
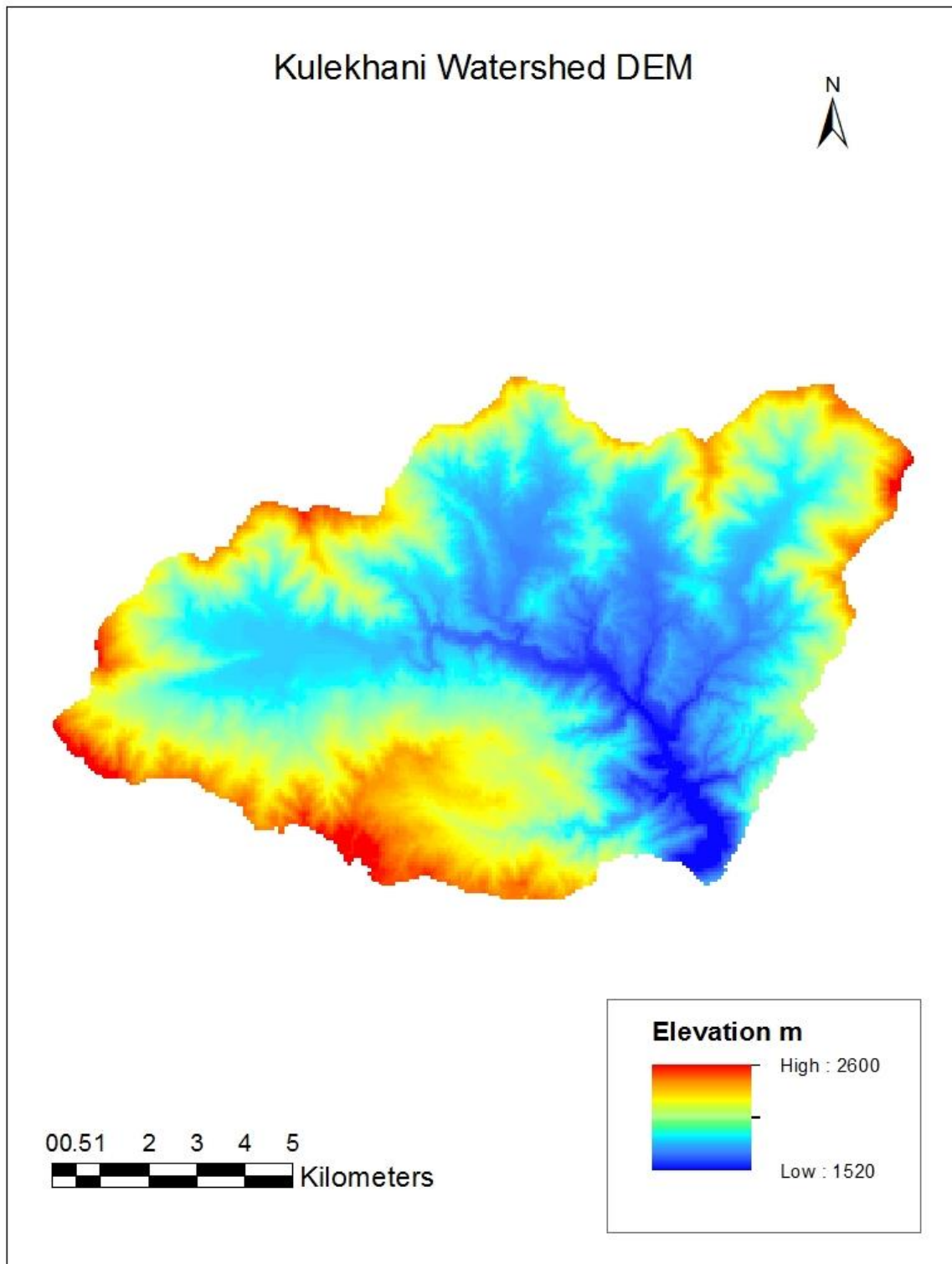
Figure 4.2: Digital elevation model of the study area.

4.2.2 Geological Setting

The study watershed is in the Lesser Himalayas (Mahabharat), which is one of the eight well-defined geomorphologic zones in Nepal (Hagen 1969). Hagen (1969) classified eight geomorphologic regions, namely: 1) Terai (the northern edge of the Indo-Gangetic plain, southern outskirts of Nepal), 2) Siwalik (Churia) Range, 3) Dun Valleys, 4) Mahabharat Range, 5) Midlands, 6) Fore Himalaya, 7) Higher Himalaya, and 8) Inner and Trans Himalayan Valleys. The bed rocks in the study area are slate, phyllite, schist, quartzite, marble, and granite. The geology of the watershed is shown in Figure 4.3. The formation of bedrock in the watershed area mostly belongs to the Bhimphedi Group and Phulchauki Group of the Kathmandu Complex (Stocklin 1981). The Bhimphedi Group consists of Chisapani Quartzite (a fine-grained quartzite), Kulekhani formation (consists of bands of schist and quartzite), and Markhu formation (alternative layer of marbles and schist). The Phulchauki Group consists of Tistune Formation, Sopyang Formation, and Chandragiri limestone. The named Tistung formation is slate and phyllite; the Sopyang Formation is slate and limestone interbedded; and Chandragiri is a single unit of limestone rock. The outcrop granite is highly weathered and changed into grey-colored residual soils in the southern part of the watershed.

The surficial soil in the watershed is colluvial, residual, and alluvial. Details of surface and subsurface profiles in the study catchment can be found in Kayastha et al. (2012), Dhital (2003), Regmi (2002) and Lamichhanne (2000). The overburden soil depths range from 1 m to more than 6 m. The colluvial soils are formed by erosion and landslides, and are found at the bottom of the hills and some moderate slope mid-hills. The major part of the watershed is covered with colluvium. Colluvium is observed up to 2500 m altitude in some locations. The residual soil from weathered granite is also found at higher altitudes. The southern part of the watershed, underlain with granite, is a major location of residual soil. The low-lying river valley area is mostly covered with alluvial soil and, sparsely in some locations, with fluvial deposits. The valley formed along the Palung Khola and its major tributaries, Kiteni Khola, Bisingkhel Khola, and Thado Khola, contains alluvial deposits. Detailed information on soil types in the area is available in Lamichhanne (2000).
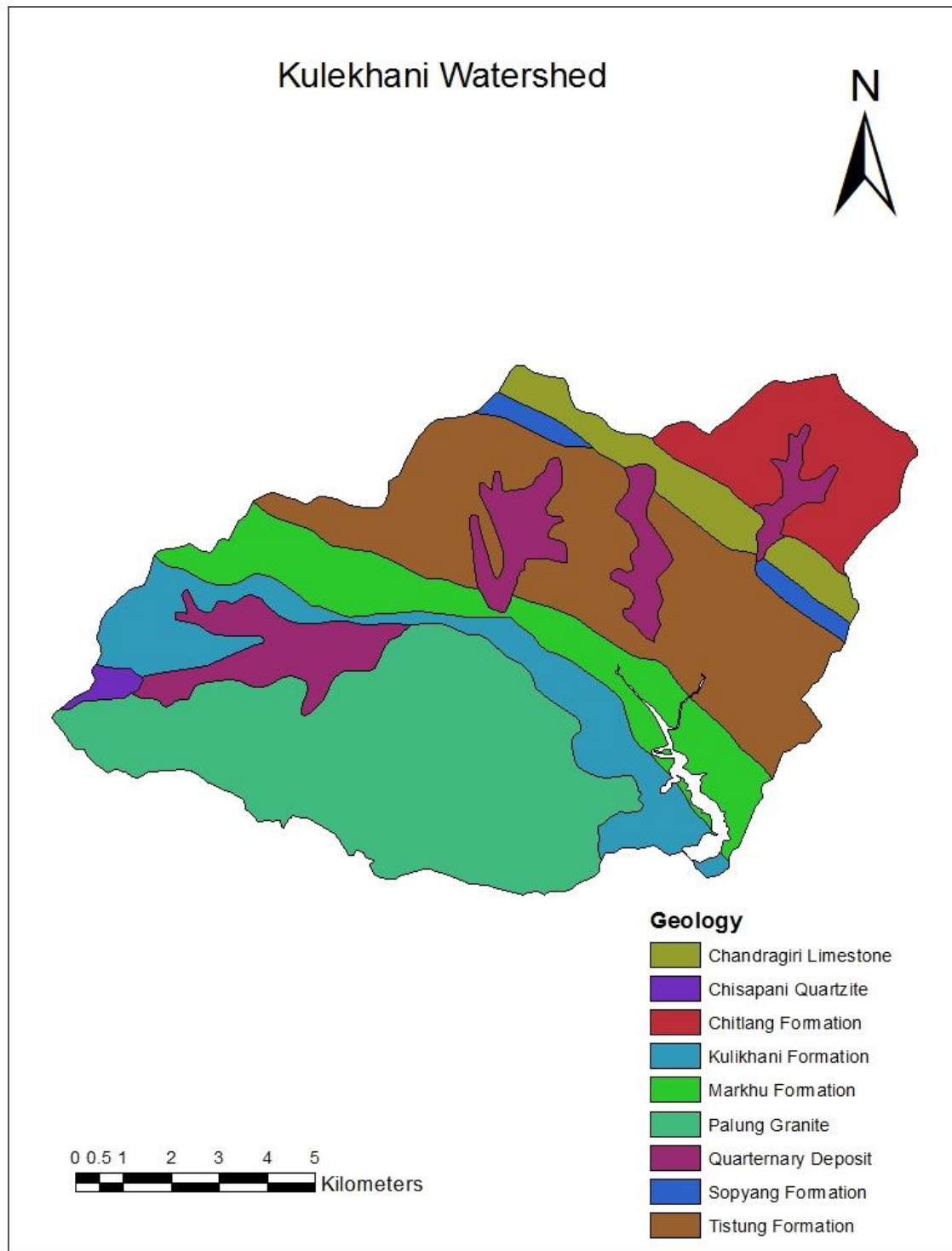
Figure 4.3: Geology in the study area (after Stocklin and Bhattrai 1977, Stocklin 1998, Regmi 2002 and Kayastha et al. 2013).

4.2.3 Climatic Conditions

The distribution of annual average rainfall is higher in the eastern than in the western region of mountainous Nepal. The study area is located in the central region, where precipitation received yearly represents the annual average of the country. Rainfall data for this study are collected from previous studies (Kayastha et al. 2013) and the Department of Hydrology and Meteorology, Nepal. Rainfall recording stations, their locations, and maximum and average recorded rainfall are shown in Table 4.1. Daman and Markhu rainfall gauge stations are located within the study watershed. One-day to five-day maximum cumulative rainfall amounts are analyzed for the period from 1980 to 2013, and are shown in Table 4.2. The recorded daily maximum rainfall at the stations shows the maximum daily recorded rainfall from 1980 to 2013 is 442.5 mm at Chisapani Ghadi. Similarly, in Daman, Markhu, and Thankot stations, the maximum recorded daily rainfall is 373.2, 385.6, and 300.1 mm, respectively.

Table 4.1 Rainfall recorded at four rain gauge stations near and within the Kulekhani watershed.

Station No.	Station Name	Altitude	Longitude Degree East	Latitude Degree North	Max. Daily Rainfall mm	Avg. Annual Rainfall mm
904	Chisapani Gadhi	1706	85° 7' 58.8"	27° 33' 0"	442	2227
905	Daman	2314	85° 4' 58.8"	27° 36' 0"	373	1725
915	Markhu	1530	85° 9' 0"	27° 36' 57.6"	385	1475
1015	Thankot	1630	85° 12' 0"	27° 40' 58.8"	300	1826

Table 4.2 shows rainfall events with one- to five-day cumulative maximum rainfall for two gauge stations within the watershed—Daman and Markhu. The maximum one-day rainfall was recorded on July 20, 1993 at both sites. However, the two-day cumulative maximum rainfall occurred on the same date in Markhu, but a different date in Daman. In Daman, the cumulative rainfall event other than one-day rainfall is higher in date proximity of July 22, 2002, such as July 22nd and 23rd (Table 4.2). The maximum recorded five-day cumulative rainfall at Daman is 730.00 mm. Chisapanighadi gauge station recorded the maximum five-day

cumulative rainfall of 891 mm, and about 40% of the annual average rainfall at the station between July 21 and 25, 2002 alone. Table 4.3 shows the estimated rainfall intensity and duration combination of Chisapani Ghadi, which has the highest recorded rainfall. Rainfall is recorded once a day for 24 hours duration. The recorded rainfall within 24 hours may not be distributed equally over the entire period. The total 24 hours' rainfall may be in a 7.02-hour period, and 48 hours' in 10.36 hours immediately before and after the recorded point of time if we consider 63 mm precipitation per hour continuously. Therefore, the seven-day recorded cumulative rainfall of 909.4 mm may have occurred over a 144.06 hours period. These combinations of assumed worst cumulative rainfall and duration for one- to seven-day recorded rainfall is given in Table 4.3. The assumed cumulative rainfall duration is the possible rainfall accumulation immediately before and after the recorded period in a rate of 63mm per hour.

Table 4.2 Cumulative rainfall record for four rain gauge stations from 1980 to 2013 in the Kulekhani watershed.

Max Rainfall	Chisapani Gadhi		Daman		Markhu		Thankot	
	Date	mm	Date	mm	Date	mm	Date	mm
One Day	July 23, 2002	442.5	July 20,1993	373.2	July 20,1993	381	July 25, 2002	300
Two Day	July 23, 24, 2002	652.6	July 22, 23, 2002	513	July 20,21, 1993	429	July 24, 25, 2002	388
Three Day	July 22, 23, 24, 2002	800.8	July 22, 23, 24, 2002	636	July 22, 23, 24, 2002	519	July 24, 25, 26, 2002	450
Four Day	July 22, 23, 24, 25, 2002	868.8	July 22, 23, 24, 25, 2002	715	July 22, 23, 24, 25, 2002	556	July 24, 25, 26, 27,2002	491
Five Day	July 21, 22, 23, 24, 25, 2002	891.1	July21, 22, 23, 24, 25, 2002	730	July 21, 22, 23, 24, and 25, 2002	561	July 23, 24, 25, 26, 27,2002	520

Table 4.3 Estimated cumulative rainfall at Chisapani Ghadi rain gauge station.

Rainfall Record in Chisapani Gadhi					
Total Recorded Duration	Date	mm	Minimum assumed Duration, hours	Each Day Rainfall, mm	Assumed, mm/hour
One Day	July 23, 2002	442.5	7.02	441	63
Two Day	July 23, 24, 2002	652.6	10.36	443 210	63
Three Day	July 22, 23, 24, 2002	800.8	29.68	148 443 210	27
Four Day	July 22, 23, 24, 25, 2002	868.8	51.43	148 443 210 68	17
Five Day	July 21, 22, 23, 24, 25, 2002	891.1	73.43	22 148 443 210 68	12
Six Day	July 20, 21, 22, 23, 24, 25, 2002	905.2	120.22	14 22 148 443 210 68	8
Seven Day	July 21, 22, 23, 24, 25, 26, 2002	909.4	144.06	14 22 148 443 210 68 4	6

4.2.4 Geotechnical Characteristics of the Study Area

The steep slopes consist of bedrock outcrops and compacted overburden soil, as compared to relatively loose mildly-sloping hills in the watershed. Hasegawa et al. (2009) observed a peak internal frictional angle of 22° to 36°, and a residual angle of 22° to 34° for slip materials along the landslide in a highway corridor in western Nepal, which is similar to the studied watershed. Geotechnical investigations have been conducted at one old landslide site in the watershed to obtain field information. The results of the geotechnical investigations are discussed in the

Section 4.3.4. Field test and laboratory test results from the investigations are used for the stability analysis.

There are mainly three types of overburden soils in the watershed. These are eluvial or residual, alluvial, and colluvial soils. The geotechnical properties of the residual soils depend on the types of parent rock, and also the depth of weathered or competent bedrock. In the study watershed, weathered granite is the parent rock for most of the residual soil. Colluvium soil is a predominant soil in the area, which originates from erosion, wind drifting, and landslides of residual soils. Colluvium consists of an unsorted matrix of soil, rock fragments, and gravel. Alluvium deposits are found in the lower altitudes of the watershed. The formation of alluvial soils is by erosion and sediment transport and deposit by slow-flowing water. Alluvium mostly consists of coarse sediment at the bottom and finer material on the top for a given batch of deposition. Different layers of unsorted materials provide sediment deposition at different times. The geotechnical properties of alluvium and colluvium both depend on the types of residual soil.

4.2.5 Types of Landslides

Landslides are observed on very steep to moderately steep mountain slopes and high-altitude locations (Figure 4.11a, Kayastha et al. 2012, Dhital 2003, Deoja et al. 1991). The majority of landslides are debris flows which travel to the foot of the hills and river courses, including hydropower reservoirs in the lowest contour of the watershed from their initiation point. Landslides are mostly initiated in natural slopes, and some in anthropogenic disturbance locations, such as near roads and other infrastructure (Kayastha et al. 2012).

Dhital (2003) studied 93 landslides in a single event in a watershed area near Kathmandu, and observed that the landslides were debris flows and slides. Dahal and Hasegawa (2008) identified 677 rainfall-induced landslides in Nepal from 1951 to 2006. These landslides were mostly debris flows in natural terrain. Petley et al. (2007) observed 397 fatal landslides during the period from 1978 to 2005 in Nepal. These landslides were debris flows, mudflows, and rock falls. In manmade slopes, such as in highway corridors, landslides are mostly shallow, translational slides (Dahal and Hasegawa 2008). Based on visual observations at the site and

previous literature (Ray and Smedt 2009, Dahal and Hasegawa 2008, Dahal et al. 2008, Petley et al. 2007, Gabet et al. 2004, Dhital et al. 1993), the types of landslides in the proposed study area are mostly slides and debris flows (Cruden and Varnes 1996). Landslides in the study area are initiated either on a natural slope or anthropogenic disturbance from infrastructure development such as road construction. Therefore, for rainfall-induced landslide danger, hazard and risk assessment, debris flow is a major type of landslide to consider.

4.3   Methodology

The approach and model developed for landslide susceptibility analysis and mapping of the study watershed is shown in Figure 4.4. The first step is collection of information, and in situ and laboratory testing. One old landslide site was used to conduct in situ geotechnical investigations, and to collect samples for laboratory testing. Soil strength parameters, such as cohesion, friction angle, and soil permeability results from the laboratory and in situ testing are considered in the analysis. The representative Soil Water Characteristics Curve (SWCC) is developed, based on the methods of Fredlund and Xing (1994) and Torres (2011), from grain size distribution. A total of 73 locations (Lamichhanne 2000) in the watershed are considered for SWCC development. Rainfall observations from four rain gauge locations are used as the duration and intensity of rainfall for infiltration depth computation. Infiltration depth is computed using the suction from SWCC, and a combination of rainfall intensity and duration. DEM (Figure 4.2) is used for developing the slope map. Maps of all parameters are developed in the GIS environment. These maps are interpolated using Inverse Distance Weighted (IDW) methods and converted into raster maps. The maps are also converted to the same extent for raster calculation. The final landslide susceptibility maps are developed for different rainfall durations and intensities. Low-intensity, long-duration and high-intensity, shorter-duration rainfall events are considered separately for the analysis. The model is verified using the recorded rainfall and observed landslides in the watershed. The threshold rainfall intensity and duration for landslide initiation is applied to unstable locations within the watershed.

66
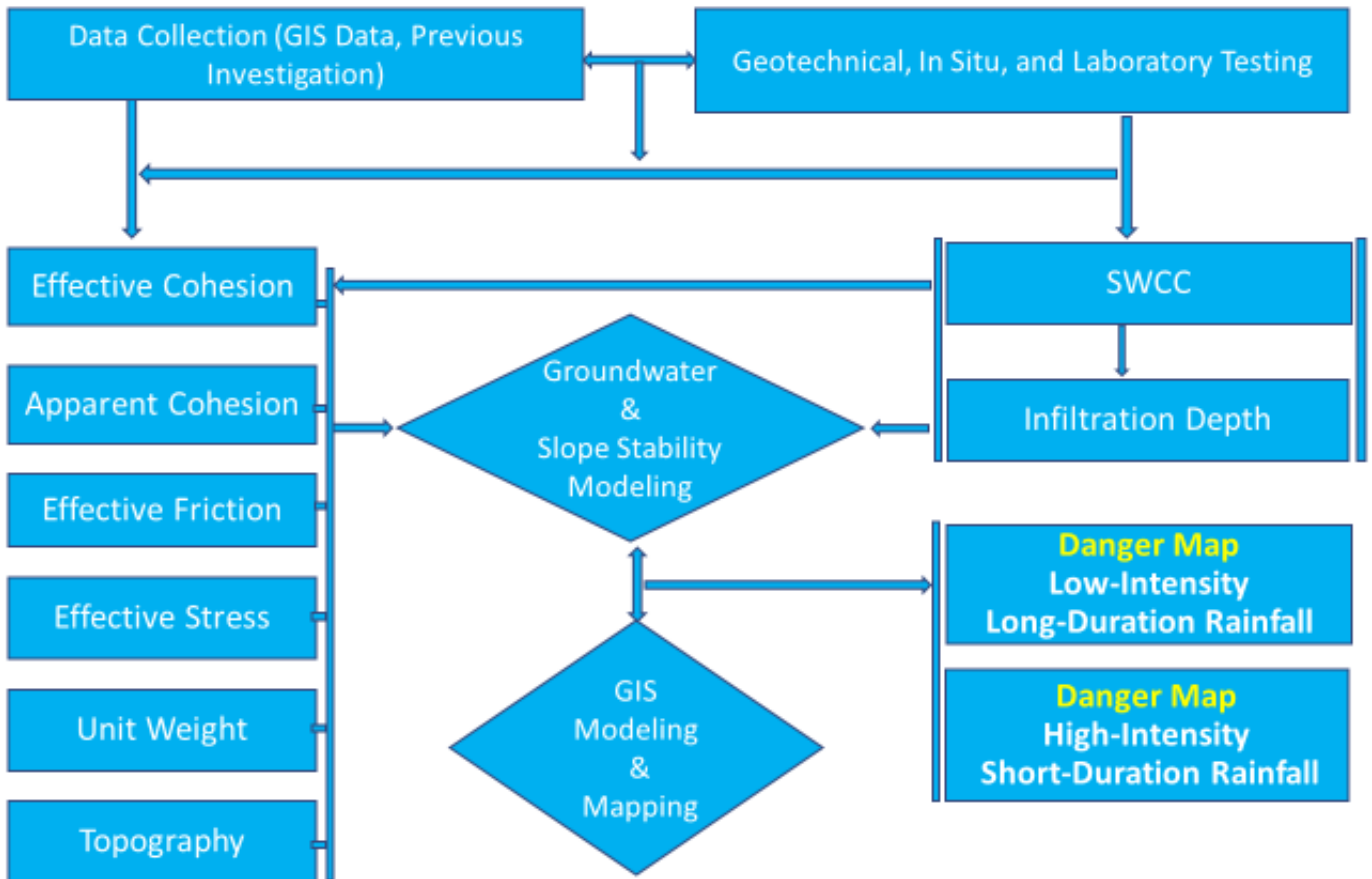
Figure 4.4: Flow chart for developing the landslide danger map model.

4.3.1 Rainfall Infiltration Model

The rainfall intensity and duration required for landslide initiation in mountainous regions has been studied by several authors, including Caine (1980), Caine and Mool (1982), Cancelli and Nova (1985), Wieczorek (1987), Ceriani et al. (1992, 1994), Crosta and Fratini (2001), Aleotti (2004), Zezere et al. (2005), and Saito et al. (2010), and empirical relations have been proposed. For mountains in Nepal, Dahal and Hasegawa (2008) recommended the following rainfall intensity and duration for landslide initiation (Equation [4.1]):

$$I = 73.90D^{-0.79} \ , \quad N_1 = 1.10D^{-0.59} \qquad [4.1]$$

where, I is the hourly intensity in mm, D is the duration in hours, and N_1 is the normalized rainfall intensity per hour—a ratio of critical rainfall to mean annual precipitation. Their empirical equation provides a warning intensity and duration of

rainfall for landslides in relation to previous events. However, it does not provide information on the location of the unstable areas or slopes. Dahal and Hasegawa (2008) proposed a threshold rainfall for the Himalayan region after studying 193 rainfall and landslide events from east to west Nepal. It can be noted from their study that the annual average rainfall distribution and rainfall intensity are in agreement with the density of landslides from the east to west of Nepal. The number of landslides recorded in Nepal is greater in the eastern and central regions than in the western region. This shows that threshold rainfall plays a significant role in the initiation of landslides, but the location of unstable slopes can only be identified with the study of subsurface physical changes on mountain slopes. The threshold rainfall triggers landslides only in a specific location of the watershed.

Hasegawa (2008) reported the threshold rainfall for a wide range of rainfall durations, from 5 hours to 90 days. In this equation, they reported that continuous rainfall of more than 12 mm per hour for 10 hours, or 2 mm of rainfall per hour for 100 hours, or daily rainfall in excess of about 144 mm as thresholds for landslide initiation. Based on these results, if there is continuous rainfall of more than 12 mm per hour for 10 hours, landslides may be triggered. Additionally, 2 mm of rainfall per hour for 100 hours will also initiate landslides. If daily rainfall exceeds about 144 mm, there will be a risk of landslide in the region. In these observations, all landslides were considered, included deep-seated or shallow landslides. The landslides considered in their study were not differentiated based on whether they were first initiated within the study period, or only retroactive within the study period. Physical parameters, such as subsurface soil characteristics and their influence on the density of landslides in specific areas of the country were not considered in their study. However, these records provide a good guide for how to proceed with further study of physical changes in the slope during threshold rainfall conditions.

The influencing factors of rainfall-induced landslides are the intensity of rainfall, topography, and soil characteristics. The initial factor of safety of the slope is influenced by the slope geometry and groundwater level, and the final factor of safety by the soil characteristics and intensity of the rainfall during the time of

failure (Rahardjo et al. 2007). Soil characteristics, initial groundwater level, and perched water conditions are factors that must be considered when identifying the instability of the slope.

The instability of a specific location depends on the geotechnical properties of subsurface soil, the groundwater profile, and threshold rainfall so that their proposed relation is a baseline for further study in the region. Dahal and Hasegawa (2008) also indicated that landslides in the Nepalese Himalayas occur after as little as a third of the required rainfall of the rest of the world, which means these mountains are more susceptible to landslides.

The consequence of rainfall on a particular soil is the focus of this study for these fragile mountains. Most of the rainfall gauge stations recorded 24-hour rainfall in the study watershed. For rainfall intensity estimations lower than 24 hours duration, Equation [4.2], proposed by Shakya (2002), is used. From Equation [4.2], rainfall for any duration can be estimated from 24 hours given rainfall. Smaller durations of estimated rainfall are necessary for infiltration depth analysis.

$$\left| \frac{P_t}{P_{24}} \right| = \left[\frac{\sin \pi t}{48} \right]^{0.4727} \quad [4.2]$$

where, P_t is rainfall in specified time t (in hours), P_{24} a total rainfall in 24 hours. Usually rainfall data are available in a 24 hours interval and amount of rainfall for t hours can be obtained from this model.

Rainfall records for the study watershed are obtained from previous research and from the Department of Hydrology and Metrology, Nepal from 1980 to 2013. Extreme cumulative rainfall for one, two, three, four, and five days are identified for the study area. It is assumed that the recorded rainfall is distributed for entire watershed and the anticipated infiltration depth is analyzed. If saturated permeability of the soil is more than rainfall precipitation rate, rainfall precipitation rate will be considered for infiltration depth computation. The condition required to understand landslide disaster from given duration and intensity of rainfall, Equation [4.1] is applied to find the threshold rainfall induced landslide condition.

Two equations are popular for rainfall infiltration: Richards, and Green Ampt. Three dimensional water filtration model based on Darcy's law and Richard's (1931) equation as given by Fredlund and Rahardjo (1993) is shown in equation [4.3].

$$\frac{\partial}{\partial x}\left(kx\frac{\partial h}{\partial x}\right) + \frac{\partial}{\partial y}\left(ky\frac{\partial h}{\partial y}\right) + \frac{\partial}{\partial z}\left(kz\frac{\partial h}{\partial x}\right) = m_2^w \rho g \frac{\partial h}{\partial t} = -\frac{\partial \theta w}{\partial t} \quad [4.3]$$

If we consider flow in vertical direction only,

$$-\frac{\partial \theta w}{\partial t} = \frac{\partial q_z}{\partial z}, \, q_z = -k_z \frac{\partial h}{\partial z} \quad [4.4]$$

where, k_x, k_y, and k_z are coefficients of permeability in the x, y, and z directions, m_2^w coefficient of soil structure volume change with respect to soil suction, θw volumetric water content, ρ is density, g is gravitational acceleration, h is hydraulic head and t is the time of infiltration. Infiltration depends on soil permeability and initial moisture content. If permeability is in a steady state condition, there is no storage, and infiltration only depends on the permeability of the soil. Richard's equation requires more information and a complex procedure for the infiltration solution. Salciarini et al. (2006) applied the "Transient Rainfall Infiltration and Grid-based Slope-stability (TRIGRS) model that couples an infinite-slope stability analysis", in which pore pressure is a triggering factor. The distribution of the depth of overburden soils in their model are assumed to vary with hill slope angle and an impervious layer is considered at the overburden soil depth. The TRIGRS model requires a solution of Richard's equation in a GIS grid and more data for analysis, and it isn't a simple model. Casadel et al. (2003) derived the overburden soil thickness based on a model proposed by Dietrich et al. (1995) for slope stability analysis and suggested that a simple model with a rainfall and slope stability relation is necessary for practical use.

The following **infiltration model** (Equation 4.5), based on a wetting front concept (Green and Ampt 1911, Lumb 1962, Mein and Larson 1973, Sun et al. 1998, Zang

et al. 2011) is used for finding the infiltration depth (Zw) for different threshold rainfall durations (Tw). The Green and Ampt infiltration model was studied and compared with the rigorous Richard's equation by Claunitzer et al. (1998) and Hsu et al. (2002). They found similar and acceptable results with the rigorous Richard's equation for infiltration. The effect of hill slope and direction of rainfall on the Green and Ampt equation was studied by Chen and Young (2006), and they compared their results with Richard's equation. They found that the Green and Ampt equation provides similar results to Richard's equation for infiltration on a hill slope. They also studied the effect of ground slope on the infiltration rate and wetting depth, and found it to be insignificant for long-duration and high-intensity rainfall. High-intensity, long-duration rainfall is important for this study, and Green and Ampt's original equation [4.5] is applied in the analysis. In the Green and Ampt equation, rainfall duration equivalent to threshold rainfall (Tw) is as given below:

$$T_w = \frac{1}{K_w}\left[Z_w - \psi\Delta\theta \ln\left[\frac{Z_w}{\psi\Delta\theta} + 1\right]\right] \qquad [4.5],$$

where T_w = time to reach the wetting front at Z_w, $\Delta\theta = \theta_1 - \theta_0$, θ_0 is the initial volumetric water content before wetting, θ_1 is the final volumetric water content after wetting, k_w is the coefficient of permeability of the soil in the wetted zone, and ψ is the wetting front capillary suction.

A total of 73 locations (Lamichhanne 2000) were chosen for infiltration depth computation in the study watershed (Figure 4.7). The depths computed in those locations were interpolated in the GIS environment for the entire watershed.

The suction head is related to the initial volumetric moisture content of the wetting front, θ_0. The suction head can be obtained from the SWCC for a given water content. The Soil Water Characteristic Curve is a primary parameter required to obtain the wetting front depth from equation [4.5]. Another parameter, the permeability of unsaturated soil, can be written as a function of the permeability of saturated soil, void ratio, and suction (Fredlund and Xing 1994, Leong and

71

Rahardjo 1997). The method applied to obtain SWCC is given in Torres (2011) and briefly discussed in the subsequent sections.

The wetting front moves downward continuously when rainfall and infiltration takes place in unsaturated soil. The permeability of unsaturated soil changes with the condition of saturation, and with the progress of the wetting front. The saturated permeability function of unsaturated soil is a function of the degree of saturation or stage of moisture content and suction in unsaturated soil (Fredlund and Xing 1994, Leong and Rahardjo 1997).

The Green and Ampt equation was also used by Freeze and Cherry (1979), Chow et al. (1988), Tsai and Yang (2006), Iverson (2000), and Chen and Young (2006) for infiltration and landslide initiation. The Green and Ampt method considers Darcy's law, equation [4.6]:

$$q = -k\left(\frac{\partial h}{\partial z}\right) \quad [4.6]$$

where q is discharge, k is the coefficient of hydraulic conductivities, and $\left(\frac{\partial h}{\partial z}\right)$ is the hydraulic gradient.

The amount of water infiltrate into the soil in a given duration to change moisture in a given depth of soil is equal to the discharge (q) into it. The Green and Ampt model of infiltration is shown in Figure 4.5. For unsaturated soil, the total head will be the suction head above the wetting front (h), (h+ψ), where ψ is the suction head at the wetting front in the water column. The quantity of water infiltrate, q, is equal to the total depth (Z_w) times the difference in moisture (θ_1-θ_0), or discharge q=$\Delta\theta$*Z_w, where, $\Delta\theta$ is the difference in volumetric water content—the difference between the initial and final water content. The infiltration depth (Z_w) is derived from the Green and Ampt (Z_w) equation [4.7] for infiltration depth for a given rainfall duration (t), permeability, suction, and initial moisture content.

$$Z_w = Kt + \psi * \Delta\theta \ln\left(1 + \frac{Z_w}{\psi * \Delta\theta}\right) \quad [4.7],$$

Chen and Young (2006) modified this equation for sloping ground, as in equation [4.8]:

$$Z_w = Kt + \frac{\psi * \Delta\theta}{\cos\beta}\ln\left(1 + \frac{Z_w\cos\beta}{\psi * \Delta\theta}\right) \qquad [4.8],$$

where β is the ground slope. T_w is the time to reach the wetting front at Z_w, and can be expressed as in equation [4.9]:

$$T_w = \frac{1}{K_w}[Z_w - \psi\Delta\theta \ln\left[\frac{Z_w}{\psi\Delta\theta} + 1\right]] \qquad [4.9],$$

where T_w = time to reach the wetting front at Z_w, $\Delta\theta = \theta_1 - \theta_0$, θ_0 is the initial volumetric water content before wetting, θ_1 is the final volumetric water content after wetting, k_w is the coefficient of permeability of the soil in the wetted zone, and ψ is the wetting front capillary suction.
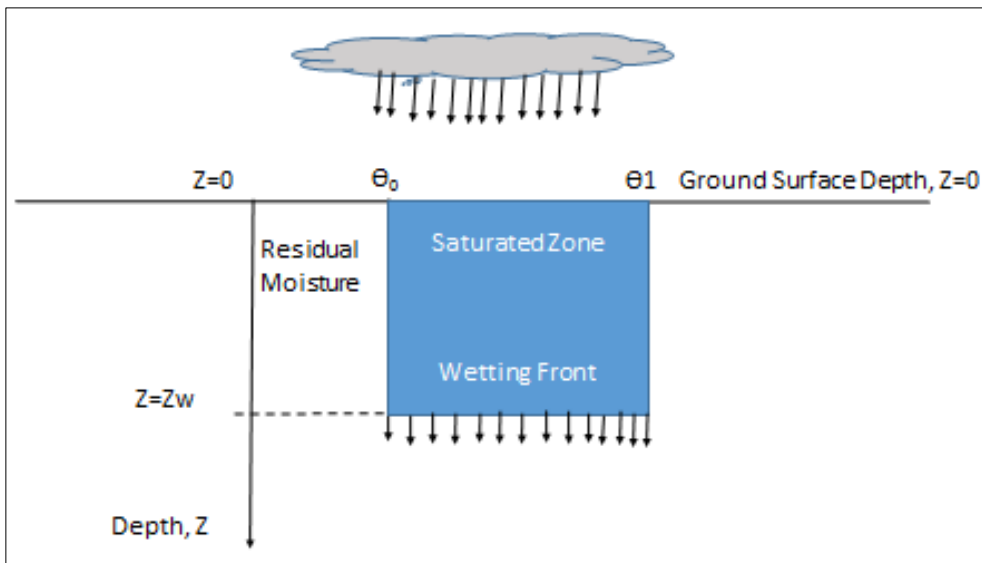
Figure 4.5: The Green and Ampt Infiltration Model.

(Note: Infiltration towards z direction, z=0, ground surface, Z=Zw, wetting front depth, θ_0 is the initial volumetric water content and θ_1 is the final volumetric water content after wetting)

The Iverson (2000) model considered constant saturated permeability for infiltration. The modified Iverson (2000) model with beta correction was proposed

73

by Tsai and Yang (2006) as a general infiltration model in groundwater conditions. Here, rainfall intensity is considered as an infiltration, the same as in the modified model used by Freeze and Cherry (1979), Chow et al. (1988), and Tsai and Yang (2006). The condition of the impervious layer in a deeper location and groundwater table is not observed in steep mountainous regions, or is at very high depth, therefore, Iverson's corrected Bita model is not applicable in this study case.

Freeze and Cherry (1979), Chow et al. (1988), and Tsai and Yang (2006) studied the variation of infiltration capacity of any ground type with rainfall intensity and duration. When the infiltration capacity is higher than the rainfall intensity, the rainfall intensity governs the infiltration, and if the rainfall intensity is greater than the permeability coefficient, infiltration will be governed by permeability. Infiltration depends on soil permeability and initial moisture content. If the permeability is in steady state condition and the soil has no moisture storage, infiltration depends on permeability alone.

The reduction of soil strength parameters due to the infiltration of rainfall on the slope is identified. The worst condition for slope instability and landslide initiation is expected to be found during the threshold rainfall on the study slope. For stability analysis, the amount of suction based on initial water content in different types of soil is measured. The water content and suction relation are developed from the grain size distribution suggested by Fredlund et al. (2002). When advancing the wetting front, Z_w, the failure conditions are tested in Equation [4.10]. Based on the different depth of overburden soil and slope angle, the infiltration depth and its role in the stability of the slope are analyzed. The role of suction in slope stability is important to identify in different saturation conditions. In steep hills, negative pore pressure (matrix suction) is the most important factor to consider for slope stability model.

4.3.2 Groundwater Flow Model

The annual average rainfall in the watershed, considering all four rainfall gauge stations, is 1813 mm. There is not any stable groundwater table in the hill portions

of the watershed. In Figure 4.2, the blue portion of the DTM with the low-lying area of river valley, which is not important for landslides, has a groundwater table, but at a significantly larger depth. The surface springs developed in the slopes are through the rock fault (Deoja et al. 1993). The seepage water moves with the wetting front in the hill slope, and its direction changes when it encounters an impervious layer or bedrock, passing through faults and joints to drain out as spring water. Figure 4.6 shows how seepage water passes through impervious or bedrock layers and moves in mountain slopes. A temporary perched water table develops and moves downward with the intensity and duration of rainfall. There is not any stable groundwater table in the hill slope that influences the slope stability in high mountains in Nepal. A water table is available in deeper locations in the valley, which is not in landslide prone areas.
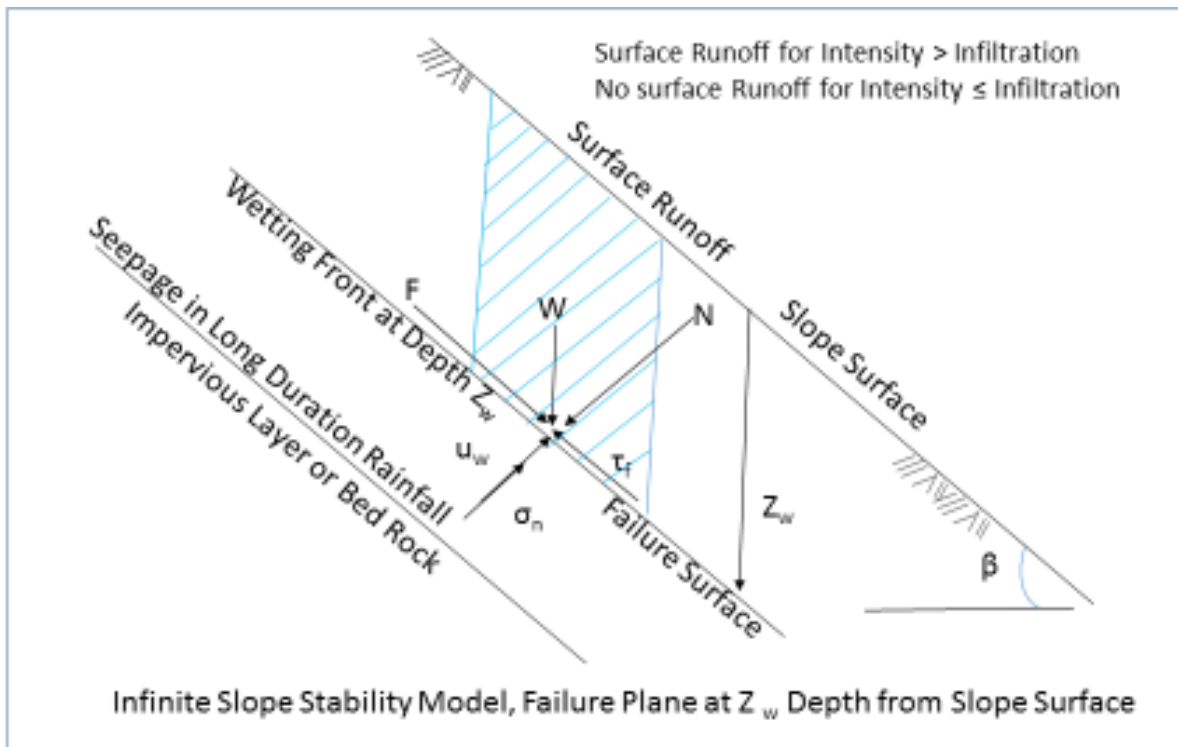
Figure 4.6: Rainfall, seepage and slope instability model.

4.3.3 Slope Stability Model

There are various infinite slope models for slope stability analysis. The slope stability for unsaturated slopes proposed by Fredlund et al. (1987) and Cho and Lee (2002) is considered for the initiation of landslides at different rainfall thresholds in this research. The depth of the wetting front Z_w will be equivalent to H in equation [4.10] for stability analysis.

$$F_s = \left[\frac{\left((c' + (u_a - u_w)\tan\phi^b) + ((\sigma_n - u_a)\tan\phi') \right)}{(\gamma_t H Sin\beta Cos\beta)} \right] [4.10]$$

where Fs = factor of safety, c' is effective cohesion, ϕ' is the effective friction angle, σ_n is the normal stress, H is the wetting front depth, β is the slope angle, γ_t is the unit weight of soil, u_a is the pore air pressure, u_w is the pore water pressure, $(u_a - u_w)$ is the matrix suction, σ_n - u_a is the effective normal stress on the slip surface, and ϕ^b is the rate of increase in shear strength due to matrix suction.

The infinite slope stability equation [4.10] has an unsaturated soil suction portion $(u_a - u_w)\tan\phi^b$. If the soil degree of saturation reaches 100%, this portion of the soil strength parameter becomes zero, and will be similar to the saturated condition. Various models are available for the identification of $(u_a - u_w)\tan\phi^b$ in terms of $\tan\phi'$ (Fredlund et al. 1996, Vanapalli et al. 1996, Khalili and Khabbaz 1998). The equivalent shear strength relation proposed by Fredlund et al. (1996) is given in equation [4.11]:

$$t_f = c' + (\sigma_n - u_a)\tan\phi' + (u_a - u_w)[(\theta^k)(\tan\phi')] \quad [4.11]$$

where t_f is shear strength, Θ is the normalized water content (Θ_w / Θ_s), Θ_w is the water content at a given suction, and Θ_s is the saturated water content. The fitting parameter k is related to the plasticity index (I_p) of the soil in percentage (Vanapalli et al. 2000, Vanapalli and Fredlund 2000, and Garven and Vanapalli 2006). Vanapalli et al. (2000) proposed two Equations [4.12] and [4.13] for compacted and expansive soils.

$$k = -0.0009I_p^2 + 0 \cdot 833I_p + 0 \cdot 9848 \quad [4.12]$$
$$k = -0.0044I_p^2 + 0 \cdot 2245I_p + 0 \cdot 9715 \quad [4.13]$$

Garven and Vanapalli (2006) proposed the fitting parameter k to the plasticity index as given in Equation [4.14]:

$$k = -0.0016I_p^2 + 0 \cdot 0975I_p + 1 \quad [4.14]$$

For non-plastic soil, I_p will be zero and fitting parameter, k equal to 1 that leads to $\tan\varnothing^b$ equal to $\Theta \tan\varnothing'$.

Garven (2009) studied seven among 25 equations for finding shear strength of unsaturated soils proposed in the literature. All of these seven equations are able to predict shear strength in different range of suction for most of 52 soil samples and 130 data sets. In her study the range points fit in the equations were 44 (Lytton 1995) to 118 (Vilar 2006) and percentage fit ranging from 34.6 to 92.9 %. Vilar (2006) equation required one tested point to develop full equation which is beyond the objective of this research. Also, Garven (2009) mentioned that this is not fully developed shear strength predicting equation. However, shear strength characteristics of eight % of samples was not captured from any of these equations. Six equations consider SWCC and are applicable to predict shear strength of unsaturated soil (Garven 2009). Among these six equations, Vanapalli et al. (1996) is applicable for entire range of suction, fit for 48 samples of 52 total tested soil samples by Garven (2009), and more relevant to the soil type in the study area (residual, and colluvial soils).

The unsaturated soil shear strength (Fredlund 1978, 1987; Vanapalli and Fredlund 1999; Fredlund and Rahardjo, 1993) can be obtained from the SWCC. The empirical relations developed based on grain size distribution by previous researchers (Fredlund and Xing 1994, Zapata 1999, and Torres 2011) are applied to obtain the soil water characteristics curve in this research. The modified SWCC model proposed by Fredlund and Xing (1994), Equation [4.15], requires various parameters. These parameters are:

- Degree of saturation (S), soil suction at residual moisture content, h_r, in kPa,
- A soil parameter related to the rate of water extraction of the soil after air entry value (a),
- n (b_f), the slope of SWCC,
- m (c_f), which is a fitting parameter or function of the residual water content,
- air soil parameter, a, which is a function of air entry value in kPa,
- Soil suction Ψ, in kPa,
- Initial volumetric water content θ_w and,
- The volumetric water content at saturated condition θ_s.

$$S(\%) = \frac{\theta_w}{\theta_s} = 1 - \frac{\ln\left(1 + \dfrac{\Psi}{h_r}\right)}{\ln\left[1 + \left(\dfrac{1,000,000}{h_r}\right)\right]} \, x \left[\frac{1}{\left\{\ln\left[e + \left(\dfrac{\Psi}{a}\right)^{b_f}\right]\right\}^{c_f}}\right] \quad [4.15],$$

There are several methods which can be used to obtain SWCC using soil grains (Zapata 1999), but the empirical model (Equation [4.16]) proposed by Torres (2011) is applied here to obtain an SWCC in which all grain sizes are used in the model. The detail of the analysis method is given in Torres (2011). The method proposed by Torres (2011) for SWCCs requires Atterberg's limits and the grain size distribution of the soils (Equation [4.16]). In Equation [4.16], suction is written as a function of the weighted plasticity index wPI and grain diameter, D. The wPI can be obtained using Equation [4.17], in which P_{200} is the percentage passed through a 200 number of sieve, and PI is the Plasticity Index. The suction on the left side can be obtained for each diameter. The percentage passed for that diameter is taken as the degree of saturation. The diameter and percentage passing can be obtained from the sigmoid function proposed by Fredlund (2002). Alternatively, the percentage and diameter can be obtained directly by reading from the grain size distribution curve. In this study, the percentage passing will be chosen as 5, 10, 15, 20, 25, 30, 40, 50, 60, 70, 80, 90, and 100, and the respective diameter (D) will be found directly using the grain size curve. The

degree of saturation will be the chosen percentage passing, and suction will be computed using the respective diameter of the percentage passing from Equation [4.16]. As the percent passing will be equivalent to the degree of saturation for the computed suction, it will be 0 to 100. Suction will be computed from grain diameter with respect to the degree of saturation.

Once suction and the degree of saturation are identified, these values are fitted into the modified SWCC equation proposed by Fredlund and Xing (1994)— Equation [4.15]. As in Fredlund and Xing (1994), Equation [4.15] is nonlinear, so identification of a, n, and m is not straight forward. A method of least squares is used to fit the Fredlund and Xing (1994) equation. The initial values of SWCC parameters a, b_f, and c_f will be found based on merging the initial curve and the Fredlund and Xing (1994) model together. Once the initial values are found, these are used as the initiation point for a, b_f, and c_f for coarse-grained soils. The typical initial values in this analysis for a, b_f, and c_f are 10, 1, and 2 for some cases.

The degree of saturation is computed with an assumed a, n, and m, and suction values obtained from the Torres (2011) model for sandy and clayey soil. The final part of the curve fitting is plotted with both curves on the same graph. Once both graphs are in the same plot, the graph obtained from the Torres (2011) model is dragged close to the Fredlund and Xing model by changing a, n, and m. If both curves are close enough, the least squares method is applied to minimize errors. The SWCC parameters will be found from the final outcome through the least squares method for the Fredlund and Xing (1994) equation.

$$\log \Psi = 0.00005(wPI)^3 - 0.003(wPI)^2 + 0.03wPI + 1.1355 - (0.0126wPI + 0.7285)\log D$$
$$- (0.0011wPI + 0.0044)\log D^2 + (0.0002wPI + 0.0056)\log D^3$$

[4.16],

$$wPI = \frac{P_{200}(PI)}{100} \quad [17],$$

where wPI = weighted plasticity index in %, P_{200} = Material passing #200 US Standard Sieve in %, PI = Plasticity Index expressed in %, and D = grain diameter.

In this study, soil samples recovered from the performed geotechnical investigations are considered for analysis. Samples were tested in the laboratory for soil grain size, plasticity index, and natural moisture content. Grain size distribution results from previous research (Lamichhanne 2000) in the watershed are also considered in the analysis. These data for a total of 73 different locations in the watershed are taken for SWCC analysis. The locations of samples recovered within the study watershed for testing are given in Figure 4.7. Typical grain size distribution curves in the study area are given in Figure 4.8. Similarly, typical soil water characteristics curves are shown in Figure 4.9.
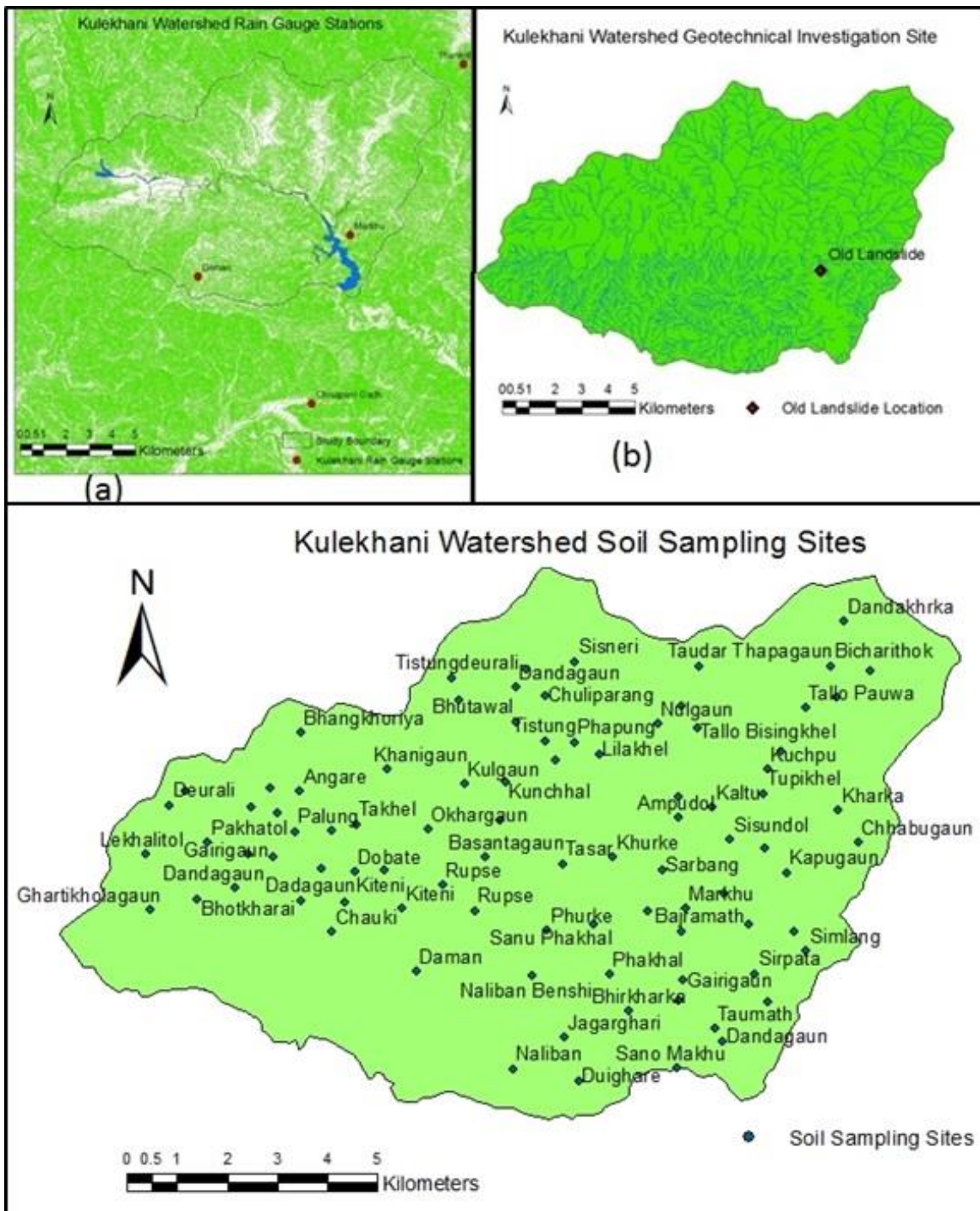
Figure 4. 7: Kulekhani Watershed (a) Rain gauge stations for rainfall data, (b) Geotechnical investigation site at old landslide area and (c) Soil sampling locations for various tests.
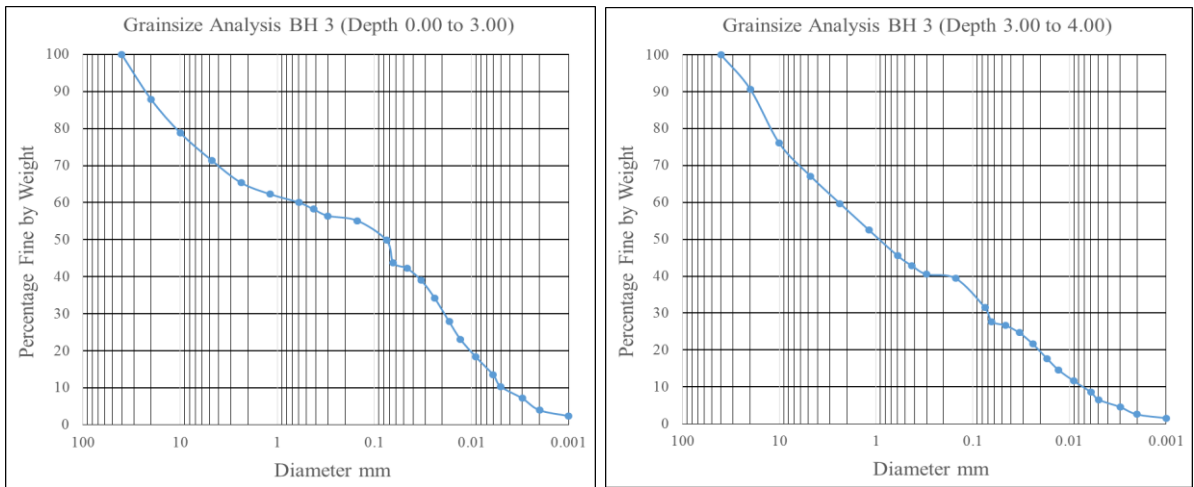
Figure 4.8: Grain size distribution for samples from BH 4, depth 0.0–1.5 and 3.0–4.0 m.
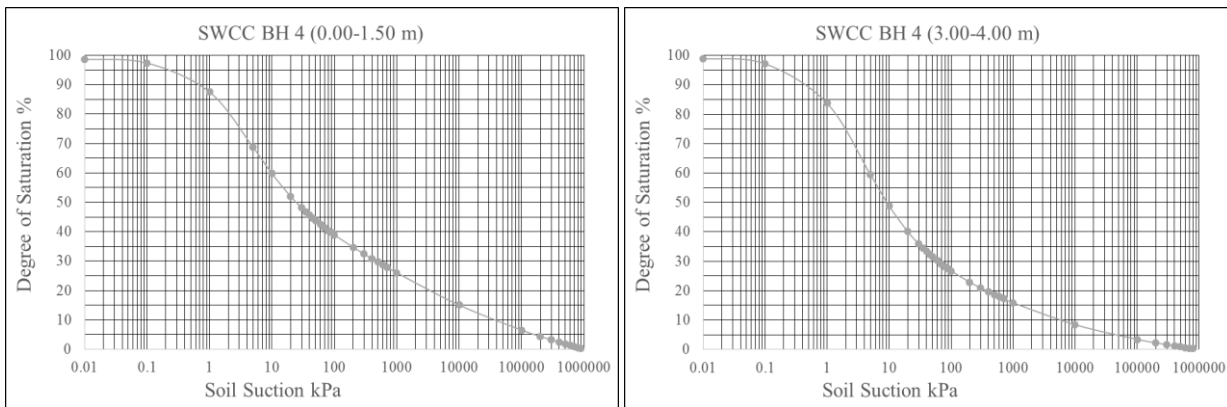
Figure 4.9: Soil Water Characteristics Curve (SWCC) for BH 4, depth 1.00–1.5 and 3.0–4.0 m. m.

4.3.4 Geotechnical Investigations and Data Collection

The geotechnical investigations were conducted in a old landslide area. In situ and infiltration tests were carried out at the site. Disturbed and undisturbed samples were collected from four boreholes at different depths. Other watershed information for the study area was collected from Dhital (1993) and Dhital (2003). A topographical map of the study area was obtained from the Topographical Survey of Nepal. The physical

conditions of subsurface soil during threshold rainfall and slope instability conditions were analyzed and used for the landslide susceptibility map of the study watershed.

The in situ testing was conducted to obtain subsurface soil geotechnical properties. Laboratory testing of disturbed and undisturbed samples for geotechnical characteristics was conducted in a soil testing laboratory in Kathmandu. Geological maps and landslide location maps are collected from previous research in the study area.

A test site was chosen within the study area at Markhu Village Development Committee, in the southeast part of the watershed near Kulekhani reservoir. The site is a landslide scrap that has been partially stabilized (Figure 4.10a). Four boreholes (BH1 to BH4) were drilled manually. All boreholes were within the partially-moving part of landslides. Boreholes were drilled to the depth of 4.0 m for in situ testing and sampling. Standard Penetration Tests (SPT) at various depths were conducted in each borehole. Some disturbed samples in various locations were also recovered for grain-size analysis. Four undisturbed samples from each BH were recovered for direct shear tests. The moisture contents of the undisturbed and disturbed samples were measured. Grain-size analyses were conducted for 14 samples recovered from various depths. In situ infiltration tests (Figure 4.10b) were conducted using the falling head method on each borehole, which was filled with a known volume of water and the time to infiltrate was observed. Eight samples at different depths were tested for moisture content and dry density. Four samples were tested for specific gravity of the soil samples. The sample associated with BHs, respective depth, and tested results are shown in Table 4.4.

83

(a)   (b)
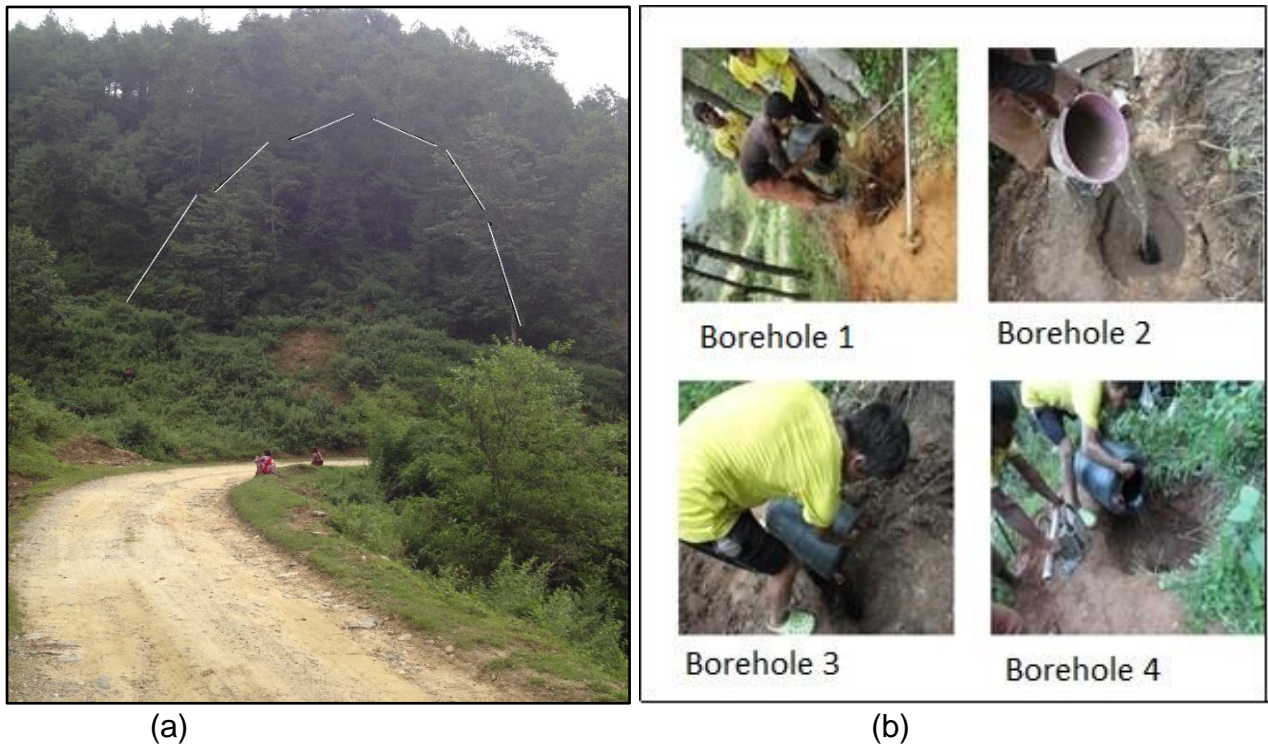
Figure 4. 10: (a) Field investigation location, Markhu, Kulekhani Watershed, (b) infiltration test.

The soil strength parameters, cohesion and angle of friction, were determined in direct shear test apparatus. Index properties of soil, such as water content and dry unit weight, were measured in the laboratory. Soil permeability was tested in situ in the open boreholes. Soil permeability was computed directly from the loss of water per unit surface area in the boreholes. The intake factor method suggested by Brand and Premchitt (1980) was used for computation, so Equation [4.18] and [4.19] were employed.

$$q = \frac{Q}{(T1 - T2)} \qquad [4.18]$$

$$K = \frac{q}{2.5DH} \qquad [4.19]$$

where the total volume of water applied is Q, the length of the permeability test hole is H, and the diameter is D. The coefficients of permeability, computed based on Brand Premchitt (1980), for all boreholes are shown in Table 4.4. The minimum coefficient of permeability from these observations is 0.00178 cm/sec. This will be used as the permeability of unsaturated soil with observed moisture conditions during testing. The degree of saturation is considered to be 100% on water content equivalent to the porosity of the soil.

The direct shear test (IS:2720-1985) was conducted for four samples. The friction angle of the samples ranged from 24 to 30 degrees, and the gravimetric water content from 18 to 25 percent. The cohesion ranged from 5 to 19 kPa. The dry unit weights of the samples ranged from 1.80 to 1.86 gm/cm^3. The strength parameters and moisture content observed in the testing were used for the slope stability computation. Soil strength parameters with associated borehole numbers are shown in Tables 4.5, and 4.6.

The initial moisture content, saturated moisture content, saturated unit weight, dry unit weight, specific gravity, void ratio, grain size distribution, and saturated cohesion and friction angle were identified from the collected samples. A SWCC from the grain size distribution of the overburden soil was developed.

Three categories of soil specific gravity values are taken for the whole watershed 2.61, 2.65, and 2.69; along with dry density of 1.46, 1.5, and 1.6 gm /cm^3; porosity of 0.40, 0.43, and 0.46; and bulk density of 1.80, 1.84, and 1.86 gm/cm^3. The observed average geotechnical properties of soil (Cohesion 11 kPa, Friction 28°) in the watershed are considered in the analysis. The moisture content conditions and grain-size analysis of

each location are used for soil suction analysis. The soil suction applied in the analysis ranges from 1 to 23 kPa. The information collected from different locations are interpolated and used for the entire watershed.

Table 4.4 Permeability of in situ soil.

Test Hole	Applied Volume of Water (cm^3/sec)	Diameter (mm)	Constant Head (cm)	Flow Rate (cm^3/sec)	Permeability (cm/sec)
1	4	101.6	400	75.76	0.00678
2	3	101.6	300	19.84	0.00237
3	3	101.6	300	36.23	0.004323
4	4	101.6	400	19.84	0.00177
				Average	0.00381

The computed matrix suction ranged from zero to 9000 kPa. The maximum matrix suction is observed in Okahrgau, sample number AS36 (Paudel 2018). The observed infiltration is very high, compared to normal rainfall intensity in the area. For the infiltration depth computation, rainfall intensity is used as a permeability coefficient in the analysis for low intensity, and infiltration rate is used for higher-intensity rainfall. Therefore, the observed infiltration rate of 0.00178 cm/sec was used as the permeability coefficient for the infiltration depth computation for high-intensity rainfall. Rainfall of four rain gauge stations Chisapani Ghadi, Daman, Markhu, and Thankot are used for the analysis. Two locations, Daman and Markhu, are within the watershed, and Chisapani Ghadi and Thankot are located close by. The maximum wetting depth is observed for a longer duration in recorded high rainfall, as infiltration is very high.

Table 4.5 Shear strength parameters of the soils tested.

Boreholes	Depth (m)	Cohesion (kPa)	Friction Angle Ø' (Degrees)	Water Content (%)	Classification	Bulk Density gm/cm^3	Specific Gravity
BH 1	0–1.5	15	30	23.03	ML, gravelly silt with sand.	1.79	2.70
	1.5–3.0	13	29	20.49	SM, silty sand with gravel.	1.81	2.65
	3.0–4.0	17	24	21.53	ML, gravelly silt with sand.	1.80	2.67
BH 2	0–1.5	15	29	21.31	SM, silty sand with gravel.	1.83	2.68
	1.5–3.0	19	25	18.21	ML, sandy silt with gravel.	1.86	2.63
	3.0–4.0	17	27	21.50	GM, silty gravel with sand.	-	2.70
BH 3	0–1.5	10	25	23.58	ML, sandy silt with gravel.	1.82	2.65
	1.5–3.0	5	32	24.49	ML, gravelly silt with sand.	1.84	2.69
	3.0–4.0	11	30	19.58	GM, silty gravel with sand.	-	2.67
BH 4	0–1.5	15	27	22.75	GM, gravelly silt with sand.	1.85	2.65
	1.5–3.0	17	26	21.15	GM, gravelly silt with sand.	1.84	2.61
	3.0–4.0	11	30	22.63	SM, silty sand with gravel.	1.83	2.48

The computed wetting front depths of all 73 locations in the watershed are used for interpolation in the GIS environment. The rainfall intensities considered in the analyses are assumed to be evenly distributed within the watershed. The average soil strength parameters observed in the old landslide area are applied to the whole watershed. The soil matrix suction analyzed from the SWCCs for 73 locations are interpolated to the whole watershed. The inverse distance weightage (IDW) method is used for interpolation of observed parameters in the raster map. Unit weight, friction, suction, and wetting depth maps are prepared as required for factors of the safety computation in map algebra. These raster maps are used to compute the factor of safety in the GIS

environment. The landslide susceptible watershed area based on the factor of safety, with respect to different rainfall, is developed.

The worst cloud burst rainfall induced landslide event is tested in the model for verification. The recorded maximum 24-hour rainfall of 540 mm at the Kulekhani dam site was used for this validation.

The selected shear strength parameters, cohesion and friction, are the tested average values applied in this study for the worst slope stability computation. The probable combination of different rainfall amounts is considered in the study. The groundwater influence is not considered because there is no stable groundwater table in the slope.

Table 4.6 Index properties of the soils tested.

Boreholes	Depth (m)	Void Ratio, e	Porosity, n	Volumetric Water, Θ	Degree of Saturation	Gravimetric Water Content	Dry Density ρ_d, (gm/cm³)	Moisture Content Residual	Tan Ø^b
BH 1	0–1.5	0.86	0.46	23.03	72.63	0.32	1.45	4.00	0.49
	1.5–3.0	0.76	0.43	20.49	71.43	0.29	1.51	5.00	0.43
	3.0–4.0	0.81	0.45	21.53	71.07	0.30	1.48	5.00	0.44
BH 2	0–1.5	0.70	0.41	21.31	68.22	0.27	1.55	4.00	0.40
	1.5–3.0	0.76	0.43	18.21	76.00	0.28	1.53	2.00	0.51
BH 3	0–1.5	0.84	0.46	23.58	78.53	0.31	1.47	4.00	0.54
	1.5–3.0	0.74	0.42	24.49	70.99	0.28	1.54	4.00	0.43
BH 4	0–1.5	0.76	0.43	22.75	79.70	0.29	1.51	5.00	0.50
	1.5–3.0	0.72	0.42	21.15	77.02	0.27	1.52	4.00	0.49
	3.0–4.0	0.66	0.40	22.63	85.30	0.27	1.49	2.00	0.61

4.4   Model verification (comparison of predicted and mapped landslide areas)

To assess the ability of the developed model to predict the landslide-susceptible zones (landslide initiation zones) in the study area, the predicted landslide initiation

zones are compared with the map of known previous landslide areas. It should be emphasized that these landslides maps include not only the landslide initiation zones but also the areas covered by the slid soil mass. Furthermore, these landslides were triggered by many different rainfall intensities and durations, not only by one duration and intensity. However, in the current validation, only one recorded rainfall event (rainfall duration and intensity) is consideted. The model analysis from the recorded rainfall of 540 mm in 24 hours is considered for validation. Figure 4.11 depicts this comparison. From this figure, it can be observed there is a relatively good agreement between the predicted landslide initiation zones and the areas affected by previous landslides. This figure also shows that the predicted landslide initiation zones are much smaller than the areas affected by previous landslides. Landslide records obtained from Kayastha et al. (2013), Dhital et al. (1993), Nippon Koei Co. Ltd. (1996), and Dhar and Dhital (2004) shows that 2.35 km^2 of the watershed area was covered with slide soil mass during the extreme rainfall. This is 1.9% of the total watershed. The predicted total unstable area from the model is 0.02% of the total watershed, and covers 0.023 km^2 of the watershed. This difference is explained by the following two factors: first, the areas affected by previous landslides not only include the initiation zones of the landslides (scrap of the landslide), but also the areas covered by the slide mass during its downhill travel (depends on the runout behavior). Second, one recorded rainfall event (540 mm rainfall in 24 hours) was considered in the simulated landslide-susceptible areas. However, the maps of the previous landslides included landslides triggered by all rainfall events that occurred in the study areas. Therefore, the area observed in the landslide is almost 102 times more than the area unstable at the moment. The area beyond the unstable area can be modeled as a debris flow, which is the objective of the next step of research.

The factor of safety and area unstable in extreme rainfall events are shown in Table 4.7.

Table 4.7 Tested Factor of Safety and watershed area in extreme rainfall.

Factor of Safety	Watershed Area (km^2)
1	0.023
1.50	0.034
2.00	0.045
2.50	0.056
3.50	0.068

4.5   Effect of rainfall duration on landslide initiation

Longer-duration low-intensity rainfall events are also identified as a threshold rainfall type for landslides in Nepal (Dahal and Hasegawa 2008). The intensity of 2 mm rainfall per hour for 100 hours or 6 mm rainfall per hour for 24 hours are considered as threshold rainfall amounts. These longer duration and low-intensity rainfall conditions are analyzed in the model. For 2 mm rainfall per hour for 100 hours, about 0.017% of the watershed area is unstable (Figure 4.12). The lowest factor of safety (FOS) observed is 0.90 for 0.017% and FOS of less than 1.5 for 0.026% of the watershed for this intensity and duration of rainfall. Similarly, for 6 mm of rainfall per hour for 24 hours, the minimum FOS observed is 0.97, as shown in Figure 4.13. The area of watershed unstable in FOS 0.97 and 1.50 are 0.015 and 0.022%, respectively, for this rainfall and intensity.
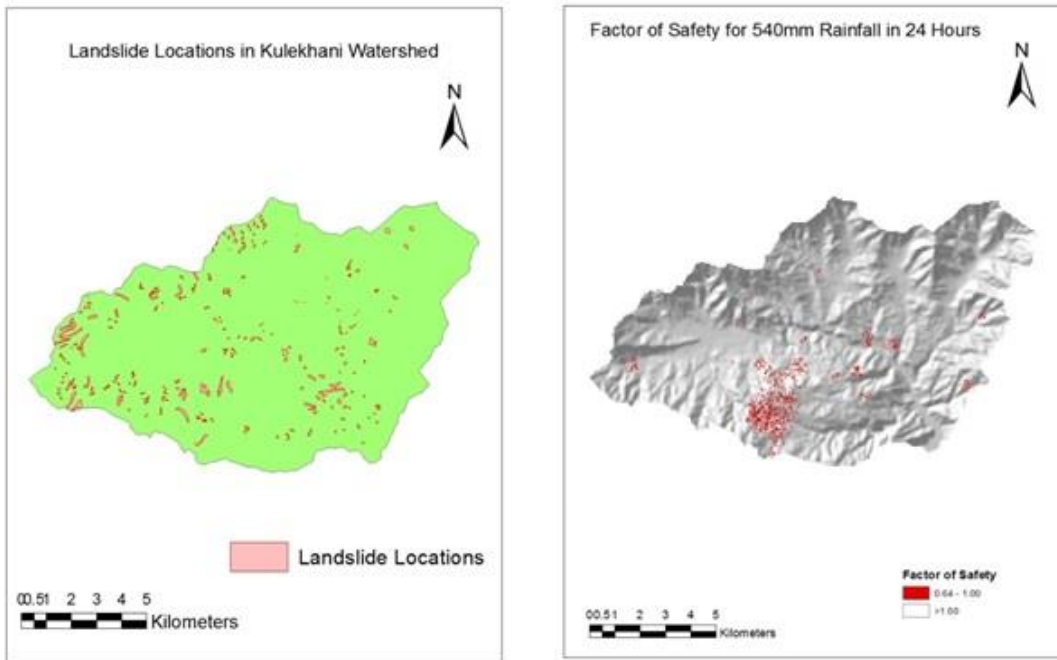
(a)   **(b)**

Figure 4.11: (a) Observed landslide areas (mainly) triggered by various rainfall durations and intensities (modified from Kayashta et al. 2013) and, b) predicted unstable slopes (landslides initiation zones) in the Kulekhani watershed for 540 mm rainfall in 24 hours.
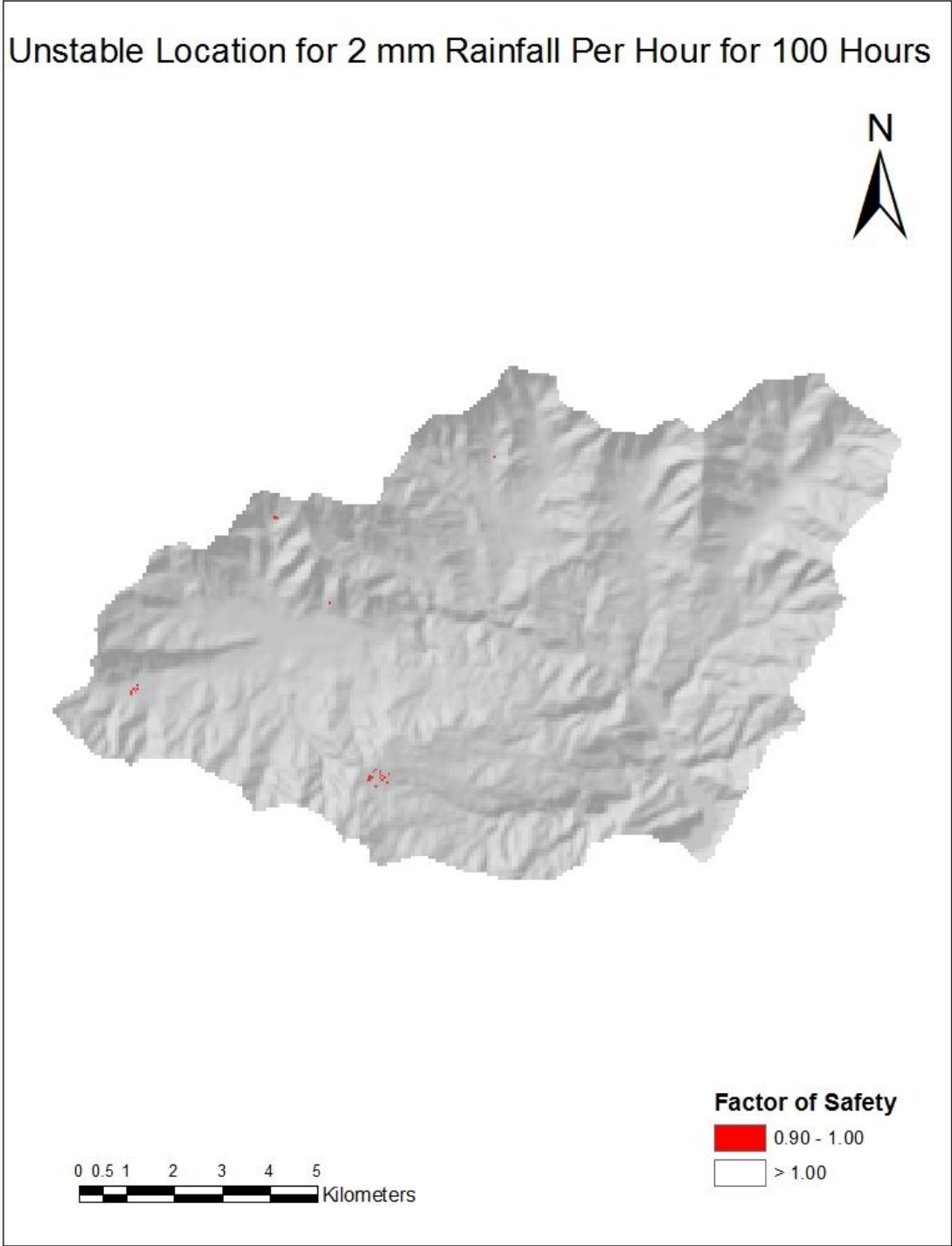
Figure 4.12: Spatial distribution of landslides for 2 mm of rainfall per hour for 100 hours.
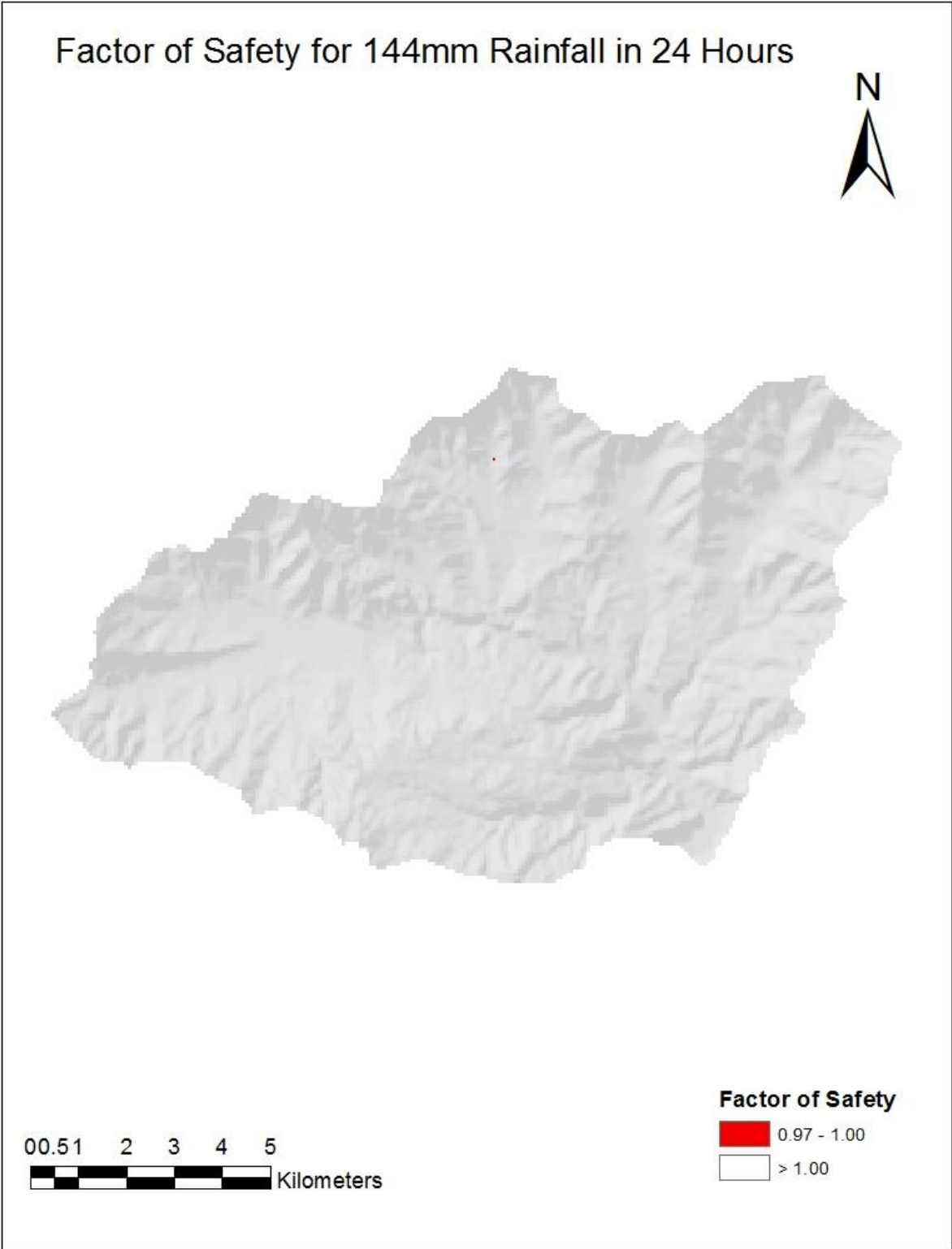
Figure 4.13: Spatial distribution of landslides for 144 mm of rainfall in 24 hours.

4.6   Effect of rainfall intensity on landslide initiation

The threshold rainfall for high-intensity short-period events is also identified for landslide initiation from previous studies (Dahal and Hasegawa 2008). One of the combinations is 12 mm of rainfall per hour for 10 hours. This intensity of rainfall and duration is tested in the model, and it is found that there are no unstable locations within the watershed, as shown in Figure 4.14. The minimum FOS observed from this rainfall intensity and duration is 1.02. The percentage of area within the watershed for FOS 1.02 and 1.5 is identified as 0.014 and 0.021, respectively. Unlike other figures, the orange color shown in Figure 4.14 does not indicate unstable areas, but areas where FOS is about 1.02. This combination of rainfall and intensity has less impact compared to the other two combinations discussed in the previous section.

Figure 4.15 shows FOS and unstable watershed area for these three threshold rainfall intensities and durations. As mentioned earlier, 2 mm rainfall per hour for 100 hours is more severe than 144 mm rainfall in 24 hours or 12 mm rainfall per hour for 10 hours in this watershed.
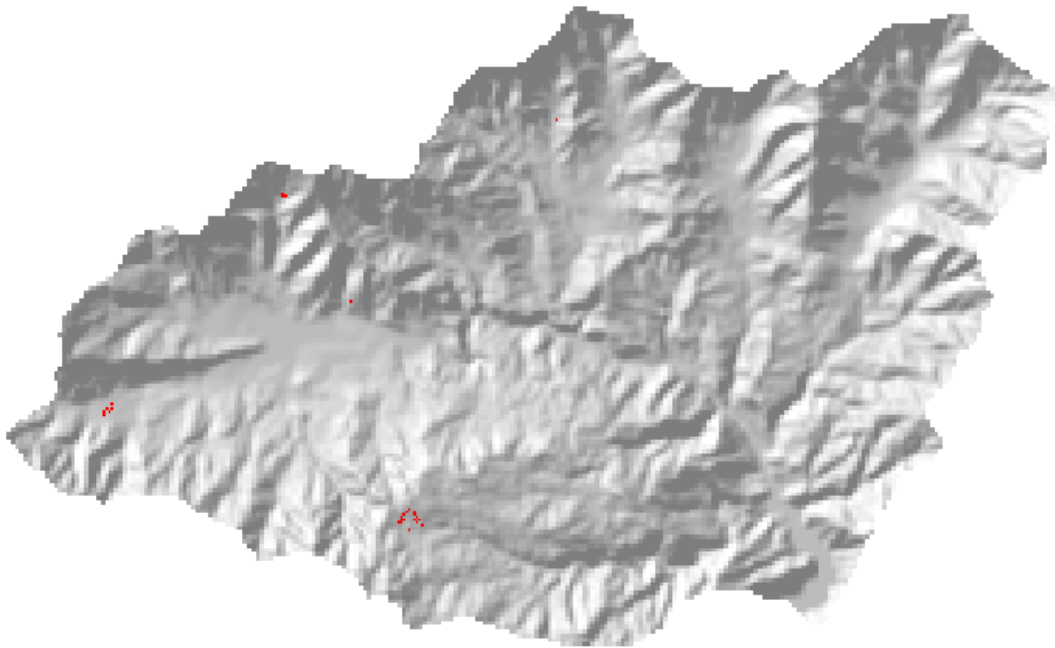
Figure 4.14: Unstable area of FOS 1.01 for 12 mm per hour rainfall for 10 hours.
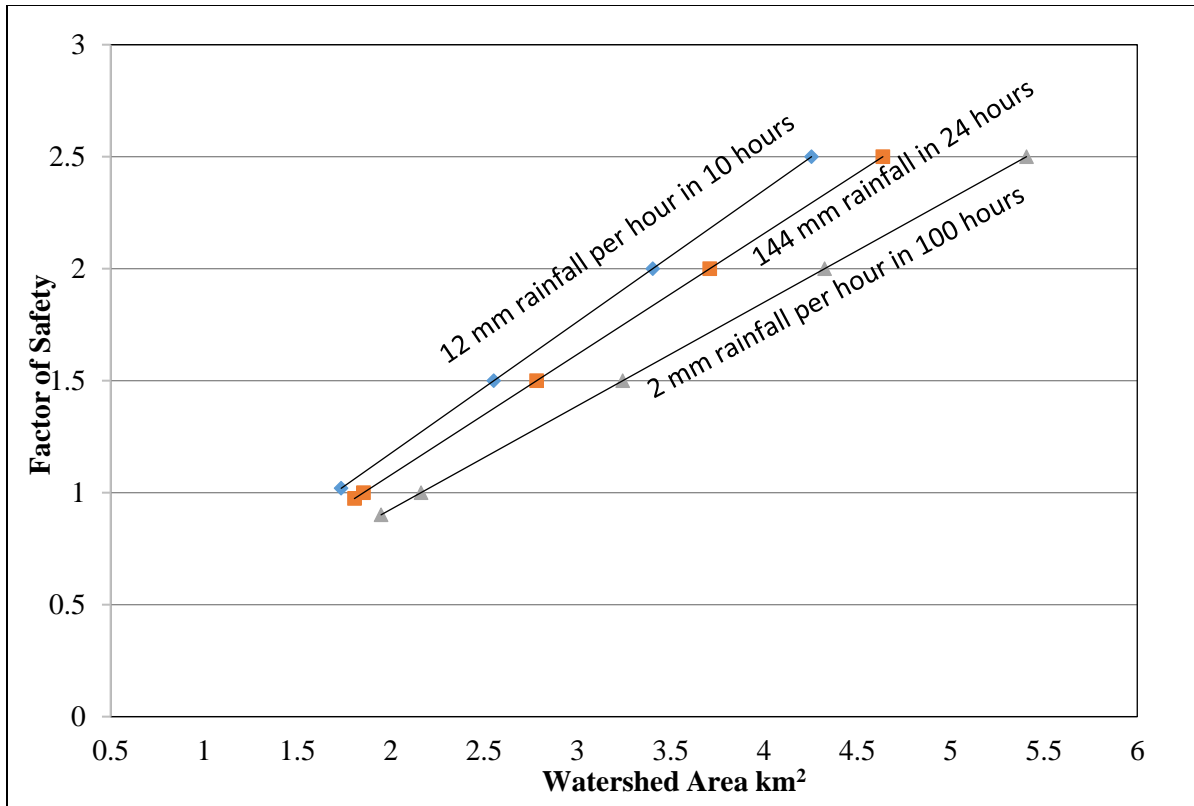
Figure 4.15: Relation of FOS to unstable slope area for threshold rainfall intensity and duration.

Further analysis has been carried out using this model for high-intensity rainfall. As infiltration of the watershed is about 63 mm per hour, the same rainfall intensity is used in the analysis. If rainfall intensity is more than 63 mm, it will have a similar effect on infiltration depth and stability of the slope as in excess of 63 mm rainfall through surface runoff. For a 24-hour recorded rainfall of 540 mm, the worst conditions of continuous rainfall could be 62.99 mm (approximately 63 mm) per hour for 8.57 hours. These combinations from one hour to 24 hours of recorded rainfall of 540 mm are used for the stability analysis. Figures 4.16 and 4.17 show a trend of landslide initiation from one to 24 hours with total rainfall of 540 mm distributed as assumed 63 mm rainfall intensity for 8.57 hours. Assumed rainfall 63 mm per hour may be continue for 8.57 hours but it may decrease with duration more than 8.57 hours. The rainfall intensity decreases for durations of more than 8.57 hours for given 540mm total rainfall. The unstable watershed area is shown as a percentage in Figure 4.16, and in km^2 in Figure 4.17. The

cumulative rainfall for this case is 540 mm, and the duration is extended from 1 hour to 24 hours. It is observed that the rate of unstable watershed area per hour in a given factor of safety gradually decreased with duration when the total maximum daily rainfall, 540 mm, was distributed from one hour to 24 hours.
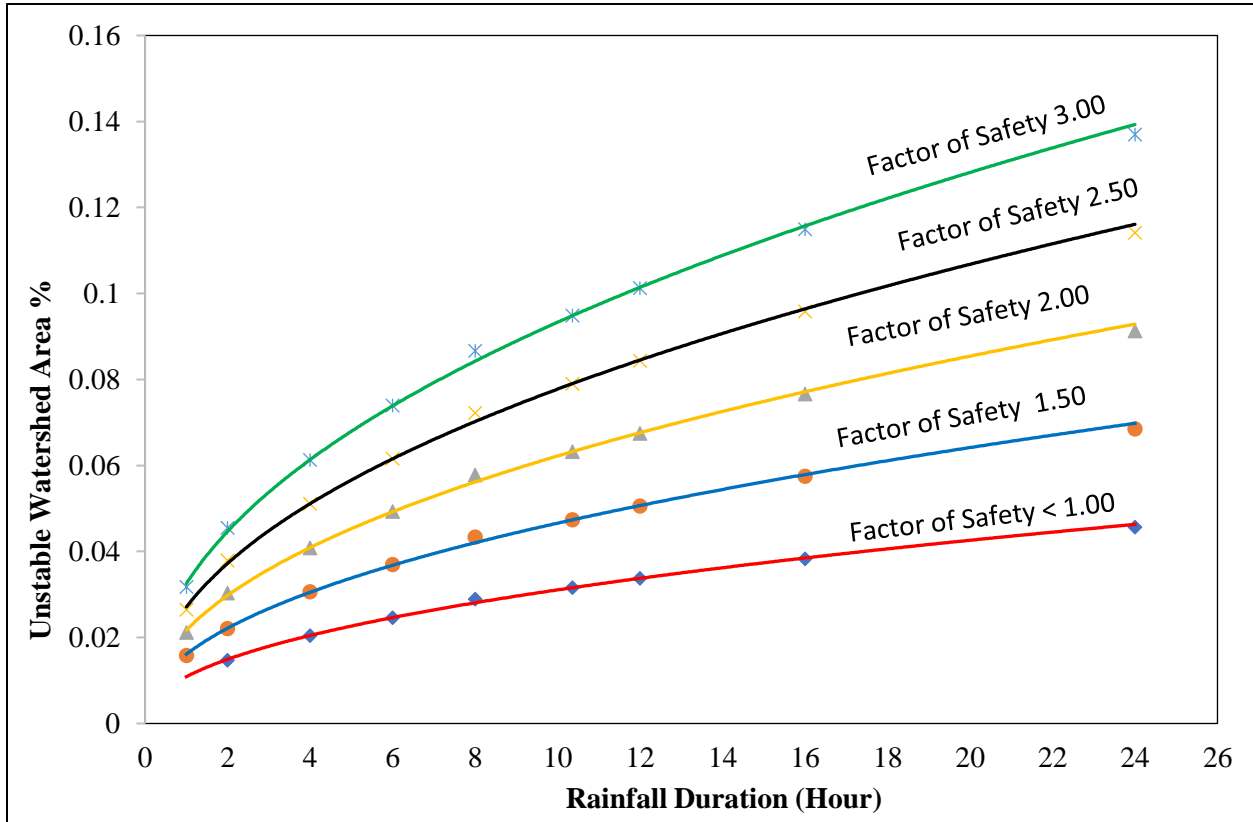
Figure 4.16: Percantage of unstable watershed area and rainfall duration with different FOS.
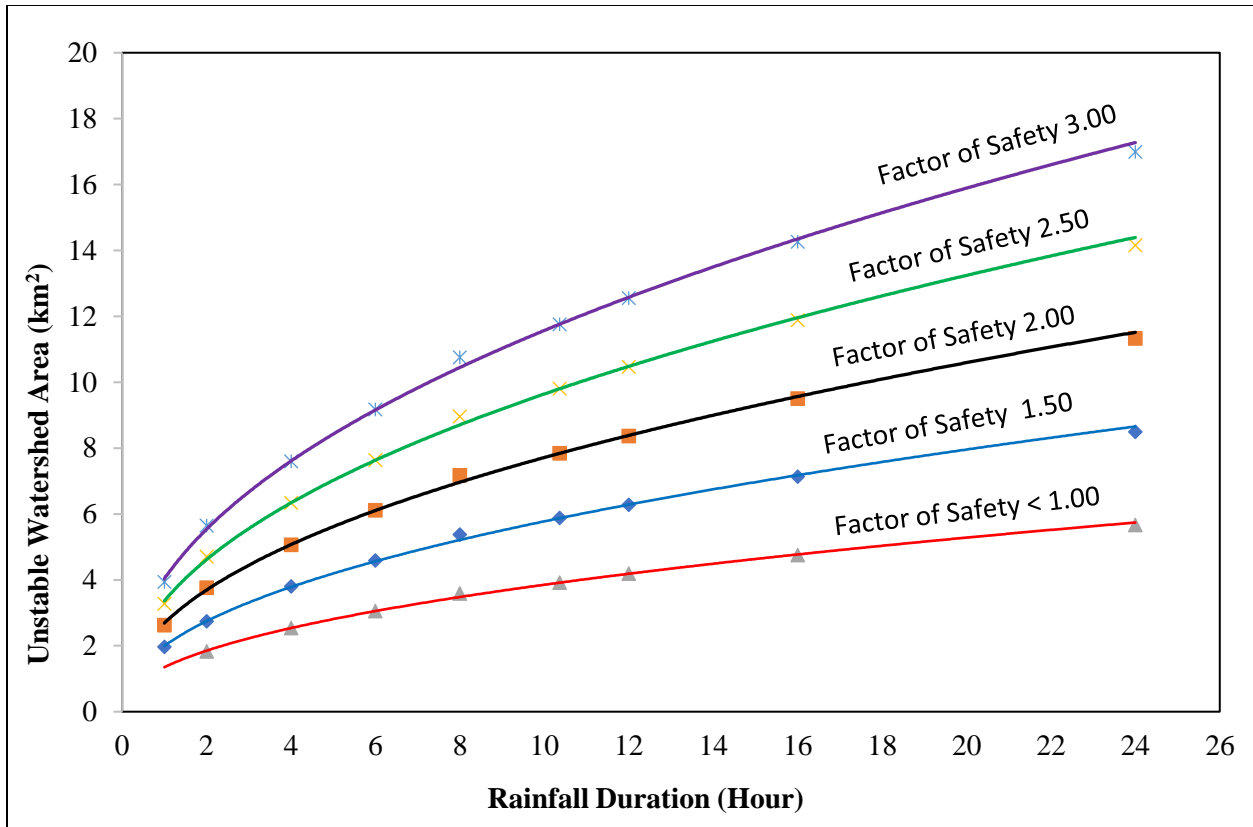
Figure 4.17: Unstable watershed area in km² and rainfall hours with different FOS.

4.7.   Summary and conclusions

In this study, a rainfall-induced landslide susceptibility map for Nepalese mountain areas has been developed within a GIS environment by including unsaturated soil conditions. Details of soil characteristics, grain size, initial moisture content, specific gravity, unit weight, in situ infiltration capacity, shear strength parameters, index property, and rainfall in the study area are applied in the unsaturated slope stability model. Wetting front depth depends mainly on rainfall, type of soil, initial moisture content, and infiltration capacity. Infiltration capacity of the watershed soil was higher than rainfall intensity in most of the cases. The wetting front increases with duration and rainfall intensity up to 63 mm per hour. Previously-identified threshold rainfall amounts for landslide initiation are tested. Some of the recommended rainfall intensity and duration for landslide initiation in the region are applied for the watershed. The spatial

distributions of landslides in those threshold conditions are identified. The expected maximum rainfall and its implication on slope stability is analyzed. Some locations are unstable at the expected higher rainfall in this watershed. The result of the combination of continuous rainfall with longer durations was an increasing trend of wetting front and instability of the slopes. This trend is studied for up to 24 hours of rainfall duration. The worst condition in the watershed is higher-intensity rainfall up to 63 mm per hour. The longer the duration of rainfall intensity close to 63 mm per hours, the higher the landslide susceptibility.

4.8   References

Acharya, G., De Smedt, F., Long, N.T. (2006), Assessing landslide hazard in GIS: a case study from Rasuwa, Nepal. Bull Eng Geol Environ, 65, (1), 99–107.

Agus, S.S, Leong, E.C. Rahardjo, H. (2004), Estimating Permeability function of Singapore residual soils, Engineering Geology 78, 119-133.

Agus, S.S, Leong, E-C. Rahardjo, H. (2004), Soil-water characteristiccurve of Singapore residual soils, Journal of Geotechnical and Geological Engineering 19, 285-309.

Aleotti, P. (2004), A warning system for rainfall-induced shallow failures, Engineering Geology, 73, 247–265.

Bhandary, N.P., Yatabe, R., Dahal, R.K., Hasegawa, S., Inagaki, H. (2013), Areal distribution of large-scale landslides along highway corridors in central Nepal, Georisk: Assessment and Management of Risk for Engineered Systems and Geohazards, pp 31.

Bijukchhen, S.M., Kayastha, P., Dhital, M.R. (2012), A comparative evaluation of heuristic and bivariate statistical modelling for landslide susceptibility mappings in Ghurmi–Dhad Khola, East Nepal. Arab J Geosci.

Brand, E.W., Premchitt, J. (1980), Shape factor of Cylindrical Piezometers, Geotechnique, 30, (4), 369-387.

Caine, N. (1980), The Rainfall Intensity: Duration Control of Shallow Landslides and Debris Flows Geografiska Annaler. Series A, Physical Geography, 62, (1/2), 23-27.

Caine, N., Mool, P.K. (1982), Landslides in the Kolpu Khola drainage, Middle Mountains, Nepal. Mt Res Dev 2,157–173.

Cancelli, A., Nova, R. (1985), Landslides in soil debris cover triggered by rainstorms in Valtellina (central Alps – Italy), in: Proceedings of the 4th International Conference and Field Workshop on Landslides, The Japan Geological Society, Tokyo, 267–272.

Carman, P.C. (1939), Permeability of saturated sands, soils and clays, Journal of Agricultural Science, 29, 263-273.

Carrier III, W.D. (2003), Goodbye, Hazen, Hello, Kozeny-Carman, ASCE J Geotech Geoenviron 129: 1054-1056.

Casadel, M. Dietrich, W.E., Miller N.L. (2003), Testing a model for predicting the timing and location of shallow landslide initiation in soil-mantled landscapes, Earth Surf. Process and Landforms 28, 925-950.

Ceriani, M., Lauzi, S., Padovan, N. (1992), Rainfalls and landslides in the alpine area of Lombardia region – Central Alps – Italy, Proc. Interpraevent, Bern, Switzerland, Band 2, 9–20.

Ceriani, M., Lauzi, S., Padovan, N. (1994), Rainfall thresholds triggering debris-flows in the alpine area of Lombardia Region, central Alps – Italy, Proc. Man and Mountain, I Conv. Intern. per laProtezione e lo Sviluppo dell'ambiente montano, Ponte di legno (BS), 123–139.

Chen, L., Young, M.H. (2006), Green-Ampt infiltration model for sloping surfaces, Water Resour. Res., 42, W07420, doi:10.1029/2005WR004468.

Chen, C.Y., Chen, T.C., Yu, F.C., Lin, S.C. (2005), Analysis of time-varying rainfall infiltration induced landslide Environ Geol 48: 466–479.

Chalise, S.R., Khanal, N.R. (2001), Rainfall and related natural disasters in Nepal. In: Tianchi, Li., Chalise S.R., Upreti, B.N. (eds), Landslide hazards, mitigation to the Hindukush-Himalayas. ICIMOD, Kathmandu, pp 63–70.

Chiang, S.H., Chang, K.T., Mondini, A.C., Tsai, B.W., Chen, C.Y. (2012), Simulation of event-based landslides and debris flows at watershed level, Geomorphology, 138, PP 306–618.

Cho, S.E., Lee, S.R. (2002), Evaluation of surficial stability for homogeneous slopes considering rainfall characteristics, Journal of Geotechnical and Geoenvironmental Engineering 128, 9, 756–763.

Claunitzer, V. Hopmans, J.W. Starr, J.L. (1998), parameter uncertainty analysis of common infiltration models. Soil Science Soc Am Journal 62, 1477-1487.

Crosta, G.B., Frattini, P. (2001), Rainfall thresholds for triggering soil slips and debris flow, in: Proceedings of the 2nd EGS Plinius Conference on Mediterranean Storms, edited by: Mugnai, A., Guzzetti, F., and Roth, G., Siena, Italy, 463–487.

Dahal, R.J., Hasegawa, S., Bhandary, N.P., Poudel, P.P., Nonomura, A., Yatabe, R. (2012), A replication of landslide hazard mapping at catchment scale, Geomatics, Natural Hazards and Risk Vol. 3, No.2, 161-192.

Dahal, R.K. and Hasegawa, S. (2008), Representative rainfall thresholds for landslides in the Nepal Himalaya, Geomorphology Vol. 100, No.3-4, pp. 429-443.

Dahal, R.K., Hasegawa, S., Nonomura, A., Yamanaka, M., Dhakal, S., Paudyal, P. (2008), Predictive modelling of rainfall-induced landslide hazard in the Lesser Himalaya of Nepal based on weights-of-evidence. Geomorphology, 102, (3–4): 496–510.

Dahal, R.K., Hasegawa S., Masuda, T., Yamanaka M. (2006), Roadside Slope Failures in Nepal during Torrential Rainfall and their Mitigation. Universal Academy Press, Inc. / Tokyo, Japan, 503–514.

Dhakal, A.S., Amada, T., Aniya, M. (1997), A GIS approach to landslide susceptibility mapping: A case study from the Kulekhani watershed, Nepal. In: Proceeding from 18th Asian Conference on Remote Sensing, Kuala Lumpur, Malaysia. Pp JS-6-1 to JS-6-6.

Dhakal, A.S., Amada, T., Aniya, M. (1999), landslide hazard mapping and the application of GIS in the Kulekhani watershed Nepal. Mountain Research and Development, v. 19(1) 3-16.

Dhakal, A.S., Amada, T., Aniya, M. (2000), landslide hazard mapping and its evaluation using GIS: An investigation of sampling scheme for grid-cell based quantitative method. Photogrammetric Engineering and Remote Sensing 66, 981-989.

Dangol, V., Upreti, B.N., Dhital, M.R., Wagner, A., Bhattarai, T.N., Bhandari, A.N., Pant, S.R., Sharma, M.P. (1993), Engineering geological study of a proposed road corridor in eastern Nepal. Bulletin of the Department of Geology, Tribhuvan University, Nepal, Special Issue, 3(1), 91-107.

Deoja, B.B., Dhital, M.R., Thapa, B., Wagner, A. (1991), Mountain risk engineering handbook, International Centre for Integrated Mountain development (ICIMOD), Kathmandu, Nepal, pp 875.

Devkota, K.C., Regmi, A.D., Pourghasemi, H.R., Yoshida, K., Pradhan, B., Ryu, I.C., Dhital, M.R., Althuwaynee, O.F. (2013), Landslide susceptibility mapping using certainty factor, index of entropy and logistic regression model in GIS and their comparison at Mugling-Narayanghat road section in Nepal Himalaya, Nat Hazard 65: 135-165.

Dhar, M.S., Dhital, M.R. (2004) Application of Morishita Spread Index in the study of landslides from the Kulekhani watershed, central Nepal. Jour. Nepal Geol. Soc., v.30, pp.123-126.

Dhital, M.R., Khanal, N., Thapa, K.B. (1993), The role of extreme weather events, mass movements, and land use changes in increasing natural hazards, A Report of the preliminary field assessment and workshop on causes of recent damage incurred in southcentral Nepal, July 19-20 1993. ICIMOD, Kathmandu, 123 pp.

Dhital M.R. (2003), Causes and consequences of the 1993 debris flows and landslides in the Kulekhani watershed, central Nepal, Debris-flow Hazards Mitigation:Mechanics, Prediction and assessment, Rickenmann &Chen (eds) pp 1931-1943.

Dhital, M.R. (2000). An overview of landslide hazard mapping and rating systems in Nepal. J Nepal Geol Soc, 22: 533–538.

Dhital, M.R., Upreti B.N., Dangol, V., Bhandari A.N., Bhattarai, T.N. (1991), Geological engineering methods applied in mountain road survey: an example from Baitadi-Darchula Road Project, Nepal. Journal of Nepal Geological Society, 7, 49-67.

Dhital, M.R. (2005), Landslide investigation and mitigation in Himalayas: focus on Nepal. In: Proceedings of International Symposium Landslide Hazard in Orogenic Zone from the Himalaya to Island Arc in Asia, Kathmandu, Nepal, 1–1.

Dietrich, W.E., Reiss, R., Hsu, M., Montgomery, D.R. (1995), A process-based model for colluvial soil depth and shallow landsliding using digital elevation data, Hydrological Process 9, 383-400.

DWIDP (Department of Water Induced Disaster Prevention (2017), Annual disaster review 2009, Ministry of Irrigation, Government of Nepal, Kathmandu pp.

Enrico, C., Antonello, T. (2012), Simplified approach for the analysis of rainfall-induced shallow landslides, Journal of Geotechnical and Geoenvironmental Engineering 138, pp 398-406.

Fall, M. (2009), A GIS-based mapping of historical coastal cliff recession. Bulletin of Engineering Geology and Environment 68(4): 473-482.

Fall, M., Azzam, R., Noubactep, C. (2006), A multi-method approach to study the stability of natural slopes and landslide susceptibility mapping, Engineering Geology 82 (2006) 241– 263.

Fredlund, D.G., Morgenstern, N.R., and Widger, R.A. (1978), Shear strength of unsaturated soils, Can. Geotech. J 15, 313–321.

Fredlund, D.G., Rahardjo, H., Can, J.K.M. (1987), Nonlinearity of strength envelope for unsaturated soils. Proceedings of the 6th International Conference on Expansive Soils, New Delhi, India, pp. 49-54.

Fredlund, D.G., Xing, A., Fredlund M.D., Barbour, S.L. (1996), The relation of the unsaturated soil shear strength to the soil-water characteristics curve. Canadian Geotechnical Journal 33, 440-448.

Fredlund, D.G. and Xing, A.E. (1994), Equation for the soil-water characteristic curve, Can. Geotech. J 31:521-532.

Fredlund, D.G., Rahardjo, H. (1993), Soil Mechanics for unsaturated Soils, John Wiley and Sons, Canada.

Fredlund, M.D., Wilson, G.W., Fredlund, D.G. (2002), Use of the grain-size distribution for estimation of the soil-water characteristic curve, Can. Geotech. J, 39: 1103-1117.

Fredlund, D.G., Rahardjo, H. (1993), Soil Mechanics for Unsaturated Soil, A Wiley –Interscience Publication, John Wiley and Sons Inc.

Garven, E., Vanapalli, S.K. (2006), Evaluation of empirical procedures for predicting the shear strength of unsaturated soils. American Society of Civil Engineers Geotechnical Special Publication No. 147, Vol. 2, pp. 2570-2581.

Ghimire, M. (2011), Landslide occurrence and its relation with terrain factors in the Siwalik Hills, Nepal: case study of susceptibility assessment in three basins. Nat Hazards, 56(1): 299–320.

Gabet, E.J., Burbank, D., Putkonen, J.K., Pratt-Sitaula, B.A., Ojha, T. (2004), Rainfall thresholds for landsliding in the Himalayas of Nepal Geomorphology 63,131 – 143.

Gerrard, J., Gardner, R.A.M., (2000), Relationships between rainfall and landsliding in the Middle Hills, Nepal. Norsk geogr. Tidsskr. 54, 74–81.

Green, W.H., Ampt, C.A. (1911), Studies on soil physics, flow of air and water through soils. Journal of Agricultural Science 4:1–24.

Hagen, T. (1969), Report on the geological survey of Nepal preliminary reconnaissance. Zürich Mémoires de la soc. Helvétique des sci. naturelles, pp185.

Horton, P., Jaboyedoff, M., Rudaz, B., and Zimmermann, M. (2013), FlowR, a model for susceptibility mapping of debris flows and other gravitational hazards at a regional scale, Nat. Hazards Earth Syst. Sci., 13, pp 869–885.

Hsu, S.M., Ni, C.F., Hung, P.E. (2002), Assessment of three infiltration formulas based on model fitting on Richard's equation, Journal of Hydrologic Engineering 7, (5) 373-379.

Hasegawa, S., Dahal, R.K., Yamanaka, M., Bhandari, N.P., Yatabe, R., Inagaki, H. (2009), Causes of large landslides in the Lesser Himalaya of central Nepal. Environ Geol 57:1423-1434.

Iverson, R.M. (2000), Landslide triggering by rain infiltration, Water Resources Research Vol 36, 7 1897-1910.

Kayastha, P., De Smedt, F. (2009), Regional slope instability zonation using GIS technique in Dhading, Central Nepal. In: Malet J P, Remaître A, Boggard T, eds. Landslide Processes: From Geomorphologic Mapping to Dynamic Modelling, CERG, France, 303–309.

Kayastha, P., Dhital, M.R., Smedt, F.D. (2013), Evaluation and comparison of GIS based Landslide Susceptibility Mapping Procedures in Kulekhani Watershhed, Nepal. Jurnal of Gelogical Society of India, v 81, 219-231.

Kayastha, P., Dhital, M.R., Smedt, F.D. (2012), Landslide Susceptibility mapping using the weight of evidence method in the Tinau Watershed, Nepal. Nat Hazards 63:479-498.

Kayastha, P., De Smedt, F., Dhital, M.R. (2010), GIS based landslide susceptibility assessment in Nepal Himalaya: a comparison of heuristic and statistical bivariate analysis. In: Malet J P, Glade T, Casagli N, eds. Mountain Risks: Bringing Science to Society. CERG Editions, 121–128.

K.C., S. (2013), Community vulnerability to floods and landslides in Nepal ecology and society 18(1): 8. (http://dx.doi.org/10.5751/ES-05095-180108.).

Kim, D., Im, S., Lee, S.H., Hong, Y., Cha, K.S. (2010), Predicting the Rainfall-Triggered Landslides in a Forested Mountain Region Using TRIGRS Model, J. Mt. Sci., 7, pp 83–91.

Kozeny, J. (1927), Ueber Kapillare Leitung des Wassers im Boden. Sitzungsber Akad. Wiss., Wien, 136 (2a) 271-306.

Khallili, N., Khabbaz, M.H. (1998), A unique relationship for the determination of the shear strength of unsaturated soils. Geotechnique, 48(5), 681-687.

Lamichhane, S.P. (2000), Engineering geological watershed management studies in the Kulekhani watershed, M,Sc. Thesis, Tribhuvan, University, Nepal

Leong, E.C., Rahardjo, H. (1997), Review of soil-water Characteristic Curve Equations, Journal of Goenvironmental Engineering, Vol.123, No 12, 1106-1117.

Lumb, P. (1962), Effect of rainstorm on slope stability. In: Proceeding of the symposium on Hong Kong Soils, Hong Kong, pp 73–87

Lu, N., Godt, J. (2008), infinite slope stability under unsaturated seepage conditions Water Resources Research v 44 w11404, pp13

Mein, R.G., Larson, C.L. (1973), Modelling infiltration during a steady rain. Water Resources Research 9(2), 384–394.

Meyer, N.K., Dyrrdal, A.V., Frauenfelder, R., Etzelmuller, B., Nadim, F. (2012), Hydrometeorological threshold conditions for debris flow initiation in Norway, Nat. Hazards Earth Syst. Sci., 12, 3059–3073, 2012.

Ministry of Home, Nepal Disaster Report (2015), public web resource: http://neoc.gov.np/en/publication/.

Muntohar, A.S. and Liao, H.J. (2009), Analysis of rainfall-induced infinite slope failure during typhoon using a hydrological–geotechnical model, Environ Geol (2009) 56:1145–1159.

Neaupane, K.M., Piantanakulchai, M. (2006), Analytic network process model for landslide hazard zonation, Eng Geol 85:281-294.

Nepal map for study area: http://www.infoplease.com/atlas/country/nepal.html.

NIPPON KOEI Co. Ltd. (2008), The study on disaster risk management for Narayangharh-Muglung Highway, Interim Report.

O'Connor J.E., Hardison, J.H. III, Costa J.E. (1997), Debris flows from moraine-dammed lakes in the Three Sisters and Mt. Jefferson Wilderness Areas, Oregon. US Geol. Surv. WaterSupply Pap.

O'Connor, J.E., Hardison, J.H., Costa J.E. (1993), Debris flows from recently deglaciated areas on central Oregon Cascade Range volcanoes, Eos Trans. AGU, 74, Fall Meet. Suppl., 314.

Pantha, B.R., Yatabe, R., Bhandary, N.P. (2010), GIS-based highway maintenance prioritization model: an integrated approach for highway maintenance in Nepal Mountains. J Transp Geogr, 18(3): 426–433.

Park, D.W., Nikhil, N.V., Lee, S.R. (2013), Landslide and debris flow susceptibility zonation using TRIGRS for the 2011 Seoul landslide, Nat. Hazards Earth Syst. Sci., 13, 2833–2849.Poudyal, C. P., Chang, C., Oh, H., Lee, S. (2010), Landslide susceptibility maps comparing frequency ratio and artificial neural networks: a case study from the Nepal Himalaya. Environ Earth Sci, 61(5), 1049–1064.

Petley, D., Hearn, G.J., Hart, A. (2007), Trends in landslide occurrence in Nepal. Natural Hazards, 43, 23-44.

Ray, R. L, Smedt De, F. (2009), Slope stability analysis on a regional scale using GIS: a case study from Dhading, Nepal. Environ Geol, 57(7): 1603–1611.

Rahardjo, H., Ong, T.H., Rezaur, R. B., Leong, E.C. (2007), Factors controlling instability of homogeneous soil slopes under rainfall. J. Geotech. Geoenviron. Eng., v 133, n12, 1532–1543.

Regmi, N.R., Giardino, J.R., Vitek., J.D. (2010), Assessing susceptibility to landslides using models to understand observed changes in slopes, Geomorphology, 122(1–3): 25–38.

Regmi, M.K. (2002), Geology of Kulekhani watershed in central Nepal with special reference to landslides and weathering, M.Sc. Thesis, Tribhuvan University, Nepal.

Saito, H., Nakayama, D., and Matsuyama, H. (2010), Relationship between the initiation of a shallow landslide and rainfall intensity duration thresholds in Japan, Geomorphology, 118, 167–175.

Salciarini, D., Godt, J. W., Savage, W., Z., Conversini, P., Baum, R. L., Michael, J.A. (2006), Modeling regional initiation of rainfall-induced shallow landslides in the eastern Umbria Region of Central Italy, Landslide (2006) 3 181-194.

Salciarini, D., Godt, J.W., Savage, W. Z., Baum, R. L., Conversini, P. (2008), Modeling landslide recurrence in Seattle, Washington, USA, Engineering Geology 102 (2008) 227–237.

Savage, W. Z., Baum, R. L. (2005), Instability of steep slopes, Chapter 4, in Debris- flow Hazards and Related Phenomena, edited by M. Jacob and O. Hungr, pp. 53–79, Praxis Publishing House and Springer, Chichester, U.K.

Shakya, B. (2002), A new approach within hydrometerological technique for the estimation of average depth of probable maximum precipitation (PMP) over Nepal. In: Wu et al. (Ed0, Flood Defence 2002, Science press, New York Ltd., pp 599-606.

Sharma, R.H., Shakya, N.M. (2008), Rain induced shallow landslide hazard assessment for ungauged catchments, Hydrogeol J, 16(5):871–877.

Stocklin, J., Bhattrai, K.D. (1981), Geology of Kathmandu area and Central Mahabharat Range, Nepal Himalaya, United Nations Mineral Exploration Technical Report, UNDP/Nepal, page 61.

Sun, H.W., Wong, H.N., Ho, K.K.S. (1998), Analysis of infiltration in unsaturated ground. In Slope Engineering in Hong Kong (Li KS, Kay JN and Ho KKS (eds)). Balkema, Rotterdam, the Netherlands, pp. 101–109.

Thapa, P.B., Dhital, M.R. (2000), Landslide and debris flows of 19–21 July 1993 in the Agra Khola watershed of central Nepal. J Nepal Geol Soc, 21: 5–20.

Torres, G.H. (2011), Estimating the soil-water characteristics curve using grain-size analysis and plasticity index, M.Sc, Thesis, Arizona State University, Tempe, AZ.

Tsai, T.L., Chiang, S.J. (2013), Modeling of layered infinite slope failure triggered by rainfall, Environmental Earth Sciences, Vol. 68, No. 5, pp 1429-1434.

Tsai, T.L., Yang, J.C. (2006), Modeling of rainfall-triggered shallow landslide Environ Geol (2006) 50: 525–534.

Upreti, B.N., Dhital, M.R. (1996), Landslide studies and management in Nepal, International Centre for Integrated Mountain Development (ICIMOD), Kathmandu, Nepal, pp 87

Upreti, B.N., Dhital M.R. (1996), Landslide studies and management in Nepal. A publication of ICIMOD (1996), Kathmandu, Nepal, 1-34.

Upreti B.N. (2001), The physiography and geology of Nepal and their bearing on the landslide problem. Tianchi L., Chalise S.R., and Upreti B.N. (eds) Landslide hazard mitigation in the Hindu-Kush Himalayas, ICIMOD, Nepal, 31-49.

Vanapalli, S.K., Fredlund, D.G. Pafahl, D.E., Clifton, A.W. (1996), Model for the prediction of shear strength with respect to soil suction, Canadian, Geotechnical, Journal 33 379-392.

Vanapalli, S.K., Fredlund, D.G. (1999), Empirical Procedures to predict the shear strength of unsaturated soils. Eleventh Asian Regional Conference on Soil Mechanics and Geotechnical Engineering, Hong et al. (eds) @Balkema, Rotterdam, ISBN 90 58090531.

Vanapalli, S.K., Fredlund, D.G. (2000), Comparison of different procedures to predict the shear strength of unsaturated soils uses the soil-water characteristic curve. Geo-Denver 2000, American Society of Civil Engineers, Special Publication, No. 99, pp. 195-209.

Wagner, A. (1997), Hazard mapping and geophysics applied to landslide study in the Himalayas and Hindukush, an unpublished brochure submitted to ITECO Nepal.

Wieczorek, G.F. (1987), Effect of rainfall intensity and duration on debris flows in central Santa Cruz Mountains, California, in: Debris Flows/Avalanches: Processes, Recognition and Mitigation, edited by: Costa, J. E. and Wieczorek, G. F., Reviews in Engineering Geology, Geological Society of America, 7, 23–104.

Yagi, H. (2001), Landslide study using aerial photographs, Landslide Hazard Mitigation in the Hindu Kush-Himalayas. In: Tianchi L, Chalise SR, and Upreti BN (eds) Landslide hazard mitigation in the Hindu-Kush Himalayas, ICIMOD, Nepal, 79

Yagi, H., Nakamura S. (1995), Hazard mapping on large scale landslides in the lower Nepal Himalayas. In: Proceedings of international seminar on water induced disasters (ISWID-1995), DPTC-JICA, Kathmandu, Nepal, 162-168.

Zhang, L.L, Zang, J., Zang, L.M., Tang, W.H. (2011), Stability of analysis of rainfall induced slope failure: a review, Geotechnical Engineering Volume 164 Issue GE5, Institute of Civil Engineers Geotechnical Engineering 164 October 2011 Issue GE5.

Zapata, C.E. (1999), Uncertainity in Soil-Water Characteristic Curve and Impacts on unsaturated shear strength Prediction. Ph.D. Dissertation, Arizona State University, Tempe, United States.

Zezere, J.L., Trigo, R.M., and Trigo, I.F. (2005), Shallow and deep landslides induced by rainfall in the Lisbon region (Portugal): assessment of relationships with the North Atlantic Oscillation, Nat. Hazards Earth Syst. Sci., 5, 331–344, 2005.

Chapter 5: Technical Paper 2 - GIS-based assessment of debris flow runout in Kulekhani Watershed, Nepal

Bhuwani Prasad Paudel, Mamadou Fall, Bahram Daneshfar

Abstract

Rainfall-induced landslide masses often change into disastrous debris flows and damage large areas in Nepal's mountainous region. The area covered by debris flow inundation is a most essential component for landslide hazard assessments leading to development of land use plans. Because debris flow is a complex natural phenomenon, runout analysis requires very detailed information and rigorous procedures. Various empirical and dynamic models are available for debris flow runout simulation. However, a simple and publicly accessible model that can provide reasonable results is the ideal option for engineers and scientists. The Flow-R model with various algorithms has the capability to analyze debris flow inundation with limited input information, and the model software is readily available in the public domain. The model can identify landslide susceptibility areas or conduct runout analysis for a user-defined debris flow source. In this research, the Flow-R model with user-defined landslide-susceptible areas was chosen for debris flow runout analysis in Kulekhani Watershed (Nepal). Two recent debris flow events are taken as case studies to identify the appropriate algorithms for runout analysis of the study areas. After comparison of observed and simulated results for debris flow runout, the algorithms proposed by Holmgren (1994) (modified) are found suitable for the study watershed. These algorithms are employed for debris flow inundation analysis in the study area with pre-defined landslide sources plus debris flow inundation map in GIS environment. The results obtained from this modeling for the debris flow area induced by 540 mm of rainfall in 24 hour period was 2.68% of the watershed, which is comparable to previously observed debris flow area in the study watershed.

5.1 Introduction

Debris flow is one of the most severe natural calamities among all forms of landslides in mountainous regions. Rainfall is one of the prime triggering factors for the formation of a debris flow from the initial landslide. Rainfall-induced shallow landslides that change into debris flows travel large distances on sloped natural terrain, and debris flows spread over more area compared to their initial landside source location. Nepal's mountainous areas are densely populated, and human life and property are vulnerable to rainfall-induced wide-spreading debris flows. As mountainous regions are prone to debris flows, prediction and remedial measures are important factors to consider for saving lives and property. Both the initiation locations and runout areas of debris flows are required for hazard analysis in these mountainous regions. An initial landslide that starts with a small mass can continue to entrain and deposit material until all energy is dissipated in the moderately mild slope to plains areas. People reside in the middle mountains and low valleys of Nepal despite vulnerability to debris flows and high risk of loss of lives and property. Every year many people lose their lives and property due to such calamities.

Recently, a number of studies have been conducted on landslide dangers for those living in these mountains (Deoja et al. 1991, Dhital et al. 1993, Dangol et al. 1993, Yagi and Nakamura 1995, Upreti and Dhital 1996, Wagner 1997, Dhital 2000, 2005, Gerrard and Gardner 2000, Chalise and Khanal 2001, Yagi 2001, Gabet et al. 2004, Dahal et al. 2006, Dahal and Hasegawa 2008, Dahal et al. 2008, Ghimire 2011, Bijukchhen et al. 2012, Bhandary 2013, Dhakal et al. 1999, Thapa and Dhital 2000, Acharya et al. 2006, Sharma and Shakya 2008, Ray and De Smedt 2009, Dahal et al. 2012, Devkota et al. 2013, Kayastha 2009, Pantha et al. 2010, Poudyal et al. 2010 and Kayastha et al. 2010, 2012, 2013). However, debris flow runout from the initial landslide and its analysis at the watershed scale has not yet been studied for hazard assessment.

The prediction methods of travel distance from the initial landslide are categorized by three methods: dynamic, semi-empirical and empirical. Dynamic methods (Wang et al.

2008, Iverson1997, Iverson et al. 1997, Savage and Baum 2005, Sassa 2000, Sassa and Wang 2005, O'Brien 2003, Pierson 2005, Pudasaini et al. 2011, Pastor et al. 2009, Takahashi et al. 1992, Takahashi 1978, 1980, Savage and Hutter 1989, Chen and Lee 2000, Hutter 1989, Hungr 1995) predict runout distance from the characteristics of debris flows that develop from an initial landside. Empirical methods (Scheidegger 1973, Hsu 1975, Corominas 1996, Finlay et al. 1999, Hunter and Fell 2003, Legros 2002, Rickenmann 1999, Fannin and Wise 2001, Rickenmann 2005, Dai et al. 2002) are derived fully from previous case studies with travel angle, volume and topography data to determine the runout distance of the debris flow. Semi-empirical methods (Crosta et al. 2002, 2003, Iverson et al. 1998, Griswold, 2004, Griswold and Iverson 2008, Takahashi and Yoshida 1979) are derived partly from dynamic methods using physical characteristics of the debris flow and partly from empirical procedures from observed debris spreading information. The research on debris flow travel distance modeling using dynamic, semi-empirical and empirical methods are further reported in Hergarten and Robl (2015), Horton et al. (2013), Blahut et al. (2010), Beguera et al. (2009), Hurlimann et al. (2008), Hungr et al. (1995), Pastor et al. (2004), Iverson and Delinger (2001), Iverson and Vallance (2001), Julien and Lan (1991), Savage and Hutter (1991), Davis et al. (1999), Sassa (1985), Hutchinson (1988), O'Brien and Julien (1985, 1987, 1988), O'Brien et al. (1993), Takahashi (1979) and Korner (1980).

Landslide area and its runout are both necessary for hazard and risk assessment (Fell et al. 2008). The study of GIS-based statistical approaches (Devkota et al. 2013, Kayasta 2009, Pantha et al. 2010, Poudyal et al. 2010, Bijukchhen et al. 2012 and Kayastha et al. 2010, 2012, 2013) has considered previous landslide events and their spatial distribution as a base factor for identification of future landslides but has not considered their runout characteristics. Obtaining the characteristics of landslide mass for debris flow hazard and risk assessment at the watershed scale is not only difficult but also expensive and unreasonable. Hazard assessment practitioners always prefer reasonable debris flow runout analysis with limited watershed information using empirical methods. Therefore, modeling debris flow runout for hazard assessment is the objective of this research. In this study, the locations of landside susceptibility and the

corresponding runout map will be identified. This information can be used for watershed hazard analysis which will be the next step of this research.

5.2   Transformation of Initial Landslide to Debris Flow

The favorable conditions for debris flow formation from an initial landslide have been studied by a number of researchers (Rickenmann and Zimmermann 1993, Takahashi 1981, Varnes 1978, Crawford and Eden 1967, Youd 1973, 1993, Iverson et al. 1997, Holzer et al. 1989, Eckersley 1990, Blackwelder 1928, Pain 1972, Pierson et al. 1990, O'Connor et al. 1997, Johnson and Rodine, 1984, Johnson and Rodine 1976, Matheson et al. 1990, Reid et al. 1997, Sassa 1985, Ellen and Fleming 1987, Takahashi 2000, Kang et al. 2003, Wong et al. 1997, Ayotte 1999, Brand 1981, Li et al. 2004, Iverson and La Husen 1989). Their research showed that the major contributing factors for debris flow formation are rainfall intensity, steep natural terrain and the type of sliding soil mass.

Debris flows in Nepal's mountains are initiated from high intensity rainfall similar to the condition studied by Cannon and Ellen (1988), Li et al. (2004) and Campbell (1975). These researchers found that matric suction and cohesion respond to prolonged moderate intensity rainfall, and bursts of high intensity rainfall lead to debris flow formation. They also found that high intensity rainfall develops a transient perched water table that mobilizes the soil mass with positive pore pressure (Iverson et al. 1997). This observation also supports the idea of rainfall-induced shallow depth landslides often changing into debris flows. The greater the depth of landslide, the lower the chance of debris flow formation, such as in landsides from man-made slopes in Nepal. The condition of saturated or nearly saturated soil prior to failure (Sidle and Swanston 1982, Johnson and Sitar 1990) and perched water tables within which positive pore pressure develops (Li et al. 2004) are common conditions in Nepal's mountains. Li et al. (2004) also observed that a transient perched water table or positive water pressure developed in the heaviest rainfall (194.5 mm per day) and volumetric water content also increased in the saturated state. After rainfall ceases, the soil remains in a tension-saturated state

even as gravity drainage occurs, and negative pore pressures or matric suction can develop. A subsequent burst of high-intensity rainfall can cause the tension-saturated zone to develop positive pore pressures almost instantaneously if there is a ground water table or a low permeability stratum underneath. Such a rapid response mechanism was also observed by Li et al. (2004) in the capillary fringe above the water table. A mechanism of this type may have initiated debris flows in the hill slope studied by Iverson (1997). This condition is considered for debris flow formation from an initial landslide in the study watershed in Nepal. In this study, a steep mountain area is considered for debris flow runout without influence of a permanent groundwater table but with a temporary perched water table developed by instantaneous rainfall above the impervious subsurface layers.

5.3   Runout Distance of a Debris Flow

The runout distance of a debris flow can be predicted by solving momentum conservation equations (Voellmy 1955, Salm 1966, Takahashi and Yoshida 1979, Hungr 1995, Wang et al. 2008). The runout distance can be related to the travel angle (Wong et al. 1997, Horton et al. 2008, Hurlimann et al. 2008).

The debris flow runout analysis provides debris flow depth and velocity in its runout area. When the probable initial location of the debris flow is identified, the selection of the appropriate method for identification of the debris flow characteristics and its runout analysis are important for hazard analysis. It is not practical to identify the spatial distribution of the debris mass and its characteristics for the whole watershed to delineate runout distance, therefore, appropriate empirical methods applied in other regions are identified and used in this research.

5.4   Modeling Debris Flow Runout

Various methods are proposed for debris flow runout modeling. Reach angle or travel angle (α), defined as the angle of elevation from the debris flow initiation point (height H)

to its end point (length L), is one of many empirical methods proposed by many researchers. Reach angle is used by Corominas (1996) for the runout distance of debris flows. Corominas (1996) proposed, after evaluating 52 debris flows, that runout distance be based on volume (V) as given in Equation [5.1].

$$\tan\alpha = \left[\frac{H}{L_{max}}\right] = 0.97V^{0.105} \qquad [5.1]$$

Rickenmann (1999) proposed using volume to determine the maximum debris flow runout length in Equation [5.2] and debris flow fan length in Equation [5.3].

$$L_{max} = 1.90V^{0.16}H^{0.83} \qquad [5.2]$$

$$L_{fan} = 15V^{1/3} \qquad [5.3]$$

where, L_{max} and L_{fan} are maximum debris flow length in natural terrain and the length of the debris flow fan, respectively.

Debris flow modeling with dynamic analysis (DAN) was proposed by Hungr (1995, 2005) with Voellmy, friction and quadratic rheology, by O'Brien et al. (1993), with FLO2D, by Pirulli et al. (2008) with RASH3D and by Horton et al. (2008, 2013) with Flow-R. Wang et al. (2008) assumed that a debris flow consists of a well-mixed flow of water and slide mass that has a homogenous, uniform, continuous, incompressible and unsteady condition. They proposed Navier-Stokes flow equations solved in a GIS grid for runout spreading, similar to a finite mesh used for numerical analysis of partial differential equations. The debris flow spreading is governed by the forms of continuity and momentum equations (Navier-Stokes flow equations) shown by Equations [5.4] to [5.7]. Debris rheology is defined in Equations [5.8] and [5.9] (Wang et al. 2008). The GIS grid in the watershed is a finite grid for solving these equations.

Continuity equation

$$(\frac{\partial u}{\partial x} + \frac{\partial v}{\partial y} + \frac{\partial w}{\partial z}) = 0 \qquad [5.4]$$

$$\rho d(\frac{\partial u}{\partial t} + u\frac{\partial u}{\partial x} + v\frac{\partial u}{\partial y} + w\frac{\partial u}{\partial z}) = -\frac{\partial p}{\partial x} + \mu(\frac{\partial^2 u}{\partial x^2} + \frac{\partial^2 u}{\partial y^2} + \frac{\partial^2 u}{\partial z^2}) \qquad [5.5]$$

$$\rho d(\frac{\partial v}{\partial t} + u\frac{\partial v}{\partial x} + v\frac{\partial v}{\partial y} + w\frac{\partial u}{\partial z}) = -\frac{\partial p}{\partial y} + \mu(\frac{\partial^2 v}{\partial x^2} + \frac{\partial^2 v}{\partial y^2} + \frac{\partial^2 v}{\partial z^2}) \qquad [5.6]$$

$$\rho d(\frac{\partial w}{\partial t} + u\frac{\partial w}{\partial x} + v\frac{\partial w}{\partial y} + w\frac{\partial w}{\partial z}) = pdg - \frac{\partial p}{\partial z} + \mu(\frac{\partial^2 w}{\partial x^2} + \frac{\partial^2 w}{\partial x^2} + \frac{\partial^2 w}{\partial z^2}) \quad [5.7]$$

$$\tau = \sigma\tan\phi \qquad [5.8]$$

$$\tau = \tau_y + \mu\left(\frac{\partial u}{\partial y}\right)^n * \sigma\tan\phi \qquad [5.9]$$

where u, v and w are the components of velocity in the x, y and z directions, respectively, ρd is the equivalent density of the debris and water mixture, p is the pressure, µ is the dynamic viscosity, g is the gravitational acceleration, σ is the normal stress, ø' is the friction parameter, n is the flow parameter and τ_y is the yield stress. The parameters required for solving these equations are the debris flow rheology and fine GIS grid for all locations in the watershed. Finding the debris flow rheology for each location in the watershed is complex and not practicable for professional practice at a reasonable cost. In this research, an empirical model that is publicly available, Flow-R (Horton et al. 2008, 2013), is applied to determine the debris flow runout.

5.5   Study Area

The study area is the Kulekhani Watershed in which the spatial distributions of landslides for different rainfall amount have been studied by Paudel et al. (2018) (Technical Paper 1 is this thesis manuscript). The details of the watershed are available in Dhital (2003), Kayastha et al. (2012), Lamichhanne (2000) and Regmi (2002). This watershed is in the middle hills of Nepal among three geographical regions, High Himalayas, Middle Mountains and Terai (plains area) (Figure 5.1). A total of 16% of the land area of Nepal is covered by high mountains which includes 8 high peaks that are among the 14 highest peaks in the world. The height of the middle hills ranges from 500 to 3000 m, and this zone covers 67% of the total land area of the country, while the

111

lowest plains area accounts for 17%. The study area represents the middle hills (67%) of Nepal which are densely populated and prone to debris flow. Among approximately 30 million people, 52% are living in steep slopes and small valleys of the high and middle mountain zones. The study watershed represents the Middle Mountains in which the residents are vulnerable by living their homes, working in the fields or walking around debris flow prone areas.

The study watershed has an approximately 124 km^2 drainage area (Figure 5.1). The elevation of the study area ranges approximately from 1500 to 2620 m above sea level (Figure 5.2). This watershed is located within Latitude 27°35'04"N to 27°41'00"N and Longitude 85°02'22"E to 85°12'8"E.

Palung Khola and Kulekhani Khola are the main rivers in the watershed. The major tributaries are Gharti Khola, Phedigaon Khola, Bhangkhoria Khola, Kitini Khola, Andheri Khola, Tistung Khola, Chitlang Khola, Chalkhu Khola, Bisingkhel Khola, Setikhani Khola and Thado Khola. The watershed is close to the capital city of Nepal and is a popular location for green vegetable cultivation, tourism and residential divisions, containing forest/barren areas and a reservoir (waterbody).
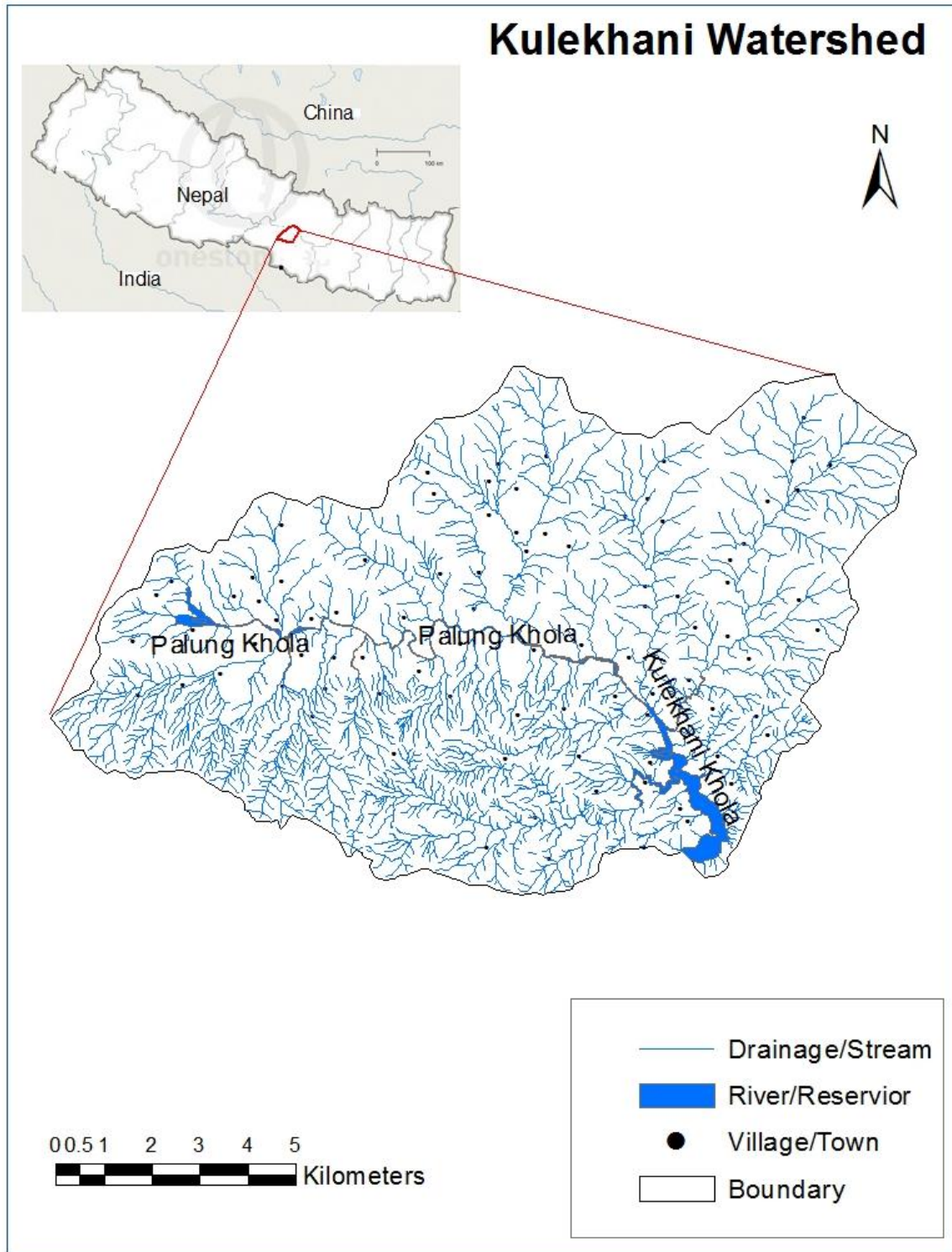
Figure 5.1: Location of the study area.
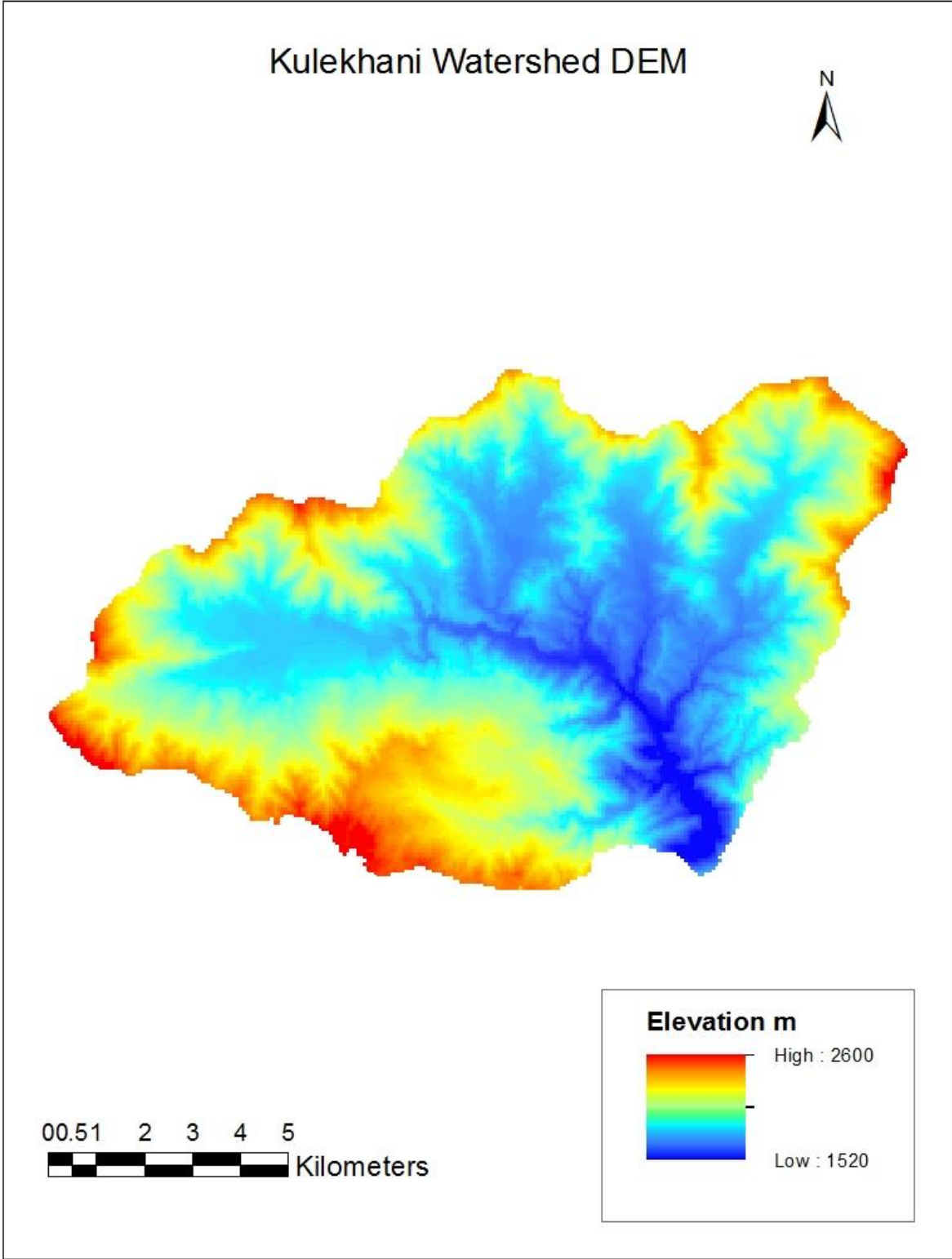
Figure 5.2: Digital elevation model of the study area.

5.5.1 Geological Setting

The geology of the watershed is shown in Figure 5.3. Hagen (1969) considered the study watershed to be in the Lesser Himalayas (Middle Mountains), which is one of the eight well-defined geomorphologic zones in Nepal, namely, "1) Terai (the northern edge of the Indo-Gangetic plain, southern outskirt of Nepal), 2) Siwalik (Churia) Range, 3) Dun Valleys, 4) Mahabharat Range, 5) Midlands, 6) Fore Himalaya, 7) Higher Himalaya, and 8) Inner and Trans Himalayan Valleys." The surficial features in the watershed are formed of bedrock covered with colluvial, residual and alluvial soils. The overburden soil depths range from 1 m to more than 6 m (Dhital 2003). The colluvial soils are formed from erosion, and landslides found at the bottom and midway up some moderately sloped hills. The major part of the watershed is covered with colluvium. The valley formed along the Palung Khola and its major tributaries, Kiteni Khola, Bisingkhel Khola and Thado Khola, contains alluvial deposits. Detailed information on the soil types in the area is available in Lamichhanne (2000).
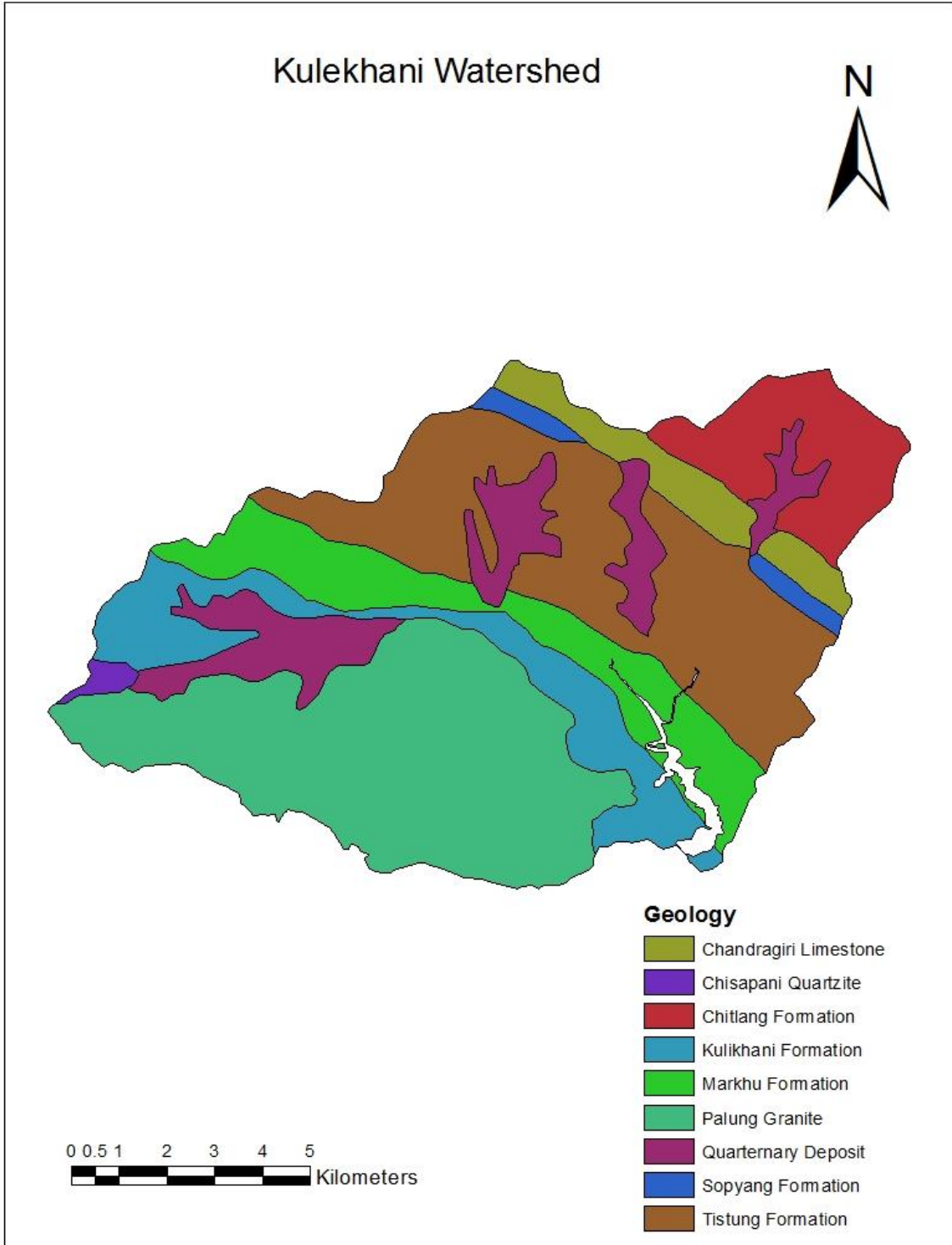
Figure 5.3: Geology in the study area (after Stocklin and Bhattrai 1977, Stocklin 1998, Regmi 2002 and Kayastha et al. 2013).

5.5.2 Rainfall Conditions

The annual average rainfall distribution gradually decreases from the eastern to western regions of mountainous Nepal. The study area is located in the central region where rainfall precipitation received yearly is equal to the annual average of the country. Rainfall data for this study can be found in Paudel et al. (2018) and Kayastha et al. (2014), which are collected from the Department of Hydrology Metrology, Nepal. Two rainfall recording stations, Daman and Markhu are located within the study watershed area and another two, Thankot and Chisapani Ghadi, just outside. The recorded rainfall at the stations shows that the maximum daily rainfall from 1980 to 2013 is 442.5 mm in Chisapani Ghadi. Similarly, at the Daman, Markhu and Thankot stations, daily maximum rainfall was recorded as 373.2, 385.6, and 300.1 mm, respectively. The maximum rainfall recorded in a temporary rain gauge station at the Kulekhani hydroelectric dam was 540 mm on July 20, 1993. The combination of intensity and duration of threshold rainfall for landslide in the region and the worst observed rainfall, 540 mm, in the study area are considered for the debris flow event in this study.

5.5.3 Landslide and Geotechnical Characteristics in the Study Area

The landslide inventory was carried out by Deoja et al. (1991), Kayastha et al. (2012) and Dhital (2003) after the 1993 devastating rainfall in the watershed. Landslides were observed in very steep to moderately steep mountain slopes at high altitude locations (Figure 5.4). Most of the landslides in the study area changed into debris flows. Landslides were initiated on both natural slopes and locations of anthropogenic disturbance such as near roads and other infrastructures.

Hasegawa et al. (2009) observed peak internal frictional angles of 22° to 36° and residual angles of 22° to 34° for landslide slip materials near the study watershed.
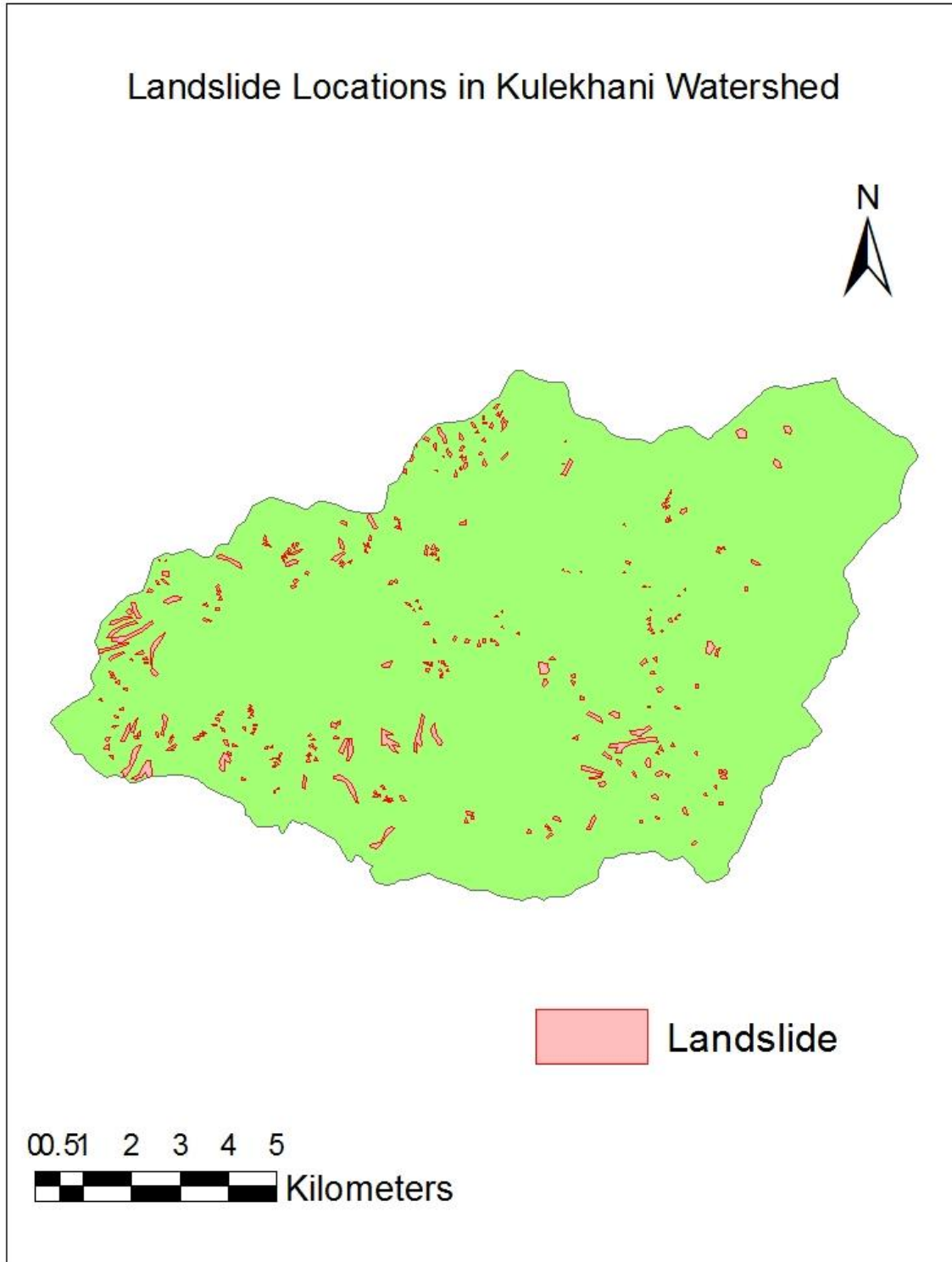
Figure 5.4: Observed landslides due to the 1993 rainfall event (modified from Kayashta et al. 2013).

For this research, Geotechnical investigations have been conducted in one old landslide site by Paudel et al. (2018) in the watershed and the results are shown in Tables 5.1 and 5.2.

Table 5.1 Shear Strength Parameters and Classification of the Tested Soils.

Borehole	Depth (m)	Cohesion (kPa)	Friction angle Ø' (Degree)	Water Content (%)	Classification	Bulk Density (gm/cm³)	Specific Gravity
BH 1	0-1.5	15	30	23.03	ML, Gravelly Silt with Sand	1.79	2.70
	1.5-3.0	13	29	20.49	SM, Silty Sand with Gravel	1.81	2.65
	3.0-4.0	17	24	21.53	ML, Gravelly Silt with Sand	1.80	2.67
BH 2	0-1.5	15	29	21.31	SM, Silty Sand with Gravel	1.83	2.68
	1.5-3.0	19	25	18.21	ML, Sandy Silt with Gravel	1.86	2.63
	3.0-4.0	17	27	21.50	GM, Silty Gravel with Sand	-	2.70
BH 3	0-1.5	10	25	23.58	ML, Sandy Silt with Gravel	1.82	2.65
	1.5-3.0	5	32	24.49	ML, Gravelly Silt with Sand	1.84	2.69
	3.0-4.0	11	30	19.58	GM, Silty Gravel with Sand	-	2.67
BH 4	0-1.5	15	27	22.75	GM, Gravelly Silt with Sand	1.85	2.65
	1.5-3.0	17	26	21.15	GM, Gravelly Silt with Sand	1.84	2.61
	3.0-4.0	11	30	22.63	SM, Silty Sand with Gravel	1.83	2.48

Mainly, there are three types of overburden soils in the watershed, eluvial or residual, alluvial and colluvial soils. The geotechnical properties of the residual soils depend on

the types of parent rock and also the depth of weathered or competent bedrock. In the study watershed, weathered granite is the parent rock for most of the residual soil. Colluvial soil is the predominant soil in the area, originating from erosion, wind drift and landslides of residual soils. Colluvium consists of an unsorted matrix of soil, rock fragments and gravel. Alluvium deposits are found at lower elevations in the watershed. The alluvial soils form from erosion and transport of sediment, which deposited in slow flowing water. Most alluvium layers are graded with coarse sediment at the bottom and finer material at the top for each episode of deposition.

Table 5.2 Physical Parameters of the Soils Tested.

Borehole	Depth (m)	Void Ratio (e)	Porosity (n)	Volumetric water (Θ)	Degree of Saturation	Gravimetric Water Content	Dry Density, ρ_d (gm/cm^3)	Moisture Content Residual	Tan Ø^b
BH 1	0-1.5	0.86	0.46	23.03	72.63	0.32	1.45	4.00	0.49
	1.5-3.0	0.76	0.43	20.49	71.43	0.29	1.51	5.00	0.43
	3.0-4.0	0.81	0.45	21.53	71.07	0.30	1.48	5.00	0.44
BH 2	0-1.5	0.70	0.41	21.31	68.22	0.27	1.55	4.00	0.40
	1.5-3.0	0.76	0.43	18.21	76.00	0.28	1.53	2.00	0.51
BH 3	0-1.5	0.84	0.46	23.58	78.53	0.31	1.47	4.00	0.54
	1.5-3.0	0.74	0.42	24.49	70.99	0.28	1.54	4.00	0.43
BH 4	0-1.5	0.76	0.43	22.75	79.70	0.29	1.51	5.00	0.50
	1.5-3.0	0.72	0.42	21.15	77.02	0.27	1.52	4.00	0.49
	3.0-4.0	0.66	0.40	22.63	85.30	0.27	1.49	2.00	0.61

The types of landslides in the study area and mountainous Nepal are predominantly debris flows. Dhital (2003) observed that most slides are debris flows in the study watershed. Dahal and Hasegawa (2008) identified 677 rainfall-induced landslides in all of Nepal and they observed mostly debris flows in natural terrain. Petley et al. (2007) observed that the 397 fatal landslides are mostly debris flows. Based on visual observations at the site and the previous literature (Dahal and Hasegawa 2008, Dahal

et al. (2008), Dhital et al. 1993, Petley et al. 2007, Gabet et al. 2004, Ray and Smedt 2009), the types of landslides in the proposed study area are identified as mostly debris flows (Cruden and Varnes 1996).

5.6   Methodology

The debris flow runout modeling requires the initial landslide location and spreading topography for the study watershed. In this study, the landslide susceptibility map previously developed by Paudel et al. (2018) was considered for debris flow initiation locations for runout modeling. Although the debris flow runout analysis can be carried out using empirical, semi-empirical and dynamic methods, for modeling work with limited information on the entire watershed, empirical methods are better options (Horton at al. 2013, Carrara et al. 2008, Finaly et al. 1999, Costta 1984, Hungr et al. 1984, Johnson 1984, Rickenmann 1999). In this research, empirical methods, the Flow-R model and the aforementioned susceptibility map for determination of the landside initiation location (source area) were considered. Flow-R is an empirical model developed by the University of Lausanne. The model can be used for both susceptibility and runout analysis of debris flows. The Flow-R model has been applied in various regions of the world and found reasonable results. It is an open source software which is freely available. Also, in the Flow-R model, options for user-defined debris flow sources are available for runout simulation only. Various algorithms are available in this model. The modeling procedure for debris flow runout with Flow-R algorithms is shown in Figure 5.5. The source identification for debris flow spreading considered in this model is described in Section 5.6.1. As shown in Figure 5.5, the landslide susceptibility map is used as the debris flow source map for runout analysis. In this model, landslide source maps are converted into an ASCII file in GIS software and applied to the runout analysis in Flow-R. The final results from Flow-R are compiled with the watershed map back in GIS. The final map shows the landslide initiation and debris flow spreading areas resulting from the selected rainfall scenario in the study watershed.

121

5.6.1 Landslide Susceptibility Maps

The details of the landside susceptibility mapping process applied in the study watershed is given in Paudel et al. (2018). However, a brief description of the process is given in this section. These maps were developed for combinations of low rainfall intensity with long duration and high intensity with short duration, which are the threshold rainfalls for landslide initiation in the study region (Dahal and Hasegawa 2008). The data for the watershed were collected, including in situ and laboratory testing, from an old landslide site within the watershed. The soil strength parameters, such as cohesion, friction, and soil permeability results from the in-situ testing and laboratory results were utilized in the analysis. Effective stress was derived at the wetting front considering the infiltration depth for the saturated soil mass at the time of the rainfall. The average unit weight was taken from the measured unit weight of soil samples at different depths. Soil samples from 73 representative locations (Lamichhanne 2000) in the watershed are considered for a Soil Water Character Curve (SWCC) based on the method of Fredlund and Xing (1994) and Torres (2011) using the grain size distribution. Infiltration depth for a given rainfall and duration at representative locations was identified from four gauges locations, two of which are within the watershed and two are closely located outside the watershed. Infiltration depths were computed using suction from the SWCC and the combination of rainfall intensity and duration. A Digital Elevation Model (DEM) was used for developing other required maps, such as a slope map of the watershed. All maps including suction, density, friction, cohesion and infiltration depth characteristics were developed in the GIS environment. These maps were interpolated with Inverse Distance Weighted (IDW) methods to create the raster maps. The same cell size and boundary extent were applied in the raster analysis. The final landslide susceptibility maps were developed for different rainfall duration and intensity. Landslides due to low intensity-long duration and high intensity-shorter duration rainfall scenarios were considered separately for the analysis and mapped on the watershed. The model was successfully verified with the recorded rainfall and observed landslides in the watershed. The threshold rainfall intensity and duration for landslide initiation was applied to unstable locations within the

watershed. These landside susceptibility maps were used to determine debris flow runout for the study watershed.
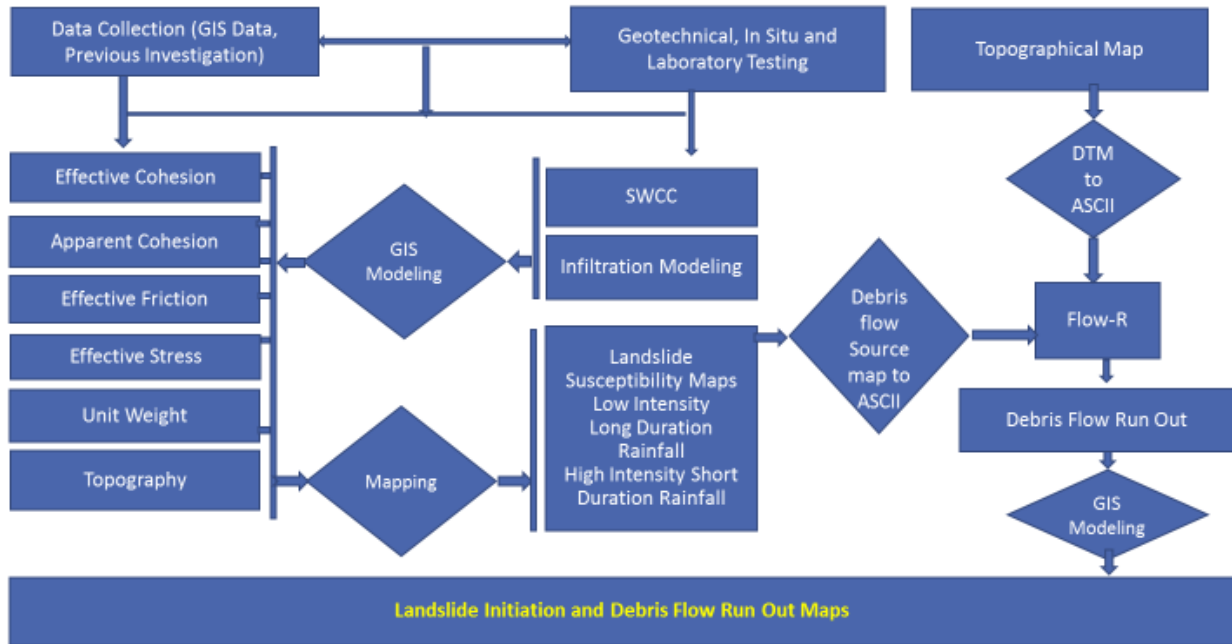
Figure 5.5: Modeling procedure for debris flow runout

5.6.2 Runout Distance

The debris flow runout distance, including spreading, was carried out with the various algorithms listed in Table 5.3 (Flow-R model) to determine the appropriate algorithms for the study watershed. The Flow-R model can be used either for identification of landslide susceptibility and debris flow runout or runout alone with user-defined sources. Through the Flow-R model, all these algorithms, including the modified Holmgren (1994) model, which was developed by Horton et al. (2013), were applied to find the most appropriate ones for this region. After validation of the various algorithms, the most appropriate algorithms were applied for the debris flow analysis of the whole watershed.

In the modified Holmgren (1994) model, Equation [5.10], the elevation of the central cell is elevated by some height (dh) at the central location. Two debris flow events outside

the watershed but within the middle hills region of Nepal were selected and the modified Holmgren (1994) model was applied for both a single flow direction and multiple flow directions. The exponent x in Equation [5.10] was tested by Claessens et al. (2005) and an appropriate value for debris flow spreading was found to be in the range of 4 to 6 as suggested by Holmgren (1994). In this study, all possible x values from 1 to 50 were tested with a selected landslide for identification of the appropriate value for debris flow inundation.

$$p_i^{fd} = \frac{(\tan Bi)^x}{\sum\limits_{j=1}^{8}(\tan Bj)^x} \forall \begin{cases} \tan B > 0 \\ x\varepsilon[1;+\infty] \end{cases} \qquad [5.10]$$

where i and j are the flow directions, p_i^{fd} the susceptibility proportion for the i direction and Bi and Bj are the slope angles at the central cell in the i and j directions. Exponent x varies from 1 to infinity. When the value of x is equal to 1 it represents the multiple flow and decrease the direction with increase in x value. Algorithm D8, proposed by O'Callaghan and Mark (1984) and Jenson and Domingue (1988) (Table 5.3), was developed for eight directions of flow. The results of all algorithms stated in Table 5.3 including the D∞ (D infinity) (Tarboton (1997) and the multiple flow direction approach (Quinn et al. 1991, Freeman 1991) are compared with observed debris flow.

5.6.2.1 Inertial Algorithms

In natural terrain, slope direction frequently changes, and a function is required to capture the new direction with respect to the initial slope. This function is called the persistence function by Horton et al. (2013). Gamma (2000) and Horton et al. (2013) used the persistence function as given in Equation [5.11] for slope direction change with respect to previous or initial direction.

$$p_i^p = w_{\alpha(i)} \qquad [5.11]$$

where p_i^p is the flow proportion in the i direction according to the weight and inertia of flow, $w_{\alpha(i)}$, and α(i) is the angle from the previous flow direction. The opposite of the previous flow direction will have an angle of 180°, which has zero flow in the next step.

For direction memory, there are three choices for determining the weights of the persistence function for debris flow propagation and inundation based on the initial direction: (1) proportional (default option in the software), (2) cosine and (3) Gamma (2000). Proportional assigns weights of 1, 0.8 and 0.4 for directions of 0, 45 and 90 degrees, respectively, and directions of 135 and 180 degrees have weights equal to zero. The cosines method assigns weights of 1 and 0.707 for the 0 and 45-degree directions, respectively, and the rest, 90, 135 and 180 degrees, have weights equal to zero. Similarly, the Gamma (2000) method assigns weights of 1.5 in the direction of flow (0 degrees), 1 for 45, 90 and 135 degrees, and zero for 180 degrees.

The direction algorithms and persistence algorithms can be written as shown in Equation [5.12] (Horton et al. 2013).

$$Pi = \frac{p_i^{fd} p_i^{p}}{\sum\limits_{j=1}^{8} p_j^{fd} p_j^{p}} p_o \qquad [5.12]$$

where i and j are the flow directions, P_i is the susceptibility value in direction i, p_i^{fd} is the flow proportion according to the flow direction algorithm, p_i^{p} is the flow proportion according to the persistence and P_o is the previously determined susceptibility, which is the total initial value or value of the central cell. The susceptibility functions will be the maximum in the original cell with po and it will be distributed in the flow direction i and j. The potentiality of flow movement in a possible direction is equal to or not more than the sum with the original central cell value which balanced and avoided loss of susceptibility in the possible flow direction cell. The susceptibility can exist until energy has not been balanced in the debris flow. Total susceptibility is distributed in all eight directions. The limit of the susceptibility is decided based on the energy available for the particular direction and the given value of energy required for the cell (grid area) in that direction. If the limit of energy requirement is higher than the available energy for any cell, the grid or cell considered for propagation may not be acceptable at that stage and ultimately

debris flow stops in that direction. If one of the cells has an unacceptably high energy requirement, the rest of the cells share the total P_o value.

5.6.2.2 Debris Flow Travel Distance

In the Flow-R model, the flow mass is considered as a unit value and energy loss is entirely from friction. The energy required to travel to another cell must be sufficient for flow to take place from one cell to another. Energy is the controlling factor for total runout and also for spreading to side cells based on the difference between the available energy and provided energy between two cells or cells adjacent to the central cell as Horton (2013) mentioned and as shown in Equation [5.13].

$$E_{kin}^i = E_{kin}^o + \Delta E_{pot}^i - E_f^i \quad [5.13]$$

where E_{kin}^i is the kinetic energy of the cell in direction i, E_{kin}^o is the kinetic energy of the central cell, ΔE_{pot}^i is the change in potential energy to the cell in direction i and E_f^i is the energy lost in friction to the cell in direction i. The friction loss can be assessed by two types of algorithms: a two-parameter friction model by Perla et al. (1980) and a simplified friction-limited model (SFLM). Both methods can result in similar propagation areas, depending on the choice of parameters (Jaboyedoff et al. 2011).

Debris flow can be simulated similar to snow avalanches as proposed by Voellmy (1955), Equation [5.14].

$$T = A_i \left[\gamma H_i \left(\cos \alpha + \frac{a_c}{g} \right) \tan \phi + \gamma \frac{v_i^2}{\xi} \right] \quad [5.14]$$

In this equation, T is a flow resistance, which is the function of friction term and turbulent term, $\emptyset$ the friction angle, a_c the centrifugal acceleration, α the slope angle, A_i the base area (ds * Bi, where ds is the length of sliding mass base and Bi is its width). The turbulence coefficient ξ has dimensions of acceleration. The centrifugal acceleration a_c, is equal to v^2/r, which depends on the vertical curvature radius of the path, v velocity of flow and r radious of the path. This model provides a satisfactory result for rockslide avalanches (Koerner 1976, Kaiser 1984). The Voellmy model has been successfully used in debris flow analysis by Hungr (1995) in a DAN model. Here, similar to the

Voellmy model, Perla et al.'s (1980) two-parameter friction model, which was tested by Zimmermann et al. (1997), was applied for the analysis. The method is derived based on a non-linear friction law (Horton 2013), considering the momentum equation as suggested by Perla et al. (1980) and can be expressed by Equations [5.15] to [5.17].

$$V_i = (aiw(1 - \exp bi) + vo^2 \exp bi)^{1/2} \qquad [5.15],$$

$$ai = g(\sin Bi - \mu \cos Bi) \qquad [5.16],$$

$$bi = \frac{-2L_i}{w} \qquad [5.17]$$

where μ is the friction parameter, V_i is velocity at i direction, ai and bi are fitting parameters, w is the mass-to-drag ratio (Perla et al. 1980), Bi is the slope angle of the segment, vo is the velocity at the beginning of the segment, Li is the length of the segment and g is the acceleration due to gravity. When the terrain slope decreases rapidly, a correction factor based on the conservation of linear momentum can be applied as given in Equation [5.18].

$$V_i^{'} = V_i \cos(B_i - B_{i+1}) \qquad [5.18]$$

In Equation [5.18], V' is the cosine of the difference in angle between Bi and Bi+1 times the initial velocity. The data for this correction factor requires more DEM area outside the attached computing cells. Large numbers of cells can be considered in the algorithms available in Flow-R (Horton 2013). The simplified friction-limited model (SFLM) suggested by Corominas (1996) is also available in Flow-R. It is based on the maximum possible runout distance by a small travel angle, as given in Equation [5.19].

$$E_i^f = g\Delta x \tan \phi \qquad [5.19]$$

where E_f^i is the energy lost in friction from the central cell to the cell in direction i, Δx is the horizontal displacement increment in direction i, tanϕ is the energy gradient in the direction of i and g is the acceleration due to gravity.

Horton et al. (2013) suggested to limit the energy for a practical approach when there are steep slopes and high spreading or propagation. They developed Equation [5.20] for limiting velocity from the given value.

$$V_i = min\{V_{max}, \sqrt{(V_o^2 + 2g\Delta h - 2g\Delta x tan\emptyset)}\}[5.20]$$

where Δh is the difference in elevation between the central cell and the cell in direction i and V_{max} is the given velocity limit. This limit can be defined by the user based on the region. A general value of V_i is always limited to Vmax and the intermediate value from the second part of Equation [5.20]. The maximum velocity can be introduced to cap the velocity on steep slopes and limit the propagation. The model is useful for hazard assessment of an area with a defined velocity condition.

5.7   Implementation of the Algorithms

Two recent landslides were chosen to verify the debris flow algorithms found to be appropriate for the study region. The observed source and debris flow inundation areas were collected for the study. The propagation calculation was carried out with the Flow-R software. Various algorithms for debris flow spreading simulation are available in Flow-R and summarised in Table 5.3. In Table 5.3, source area selection, spreading algorithms and control mechanism or energy control are given in separate columns and can be selected individually. Any combination of all alternatives from each column and sub-column can be applied for modeling. All these choices were applied for debris flow model identification for the study region.

Table 5.3 Available Algorithms for Debris Flow Propagation

Source Area Selection	Spreading Algorithms				Energy Calculation			
	Direction Algorithm		Initial Algorithm		Friction Loss Function		Energy Limitation	
Only Superior Sources (Debris Flows only), Energy Base Discrimination Complete Propagation of all source areas (long)	Holmgren (1984)	Exponent 1 to 50	Weights	Default, Cosinus, Gamma 2000	Perla et al. (1980) Perla et al (1980) no correction	Md 0010 to 7500 mu= 0.01 to 0.5	Velocity	1 mps to 50 mps
	Holmgren (1994) Modified	Dh from 0.25m to 70 Exponent 0.1 to 50	Direction memory	Len=005 to 100, Open 090 to 300	Travel angle	From 0.1 ° to 50 °		
	D8	Threshold 10 to 50, Exponent 1 to 50			Variable Travel Angle			
	D Infinity							
	Freeman (1991)							
	Quinn et al. (1991)							
	Wichmann &Becht (2003)	Threshold 10 to 50, Exponent 1 to 50						
	Gamma (2000)	Threshold 10 to 50, Exponent 1 to 50						
	Rho8	-						

5.5 Comparison of the Computed Debris Flows with Observed Debris Flows in the Study Region

Two recent landslide sites were chosen for identification and validation of the algorithms: Jure landslide shown in Figure 5.6, located in Jure Village, Sindhuplanckowk District, Nepal, and Taprang landslide shown in Figure 5.7, located in Naune, Taprang Village in Sildjure VDC, Kaski District, Nepal. The Jure landslide location is about 72 km east (slightly northeast) and Taprang 130 km northwest from the study watershed. Both of these landslides took lives and devastated large amounts of residential property and farm land.

(a)   (b)

Figure 5. 6 Jure landslide: (a) from Google map and (b) from Kantipur online.

(a)   (b)

Figure 5. 7: Taprang landslide: (a) from Google map and (b) from Department of Water Induced Disaster Prevention (DWIDP).

Jure landslide is located at 27°46'3.73"N, 85°52'14.37"E, and its average elevation is 1142 m above msl. This landslide occurred early in the morning on August 2, 2014. The landslide initiation and spreading area was located in Ward no. 1 and 5 of the Mankha Village Development Committee (VDC) and Ward no. 5 of the Ramche VDC and killed

130

156 people. This gigantic landslide dammed the Sunkoshi River, major tributaries of the Koshi River, the largest river in Nepal, and formed a temporary lake for several months. The elevation difference from crown to toe is approximately 800 m. The debris flow deposit area was approximately 800 m long, 300 m wide and about 25 to 50 m in depth. The details of this landslide are available in Jha et al. (2014). The mechanism of failure and any further detail of this landslide are beyond the scope of this research.

Taprang landslide is located at 28°18'31.73"N, 84°4'48.75"E, and its average elevation is 1478 m above msl. Figure 5.7 shows the landslide area in the Taprang VDC of Kashki Distric, Nepal. Taprang landslide killed 7 people and dammed the Madi River for five hours. The landslide occurred on August 3, 2010, almost 4 years before the Jure landslide. While the river was dammed, the downstream riparian life in the Kaski, Lamajung and Tanahun districts of Nepal was threatened. This landslide was active after several years. The detail of the failure mechanism and characteristics of this landslide are also beyond the scope of this research. More information about the landslide is available in Singh (2014).

The outcomes of all algorithms (Table 5.3) were compared with the observed debris flow area for both landslides. The observed debris flow spreading outline for the Jure landslide is shown in Figure 5.8, and the source area of the Jure landside is shown in Figure 5.9. As discussed before, in Flow-R, the source area is considered unitary, spreading is energy balanced and the mass of the sliding debris does not influence its runout distance. The three available options for source selection in column 1 of Table 5.3, "Only Superior Sources (Debris-Flows Only)," "Energy Base Discrimination" and "Complete Propagation of all Source Areas (long)," all provided similar results; no difference was observed by choosing any of these three methods. All combinations of column 2 and its sub-column and column 3 and its sub-column in Table 5.3 were applied in the analysis. Propagation was not observed using D8, Rho8 and D-infinity with all other combinations. Similarly, other algorithms with large travel angles also did not produce the observed debris flows. Some combinations of algorithms produced more than the observed debris flows, spreading in small travel angles at limited velocity (Vmax). Figure 5.9 shows the source of the debris flow and outline of the observed

131

spreading for the Jure landslide. Figure 5.10 shows the debris flow which is most similar to this observed debris flow. The Holmgren (1994) and modified Holmgren (1994) algorithms produced large runout as well as the Gamma (2000) and Perla et al. (1980) algorithms. The modeled spreading was more than observed when the modified Holmgren (1994), Equation [5.10] dh was 10 m and the exp was set to 40 and inertial algorithms with weights and proportional (default) option and low travel angle. The results of these combinations are shown in Figure 5.11. Also, debris flow analyses with the "Weights" and "Cosinus" initial algorithms produced large spreading. The velocity limit in this case did not make any difference in the propagation as compared to limiting the travel angles; the spreading is mostly governed by the travel angle. The algorithms applied to find the spreading shown in Figure 5.11 were applied for the computation of debris flow in the entire study watershed.

Validation was also conducted for the Taprang landslide. Figure 5.12 shows the debris flow source. In the Taprang landslide, source area selection, spreading algorithms and energy calculation were selected as discussed above and their results compared to the observed landslide. Selecting source area did not produce any change in the debris flow propagation, similar to the previous landslide simulation observations. The Holmgren (1984) algorithm with exponent 1 to 50 and weights with proportional option (default) together with low travel angle produced the spreading shown in Figure 5.13. Figure 5.14 shows a large spreading result from the combination of low velocity, low travel angles and modified Holmgren (1984) algorithm.
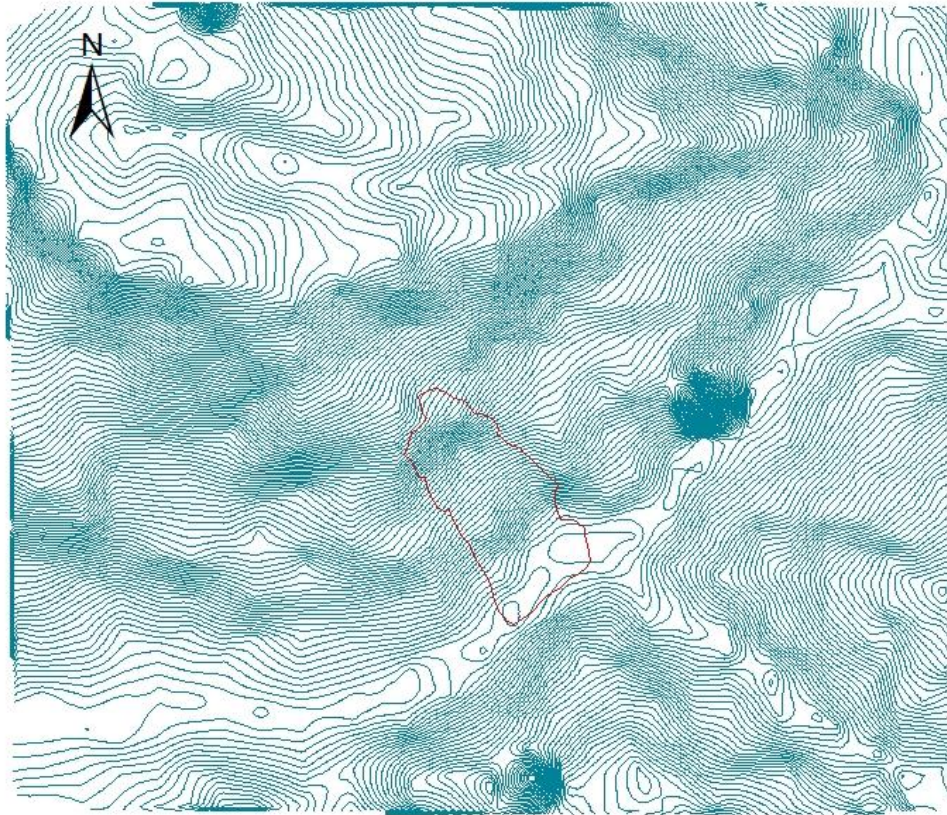
Figure 5.8: Observed debris flow outlines, Jure landslide.
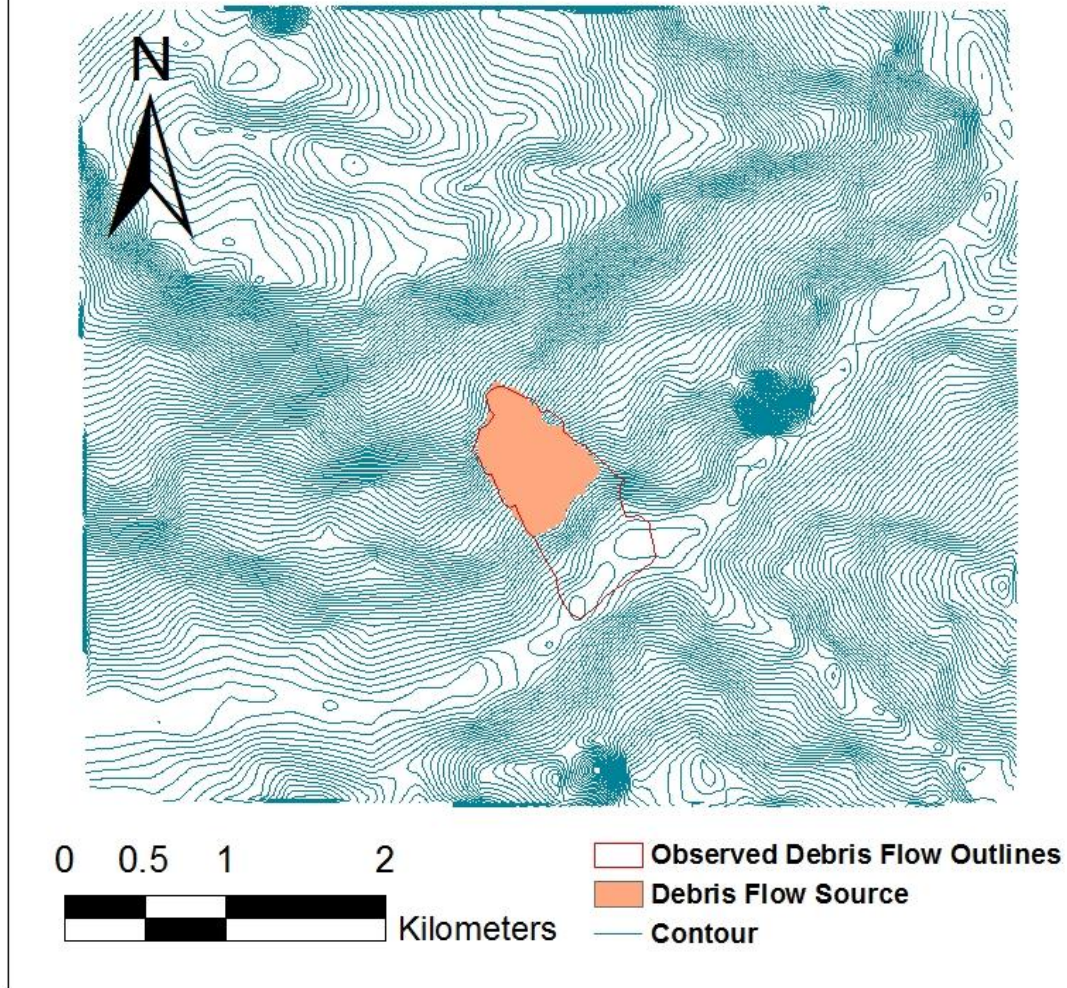
Figure 5.9: Source area with observed debris flow outline, Jure landslide.

Figure 5.10: Modeled debris flow outline for the Jure landslide.
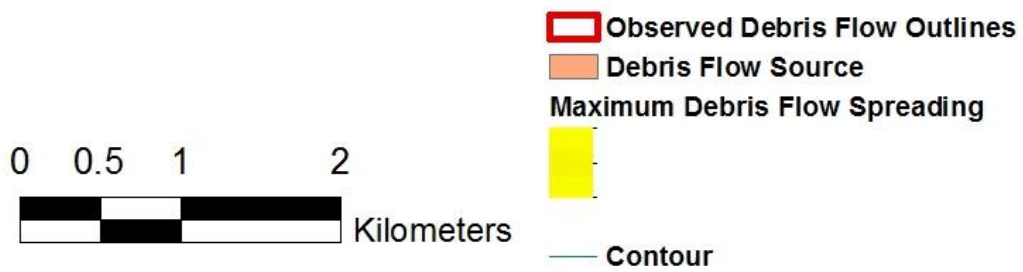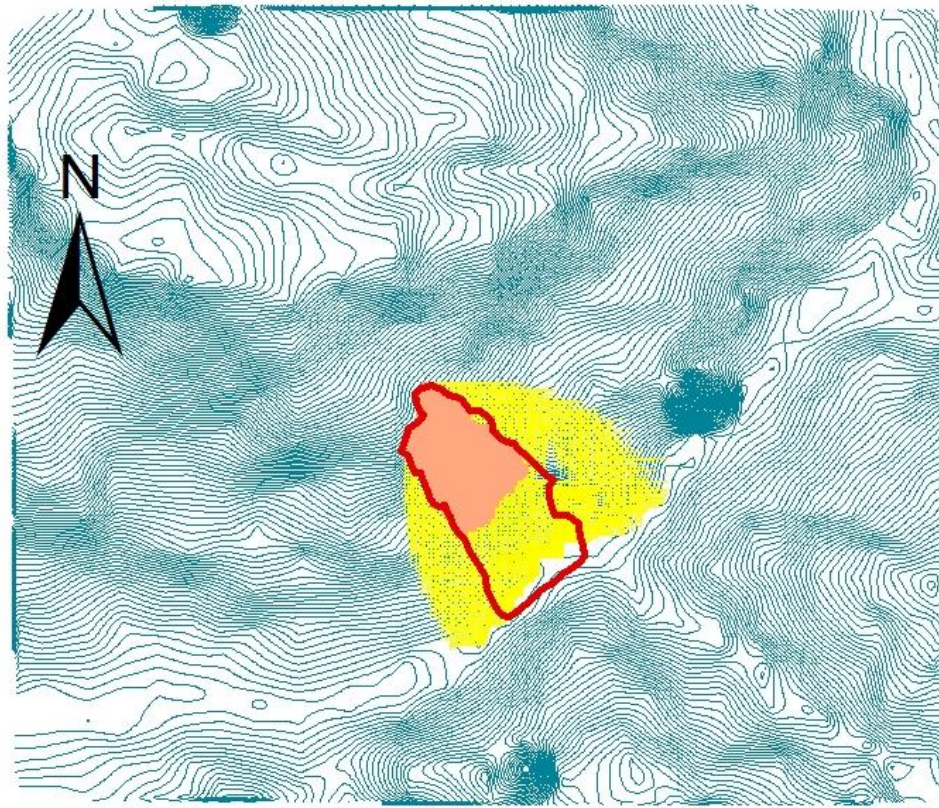
Figure 5.11: Maximum debris flow from model study, Jure landslide.
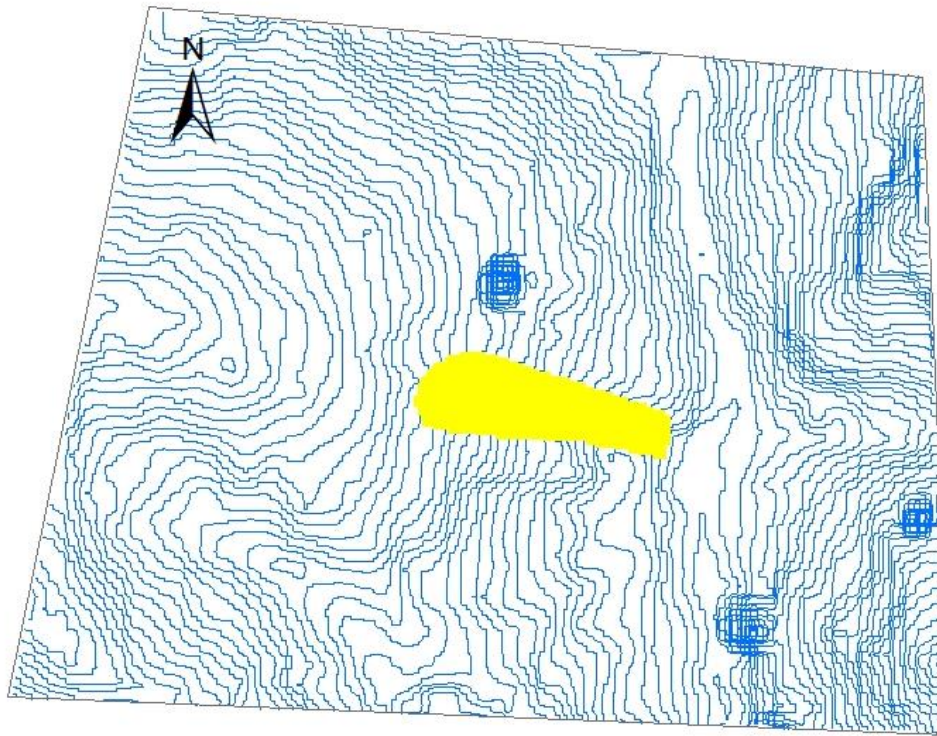
Figure 5.12: Debris flow from model study, Taprang landslide.
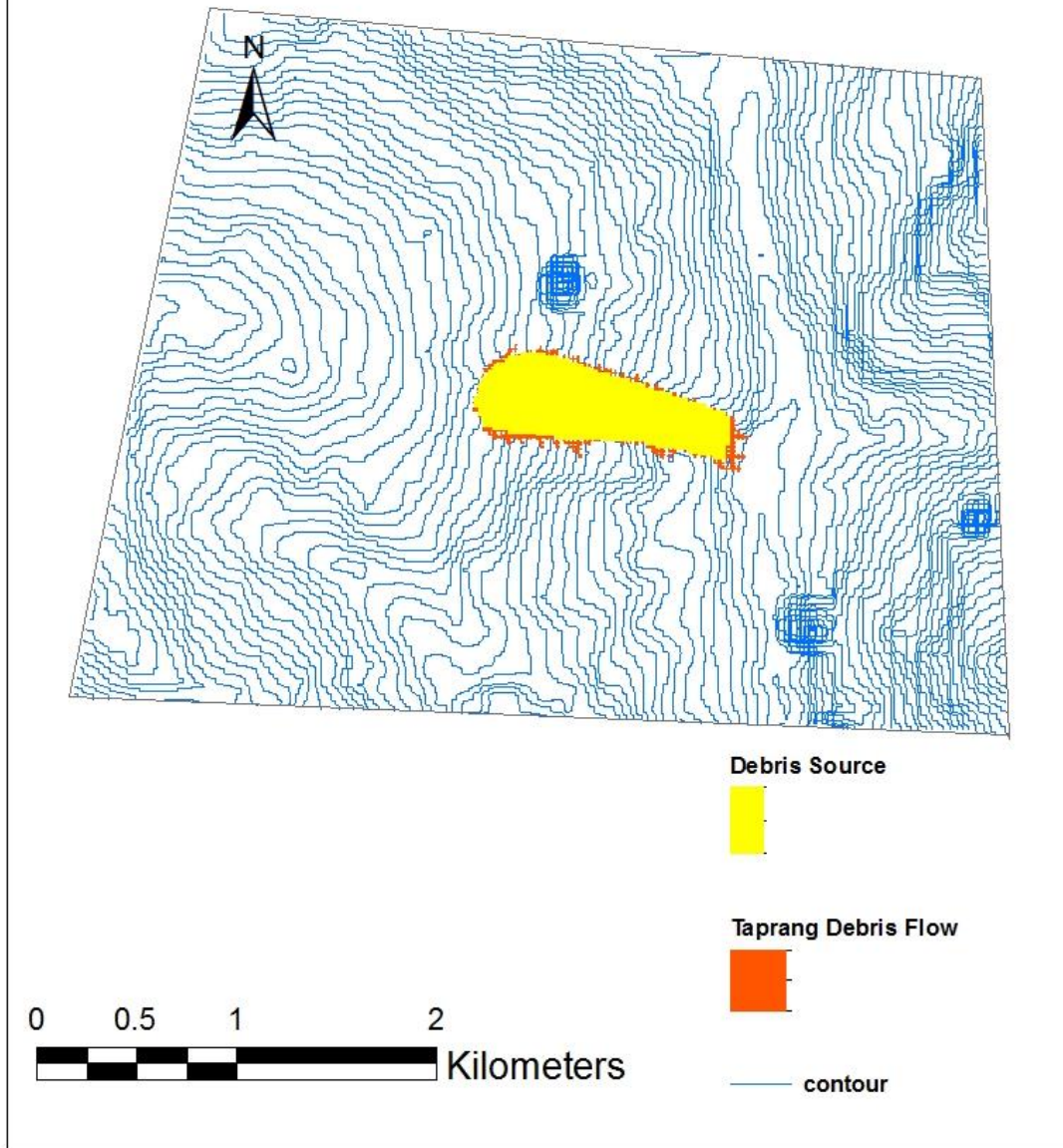
Figure 5.13: Debris flow from model study, minimum runout, Taprang landslide.
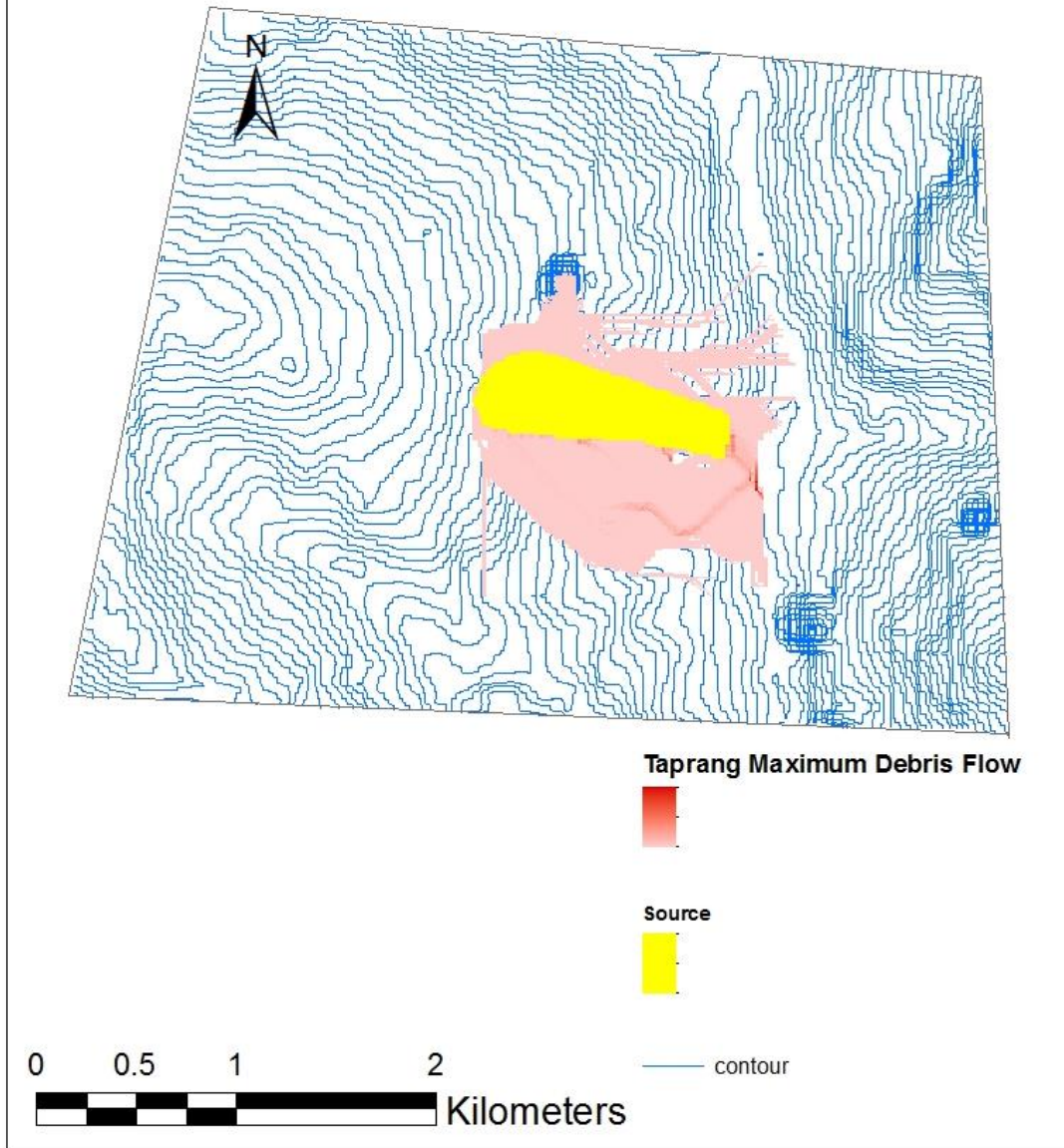
Figure 5.14: Maximum debris flow from model study, Taprang landslide.

5.8 Results and Discussion

5.8.1 Two Recent Landslides

The results of the application of the algorithms in Table 5.3 were compared with previous research by others in different regions. The result of the analysis for the D8 algorithm (O'Callaghan and Mark 1984) found no spreading, similar to the results found by Desmet and Govers (1996), Endreny and Wood (2003), Erskine et al. (2006) and Tarboton (1997). For this reason, this method was not applied for the analysis of the study watershed in this research. Tarboton (1997) proposed the D∞ (D infinity) algorithm, also used for the analysis of the observed debris flows, but spreading was small as also found by Horton et al. (2013). Fairfield and Leymarie (1991) proposed the Rho8 algorithm, a stochastic method, but the result was unable to capture the observed debris flow location, similar to the findings of Erskine et al. (2006). The result of the multiple flow direction model proposed by Quinn et al. (1991) provided satisfactory results compared to those observed in the field, similar to Huggel et al. (2003). The Freeman (1991) model was tested with the observed debris flows but the result found only small spreading. The modified Holmgren (1984) algorithm provided a little more spreading than that observed.

The modified Holmgren (1984) algorithm with low travel angle and low velocity found spreading similar to the Jure landslide (Figure 5.11) and the Taprang landslide (Figure 5.14). This will provide a more conservative spreading area, which is reasonable as the observed spreading area was not instantly measured in the field and observations of debris flows after several days or months may be smaller than the actual spreading during the debris flow incident. Therefore, this combination of algorithms was applied for the computation of debris flows in the study watershed, Kulekhani.

5.8.2 The Study Watershed

Three combinations of rainfall-induced landslide locations identified in Paudel et al. (2018) were applied as the debris flow source. The debris flow spreading results for the landslide source with 144 mm of rainfall in 24 hours are shown in Figure 5.15. The initial

landslide source covered 0.0012% of the watershed area, or the unstable area was 0.16 hectare (1600 m^2). The spreading area at this rainfall intensity and duration is 0.44 hectare (4400 m^2). The ratio of landslide spreading area to source area is almost 3:1. Thus, the spreading area is about 3 times larger than the source area for 144 mm of rainfall over a 24-hour period in the watershed.

The second combination of rainfall and duration applied in the model is 2 mm of rainfall per hour for 100 hours. The source area for this combination was identified to cover 0.017% of the watershed area or 2.16 hectares. The debris flow observed in this rainfall source covered 12.40 hectares. The debris spreading area is thus 5.70 times greater than the source area. Figure 5.16 shows the debris flow spreading for this rainfall scenario.

The unstable area for the extreme rainfall condition (540 mm in 24 hours) was also modeled in this study and is shown in Figure 5.17. The unstable locations in the watershed were 1.38% (1.715 km^2) of the total area. The debris flow spreading in this area was 2.68% of the total watershed (3.325 km^2) or 332.53 hectares. The ratio of spreading area to source area for this extreme case is about 2:1. It is understood from the model study that the debris flow source to spreading ratio decreases with minor to major (extreme) events.
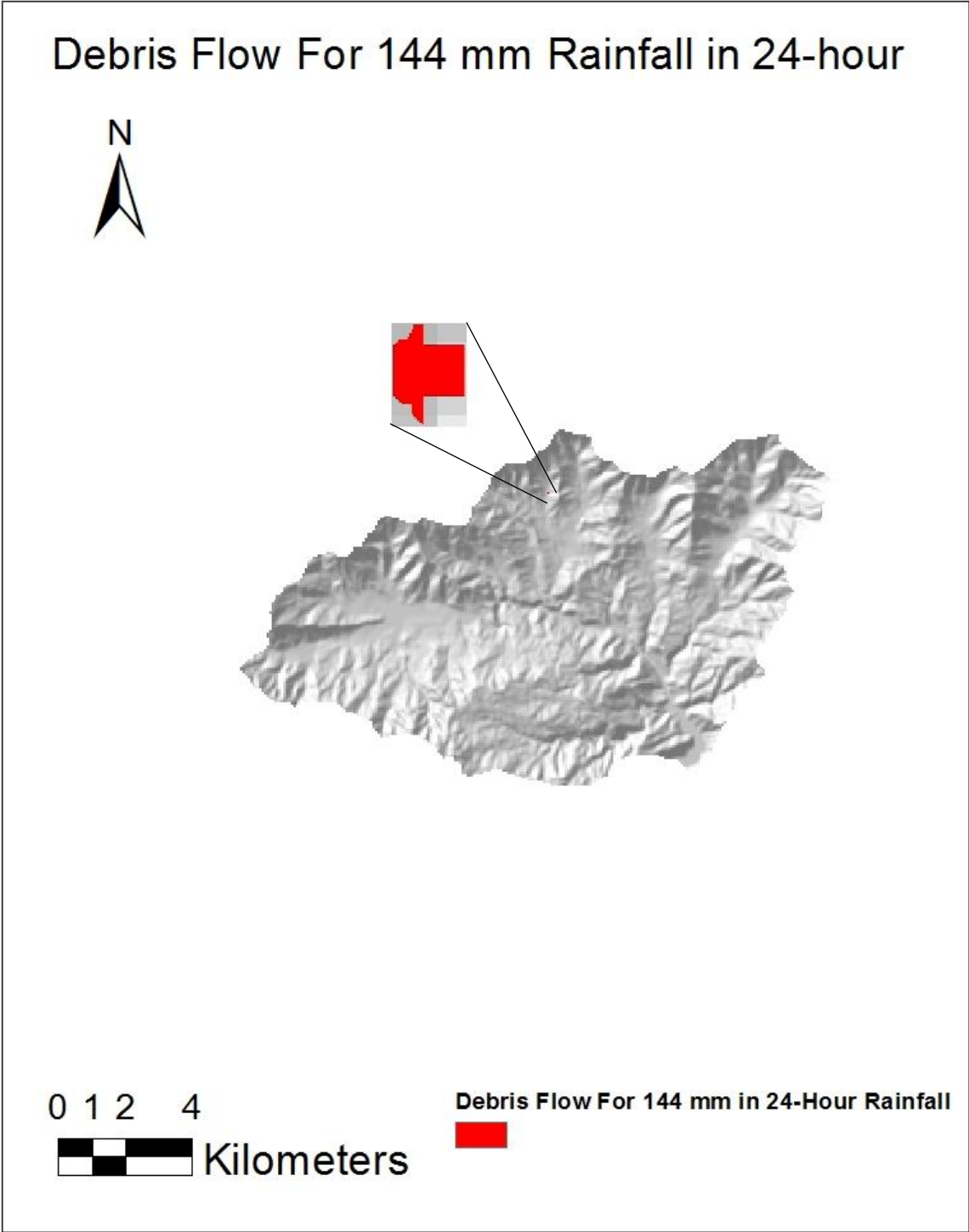
Figure 5.15: Maximum debris flow from the model study for 144 mm of rainfall in 24 hours.
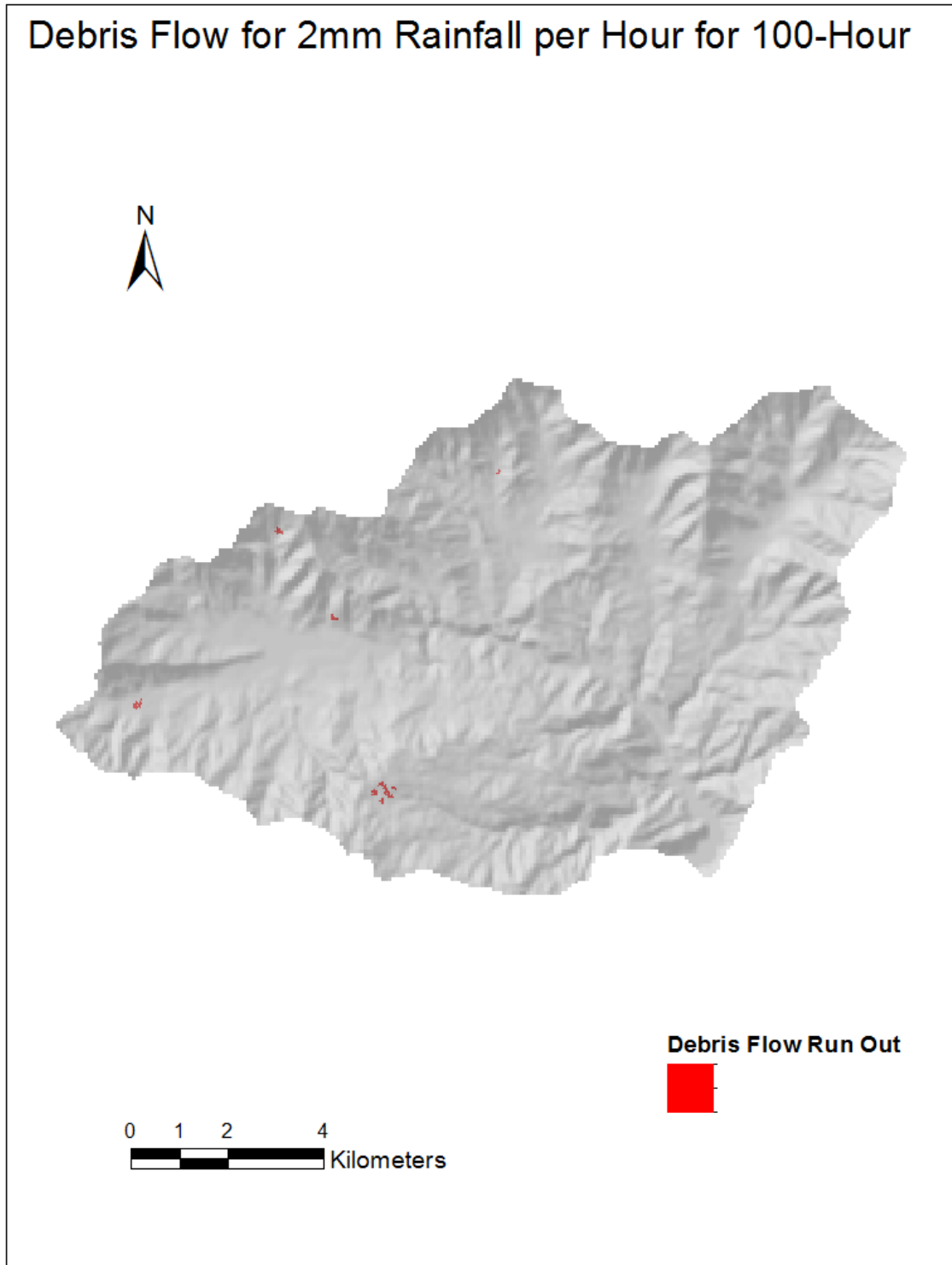
Figure 5.16: Maximum debris flow from the model study for 2 mm rainfall per hour for 100 hours.
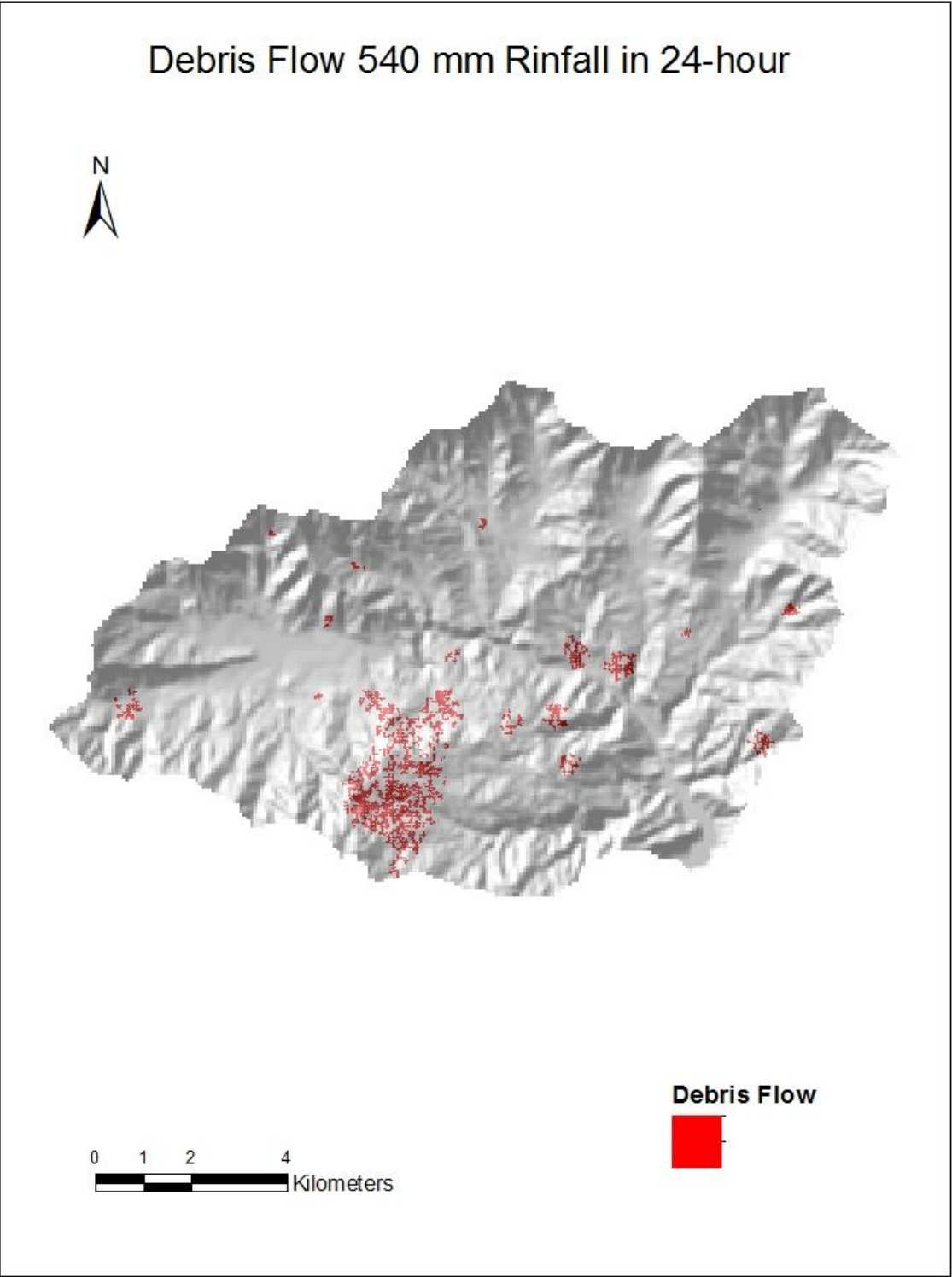
Figure 5.17: Maximum debris flow from the model study for 540 mm rainfall in 24 hours.

5.9 Summary and Conclusions

Rainfall-induced landslides change into debris flows and devastate large areas in mountainous Nepal. Both the initial landslide and debris flow inundation locations are important considerations for landslide hazard analysis. Debris flow runout assessment requires a large amount of information and computational processing. A simple model with a reasonable result from minimal resources and accessible computing tools is preferred by engineers and scientists for debris flow runout analysis. The Flow-R model is an empirical method requiring minimal data for susceptibility and runout analysis. The model is also capable of simulating runout from a user-defined debris flow source.

The Flow-R model was applied for two recent landslides that changed into debris flows. Various algorithms available in Flow-R were applied to simulate runout with the observed travel area. The model showed that it can predict debris flow from rainfall-induced initial landslides using selected algorithms for Nepal's mountains.

The appropriate algorithms obtained from the simulation of two recent landslides were then applied to the study watershed. The debris flow source was landslide susceptible areas previously obtained by Paudel et al. (2018). The results show that the debris flow spreading from the model study of the Kulekhani watershed covers 2.68% of the total area for the extreme rainfall event that occurred in the region in 1993. The model study results match with the debris flow observed by Kayastha et al. (2013), Dhital et al. (1993), Nippon Koei Co. Ltd. (2008) and Dhital (2003). The modeled debris flow spreading from the landside source shows that the minor rainfall event produces landslides with a greater spreading area to source area ratio than the extreme events with the selected algorithms.

5.10 References

Acharya, G., De Smedt, F., Long, N.T. (2006), Assessing landslide hazard in GIS: a case study from Rasuwa, Nepal. Bull Eng Geol Environ, 65 (1): 99–107.

Ayotte, D., Evans, N., Hungr, O. (1999), Runout analysis of debris flows and avalanches in Hong Kong. Proceeding of Symposium on Slope Stability and Landslides, organized by the Vancouver Geotechnical Society, Vancouver, B.C., Canada, May 1999, pp 39-46.

Beguera, S., Van Asch, Th.W. J., Malet, J.-P., Grondahl, S. (2009), A GIS-based numerical model for simulating the kinematics of mud and debris flows over complex terrain, Nat. Hazards Earth Syst. Sci., 9, 1897–1909.

Bhandary, N.P., Yatabe, R., Dahal, R.K., Hasegawa, S., Inagaki, H. (2013), Areal distribution of large-scale landslides along highway corridors in central Nepal, Georisk: Assessment and Management of Risk for Engineered Systems and Geohazards, pp 31.

Bijukchhen, S.M., Kayastha, P., Dhital, M.R. (2012), A comparative evaluation of heuristic and bivariate statistical modelling for landslide susceptibility mappings in Ghurmi–Dhad Khola, East Nepal. Arab J Geosci.

Blackwelder, E. (1928), Mudflow as a geological agent in semi-arid mountains, Geological Society of America, Bulletin, 39, 465-484.

Blahut, J., Horton, P., Sterlacchini, S., Jaboyedoff, M. (2010), Debris flow hazard modelling on medium scale: Valtellina di Tirano, Italy, Nat. Hazards Earth Syst. Sci 10 pp 2379-2390.

Brand, E.W. (1984), State-of-the-art report on landslides in Southeast Asia. Proc 4th Int Symp Landslides, Toronto, Canada 3: 105–106

Brand, E.W. (1981), Some thoughts on rain-induced slope failures. In: Proc 10th Int Conf Soil mechanics and foundation engineering, Stockholm. Balkema, Rotterdam, 3, pp 373–376.

Campbell, R.H. (1975), Soil slips, debris flows and rainstorms in the Santa Monica Mountains and vicinity, southern California, U.S.G.S. Prof. Paper, 851, 51 pp.

Cannon, S.H., Ellen, S.D. (1988), Rainfall that resulted in abundant debris-flow activity during the storm, In: Ellen S.D., Wieczorek G.F., Eds., "Landslides, floods, and marine effects of the storm of January 3-5, 1982, in the San Francisco Bay area", U.S.G.S. Prof. Paper, 1434, 27-34.

Carrara, A., Crosta, G., Frattini, P. (2008), Comparing models of debris-flow susceptibility in the alpine environment, Geomorphology, 94, 353–378.

Chen, H., Lee, C.F. (2002), Runout Analysis of slurry flow with Bingham model, Journal of Geotechnical and Geo-environmental Engineering Vol 128 No 12 pp 1032-1042.

Chen, H., Le, C.F. (2000), Numerical simulation of debris flows, Canadian Geotechnical Journal 37, 14-160.

Claessens, L., Heuvelink, G.B.M., Schoorl, J.M., Veldkamp, A. (2005), DEM resolution effects on shallow landslide hazard and soil redistribution modelling, Earth Surf. Proc. Land., 30, 461–477.

Corominas, J. (1996), The angle of reach as a mobility index for small and large landslides, Can. Geotech. J., 33, 260–271.

Crawford, C.S., Eden, W.J. (1967), Stability of natural slopes in sensitive clay. Journal of Soil Mechanics and Foundation Engineering, American Society of Civil Engineers, SM4, 419-436.

Crosta G.B., Cucchiaro S. & Frattini, P. (2002), Determination of the inundation area for debris flow through semi-empirical equations. Mediterranean Storms (Proceedings of the 4th EGS Plinius Conference, Spain Universitat de les Illes Balears.

Crosta G., Cucchiaro, S., Frattini, P. (2003), Validation of semi-empirical relationships for the defi nition of debris-fl ow behavior in granular materials. In Debris-fl ow Hazards Mitigation: Mechanics, Prediction, and Assessment, Rickenmann D, Chen C (eds). Millpress: Rotterdam; 821–832.

Cruden, D., Varnes, D. (1996), Landslide Types and Processes in Landslides: Investigation and Mitigation. ed. Turner, A. and Schuster, R. Transportation Research Board, National Research Council; 247. p. 36-75.

Dahal, R.J., Hasegawa, S., Bhandary, N.P., Poudel, P.P., Nonomura, A., Yatabe, R. (2012), A replication of landslide hazard mapping at catchment scale, Geomatics, Natural Hazards and Risk Vol. 3, No.2, 161-192.

Dahal, R.K., Hasegawa, S. (2008), Representative rainfall thresholds for landslides in the Nepal Himalaya, Geomorphology Vol. 100, No.3-4, pp. 429-443.

Dahal, R.K., Hasegawa, S., Nonomura, A., Yamanaka, M., Dhakal, S., Paudyal, P. (2008), Predictive modelling of rainfall-induced landslide hazard in the Lesser Himalaya of Nepal based on weights-of-evidence. Geomorphology, 102, (3–4): 496–510.

Dahal, R.K., Hasegawa S., Masuda T., Yamanaka, M. (2006), Roadside slope failures in Nepal during torrential rainfall and their mitigation. Universal Academy Press, Inc./ Tokyo, Japan, 503–514.

Dai, Z.L., Huang, Y., Cheng, H.L., Xu, Q. (2014), 3D numerical modeling using smoothed particle hydrodynamics of flow-like landslide propagation triggered by the 2008 Wenchuan earthquake. Eng Geol 180:21–23.

Dai, F.C., Lee, C. F and Nagi. Y. Y. (2002), Landslide risk assessment and management: an overview. Engineering Geology, 64: 65-87.

146

Dai, F.C., Lee, C.F. (2001), Frequency–volume relation and prediction of rainfall-induced landslides. Engineering Geology 59, 253–266.

Dangol, V., Upreti, B.N., Dhital, M.R., Wagner, A., Bhattarai, T.N., Bhandari, A.N., Pant S.R., Sharma, M.P. (1993), Engineering geological study of a proposed road corridor in eastern Nepal. Bulletin of the Department of Geology, Tribhuvan University, Nepal, Special Issue, 3(1), 91-107.

Davis, A.P., Poulas, S.J., Castro, G. (1999), A fragmentation-spreading model for long-runout rock avalanches, Canadian Geotechnical Journal, 36, 1096-1110.

Denlinger, R.P., Iversion, R.M. (2004), Granular avalanches across irregular three-dimensionsl terrain, 1 theory and computation, Journal of Geophysical Research – Earth Surface, 109, F01014.

Deoja, B.B., Dhital, M.R., Thapa, B., Wagner, A. (1991), Mountain risk engineering handbook, International Centre for Integrated Mountain Development (ICIMOD), Kathmandu, Nepal, pp 875.

Desmet, P.J.J., Govers, G. (1996), Comparison of routing algorithms for digital elevation models and their implications for predicting ephemeral gullies, Int. J. Geogr. Inf. Syst., 10, 311 – 331.

Devkota, K.C., Regmi, A.D., Pourghasemi, H.R., Yoshida, K., Pradhan, B., Ryu, I.C., Dhital, M.R., Althuwaynee, O.F. (2013), Landslide susceptibility mapping using certainty factor, index of entropy and logistic regression model in GIS and their comparison at Mugling-Narayanghat road section in Nepal Himalaya, Nat Hazard 65, 135-165.

Dhital, M.R. (2000), An overview of landslide hazard mapping and rating systems in Nepal. J of Nepal Geol Soc, 22: 533–538.

Dhital, M. R. (2005), Landslide investigation and mitigation in Himalayas: focus on Nepal. In: Proceedings of International Symposium Landslide Hazard in Orogenic Zone from the Himalaya to Island Arc in Asia, Kathmandu, Nepal, 1–1.

Dhital, M.R., Khanal, N., Thapa, K.B. (1993), The role of extreme weather events, mass movements, and land use changes in increasing natural hazards, A Report of the preliminary field assessment and workshop on causes of recent damage incurred in southcentral Nepal, July 19-20 1993. ICIMOD, Kathmandu, 123 pp.

Dhital, M.R. (2003), Causes and consequences of the 1993 debris flows and landslides in the Kulekhani watershed, central Nepal, Debris-flow Hazards Mitigation:Mechanics, Prediction and assessment, Rickenmann &Chen (eds) pp 1931-1943.

Dhakal, A.S., Amada, T., Aniya, M. (1999), Landslide hazard mapping and the application of GIS in the Kulekhani watershed Nepal. Mt Res Dev, 19(1): 3–16.

Eckersley, J.D. (1990), Instrumented laboratory flow slides, Geotechnique, 40(3), 489-502.

Ellen, S.D. and Fleming R.W. (1987), Mobilization of debris flows from soil slips, San Francisco Bay region, California. See Costa & Wieczorek 1987, pp. 31–40.

Endreny, T.A., Wood, E.F. (2003), Maximizing spatial congruence of observed and DEM-delineated overland flow networks, Int. J. Geogr. Inf. Sci., 17, 699–713.

Erskine, R., Green, T., Ramirez, J., MacDonald, L. (2006), Comparison of grid-based algorithms for computing upslope contributing area, Water Resour. Res., 42, W09416.

Fairfield, J., Leymarie, P. (1991), Drainage networks from grid digital elevation models, Water Resour. Res., 27, 709–717.

Fannin, R.J., Wise, M.P. (2001), An empirical-statistical model for debris flow travel distance, Canadian Geotechnical Journal, 38, 982-994.

Finlay, P.J., Mostyn, G.R., Fell, R. (1999), Landslide risk assessment prediction of travel distance Canadian Geotechnical Journal 36, 556-562.

FLO-2D User's manual (2003), Version 2003.06, FO-2D Software Inc. P. O. Box 66 Nutrioso, Arizona 85932.

Freeman, T. G. (1991), Calculating catchment area with divergent flow based on a regular grid. Comput. Geosci., 17, 413–422,

Fredlund, D. G., Xing, A.E. (1994), Equation for the soil-water characteristic curve, Can. Geotech. J 31:521-532.

Fell, R., Corominas, J., Bonnard, C., Cascini, L., Leroi, E., Savage, W.Z. (2008), Guidelines for landslide susceptibility, hazard and risk zoning for land use planning, Eng. Geol., 102, 85–98.

Gabet, E.J., Burbank, D., Putkonen, J.K., Pratt-Sitaula, B.A., Ojha, T. (2004), Rainfall thresholds for landsliding in the Himalayas of Nepal Geomorphology 63,131 – 143.

Gerrard, J., Gardner, R.A.M., (2000), Relationships between rainfall and landsliding in the Middle Hills, Nepal. Norsk geogr. Tidsskr. 54, 74–81.

Ghimire, M. (2011), Landslide occurrence and its relations with terrain factors in the Siwalik Hills, Nepal: case study of susceptibility assessment in three basins. Nat Hazards, 56(1): 299–320

Griswold J.P. (2004), Mobility Statistics and Hazard Mapping for Nonvolcanic Debris-fl ows and Rock Avalanches. Master Thesis, Portland State University, Portland, OR.

Griswold, J.P., Iverson R.M. (2008), Mobility Statistics and Automated Hazard Mapping for Debris-fl ows and Rock Avalanches, US Geological Survey Scientifi c Investigations Report 5276. US Geological Survey: Reston, VA; 59.

Hagen, T. (1969), Report on the geological survey of Nepal preliminary reconnaissance. Zürich Mémoires de la soc. Helvétique des sci. naturelles, pp185.

Hergarten, S., Robl, J. (2015), Modelling rapid mass movements using the shallow water equations in Cartesian Coordinates, Nat. Hazards Earth Syst. Sci., 15 pp671-685.

Holzer, T. Youd, T.L, Hanks, T.C. (1989), Dynamics of liquefaction during the 1987 Superstition Hills, California, earthquake. Science 244:56–59

Holmgren, P. (994), Multiple flow direction algorithms for runoff modelling in grid based elevation models: An empirical evaluation, Hydrol. Process., 8, 327–334.

Horton, P., Jaboyedoff, M., Rudaz, B., Zimmermann, M. (2013), Flow-R, a model for susceptibility mapping of debris flows and other gravitational hazards at a regional scale, Nat. Hazards Earth Syst. Sci.,13, pp 869-885.

Horton, P., Jaboyedoff, M., Bardou, E. (2008), Debris flow susceptibility mapping at a regional scale, in: Proceedings of the 4th Canadian Conference on Geohazards, edited by: Locat, J., Perret, D., Turmel, D., Demers, D., and Leroueil, S., Qu´ebec, Canada, 20–24 May pp 339–406.

Horton, P., Loye, A., Jaboyedoff, M. (2009), Debris flows and avalanches susceptibility hazard mapping for Pakistan – modelling of the two pilot districts Muzaffarabad and Manshera, Technical Report, Faculty of Geosciences and Environment, Institute of Geomatics and Risk Analysis, University of Lausanne, Switzerland.

Hsu, S.M, Ni, C.F., Hung, P.E. (2002), Assessment of three infiltration formulas based on model fitting on Richard's equation, Journal of Hydrologic Engineering 7, (5) 373-379.

Hsu, K.J. (1975), Catastrophic debris streams (Sturzstroms) generated by rock falls, Geological Society of America Bulletin, 86, 129-140.

Huggel, C.K.A., Haeberli, W., Krummenacher, B. (2003), Regional-scale GIS-models for assessment of hazards from glacier lake outbursts: evaluation and application in the Swiss Alps, Nat. Hazards Earth Syst. Sci., 3, 647–662.

Hutchinson, J.N. (1988), General report: morphological and geotechnical parameters of landslides in relation to geology and hydrogeology. In: Bonnard Ch (ed.) Landslides. Proc 5th Int Symp on Landslides. AA Balkema, Rotterdam, pp 3–35

Hungr, O., Evans, S.G. (1985), An example of a peat flow near Prince Rupert, British Columbia, Canadian Geotechnical Journal Vol 22 pp 246-249.

Hungr, O., Sun, H.W., Ho, K.K.S. (1999), Mobility of selected landslides in Hong Kong- pilot back-analysis using a numerical model, proceeding of the HKIE Geotechnical Division Seminar on Geotechnical Risk Management, May 1999, Hong Kong Institute of Engineers, pp169-175.

Hungr, O., Corominas, J., Eberhardt, E. (2005), State of the art paper #4, estimating landslide motion mechanism, travel distance and velocity. In: Hungr, O., Fell, R., Couture, R., Eberhardt, E. (Eds.), Landslide Risk Management. Proceedings, Vancouver Conference. A.A. Balkema Publishers, Rotterdam.

Hungr, O. (1995), A model for the runout analysis of rapid flow slides, debris flows, and avalanches, Canadian Geotechnical journal, Vol. 32, pp610-623.

Hungr, O., Evans, S.G. Bovis, M.J., Hutchinson, J.N. (2001), A review of the classification of Landslide of the flow type, Environmental and Engineering Geoscience, Vol VII No. 3 pp221-238.

Hungr, O., Morgenstern, N.R. (1984), Experiments on the flow behavior of granular materials at high velocity in an open channel, Geotechnique, 34, 3 405-413

Hurlimann, M. Rickenmann D., Medina, V. Medina, V., Beteman, A. (2008), Evaluation of approach to calculate debris-flow parameters for hazard assessment Engineering Geology 102, pp 152-163.

Hutter, K., Svendsen, B., Rickenmann, D. (1996), Debris flow modeling: A review, Continuum Mech. Thermodyn. 8 1-35 @ Springer-Verlag 1996.

Hunter, G., Fell, R. (2003), Travel distance angle for 'rapid' landslides in constructed and natural soil slopes. Canadian Geotechnical Journal, 40(6): 1123‑1141.

Iverson, R.M. (1997), The physics of debris flow, Reviews of Geophysics, Vol. 35(3) pp245-296.

Iverson, R.M., LaHusen, R.G. (1989), Dynamic pore-pressure fluctuations in rapidly shearing granular materials: Science, 246:796-799.

Iverson, R.M. (1990), Groundwater flow fields in infinite slopes, Geotechnique, 40, 139–143, 1990.

Iverson, R.M., Denlinger, R. P. (2001), Mechanics of debris flows and debris-laden flash floods, Seventh Federal Interagency Sedimentation Conference, Reno, Nevada, USA, 2001.

Iversion, R.M., Vallance, J.W. (2001), New views of granular mass flows, Geology 29, 2, 115-118.

Iverson, R.M., Reid, M.E., La Husen, R.G. (1997), Debris flow mobilization from landslides, Annual Review Earth Planet Science Volume 25 pp85-138.

Iverson R.M., Schilling S.P., Vallance J.W. (1998), Objective delineation of lahar-inundation hazard zones. GSA Bulletin 110(8): 972– 984.

Jaboyedoff, M., Labiouse, V. (2011), Technical Note: Preliminary estimation of rockfall runout zones, Nat. Hazards Earth Syst. Sci., 11, 819–828.

Jaboyedoff, M., Rudaz, B., Horton, P. (2011), Concepts and parameterization of Perla and FLM model using Flow-R for debris flow, Proceedings of the 5th Canadian Conference on Geotechnique and Natural Hazards, 15–17 May 2011, Kelowna, BC, Canada.

Jenson, S.K., Dominque, J.O. (1988), Extracting topographic structure from digital elevation data for geographic information system analysis, Photogramm. Eng. Rem. S., 54, 1593–1600.

Jha, B.K., Dhital, M.R., Dwibedi, S., Banskota, N., Amatya, S.C. (2014), Nepal Government Ministry of Irrigation (2014) Report on Jure Landslide, Mankha VDC, Sindhupalchowk District, http://dpnet.org.np/index.php?pageName=activities

Johnson, A.M. (1970), Physical processes in Geology. San Francisco, Freeman, Cooper. 577pp.

Johnson, A., Rodine, J.R. (1984), Debris Flow, Brundsden, D., and Prior, D.B., eds., Slope Instability, John Wiley & Sons. p. 257-361.

Johnson, K.A., Sitar, N. (1990), Hydrologic conditions leading to debris flow initiation. Canadian Geotechnical. J. 27,789–801.

Julien, P.Y., Lan, Y.Q. (1991), Rheology of hyperconcentrations, J. Hydraul. Eng., 117 (3), 346–353.

Kaiser, P.K., Simmons, J.V. (1989), A reassessment of transport mechanism of some rock avalanches in the Northwest Territories, Canada, Cana.Geotechnical Journal, Vol. 27, 129-144.

Kayastha, P., De Smedt, F. (2009), Regional slope instability zonation using GIS technique in Dhading, Central Nepal. In: Malet J P, Remaître A, Boggard T, eds. Landslide Processes: From Geomorphologic Mapping to Dynamic Modelling, CERG, France, 303–309.

Kayastha, P., Dhital, M.R., Smedt, F.D. (2013), Evaluation and comparison of GIS based landslide susceptibility mapping procedures in Kulekhani watershhed, Nepal. Jurnal of Gelogical Society of India, v 81, 219-231.

Kayastha, P., Dhital, M.R., Smedt, F.D. (2012), Landslide Susceptibility mapping using the weight of evidence method in the Tinau Watershed, Nepal. Nat Hazards 63:479-498.

Kayastha, P., De Smedt, F., Dhital, M.R. (2010), GIS based landslide susceptibility assessment in Nepal Himalaya: a comparison of heuristic and statistical bivariate analysis. In: Malet J P, Glade T, Casagli N, eds. Mountain Risks: Bringing Science to Society. CERG Editions, 121–128.

Kang, Z.C., Law, K.T., Lee, C. F. (2003), Movement pattern of debris flow SPISODE, Beijing, China.

Kang, Z. & Zhang, S. (1980), A preliminary analysis of the characteristics of debris flow, Proceedings of the International Symposium on River Sedimentation, Chinese Society for Hydraulic Engineering: Beijing 225-226.

Kang, Z. Wang, S.J., Lee, C.F., Law K.T. (2000), A study of debris flow hazard prevention, Institute of Mountain disasters and Environment Chinese Academy of Science, Department of Civil Engineering the University of Hong Kong, The Jockey Club Research and Information Centre for landslip prevention and land development.

Koerner, H.J. (1976), Reichweite und Geschwindigkeit von Bergsturzen und fleisschneelawinen. Rock Mech. 8, 225–256.

Korner, H.J. (1980), The energy-line method in the mechanics of avalanches, Journal of Geology, 26, 501-505.

Lamichhanne, S.P. (2000), Engineering geological watershed management studies in the Kulekhani watershed, M.Sc. Thesis, Tribhuvan, University, Nepal.

Legros F (2002), The mobility of long-runout landslide. Eng Geol 63:301–331.

Li, A.G., Yue, Z.Q., Tham, L.G., Lee, C. F. Law, K.T. (2004), Field monitored variation of soil moisture and matric suction in a saprolite slope, Canadian Geotechnical Journal.

Mathewson C.C., Keaton, J.R., Santi, P.M. (1990), Role of beedrock groundwater in the initiation of debris flows and sustained post-flow, Debris Flow Mobilization Sream Discharge Bull Assoc. Eng.Geo.27, 73-84.

McLellan, P.J., Kaiser, P.K. (1984), Application of a two parameters model to avalanches in the Mackenzi Mountains, Proceedings, 4th International Symposium on Landslides, Toronto, Vol 1 pp 135-140.

Nippon Koei Co. Ltd. (2008), The study on disaster risk management for Narayangharh-Muglung Highway, Interim Report.

O'Brien, J. S. (2003), FLO-D Users Manual, version 2003, FLO-2D Software Inc.

O'Brien, J.S. (1986), Physical process rheology and modeling of mudflows Doctoral dissertation, Colorado State Univerity, Fort Collins, Colorado.

O'Brien, J.S., Julien, P. Y. (1988), Laboratory analysis of mudflow properties, ASCE, Journal of Hydraulic Engineering, 114(8): 877-887.

O' Brien, J.S., Julien, P.Y. (1985), Physical processes of hyperconcentrated sediment flows, Proc. Of the ASCE Speciality Conf. On the Delineation of Landslides, Floods, and Debris Flow Hazard in Utah, Utah Water Research Laboratory, Series UWRL/G-85/03, 260-279.

O' Brien J. S., Julien, P.Y. (1987), Discussion on mountain torrent erosion, By K. Ashida in sediment transport in gravel-bed rivers, John Wiley and Sons, 537-539.

O' Brien, J. S., Julien, P.Y., Fullerton, W. T. (1993), Two-dimensional water flood and mudflow simulation, J. of Hydraulic Engineering, ASCE, 119(2)244-259.

O'Callaghan, J.F., Mark, D.M. (1984), Extraction of Drainage Networks from Digital Elevation Data, Computer Vision, Graphics and Image processing 20, 323-344.

O'Connor, J.E., Hardison, J.H. III, Costa, J.E. (1997), Debris flows from moraine-dammed lakes in the Three Sisters and Mt. Jefferson Wilderness Areas, Oregon. US Geol. Surv. WaterSupply Pap.

O'Connor, J. E., Hardison, J. H., Costa, J.E. (1993), Debris flows from recently deglaciated areas on central Oregon Cascade Range volcanoes, Eos Trans. AGU, 74, Fall Meet. Suppl., 314.

Pain, C.F. (1972), Characteristics and geomorphic effects of earthquake-initiated landslides in the Adelbert Range, Papua New Guinea, Engineering. Geol., 1972, 6(4), pp. 261-264.

Pantha, B. R., Yatabe, R., Bhandary, N.P. (2010), GIS-based highway maintenance prioritization model: an integrated approach for highway maintenance in Nepal Mountains. J Transp Geogr, 18(3): 426–433.

Pastor, M., Herreros, I., Fernandez Merodo, J.A., Mira, P., Haddad, B., Quecedo, M., Gonzalez, E., Alvearez,-Cedron, C., Drempetic, V. (2009), Modelling of fast catastropic landsides and impulse wave induced by them in fjords, lakes and reservoirs, Engineering Geology 109 pp124-134.

Pastor, M., Quecedo, M., Gonza´lez, E., Herreros, I., Ferna´ndez Merodo, J.A., Mira, P. (2004), A simple approximation to bottom friction for Bingham fluid depth integrated models. J Hydraul Eng ASCE 130(2),149–155.

Paudel, B., Fall, M., Danesfar, B. (2018), GIS-based landslide susceptibility modeling in Kulekhani watershed, Nepal (submitted).

Perla, R., Cheng, T.T., McClung, D.M. (1980), A two-parameter model of snow-avalanche motion, J. Glaciol., 26, 197–207.

Pierson, T.C. (2005), Hyperconcentrated flow - transitional process between water flow and debris flow. In Debris-flow Hazards and Related Phenomena. Praxis Publishing Ltd, Chichester, pp. 159-202.

Pierson, T.C., Janda, R., Thouret J.C., Borrero C.A. (1990), Perturbation and melting of snow and ice by the 13, November 1985 eruption of Nevado del Ruiz, Colombia, and consequent mobilization, flow and deposition of lahars, J. Volcanol. Geotherm. Res., 41, 17-66.

Pirulli, M., Mangeney, A. (2008), Results of back-analysis of the propagation of rock avalanches as a function of the assumed rheology, Rock Mech. Rock Eng., 41, 59–84.

Pudasaini, S.P. (2011), Some exact solutions for debris and avalanche flows, Phys. Fluids, 23(4), 043301, doi:10.1063/1.3570532.

Poudyal, C.P., Chang, C., Oh, H., Lee, S. (2010), Landslide susceptibility maps comparing frequency ratio and artificial neural networks: a case study from the Nepal Himalaya. Environ Earth Sci, 61(5), 1049–1064.

Pudasaini, S.P., Wang, Y., Hutter, K. (2005), Modelling debris flows down general channels, Nat. Hazards Earth Syst. Sci., 5, 799–819.

Quinn, P., Beven, K., Chevallier, P., Planchon, O. (1991), The prediction of hillslope flow paths for distributed hydrological modelling using digital terrain models, Hydrol. Process., 5, 59–79.

Ray, R.L, Smedt De, F. (2009), Slope stability analysis on a regional scale using GIS: a case study from Dhading, Nepal. Environ Geol, 57(7): 1603–1611.

Reid, M.E., LaHunsen, R.G., Iverson, R.M. (1997), Debris-flow initiation experiments using diverse hydrologic triggers, Cheng-lung Chen Ed., "Debris-Flow Hazard: Mechanics, Prediction, and Assessment", Proc. 1st int. conf., ASCE, S.Francisco, 1-11

Regmi, M.K. (2002), Geology of Kulekhani watershed in central Nepal with special reference to landslides and weathering, M.Sc. Thesis, Tribhuvan University, Nepal.

Rickenmann, D. (1991), Hyperconcentrated flow and sediment transport at steep slopes, Journal of Hydraulic Engineering, 117, 1419-1439.

Rickenmann, D. (1999), Empirical relationships for debris flows, Nat. Hazards, 19, 47–77.

Rickenmann, D., Zimmermann, M. (1993), The 1987 debris flows in Switzerland: documentation and analysis, Geomorphology, 8, 175–189.

Rickenmann, D. (2005), Runout prediction methods, In: Jakob, M., Hungr, O. (Eds.), debris flow hazards and related phenomena., Springer Berlin pp305-324.

Rickenmann, D., Laigle D., McArdell, B.W., Hubl, J. (2006), Comparison of 2D debris-flow simulation models with field events. Comput Geosci 10(1):241–264.

Rodine, J.D. (1974), Analysis of the mobilization of debris flows, Final Report to U.S. Army Research Office, Grant no. DA-ARO-D-31-124- 71-G158, pp.226.

Rodine, J.D., and Johnson, A.M. (1976), The ability of debris, heavily freighted with coarse clastic materials, to flow on gentle slopes, Sedimentology, v.23, 213-234.

Salm, B., Burkard, A., Gubler H. (1990), Berechnung von Fliesslawinen, eine Anleitung für Praktiker mit Beispielen. Mitteilungen des Eidgenössischen Institutes für Schnee und Lawinenforschung, No. 47, Davos, Switzerland.

Sassa, K. (2000), Mechanism of flows in granular soils. In GeoEng 2000: An International Conference on Geotechnical and Geological Engineering.

Sassa, K. (1988), Geotechnical model for the motion of landslides, In preoceeding of the seenth international symposium on landslide, edited by C. Bonnard, Laussane, Switzerland, 10-15 July 1988, A.A. Balkema, Rotterdam, Vol 1, pp37-55.

Sassa, K. (1985), The mechanism of debris flows. Proceedings of XI International Conference on Soil Mechanics and Foundation Engineering, San Francisco, 3, pp. 1173-1176.

Sassa, K., Wang, G. (2005), Mechanism of landslide-triggered debris flows: Liquefaction phenomena due to the undrained loading of torrent deposits. In Debris-flow Hazards and Related Phenomena. Praxis Publishing Ltd, Chichester, pp. 81-104.

Savage, W.Z., Baum R.L. (2005), Instability of steep slopes, Chapter 4, in Debris- flow Hazards and Related Phenomena, edited by M. Jacob and O. Hungr, pp. 53–79, Praxis Publishing House and Springer, Chichester, U.K.

Savage, S.B., Hutter, K. (1989), The motion of a finite mass of granular material down a rough inclined, Journal of Fluid Mchanics, 199, 177-215.

Savage, S.B., Hutter, K. (1991), The dynamics of avalanches of granular materials from initiation to runout, Part I Analysis, Acta Mechanica, 86 201-223.

Scheidegger, A.E. (1973), On the prediction of the reach and velocity of catastrophic landslide, Rock Mechanics, 5 231-236.

Sharma, R.H, Shakya, N.M. (2008), Rain induced shallow landslide hazard assessment for ungauged catchments. Hydrogeol J, 16(5): 871–877 Soeters R, van Westen C J (1996). Slope instability recognition, analysis and zonation. In: Turner K T, Schuster R L, eds. Landslide: investigation and mitigation. Special Report 247. Transportation Research Board, National Research Council, Washington DC, 129– 177.

Sidle, R.C., Swanston, D.N. (1982), Analysis of a small debris slide in coastal Alaska. Can. Geotech.J. 19 (2), 167-174.

Singh, M. (2014), Geotechnical Investigation of Madi landslide dam, Nepal, http://undergroundwaterresources.com/author/ms1573163gmail-com.

Takahashi, T., Yoshida, H. (1979), Study on the deposition of debris flows, Part I deposition due to abrupt change of bed slope. Annals of the Disaster Prevention Research Institute, Kyoto University, Kyoto, Japan, 22 B-2.

Takahashi, T., Nakagawa, H., Tarada, T., Yamashike, Y. (1992), Routing debris flows with particle segregation, Journal of Hydroulic Engineering, 118 (11), 1490-1507.

Takahashi, T. (1981), Estimation of potential debris flows and their hazardous zones: Soft counter (1981) measures for a disaster, Journal of Natural Disaster Science, 3, 57–89.

Takahashi, T., Nakagawa, H. (1989), Debris flow hazard zone mapping, Proc. Of the Japan-China (Taipai) Joint seminar on Natural Hazard Mitigation Kyoto, Japan, 363-372.

Takahashi, T., Nakagawa, H., Satofuka, Y. (2000), Newtonian fluid model for viscous debris flow, Wieczorek and Naeser (eds) Debris flow Hazards Mitigation: Mechanics, Prediction, and Assessment, Balkema, Rotterdam, ISBN 90 5809 149 X.

Takahashi, T., Satofuka, Y., Chishire, K. (2000), Dynamics of debris flows in the inertial regime Newtonian fluid model for viscous debris flow, Wieczorek and Naeser(eds) Debris Flow Hazards Mitigation: Mechanics, Prediction, and Assessment, Balkema, Rotterdam.

Tarboton, D.G. (1997), A new method for the determination of flow directions and upslope areas in grid digital elevation models, Water Resour. Res., 33, 309–319.

Thapa, P.B., Dhital M.R. (2000), Landslide and debris flows of 19–21 July 1993 in the Agra Khola watershed of central Nepal. J Nepal Geol Soc, 21: 5–20

Torres, G.H. (2011), Estimating the soil-water characteristics curve using grain-size analysis and plasticity index, M.Sc. Thesis, Arizona State University, Tempe, AZ.

Upreti, B.N., Dhital, M.R. (1996), Landslide studies and management in Nepal. International Centre for Integrated Mountain Development (ICIMOD), Kathmandu, Nepal, 87p

Varnes, D.J. (1978), Slope movement types and processes, in Schuster, R.L. and R.J. Krizek (ed.), Landslides Analysis and Control: National Academy of Sciences Transportation Research Board Special Report No. 176, p. 12-33.

Voellmy, A. (1955), Uber die Zerstorungskraft von Lawinen Schweizerische Bauzeitung, Jahrg 73. Heft 12, 159 - 162, 15, 212 - 217, 17, 246 - 249, 19, 280-285.

Wagner, A. (1997), Hazard mapping and geophysics applied to landslide study in the Himalayas and Hindukush, an unpublished brochure submitted to ITECO Nepal.

Wang, C., Li, S., Esak, T. (2008), GIS-based two-dimensional numerical simulation of rainfall-induced debris flow Nat. Hazards Earth Syst. Sci., 8, 47–58, 2008 www.nat-hazards-earth-syst.

Wong, H.N. Chen, Y.M., Lam, K.C. (1996), Factual Report on the November 1993 Natural Terrain Landslides in three study areas on Lantau Island, Geotechnical Engineering Office, Civil Engineering Department, Hong Kong.

Wong, H.N., Lam, K.C., Ho, K.K.S. (1997), Diagnostic report on November 1993 Natural Terrain Landslides on Lantau Island, GEO special report number 6/97.

Yagi, H. (2001), Landslide study using aerial photographs, Landslide Hazard Mitigation in the Hindu Kush-Himalayas. In: Tianchi L, Chalise SR, and Upreti BN (eds) Landslide hazard mitigation in the Hindu-Kush Himalayas, ICIMOD, Nepal, 79

Yagi H., Nakamura S. (1995), Hazard mapping on large scale landslides in the lower Nepal Himalayas. In: Proceedings of international seminar on water induced disasters (ISWID-1995), DPTC-JICA, Kathmandu, Nepal, 162-168.

Youd, T.L. (1993), Liquefaction-Induced Damage to Bridges, Transportation Research Record No. 14311, National Research Council, National Academy Press, Washington, D.C., 35-41.

Youd, T. (1973), Liquefaction, flow and associated ground failure Geological Survey Circular 688, United States Department of the Interior, U. S. Geological survey, Washington, D.C.2044.

Zimmermann, M., Mani, P., Gamma, P. (1997), Murganggefahr und Klima¨anderung – ein GIS-basierter Ansatz, NFP 31 Schlussbericht, Hochschulverlag an der ETH, Z¨urich, 1997 (in German).

Chapter 6: Technical Paper 3 - GIS-based assessment of debris flow hazards in Kulekhani Watershed, Nepal

Bhuwani Prasad Paudel, Mamadou Fall, Bahram Daneshfar

Abstract

Debris flows are a hazardous natural calamity in mountainous regions of Nepal. Torrential rainfall within a very short period of the year is the main triggering factor for instability of slopes and initiation of landslides. Furthermore, the topography of the mountains and poor land use practices are additional factors that contribute to these instabilities. In this research, a GIS model has been developed to assess the debris flow hazard in mountainous regions of Nepal. Landslide-triggering threshold rainfall frequency is related to the frequency of landslides and the debris flow hazard in these mountains. Rainfall records from 1980 to 2013 are computed for one- to seven-day cumulative annual maximum rainfall. The expected rainfall for 1 in 10 to 1 in 200 years return periods are analyzed. The expected threshold rainfall is modeled in the GIS environment to identify the factor of safety of mountain slopes in a study watershed. A relation between the frequency of rainfall and debris flow hazard area is derived for return periods of 25, 50, 100, and 200 years. The debris flow hazard results from the analysis are compared with a known event in the watershed and found to agree. This method can be applied to anticipated rainfall-induced debris flow from the live rainfall record to warn the hazard-prone community in these mountains.

6.1   Introduction

Rainfall-induced landslides that often change into debris flows are highly hazardous in mountainous Nepal. Nepal has diverse seasonal rainfall. Approximately 80% of annual rainfall occurs in the monsoon season (June to September) alone. The majority of land is mountainous terrain (almost 83%), and 67% of the total population live in these landslide-prone mountains. Landslides were the second most common cause of human death after epidemics in Nepal from 1971 to 2015.

153

From 1983 to 2016, the total number of deaths and missing from landslides was 9,153. This represents 269 lives lost per year (Ministry of Home 2016). Landslide leads to flooding in the lower part of the mountains that killed on an average 729 people per year between 1971 to 2016. Landslide and flooding destroyed about 5337 houses per year during the period from 1971 to 2014 (DWIDP 2017). The plain area of Nepal, which is about 17% of the total land in lower watersheds, is affected and damaged by flooding and debris flow following rainfall induced landslide. The loss of life and property is increasing every year as suitable land is unable to match the needs of the growing population for safe residential and commercial premises. This effect is further worsened by the unplanned use of land for various activities and infrastructure development. Because of limited resources and lack of understanding, the vulnerability to landside hazard and other hazard loss is at a high level in Nepal, as pointed by Corominas et al. (2014), compared to other developing countries. Assessment of hazard, vulnerability, and risk for development activities is not a common practice, as it is hindered by a lack of understanding of landslide initiation and its associated hazards.

The overall objective of this research is to develop models for landslide (debris flow) hazard assessment for Nepal's mountains. For landslide hazard assessment in a study area, knowledge of the temporal and spatial distribution of landslides for a given rainfall return period is necessary. Models of landslide initiation and debris flow assessment for different rainfall amounts in these mountains have been studied by Paudel et al. (2018). As a further step towards discovering landslide hazards, research on the probability of rainfall and its effect on the spatial distribution of landslides for different return periods will be assessed. Finally, a model for hazard assessment will be developed, and it will be employed for developing hazard maps of the study area.

6.2 Study Area

The area chosen for this study is the Kulekhani watershed, located in central Nepal, about 30 km south of the capital city, Kathmandu (Figure 6.1). The size of the watershed is approximately 124 km^2. The details of the watershed are available in Paudel et al. (2018), Kayastha et al. (2013), Dhital (2003), Dhakal et al. (2000, 1999,

1997), Lamichhanne (2000), and Dhital et al. (1993). The study watershed was devastated in 1993 by a landslide event that took the lives of 1,138 people in a single incident in the region. This landslide event was associated with extreme rainfall, which triggered more than 300 landslides, most of which changed into debris flows over a two-day period, July 19 and 20, 1993. The landslide event caused flooding in the lower watershed of the river system, and the total number of recorded deaths was more than 1,500 (Dhital 2003).
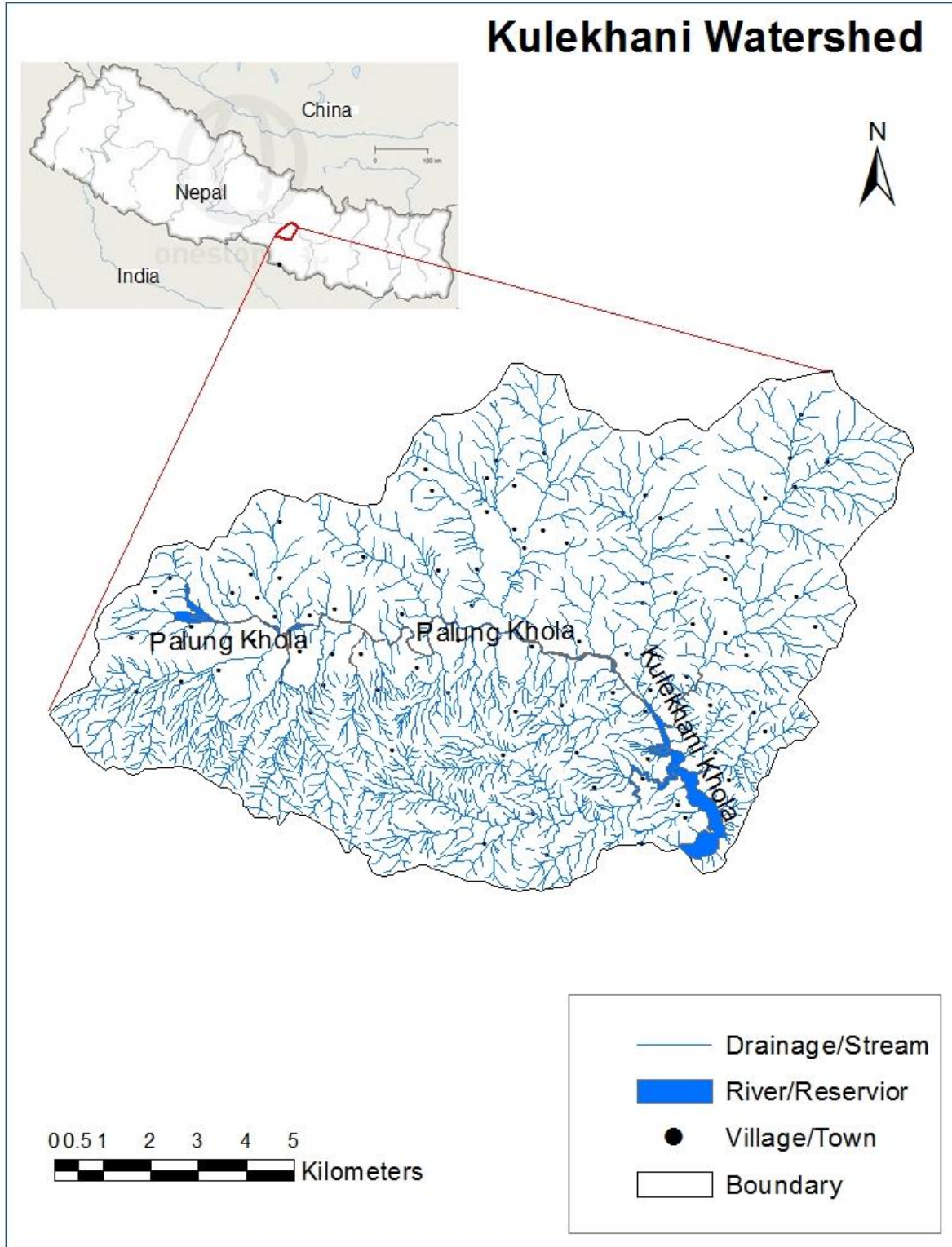
Figure 6.1: Location of the study area, Kulekhani, Nepal.

6.3 Methodology

A landslide hazard, as defined by Varnes et al. (IAEG Commission, 1984) in 1984, is "a probability of occurrence of a potentially damaging event in a given area and period of time". After 15 years of Varnes et al.'s work, Guzzetti et al. (1999) further defined landslide hazard by adding "magnitude" and redefining the probability of occurrence of a given magnitude of landslide in a given duration and location. Therefore, it is important to consider three components: probability of occurrence of a landside, its location, and its size when one conducts landslide hazard assessment. Fall (2009) further clarified the term, stating that landslide hazard is characterized by "its location, intensity (magnitude), frequency and probability". The probability of the landside initiation, debris flow inundation, and the magnitude of the event to create vulnerability to the element at risk are important factors for landslide hazard and risk assessment.

In this paper, the model for the "hazard" is assessed by applying landslide-triggering threshold rainfall duration, intensity, and annual probability (Corominas 2014; Guzzetti et al. 2008, 2007, 2006; Guzzetti 2005). Paudel et al. (2018) (Technical Paper I) verified the critical rainfall intensity and durations for landside initiation while studying these mountains. These combinations of duration and intensity of rainfall with their return period (annual probability) are applied to obtain the probability of landslide-susceptible areas. This method is applied to the study watershed area to estimate the potential locations of probable landslide occurrence regions for a given rainfall return period. The relation of landslide area and rainfall return period is derived for different rainfall recurrence within the watershed to use in hazard analysis, as proposed by Reid and Page (2003).

Many models for landslide hazard assessments are GIS-based statistical methods, which use previous landslide events as a base factor for the identification of potential landslides in the future (Jaiswal 2011, Remondo 2008). However, when a landslide occurs, the topography of the area changes, and a similar rainfall intensity and duration may not still be the threshold rainfall, even though its recurrence period is the same. When one landslide event occurs, new analysis is required to consider the associated

157

morphological change. A model that can consider physical features of the watershed during landslide-triggering threshold rainfall is necessary for finding potential landslide locations, independent of previous events. By using rainfall events, determination of related landslide-susceptible areas, debris flow inundation, and the probability of hazard are carried out in a GIS environment in this research. The outcome is the identification of the phenomenon that makes particular hill slopes severely unstable for a given annual probable rainfall intensity and duration, and its application to hazard analysis.

Figure 6.2 shows the methodology developed for the assessment of debris flow hazard in the study area, as well as the relationship between the different work steps of the investigations carried out. This approach includes four main stages. The first stage consists of the acquisition of data and development of the database, which are required to conduct the work described in the other stages of this study. In the second stage of this investigation, a GIS-based assessment of landslide susceptibility and probability in the study area is performed. The frequency of annual maximum rainfall is analyzed and their related landslide events in temporal and spatial dimension are derived for the study watershed. These landslide locations are considered as debris flow sources or debris flow initiation points. The third stage deals with the GIS-based assessment of debris flow runout. The debris flow runout distances are modeled from the identified landslide initiation points. This assessment results in the development of a debris flow inundation map of the study area. Finally, in the fourth stage of this study, the results obtained in stages 2 and 3 are used to conduct a GIS-based assessment of debris flow hazards to develop a debris flow hazard map for the study area. The main stages are described in detail below.
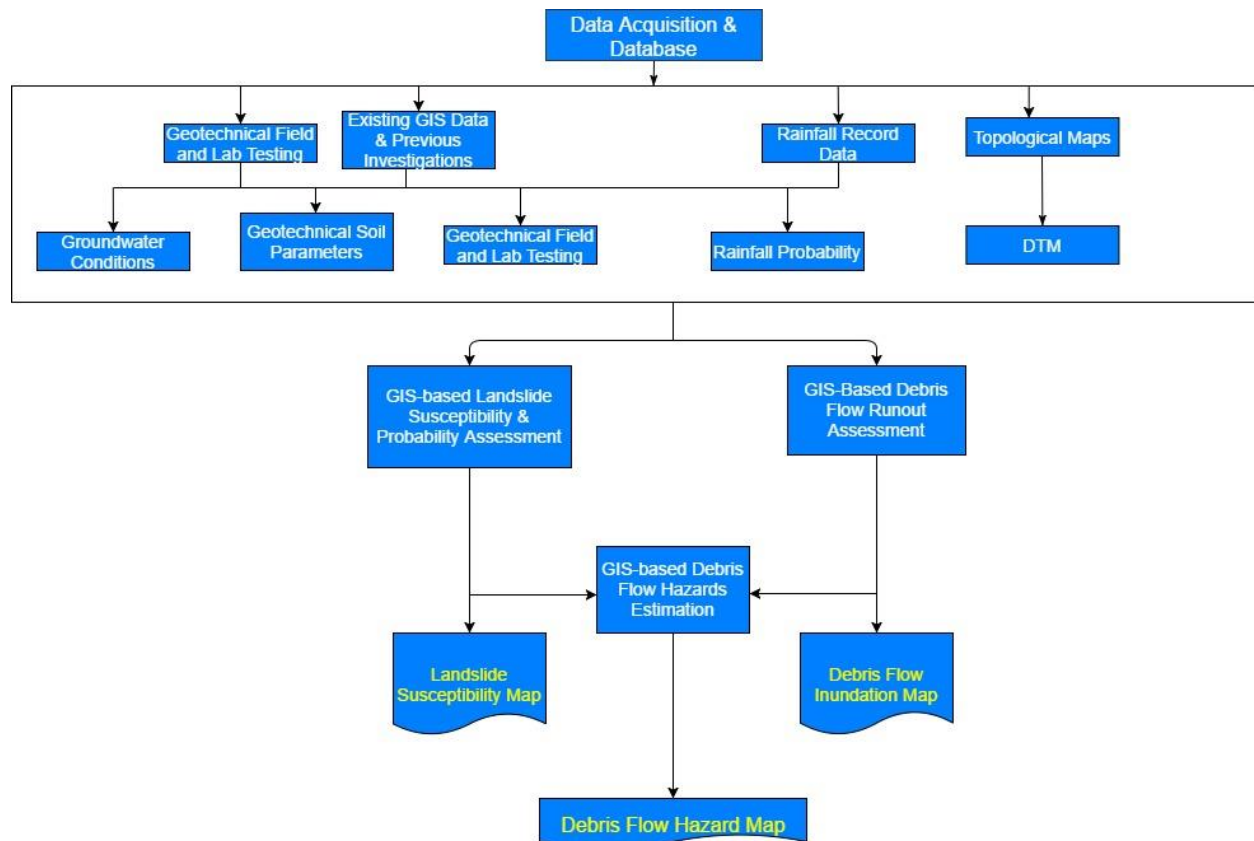
Figure 6.2: Landslide (debris flow) hazard analysis methodology. (GIS = Geographical Information System, DTM = Digital Terrain Model).

6.3.1 Data Acquisition and Database

Data required for this study include: (i) a topographical map of the study area that was obtained from the Topographical Survey of Nepal. Digital elevation Model (DEM) was then developed from the topographical map. Slope maps were developed from the DEM as shown in Figure 6.3; (ii) a geological map and previous landslide location maps, which were collected from previous research in the study watershed (Paudel et al. 2018, Lamichhanne 2000, Kayastha 2013); (iii) geotechnical parameters of the soils present in the study area. These geotechnical parameters were obtained from the results of the field and laboratory investigations performed in this study, as well as from previous geotechnical investigations in the study area (Paudel et al. 2018, Lamichhanne 2000);

(iv) Rainfall data from the Department of Hydrology and Meteorology of Nepal; (v) Soil Water Characteristics Curves (SWCC) developed from the above information.

6.3.1.1　　Rainfall Data

In the study watershed, rainfall is recorded at four rain gauge stations. Two rainfall recording gauge stations, Daman and Markhu, are within the watershed and two, Chissapani and Thankot, are located close to it. Among these four rain gauge stations, the rainfall recorded in Chissapani is the highest. Rainfall is recorded once in each 24-hour period for all of these stations. The rainfall data is available for the period from 1980 to 2013. As Chissapani Ghadi rain gauge station received the maximum rainfall of the four stations, this station is considered for finding the worst conditions for rainfall-induced landside hazard in the study watershed.

From the daily recorded rainfall during the period 1980 to 2013, the maximum rainfall for one-day to seven-day periods is analyzed. These series of rainfall are used for probability analysis. The probability of rainfall for one to seven days, and the consequences for landslide susceptibility are derived.

6.3.1.2　　Topographical Map and DEM

The topographical map is modeled as a Triangulated Irregular Network (TIN) to develop DEM, a raster map, Figure 6.3. Figure 6.3 is further used for developing slope maps. Maps of all parameters are developed in the GIS environment. All individual maps are interpolated using Inverse Distance Weighted (IDW) methods to create continuous raster maps for the whole watershed. The extent of these maps and their cell numbers are sized to the same scale for raster analysis.
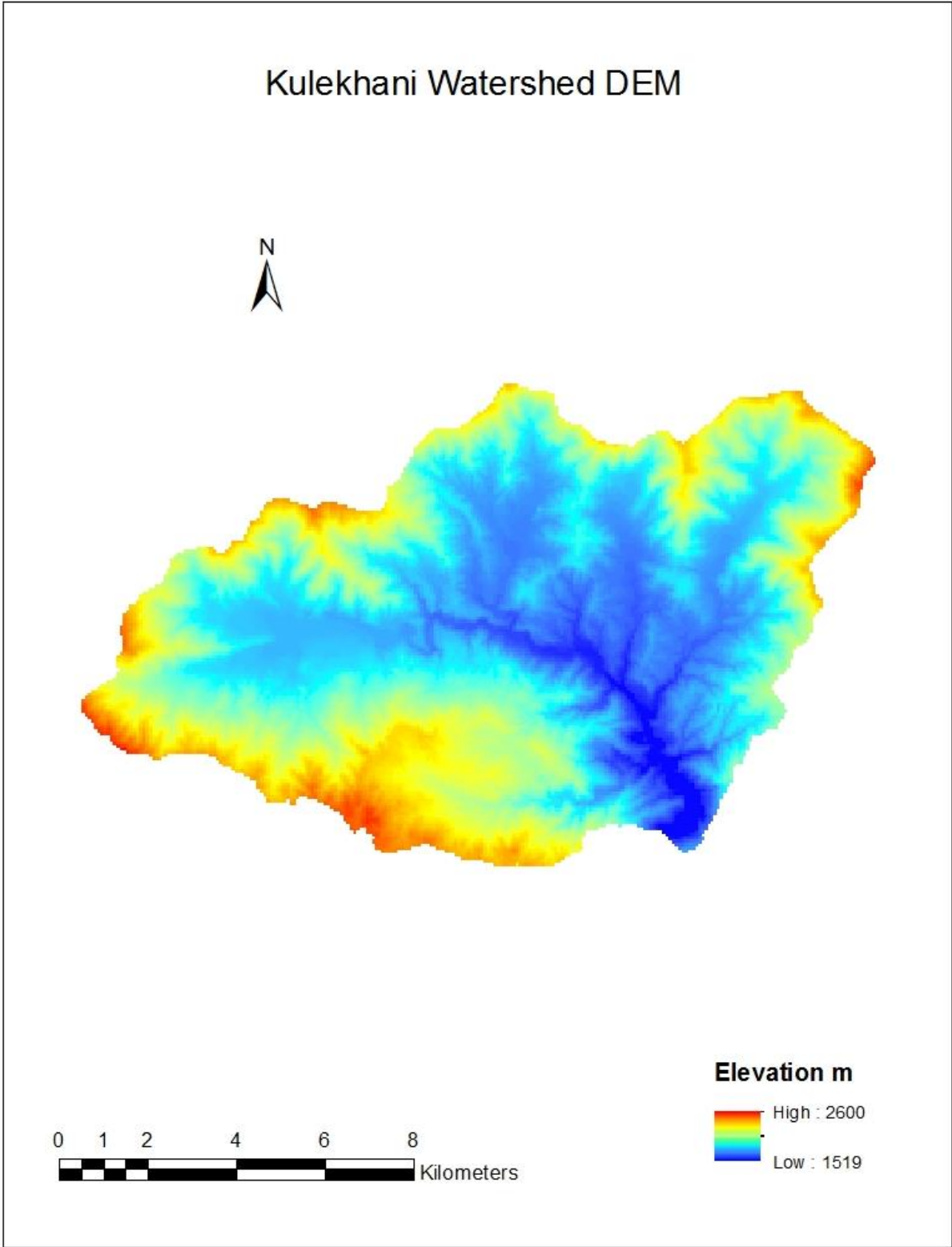
Figure 6.3: Digital Elevation Model (DEM) for the study watershed, Kulekhani.

6.3.1.3 Groundwater Conditions

There is no stable groundwater table in the hill portions of the studied watershed, although the annual average rainfall from four rain gauge stations is 1,813 mm. The groundwater flow pattern and its significance for landslides in this watershed can be found in Deoja et al. (1993). Some natural water springs are found in the lower part of the watershed, but those pass through the rock faults. A temporary perched water table develops and moves downward based on the intensity and duration of rainfall. There is no stable groundwater table in the hill slope that influences the slope stability in higher mountains in Nepal. A water table is available in deeper locations in the valley which have no to very mild slopes, therefore, groundwater effects are not considered in the analysis.

6.3.1.4 Geotechnical Data

One previous landslide location was chosen for the geotechnical investigations of the site to obtain additional relevant geotechnical data (e.g., cohesion and friction angle, representing soil strength parameters). The cohesion and friction angle were obtained from direct shear testing (IS:2720-1985). On-site infiltration tests were conducted on two boreholes to ascertain infiltration capacity and permeability of in situ soils. The initial moisture content, saturated moisture content, saturated unit weight, dry unit weight, specific gravity, void ratio, grain size distribution, and saturated cohesion and friction angle were obtained from collected samples. Other watershed information of the study area is given in Dhital (2003 and 1993).

The observed infiltration (0.00178 cm/sec) is very high as compared to normal rainfall intensity in the area. For infiltration depth computation, rainfall intensity is used as the permeability coefficient in the analysis for low-intensity rainfall, and the infiltration rate is used for higher-intensity rainfall. Therefore, the observed infiltration rate was used as the permeability coefficient for the infiltration depth computation for high-intensity rainfall. The maximum wetting depth is observed for a longer duration during recorded high rainfall, as infiltration is very high.

162

GIS layers representing each parameter required for Equation [6.14] are developed and analyzed in the GIS environment.

6.3.1.5   SWCC

A total of 73 locations in the watershed were considered for SWCC development. Soil grain size distribution, plasticity index, and natural moisture content information from those locations (Lamichhanne 2000) was applied to find matric suction. The results were interpolated to the whole watershed using Inverse Distance Weighted (IDW) methods in GIS. The infiltration depth of probable maximum rainfall for one-day to seven-day cumulative maxima for 25-, 50-, 100-, and 200-year return periods are analyzed.

6.3.2 Landslide Probability

Corominas et al. (2014) indicated that the probability of landslide occurrence in a given area can be obtained using different methods: heuristic (or expert judgement) methods, rational (geomechanical approach) methods, empirical probability, and indirect methods. Corominas (2014) also suggested an indirect approach to obtain the probability of landside occurrence by relating the frequency of triggering factors, such as earthquakes or rainfall for any watershed. In this research, the indirect approach is applied to estimate landside frequency from the frequency of landslide-triggering rainfall events. A landslide-triggering rainfall event X occurs for precipitation more than the threshold rainfall Xt in a given time period for any watershed. The return period of the threshold rainfall may be defined as the average recurrence interval between events equal to or exceeding the threshold rainfall for this watershed. The probability of any rainfall event more than the threshold rainfall is the product of the probability of a rainfall event less than the threshold rainfall times the probability of one event more or equal to the threshold rainfall. The expectation of recurrence period E(t) can be defined as given below (Chow et al. 1988):

$$\mathrm{E}(t) = \sum_{t=1}^{\infty} t(1-p)^{t-1} p \qquad\qquad [6.1]$$

163

where p is the probability of the event and t is the time period:

$$= p + 2(1-p)p + 3(1-p)^2 p + \ldots\ldots\ldots\ldots\ldots$$

$$= p\left[1 + 2(1-p) + 3(1-p)^2 + \ldots\ldots\ldots\right]$$

$$E(t) = p\left[(1-(1-p)\right]^{-2} \qquad\qquad [6.2]$$

$$E(t) = \frac{p}{\left[1-(1-p)\right]^2} = \frac{1}{p} = T \qquad\qquad [6.3]$$

where the return period T of a rainfall event is the inverse of the probability, as the rainfall event is a random event, independent of space and time.

The probability of a rainfall event X exceeding the threshold rainfall, Xt, for landslide initiation in a watershed can be written as P(X≥Xt) =1/T. This is an annual probability of the rainfall. The probability of any rainfall greater than the threshold rainfall for a given year period N is

$$= 1 - (1-p)^N \quad [6.4],$$

or, the probability of threshold rainfall at least once in N year $= 1 - \left(1 - \dfrac{1}{T}\right)^N$ [6.5]

Landslides do not occur during the maximum rainfall of every year, but may occur when both rainfall duration and intensity increase beyond the threshold value. These rainfall durations and intensities, which trigger landslides, are extreme values in the probability distribution function. These extreme values may appear a couple of times in a single year, or not at all in some years. The probability distribution of these events must consider them as extreme value events, and therefore requires the application of an extreme value distribution function for probability analysis (Chow et al. 1988).

Extreme value observation lies in the initial or end of the probability distribution function of all observations. Chow at al. (1988) mentioned that there are three ways to analyze these observations based on the location of interest in the distribution function such as high, low, or normal rainfall. These are extreme value distribution Type I, Type II, and Type III. Extreme rainfall events are mostly modeled by the extreme value type I

distribution (Chow et al. 1988, Tomlinson 1980, Chow 1953). The extreme value Type I probability distribution function can be written as given below (Chow et al. 1988):

$$F(x) = \exp\left[-\exp\left(-\frac{x-u}{\alpha}\right)\right] \qquad -\infty \leq x \leq \infty \quad [6.6]$$

Parameters $\alpha = \dfrac{\sqrt{6}s}{\pi}$ $\qquad\qquad$ [6.7]

$$u = \bar{x} - 0.5772\alpha \qquad\qquad [6.8]$$

where u is the mode of distribution (almost at the maximum probability density location), $\bar{x}$ is the average, s is the standard deviation,

If $\left(\dfrac{x-u}{\alpha}\right)$ is replaced with y $\qquad\qquad$ [6.9]

From equation [6.6]:

$$y = -\ln\left[\ln\left(\frac{1}{F(x)}\right)\right] \qquad\qquad [6.10]$$

For return period T:

$$y_T = -\ln\left[\ln\left(\frac{T}{T-1}\right)\right] \qquad\qquad [6.11]$$

From Eq. [6.10]:

$$X_T = u + \alpha y_T \qquad\qquad [6.12]$$

$$X_T = u + \alpha\left[-\ln\left[\ln\frac{T}{T-1}\right]\right] \qquad\qquad [6.13]$$

For a given return period T, the probability of rainfall X_T at least once, other parameters as defined above.

Rainfall data from 1980 to 2013 in the selected gauge station (Chhisapani Ghadi) were used in the analysis (Paudel et al. 2018). From these data, one-day to seven-day period cumulative annual maximum rainfall dates were identified. The cumulative rainfall on those dates was developed for each year from 1980 to 2013. Among these data, one-day (24-hour) maximum annual events were modeled using Log Pearson type II and

165

type I. It is found that the extreme values obtained from the frequency analysis are significantly lower in type II than the extreme value of type I distribution. For further frequency analysis, the extreme value of type I is considered. The annual probability of one-day cumulative maximum rainfall to seven-day cumulative maximum rainfall is analyzed. The associated probability of rainfall-induced landslide area is computed. Analysis of the return periods of 25, 50, 100, and 200 years are used for probable rainfall at least once annually. The rainfall event within the given duration from one to seven days, and return period of 25 to 200 years are applied in the landslide initiation analysis.

6.3.3 Landslide Initiation or Susceptibility Assessment

The identification and mapping of landslide-susceptible zones with threshold rainfall is necessary for hazard assessment. Rainfall-induced landslide susceptibility has been studied by several authors, such as Horton et al. (2013, 2009, 2008), Park et al. (2013), Tsai and Chiang (2013), Chiang et al. (2012), Enrico and Antonello (2012), Meyer et al. (2012), Kim et al. (2010), Muntohar and Liao (2009), Salciarini et al. (2008), Tsai and Yang (2006), Chen et al. (2005), Fell et al. (2005), and Hsu et al. (2002). Some of the models used by these researchers required a large number of input data and complex procedures. Besides dealing with a huge data-driven complex relation of rainfall and slope instability, a simple model coupled with rainfall thresholds is a more practical approach for landslide susceptibility assessment (Casadel et al. 2003). Furthermore, the empirical relation of rainfall intensity and duration to landslide initiation can be found in Saito et al. (2010), Zezere et al. (2005), Aleotti (2004), Crosta and Fratini (2001), Ceriani et al. (1992, 1994), Wieczorek (1987), Cancelli and Nova (1985), Caine and Mool (1982), and Caine (1980). For mountains in Nepal, Dahal and Hasegawa (2008) recommended a relation of threshold rainfall intensity and duration for landslide initiation. However, their method does not consider influencing factors such as topography, soil characteristics, and groundwater (Rahardjo et al. 2007). After comparing various models, Chen and Young (2006), Casadel et al. (2003), Hsu et al. (2002), and Claunitzer et al. (1998) suggested a simple rainfall and slope stability model

166

for practical applications. Considering this, the following models are selected for landslide susceptibility assessment.

Slope Stability Model: The slope stability for an unsaturated slope proposed by Fredlund et al. (1987) and Cho and Lee (2002) is considered in this research. This method can consider the initiation of landslide at different rainfall thresholds. The depth of the wetting front Z_w will be equivalent to H in equation [6.14] for the stability analysis.

$$F_s = \left[\frac{\left((c' + (u_a - u_w)\tan\phi^b) + ((\sigma_n - u_a)\tan\phi') \right)}{(\gamma_t HSin\beta Cos\beta)} \right] [6.14]$$

where F_s = factor of safety (FoS), c' is effective cohesion, ϕ' is effective friction angle, σ_n is normal stress, H is wetting front depth, β is slope angle, γ_t, is the unit weight of soil, u_a is pore air pressure, u_w is the pore water pressure, $(u_a - u_w)$ is matric suction, $\sigma_n - u_a$ is effective normal stress on the slip surface, and ϕ^b is the rate of increase in shear strength due to matric suction.

The infinite slope stability equation [6.14] has an unsaturated soil suction portion $(u_a - u_w)$ $\tan\phi^b$. If the soil degree of saturation reaches 100%, this portion of the soil strength parameter becomes zero, and will be similar to saturated conditions. Various models are available for identification of $(u_a - u_w)$ $\tan\phi^b$ in terms of $\tan\phi'$ (Khalili and Khabbaz 1998, Fredlund et al. 1996, Vanapalli et al. 1996). The equivalent shear strength relation proposed by Fredlund et al. (1996), given in equation [6.15], is used in this study.

$$t_f = c' + (\sigma_n - u_a)tan\phi' + (u_a - u_w)[(\theta^k)(tan\phi')] \qquad [6.15]$$

where t_f is shear strength, Θ is the normalized water content (Θ_w / Θ_s), Θ_w is water content at a given suction, and Θ_s is saturated water content. After Garven and Vanapalli (2006), and Vanapalli and Fredlund (2000), the fitting parameter k is related to the plasticity index (I_p) of soil in %, and is given in equation [6.16].

$$k = -0.0016I_p^2 + 0 \cdot 0975I_p + 1 \qquad [6.16]$$

For non-plastic soil, I_p will be zero and the fitting parameter k is equal to 1, which leads to tan$\varnothing^b$ equal to Θ tan$\varnothing'$.

Unsaturated soil shear strength (Vanapalli and Fredlund 1999, Fredlund et al. 1987, 1978, Fredlund and Rahardjo, 1993) can be obtained from Soil Water Characteristics Curve (SWCC). Empirical relations developed based on grain size distribution by previous researchers, Torres (2011), Fredlund and Xing (1994, Equation [6.17]), and Zapata (1999), are applied to obtain the soil water characteristics curve. The modified SWCC model proposed by Fredlund and Xing (1994), Equation [6.17], requires various parameters. These parameters are: degree of saturation (S); soil suction at residual moisture content, h_r in kPa; a soil parameter related to the rate of water extraction of the soil after air entry value (a), n (b_f); the slope of the SWCC; m (c_f), which is a fitting parameter or function of the residual water content; air soil parameter, a, which is a function of the air entry value in kPa; soil suction Ψ, in kPa; the initial volumetric water content Θ_w; and the volumetric water content in saturated conditions Θ_s.

$$S(\%) = \frac{\theta_w}{\theta_s} = 1 - \frac{\ln\left(1 + \frac{\Psi}{h_r}\right)}{\ln\left[1 + \left(\frac{1,000,000}{h_r}\right)\right]} x \left[\frac{1}{\left\{\ln\left[e + \left(\frac{\Psi}{a}\right)^{b_f}\right]\right\}^{c_f}}\right] \qquad [6.17]$$

The empirical model (Equation [6.18]) proposed by Torres (2011) is applied here to obtain SWCCs in which all grain sizes are used in the model. The detail of the analysis method is given in Torres (2011) and implemented in Paudel et al. (2018). The wPI term in Equation [6.18] can be obtained from Equation [6.19], in which P_{200} is percentage passed through a 200-number of sieve, and PI is the Plasticity Index.

$$\log \Psi = 0.00005(wPI)^3 - 0.003(wPI)^2 + 0.03wPI + 1.1355 - (0.0126wPI + 0.7285)\log D$$
$$- (0.0011wPI + 0.0044)\log D^2 + (0.0002wPI + 0.0056)\log D^3 \qquad [6.18]$$

$$wPI = \frac{P_{200}(PI)}{100} \quad \text{[6.19]}$$

where, wPI = weighted plasticity index in %, P_{200} = Material passing through a #200 US Standard Sieve in %, PI = Plasticity Index, expressed in %

Infiltration model: based on a wetting front concept (Zhang et al. 2011, Chen and Young 1979, 2006, Tsai and Yang 2006, Iverson 2000, Sun et al. 1998, Chow et al. 1988, Freeze and Cherry 1979, Mein and Larson 1973, Lumb 1962, Green and Ampt 1911) Green and Ampt's original equation [6.20] is applied in the analysis for finding the infiltration depth (Z_w) for different threshold rainfall durations T_w. Equation [6.21] is for the iteration process.

$$T_w = \frac{1}{K_w}\left[Z_w - \psi\Delta\theta \ln\left[\frac{Z_w}{\psi\Delta\theta} + 1\right]\right] \quad \text{[6.20]}$$

Or

$$Z_w = Kt + \psi * \Delta\theta \ln\left(1 + \frac{Z_w}{\psi * \Delta\theta}\right) \quad \text{[6.21]}$$

$$\Delta\theta = \theta_1 - \theta_0 \quad\quad\quad \text{[6.22]}$$

where, ψ is the suction head at the wetting front in the water column, $\Delta\theta$ is the difference in volumetric water content between the initial and final water content, t is rainfall duration, Tw is rainfall duration equivalent to threshold rainfall, θ_0 is the initial volumetric water content before wetting, θ_1 is the final volumetric water content after wetting, k is the coefficient of permeability of the soil in the wetted zone.

Tsai and Yang (2006), Chow et al. (1988), and Freeze and Cherry (1979), studied the variation of infiltration capacity of any soil with rainfall intensity and duration. When the infiltration capacity is higher than the rainfall intensity, rainfall intensity governs the infiltration; and if rainfall intensity is greater than the permeability coefficient, infiltration will be governed by permeability. Infiltration depends on soil permeability and initial

moisture content. If permeability is in a steady state condition and the soil has no moisture storage, infiltration depends on permeability alone.

The rainfall intensity considered in this analysis is assumed to be evenly distributed within the watershed.

The average soil strength parameters observed in old landslide areas are applied to the entire watershed (Cohesion 11 kPa, Friction 28°). The soil suction applied in the analysis range from 1 to 23 for 73 locations. Unit weight, friction angle, suction, and wetting depth maps are prepared as required for FoS computation in map algebra. These raster maps are used to compute the FoS in the GIS environment. The landslide-susceptible watershed area based on an FoS of less than one for different rainfall is developed. The final landslide susceptibility maps are developed for different rainfall durations and intensities. Landslide susceptibility is classified in three categories: low-susceptibility areas with a FoS greater than two; medium susceptibility with an FoS between one and two; and highly susceptible area with an FoS of less than one. From the highly-susceptible areas, landslides initiate and change into debris flows, then travel to the other parts of the watershed. This information is used in the GIS environment for debris flow hazard map development.

6.3.4 Debris Flow Runout Assessment

Most of the rainfall-induced initial landsides in the study watershed change into destructive debris flows (Dhital 1993, 2003). Landslide source area and travel distance covered by debris must be assessed separately, as the extent of these areas depends on different factors (Fell et al. 2008). Various models have been proposed for debris flow runout assessment. These are empirical (Hurlimann et al. 2008, Hunter and Fell 2003, Legros 2002, Fannin and Wise 2001, Finlay et al. 1999, Rickenmann 1999, Corominas 1996, Hsu 1975, Scheidegger 1973), semi-empirical, and dynamic models (Wang 2008; Iverson 1997; Iverson et al. 1997; Savage and Baum 2005; Sassa 2000; Sassa and Wang 2005; et al. 1997; O'Brien 2003; Pierson 2005; Takahashi et al. 1992; Takahashi 1978, 1980; Savage and Hutter 1989; Chen and Lee 2000; Hungr 1995; Hutter et al. 1996). Debris flow is a complex physical phenomenon and requires detailed

information of debris characteristics, terrain topography, in situ moisture conditions, and information about other influencing factors for its runout analysis (Wieczorek and Naeser 2000). The dynamic analysis models require the above information in detail. To obtain a reasonable result from analysis based on limited information, empirical methods present better options (Horton et al. 2013, Carrara et al. 2008, Finaly et al. 1999, Rickenmann 1999, Costa 1984, Hungr et al. 1984, Johnson 1984). In this research, empirical methods are considered for debris flow runout assessment. Previously-developed landslide susceptibility maps (Paudel et al. 2018) are considered as debris flow source maps for debris flow analysis. The probable cumulative rainfall for one- to seven-day periods for return periods of 25, 50, 100, and 200 years are used for landslide susceptibility and probability analysis. Later, a landside susceptible area, which has a slope stability FoS of less than one is used as a debris flow source.

Debris flow runout analysis is carried out with various algorithms using the Flow-R software (Horton et al. 2013). The Flow-R model can be used for the identification of landslide susceptibility and debris flow runout (Horton et al. 2013). An application of this software can be found in Paudel et al. (2018b) (Technical Paper 2 in this thesis manuscript). Flow-R is an empirical model developed at the University of Lausanne. The Flow-R model has been applied in various regions of the world with valid and reasonable results (Horton et al. 2013). Also, in the Flow-R model, options for user-defined debris flow sources are available for runout- only simulations. There are various algorithms available in this model; however, the algorithm identified by Paudel et al. (2018b) for the study watershed is employed for the debris flow runout analysis. The debris flow source is user defined in this analysis as the source which is analyzed and discussed in Paudel et al. (2018) and Section 6.3.2.

The Flow-R model models listed in Table 6.1 are selected for analysis in this research (Paudel et al. 2018b). In Table 6.1, the first column contains a list of source identifications. In this research, the model selected for the source identification and definition of source areas does not make any difference. For spreading algorithms, the Holmgren (1994) or Holmgren modified algorithms (Horton et al. 2013) are both appropriate for use in this watershed. Modified Holmgren (1994) algorithms were

developed by Horton et al. (2013) by adding with some height (dh) at a central cell location. The details of these algorithms are available in Horton et al. (2013). In the second sub-column of the second main column, there are two options for initial algorithms, Weights and Direction memory. Direction memory does not show actual debris flow spreading but any of the default (proportional), Cosinus, and Gamma (2000) algorithms provide appropriate runout results. For the friction loss function and energy loss function, algorithms available are two parameters friction model Perla et al. (1980) and the Simplified Friction Limited Model (SFLM) (Corominas 1996). However, a lower travel angle and lower velocity are sufficient to model debris flow runout.

Table 6. 1 Available Algorithms in Flow-R Model for Debris Flow Propagation.

Source Area Selection	Spreading Algorithms				Energy Calculation			
	Direction Algorithm		Initial Algorithm		Friction Loss Function		Energy Limitation	
(Only Superior Sources (Debris-Flows only), Energy Base Discrimination, Complete Propagation of all source areas (long)	Holmgren (1994)	Exponent 1 to 50	Weights	Default, Cosinus, Gamma (2000)	Travel angle	From 0.1 ° to 50 °	Velocity	1 mps to 50 mps
	Holmgren (1994) Modified	Dh from 0.25m to 70 Exponent 0.1 to 50	Direction memory	Len=005 to 100, Open 090 to 300				

Mps = meter per second

The algorithm suggested by Holmgren (1994) is given in Equation [6.23]:

$$p_i^{fd} = \frac{(\tan Bi)^x}{\sum_{j=1}^{8}(\tan Bj)^x} \forall \begin{Bmatrix} \tan B > 0 \\ x\varepsilon[1;+\infty] \end{Bmatrix} \qquad [6.23]$$

where i and j are the flow directions, p_i^{fd} is the susceptibility proportion for i direction, Bi and Bj are the slope angle from the central cell in i and j directions. Exponent x varies from one to infinity. When the value of x is equal to one, it represents the multiple flow, and decreases the direction with the increase in its value. In modified Holmgren (Horton

et al. 2013), the central cell is raised with some height (dh) at a central location, which can be defined by the user in the Flow-R model.

In a natural terrain, slope direction frequently changes with downslope distance, and a function should be capable of capturing the new direction at a new location. This functional process is defined as the persistence function by Horton et al. (2013). Gamma (2000) and Horton et al. (2013) used the persistence function given in Equation [6.24] for change in direction with respect to the previous or initial direction:

$$p_i^p = w_{\alpha(i)} \qquad [6.24]$$

where p_i^p is the flow proportion in direction i, according to the weight and inertia of the flow, $w_{\alpha(i)}$, α(i) is the angle from the previous flow direction. The direction algorithms and persistence algorithms can be written as shown in Equation [6.25] (Horton et al. 2013). The combined susceptibility of both functions will be at a maximum value in the original cell with p$_o$, and it will be distributed in the flow directions i and j.

$$Pi = \frac{p_i^{fd} p_i^p}{\sum\limits_{j=1}^{8} p_j^{fd} p_j^p} p_o \qquad [6.25]$$

where i and j are the flow directions, p$_i$ is the susceptibility value in direction i, p_i^{fd} the flow proportion according to the flow direction algorithm, p_i^p the flow proportion according to the persistence, and P_o the previously determined susceptibility, which is the total initial value or value of the central cell.

In the Flow-R model, the flow mass is considered to be a unit value, and energy loss results entirely from friction. The energy required to travel to another cell must be sufficient for flow to take place from one cell to another. Energy is the controlling factor for runout and spreading to adjacent cells based on the available energy, and the required energy is different between two cells or adjacent cells. The energy required value between cells can be defined by the user. Equation [6.26] shows this relation (Horton 2013).

$$E_{kin}^i = E_{kin}^o + \Delta E_{pot}^i - E_f^i \qquad [6.26]$$

173

where, E^i_{kin} is the kinetic energy of the cell in direction i, E^o_{kin} is the kinetic energy of the central cell, ΔE^i_{pot} is the change in potential energy to the cell in direction i, and E^i_f is the energy lost in friction to the cell in direction i.

The simplified friction-limited model (SFLM) suggested by Corominas (1996), and known as Default in the software, is given in Equation [6.27]:

$$E^f_i = g\Delta x \tan \phi \qquad [6.27]$$

Where, E^f_i is the energy lost function from the central cell to the cell in i direction, Δx, the horizontal displacement increments in direction i, tanø, the energy gradient in the direction of i, and g the acceleration due to gravity.

Horton et al. (2013) developed Equation [6.28] for a limiting velocity from a given value. The maximum velocity can be introduced to cap the velocity on the steep slopes, and limit the propagation:

$$V_i = min\{V_{max,} \sqrt{(V_o^2 + 2g\Delta h - 2g\Delta x tan\emptyset)}\} \qquad [6.28]$$

where, Δh is the difference in elevation between the central cell and the cell in direction i, and V_{max} is the given velocity limit. This limit can be defined based on region by the user. The general value of V_i is always limited to V_{max}, and the intermediate value from the second part of Equation [6.28].

6.3.5 Debris Flow Hazard Assessment

The final stage of this study is the debris flow hazard area mapping for the study watershed. When all information is derived, and analyzed using the above-mentioned methodology and work steps, these results are applied in the final model as shown in Figure 6.2 to create debris flow hazard maps. In this model, landslide-susceptible maps developed using the methodology mentioned in the previous section and a given probability are categorized in three areas. These are: FoS less than one, one to two and more than two in the stability analysis. The watershed areas associated with FoS of less

174

than one in the slope stability analysis are considered to be landslide-susceptible regions. These unstable areas are considered for debris flow runout analysis and developed debris flow inundation maps. Debris flow inundation areas in the study watershed maps are converted into polygons and included in landslide-susceptible regions, called a debris flow zone, for a given probability. An FoS of one to two is defined as a medium landslide susceptibility zone. The area which has an FoS of more than two is considered a low landslide susceptibility zone for a given probability. Finally, the debris flow zone includes debris flow initiation, inundation, and a buffer of 10 m outlines of these areas.

These debris flow areas are associated directly with the probability of rainfall (annual frequency of return rainfall) in the watershed. The debris flow area, medium-susceptibility, and low-susceptibility zones are analyzed for different return periods. The rainfall return periods used in this study are 25, 50, 100, and 200 years, and rainfall durations cover one-day to seven-day periods. The duration selected is based on conversations with the local elderly people who have extensive experience with rainfall-induced landslide events. Seven-day rainfall has a mythical status in Nepal in relation to landslides. People become scared if rainfall continues up to seven days with considerable intensity, because they believe that a landslide in their area is imminent if such rainfall occurs at any time of the year. However, such events occur mostly between late April and late November. In another study, continuous and longer rainfall caused more landslides in these mountains (Dahal and Hasegawa 2008). The annual probability of the hazard area is analyzed and the trend of highly hazardous areas and their probability or return period are derived.

6.4   Debris Flow Hazard in the Study Watershed

6.4.1 Landslide Susceptibility Maps

The data for landslide-triggering factors in the watershed are applied in Equation [6.14] to identify landslide-susceptible areas, as discussed in Section 6.3. Rainfall probability is derived for the probability of landslide-susceptible locations. The rainfall data of the study area are available from 1980 to 2013, and are recorded once every day. The maximum one-day to seven-day rainfall in every year from 1980 to 2013 period are identified and shown in Figure 6.4. From Figure 6.4, the cumulative rainfall date for one-day maximum, two-day maximum and so on up to seven days may not concede each other. However, most of these maximum rainfall event days are on similar dates (Figure 6.4). Figure 6.4 also shows the cumulative one-day rainfall of 443 mm, and seven-day rainfall of 1,033 mm. The rainfall amount of 1,033 mm is almost half of the average annual rainfall in the watershed. Within the study period 1980 to 2013, up to half of the annual precipitation can occur in one seven-day event.
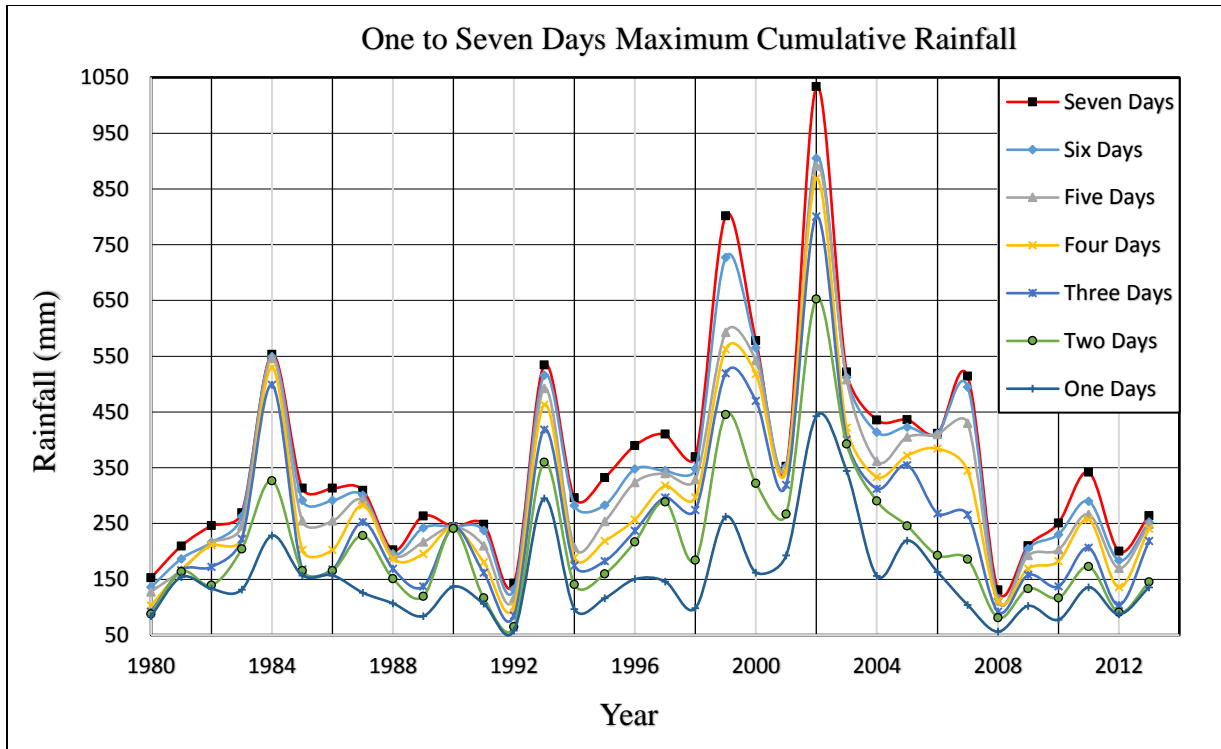
Figure 6.4: One- to seven-day maximum cumulative rainfall.

These maximum cumulative rainfall amounts are used for annual probability and recurrence period analysis. The return periods chosen for analysis are from 1.01 year to 200 years. Figure 6.5 shows the probability and return period of rainfall for events of one to seven days' duration.

From Figure 6.5 a higher return period or lower annual probability is linked to more cumulative rainfall. The probability of one-day and seven-day events remains the same, as it is a cumulative maximum taken from each year from 1980 to 2013. The rainfall for a return period of 200 years and an annual probability of 0.005 for one-day's duration is 458.39 mm, while for seven days it is 1,051mm. Similarly, for a return period of 500 years and a probability 0.002, one-day's rainfall is 519 mm, and seven-days' rainfall 1,185 mm. Higher intensity and longer duration rainfall are triggering factors for landslide initiation. The duration of one to seven days, and expected rainfall from probability analyses are applied for hazard assessment of the area.
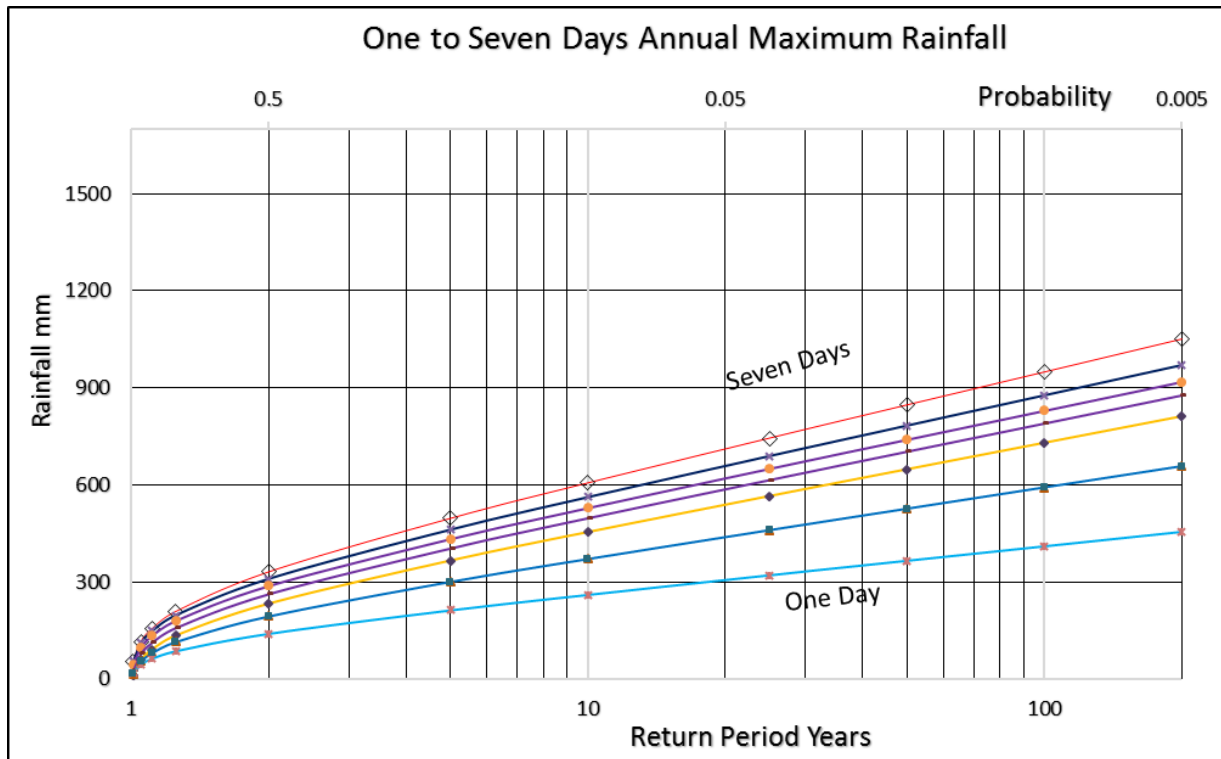
Figure 6.5: One-day to seven-day annual maximum rainfall probability and return period.

The annual probability of rainfall is computed for up to a 200-year return period. The further analysis of landslide susceptibility is carried out for selected rainfall return periods—once in 25, 50, 100, and 200 years—to obtain a trend of hazard in the watershed rather than all analyses. The expected rainfall for these probabilities and return periods are given in Table 6.2 and 6.3. Also given in these tables is infiltration rate, which is equivalent to rainfall intensity over the period of one to seven days. These infiltration rates and durations of expected rainfall (such as one-day to seven-day) are used for infiltration computations. Landslide susceptibility is computed as in Equation [6.14]. The location and areas identified as unstable for different rainfall return periods are shown in Figure 6.6 and 6.7. Figure 6.6 a), b), and c) show an annual probability of 0.04 for landslide susceptibility for continuous rainfall over one-, four-, and seven-day

periods while Figure 6.6 d), e), and f) show a probability of 0.02 for the same duration one, two, and seven days' rainfall. Similarly, Figure 7.7 a), b), and c) show an annual landslide susceptibility probability of 0.01 for one-, four-, and seven-day rainfall period, and Figure 7.7 d), e), and f) shows a probability of 0.005 for one-, two-, four-, and seven-day rainfall periods. The area of landslide susceptibility increases with the higher return period rainfall and number of days' duration.

Table 6.2 Annual rainfall probability and return period for one- to four-day rainfall

Annual Rainfall Probability	Return Period	One-day Rainfall		Two-day Rainfall		Three-day Rainfall		Four-day Rainfall	
P	Year	mm	In (cm/sec)	mm	In (cm/sec)	mm	In (cm/sec)	mm	In (cm/sec)
0.04	25	320	0.00037	460	0.00027	565	0.00022	614	0.00018
0.02	50	367	0.00042	526	0.00030	647	0.00025	702	0.00020
0.01	100	413	0.00048	591	0.00034	729	0.00028	789	0.00023
0.005	200	458	0.00053	657	0.00038	811	0.00031	875	0.00025

P = Probability, In = Infiltration

The summary of the analysis above is shown in Figures 6.8 and 6.9. The landslide-susceptible area does not change much for up to a two-day period of rainfall, but it increases with duration rapidly after that. The rainfall events with low annual probability are linked to a higher landslide-susceptible area. The watershed is 124 km^2 and unstable areas are up to 400 hectares for seven-day rainfall, with a probability of 0.005. The recurrence period of this event is 200 years, and the landslide-susceptible area is 3.25%. The lower the annual probability of rainfall or extreme event, the higher the rainfall intensity and the unstable areas.

Table 6.3 Continued annual rainfall probability and return period for five-, six-, and seven-day rainfall.

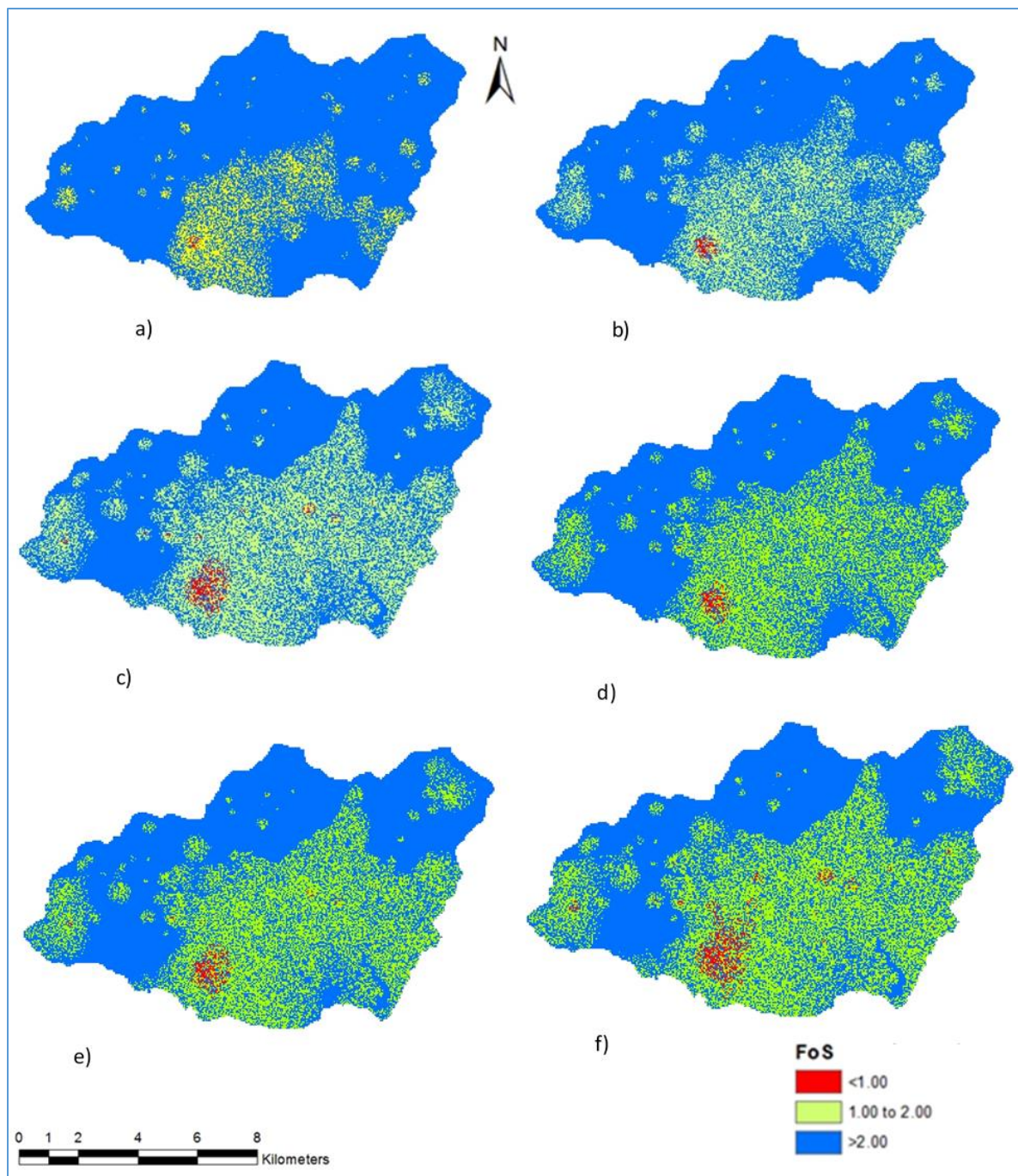| Annual Rainfall Probability	Return Period	Five-day Rainfall		Six-day Rainfall		Seven-day Rainfall	
P	Year	mm	In (cm/sec)	mm	In (cm/sec)	mm	In (cm/sec)
0.04	25	651	0.00015	689	0.00027	744	0.00015
0.02	50	741	0.00017	783	0.00030	847	0.00017
0.01	100	830	0.00019	877	0.00034	949	0.00019
0.005	200	919	0.00021	970	0.00038	1051	0.00021

P = Probability, In = Infiltration

Figure 6.6: Landslide susceptibility area for 25-year return period, a) one-day rainfall, b) four-day rainfall, and c) seven-day rainfall; and landslide susceptibility area for 50-year return period, d) one-day rainfall, e) four-day rainfall, f) seven-day rainfall.
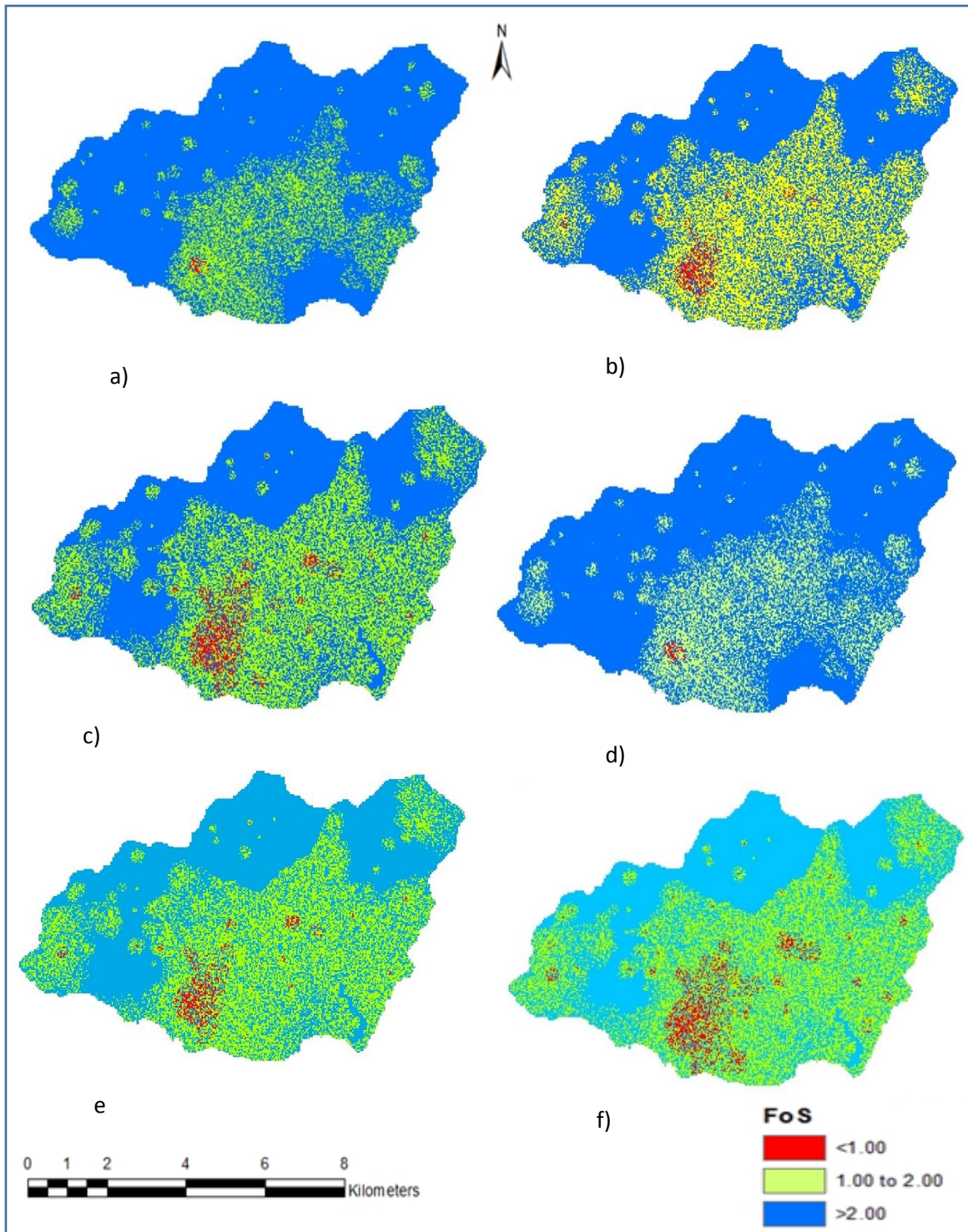
181

Figure 6.7: Landslide susceptibility area for 100-year return period, a) one-day rainfall, b) four-day rainfall, and c) seven-day rainfall; and landslide susceptibility area for 200-year return period, d) one-day rainfall, e) four-day rainfall, and f) seven-day rainfall.
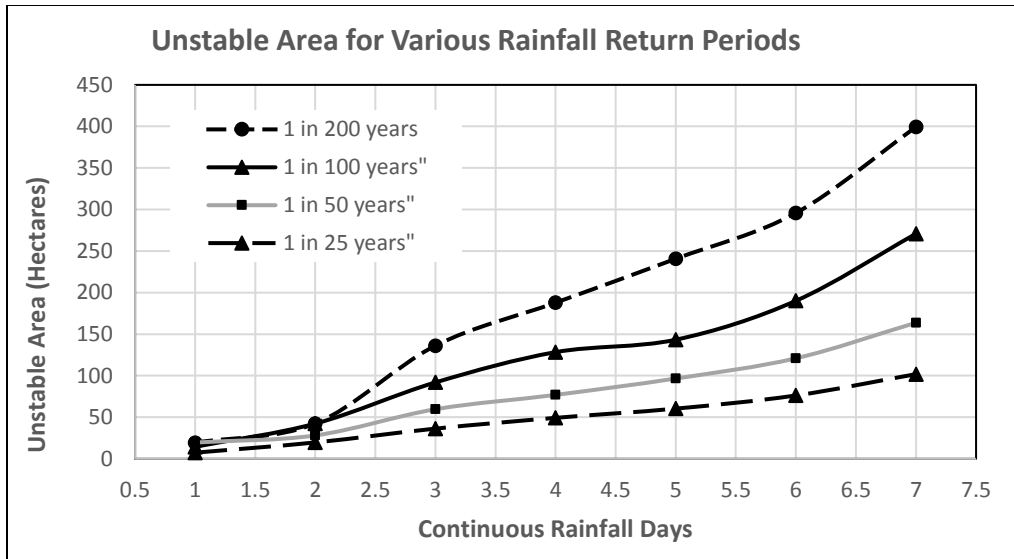
Figure 6.8: Landslide-susceptible area in hectares for different return periods and rainfall durations.
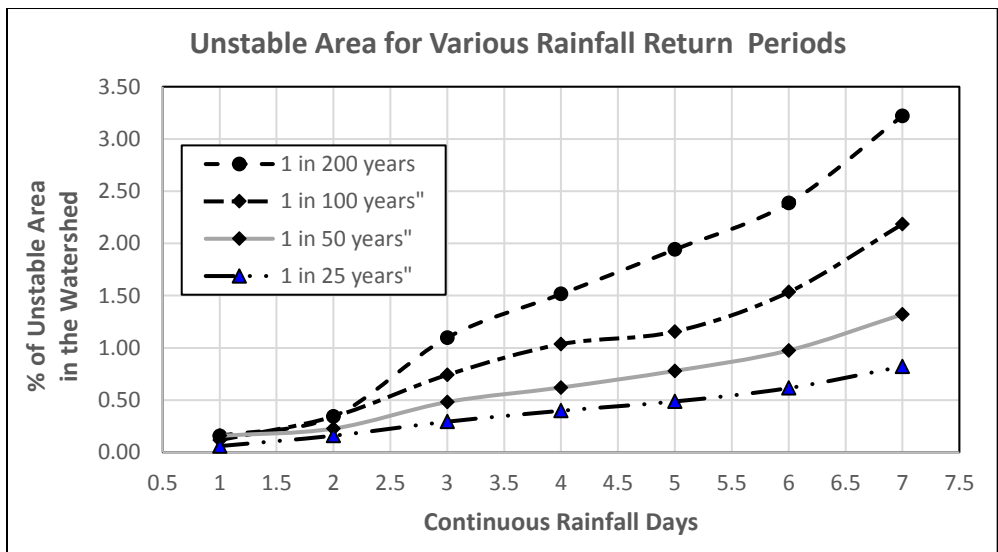

Figure 6.9: Landslide-susceptible area (%) of the watershed for different return periods and rainfall durations.

6.4.2 Debris Flow Inundation with Susceptibility Maps

The landslide susceptibility maps discussed in the previous section are considered to be debris source maps for runout distance analysis. The total landslide initiation areas and debris flow runout areas are merged. These areas are converted into polygons. The total identified unstable and runout debris flow area must have some setback distance. The setback distance depends on the location of the area, physical features, type of development, existing terrain slope, type of slope, and length of slope (Ontario Hazard Analysis Guidelines 2002). Obtaining these features is beyond the scope of this research. Therefore, a constant value of 10 m outer setback distance is used. These polygons are enclosed with a 10-m buffer around the outer area as a setback distance. The final results of this analysis are shown in Figure 6.10. Figure 6.10 a), b), c), and d) show the landslide and debris flow susceptibility area, with a buffer of 10 m, for continuous rainfall over one day with annual probabilities of 0.04, 0.02, 0.01, and 0.005, respectively. Figure 6.10 e), f), g), and h) show a similar susceptibility area, buffer, and annual probability, but for seven days' continuous rainfall.
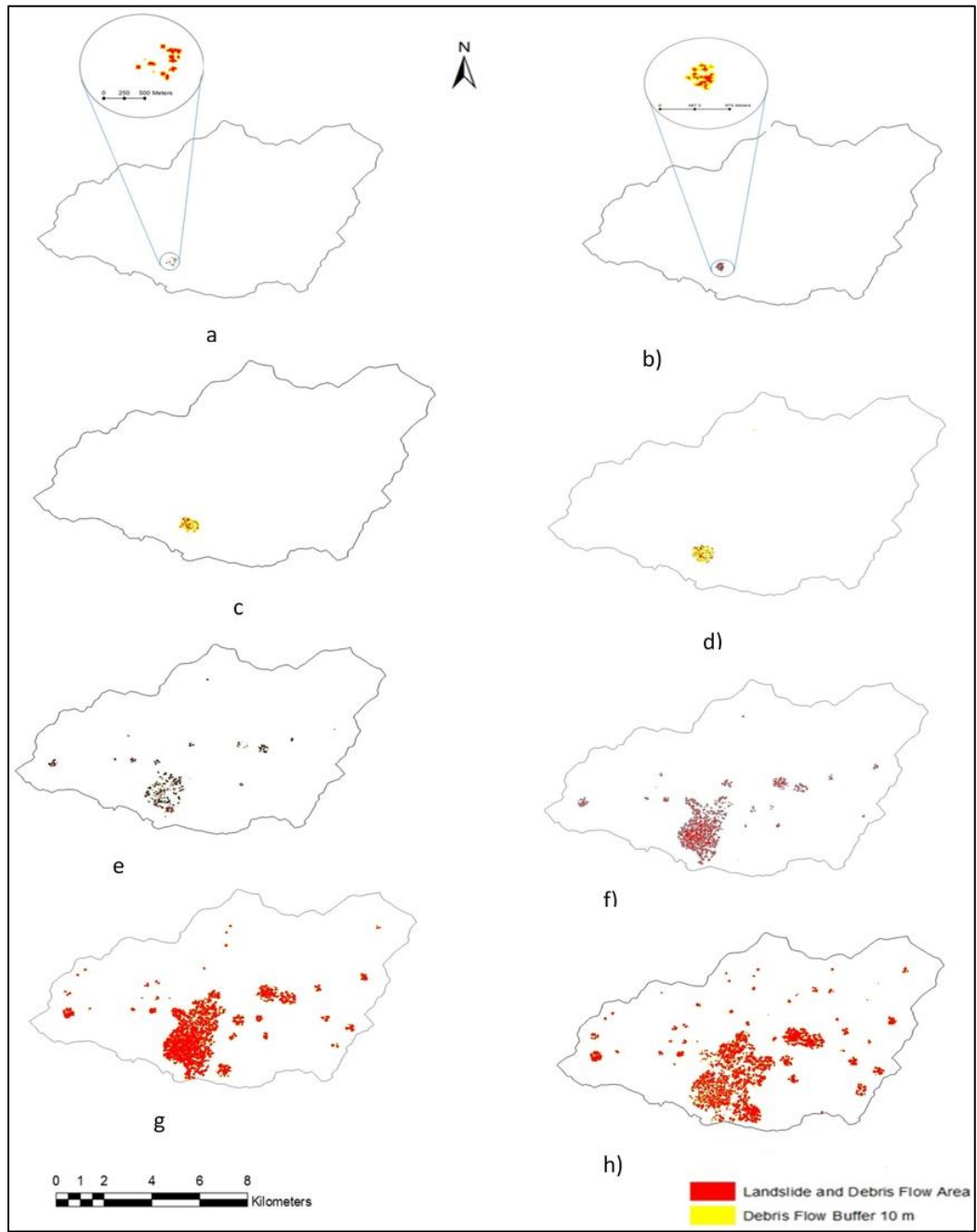
Figure 6.10: Landslide initiation and debris flow susceptible area and buffer areas for one-day rainfall with return periods of a) 25 years, b) 50 years, c) 100 years, and d) 200 years; and seven-day rainfall with return periods of e) 25 years, f) 50 years, g) 100 years, and h) 200 years.

6.4.3 Debris Flow Hazard Maps

Debris flow hazard maps are developed by combining landslide initiation and debris flow runout areas. The (probable) debris flow area has an FoS of less than one in the initial slope, debris flow susceptible area, and their buffer of 10 m outlines. The watershed area beyond the debris flow area is also categorized as medium and low landslide-susceptibility areas based on the FoS of the stability of the initial slope. The watershed area which has an FoS of one to two is considered to be a medium-(landslide) susceptibility area, and that with more than two as low-susceptibility. The medium-susceptibility area is the map area for FoS of less than two, minus debris flow areas. The low-susceptibility zone has an FoS of more than two, minus the debris flow area and the medium-susceptibility areas. This analysis is carried out for seven-day rainfall and one-day rainfall only, and is summarized in Table 6.4. The hazard area in the watershed for one-day and 25-, 50-, 100-, and 200-year return rainfall is shown in Figure 6.11. Figure 6.12 shows seven-day rainfall and return periods of 25, 50, 100, and 200 years.

Table 6.4 Hazard area with probability and return period.

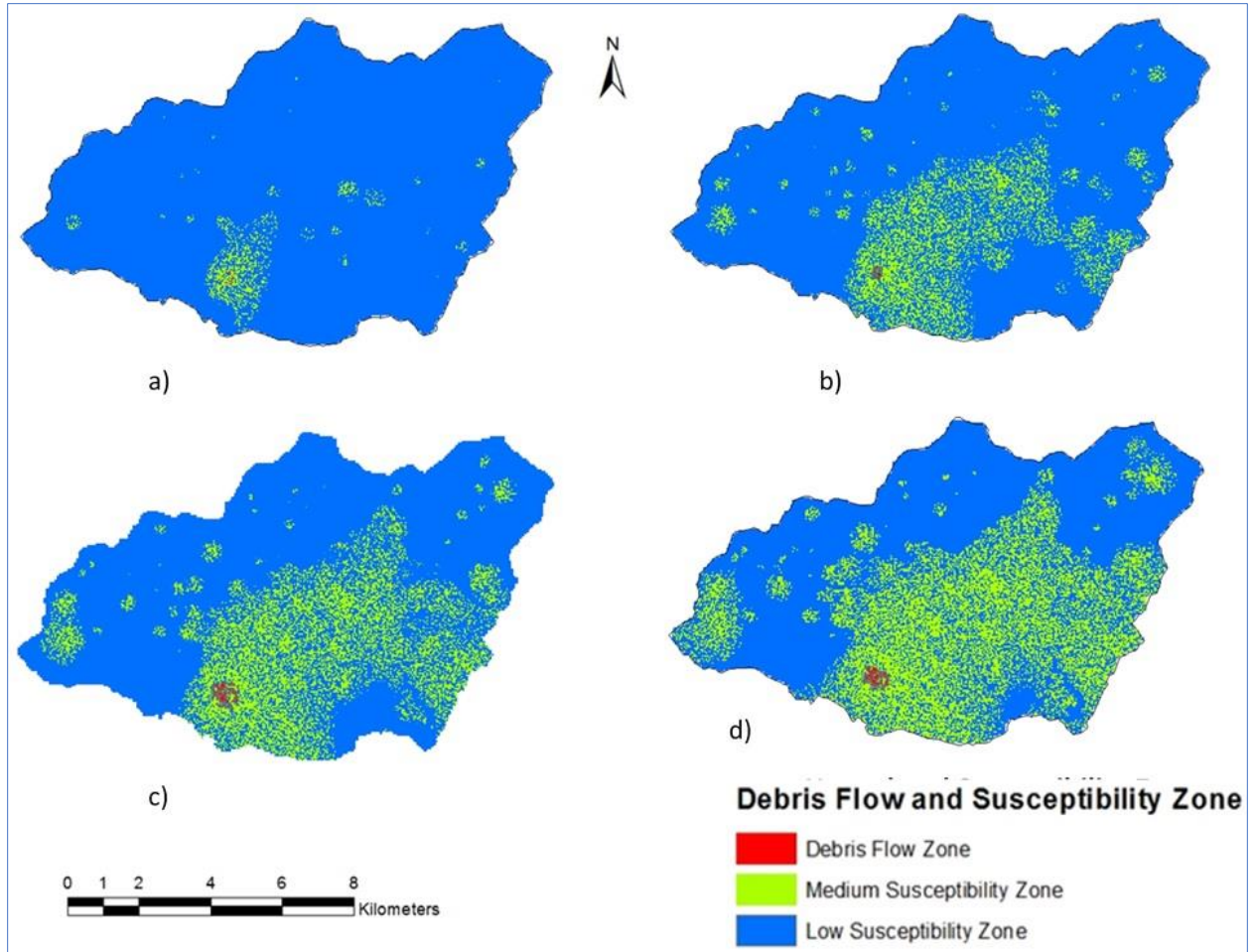| Return Period (Years)	Annual Probability	Days of Rainfall	Total Watershed Area (Ha)	Hazard Area (Ha)	Medium-susceptibility Area (Ha)	Low-susceptibility Area (Ha)
25	0.04	1	12,400	13	1,387	11,001
50	0.02	1	12,400	18	2,624	9,740
100	0.01	1	12,400	24	4,998	7,802
200	0.005	1	12,400	36	5,009	7,355
25	0.04	7	12,400	77	3,960	8,364
50	0.02	7	12,400	154	4,365	8,035
100	0.01	7	12,400	284	4,706	7,409
200	0.005	7	12,400	418	8,403	7,384

Figure 6.11: Debris flow hazard map with 10-m buffer for one-day rainfall with return periods of a) 25 years (P= 0.04), b) 50 years (P= 0.02), c) 100 years (P= 0.01), d) 200 years (P= 0.005). (P: annual probability).
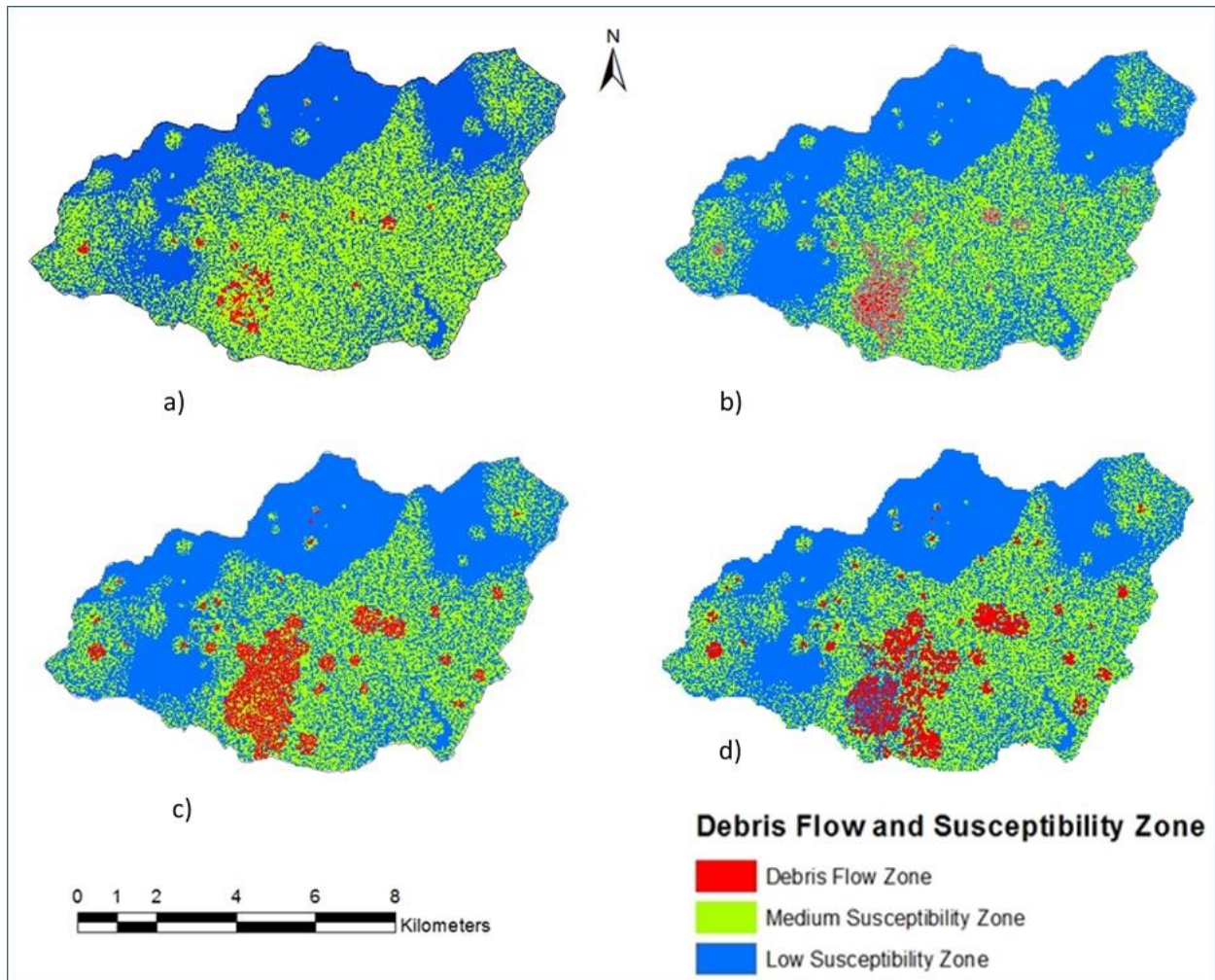
Figure 6.12: Landslide hazard map with a 10-m buffer for seven-day rainfall with return periods of a) 25 years (P= 0.04), b) 50 years (P= 0.02), c) 100 years (P= 0.01), d) 200 years (P= 0.005). (P: annual probability).

6.5   Results and Discussions

The relation of hazard and susceptibility area to its annual probability for one-day rainfall is shown in Figure 6.13. The large high-hazard area is associated with low-probability events, and the low-hazard area with high-probability events, which means that short rainfall return periods are associated with small hazard areas. For seven-days' rainfall duration, this relation is shown in Figure 14. The relation of high hazard areas to their

188

annual probability of occurrence is given in Equation [6.28] and [6.29]. The regression coefficients (R) for Equation [6.29] and [6.30] are 1.00 and 0.99, respectively.

$$H_1 = 2.7185\, P_1^{-0.482} \qquad\qquad [6.29]$$

$$H_7 = 5.8841\, P_7^{-0.82} \qquad\qquad [6.30]$$

Where, H_1 and H_7 are hazard areas, and P_1 and P_7 are the annual probability of occurrence in one-day and seven-day rainfall.
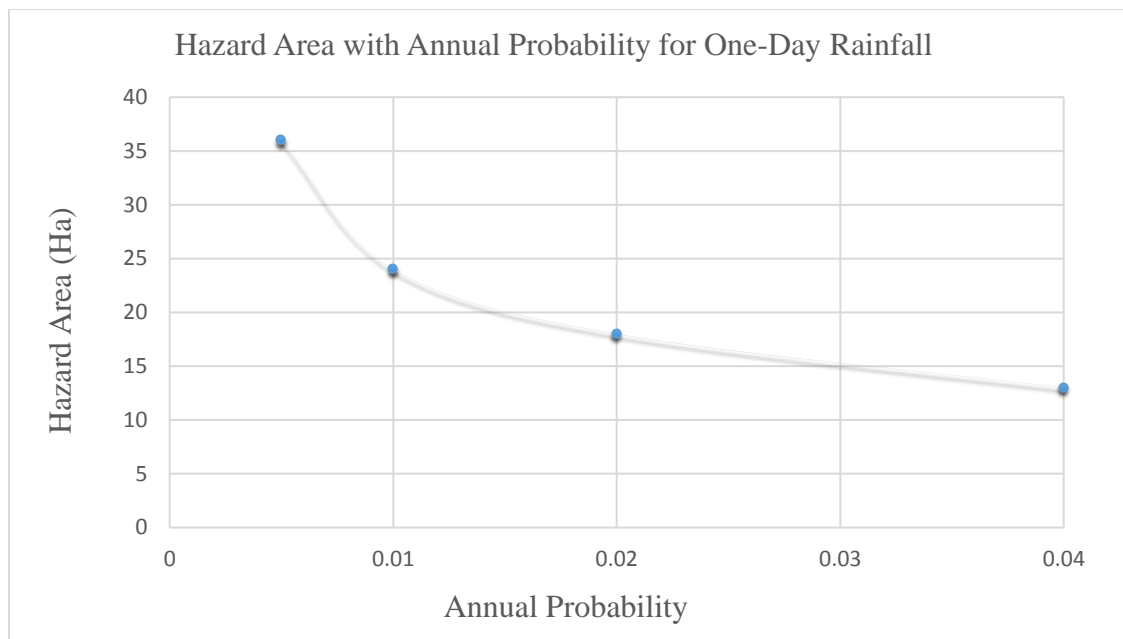

Figure 6.13: Landslide hazard area with 10-m buffer for annual probability for one-day rainfall.
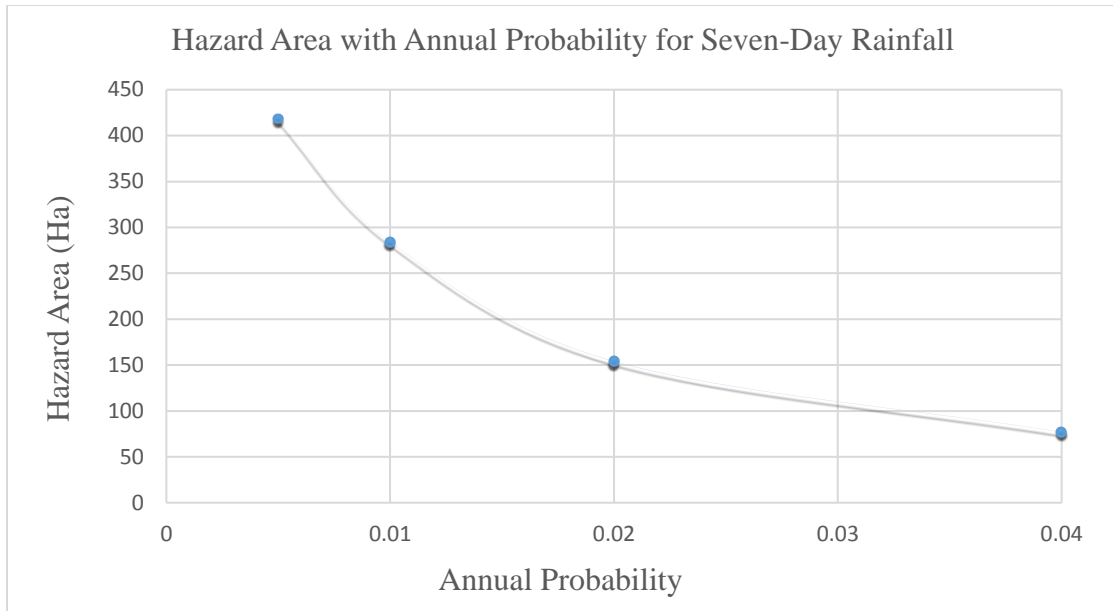
Figure 6.14: Landslide hazard area with 10-m buffer for annual probability for seven-day rainfall.

The relation between high hazard area and rainfall return period is derived for a rainfall duration of one day and shown in Figures 6.15 and 6.16. A high hazard area as small as 13 ha is observed for 25-year return period rainfall for one-day duration, and up to 77 hectares for seven-days. Equation [6.31] and [6.32] are the relationships of high hazard with return period for this watershed. The R values for these equations are 1 and 0.9972 for one-day and seven-day rainfall periods, respectively.

$$H_{1D} = -0.0081(RP^2) + 3.771(RP) + 13 \qquad [6.31]$$

$$H_{7D} = -0.0002(RP^2) + 0.1675(RP) + 9.33 \qquad [6.32]$$

where, H_{1D} and H_{7D} are high hazards for one- and seven-day periods, and RP is the return period.
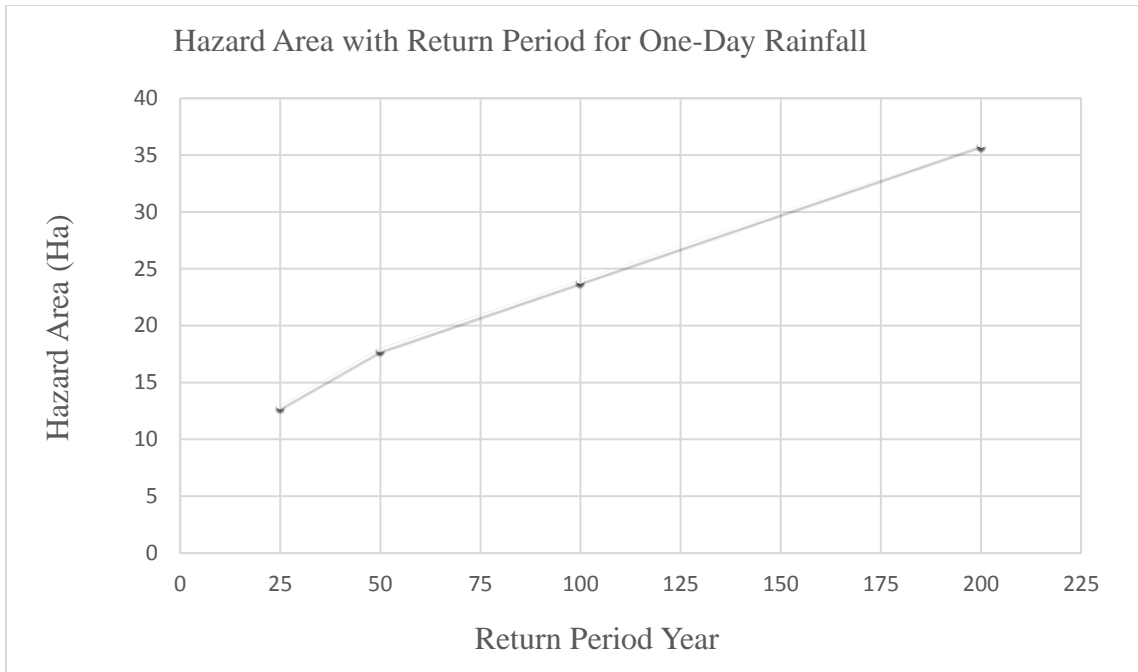
Figure 6.15: Landslide hazard and return period with 10-m buffer for one-day rainfall.
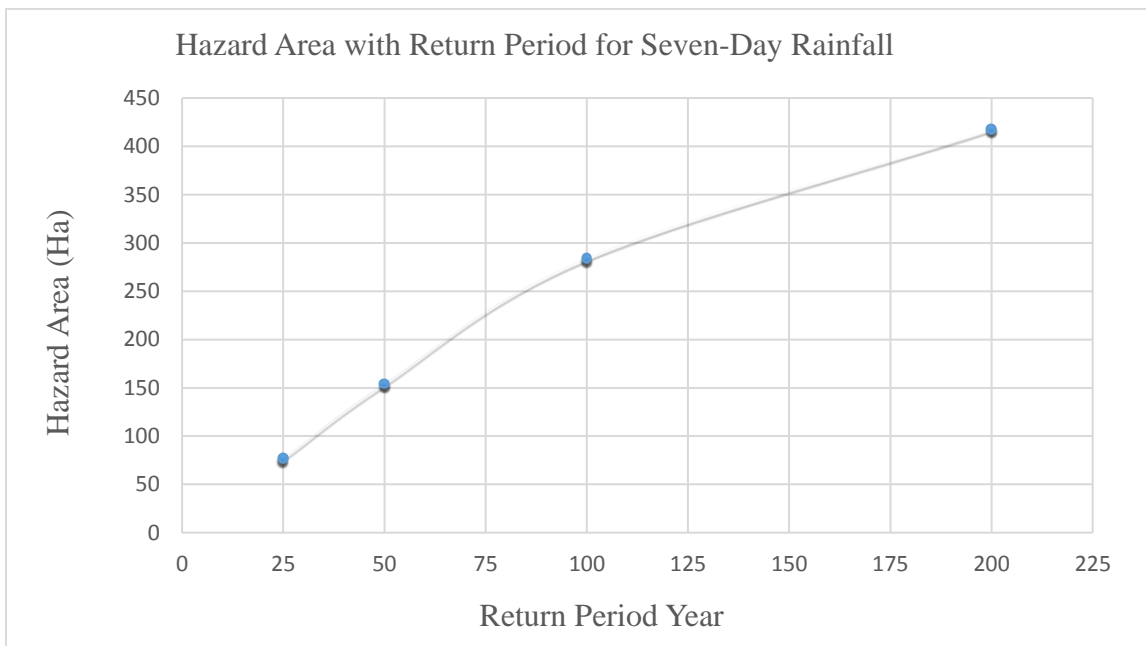

Figure 6.16: Landslide hazard area and return period with 10-m buffer for seven-day rainfall.

6.6   Summary and Conclusions

Recorded rainfall and physical changes are modeled to predict instability in mountain slopes in the study watershed. Annual rainfall probability or respective return periods are applied for rainfall-induced landslide probability assessment. Rainfall records for 34 years (from 1980 to 2013) are available to identify annual one-day to seven-day maximum rainfall. Information regarding the maximum annual cumulative rainfall of the 34-year period is used to calculate annual rainfall probability and return periods. One-day and seven-day maximum cumulative rainfall from the analysis is 443 and 1,033 mm, respectively. The annual probability of rainfall computed for 1.01 to 200-year return periods have annual probabilities of 0.990099 to 0.005. The rainfall for a return period of 200 years and an annual probability of 0.005 for one-day duration is 458 mm, while for seven days it is 1,051 mm. The infiltration rate is identified from the rainfall intensity duration of the selected annual probability. For the landslide susceptibility analysis, only four return periods 25, 50, 100, and 200 years (annual probability 0.04 to 0.005) are selected to find a trend of landslide susceptibility with annual probability or return period in the watershed.

Data from a geotechnical investigation conducted in one recent landslide location within the study area is considered for stability analysis. SWCC is developed using a grain size distribution model from soil samples received from 73 locations (Lamichhanne 2000) in the watershed. The grain size distribution model is used for matric suction with respect to the in situ moisture content of these locations. The landslide-susceptible locations and area of the watershed with a given probability is identified. The landside susceptibility is analyzed for one-, four-, and seven-day periods and the return periods mentioned above. The area of landslide susceptibility increases with the higher return period rainfall and number of days.

Susceptibility areas are categorized as high, medium, or low-susceptibility based on an FoS of less than one, one to two, and more than two, respectively. The watershed area is 124 km^2 and the unstable portion is up to 400 hectares for seven-day rainfall with an

192

annual probability of 0.005. The recurrence period of this event is 200 years. The landslide-susceptible area is 3.25% of the total watershed area. The longer duration and higher intensity rainfall are trigger factors for rainfall-induced landslides.

The hazard zone (FoS less than one) of the watershed is considered as a source of landslides for debris flow analysis. The Flow-R model is applied for debris flow runout and inundation area computation. In the Flow-R model, susceptible areas developed from slope stability analysis are considered as a user-defined debris flow source. The Holmgren (1994) modified algorithm developed by Horton et al. (2013) is used for debris flow spreading. For the initial algorithm, Weights was chosen. The Weights algorithms have three sub-algorithms: the default algorithm, Gamma 2000, and Cosinus. Any of these algorithms provides appropriate debris flow spreading in this region; however, the default is chosen for the analysis, which is a proportional method of spreading to adjacent cells. Friction loss function and energy limitation algorithms are available and used in the energy calculation. The low travel angle and low velocity were appropriate for debris flow runout analysis for this watershed, and these are chosen for friction loss function and energy limitation.

The debris flow area and landslide initiation area from the susceptibility analysis are combined in a single map to develop hazard maps. These combined total areas are transformed into polygons. The landslide hazard area required a setback distance which depends on various factors, including type of soil, proximity of river or water body, and topography. Individual polygon setback distance analysis is beyond the scope of this research, and therefore a 10-m setback distance is chosen for all polygons and buffers them from the outer side. The final area within the buffered mark is termed the hazard area. For return periods of 25, 50, 100, and 200 years, one-day and seven-day duration rainfall intensity are used for these analyses. For the 25-year return period and one-day duration rainfall, the computed hazard area is 13 hectares (ha), while for the 200-year return period it is 36 ha. This area drastically changed for seven-day rainfall as it is 77 ha for a 25-year return period. and 418 ha for a 200-year return period. Large return periods with high duration rainfall are hazardous in the study watershed.

The landslide hazard areas for different return periods are developed for the study watershed. The annual rainfall probability (recurrence period) and hazard location in any watershed is important for policy makers. For instance, if an area is hazardous for a 1 in 25 year event, it should be avoided for hospitals, school buildings, or any such community facility services. It may or may not be suitable for residential development depending on other factors and the decision of the local authority.

This study is a part of landslide risk assessment modeling for the watershed scale. The hazard is assessed using unsaturated soil technology and rainfall effects on sloping ground. Methods used for analysis are open-source computing tools for hazard assessment. The method can be used for developing landslide hazard risk and as support for making land use plans in similar hazardous areas. This study provides an indirect probability assessment for potential rainfall-induced landslide locations within the watershed. The areas of landslide susceptibility, debris flow inundation, and setback distance are considered as a landslide hazard area within the study area for a given time and location. Based on government policies for any watershed or location, these methods can be applied to estimate the risk of any development in any proposed area before planning these activities. This will reduce physical, societal, environmental, and economic hazard in the study watershed. Hazard return periods and the design life of a proposed development plan or structure can be compared before implementing their construction in the area.

6.7   References

Aleotti, P. (2004), A warning system for rainfall-induced shallow failures, *Engineering Geology*, 73, 247–265.

Caine, N. (1980), The Rainfall Intensity: Duration Control of Shallow Landslides and Debris Flows Geografiska Annaler. Series A, Physical Geography, Vol. 62, No. 1/2 (1980), pp. 23-27.

Caine, N., Mool, P.K. (1982), Landslides in the Kolpu Khola drainage, Middle Mountains, Nepal. Mt Res Dev 2:157–173.

Cancelli, A., Nova, R. (1985), Landslides in soil debris cover triggered by rainstorms in Valtellina (central Alps – Italy), in: Proceedings of the 4th International Conference and Field Workshop on Landslides, The Japan Geological Society, Tokyo, 267–272.

Carrara, A., Crosta, G., Frattini, P. (2008), Comparing models of debris-flow susceptibility in the alpine environment, *Geomorphology*, 94, 353–378.

Casadel, M., Dietrich, W.E., Miller N.L. (2003), Testing a model for predicting the timing and location of shallow landslide initiation in soil-mantled landscapes, Earth Surf. Process and Landforms 28, 925-950.

Ceriani, M., Lauzi, S., Padovan, N. (1992), Rainfalls and landslides in the alpine area of Lombardia region – Central Alps – Italy, Proc. Interpraevent, Bern, Switzerland, Band 2, 9–20.

Ceriani, M., Lauzi, S., Padovan, N. (1994), Rainfall thresholds triggering debris-flows in the alpine area of Lombardia Region, central Alps – Italy, Proc. Man and Mountain, I Conv. Intern. per laProtezione e lo Sviluppo dell'ambiente montano, Ponte di legno (BS), 123–139.

Chen, H., Lee, C.F. (2000), Numerical simulation of debris flows. Canadian Geotechnical Journal, 37: 146-160.

Chen, L., Young, M. H. (2006), Green-Ampt infiltration model for sloping surfaces, Water Resour. Res., 42, W07420, doi:10.1029/2005WR004468.

Chen, C.-Y., Chen, T.-C., Yu, F.-C., Lin, S.-C. (2005), Analysis of time-varying rainfall infiltration induced landslide Environ Geol 48: 466–479.

Cho, S.E., Lee, S.R. (2002), Evaluation of surficial stability for homogeneous slopes considering rainfall characteristics. Journal of Geotechnical and Geoenvironmental Engineering 128(9): 756–763.

Chiang, S.H., Chang, K.T., Mondini, A.C., Tsai, B.W., Chen, C.Y. (2012), Simulation of event-based landslides and debris flows at watershed level, Geomorphology, 138, PP 306–618.

Chow, V.T, Maidment, D.R., Mays, L.W. (1988), Applied Hydrology, McGraw Hill Book Company, International Editions ISBN 0-07-010810-2.

Chow, V.T, (1953), Frequency analysis of hydrologic data with special application to rainfall intensities bulletin no 414 University of Illinois Eng. Expt. Station.

Claunitzer, V. Hopmans, J.W. Starr, J.L. (1998), parameter uncertainty analysis of common infiltration models. Soil Science Soc Am Journal 62, 1477-1487.

Corominas, J. (1996), The angle of reach as a mobility index for small and large landslides. Canadian Geotechnical Journal, 33: 260-271.

Corominas, J., Van Westen, C., Frattini, P., Cascini, L., Malet, J.-P., Fotopoulou, S., Catani F., Van Den Eeckhaut, M., Mavrouli, O., Agliardi, F., Pitilakis, K. • Winter, M. G. Pastor M.• Ferlisi S., Tofani, V., Hervas J., Smith, J.T. (2014), Recommendations for the quantitative analysis of landslide risk Bull Eng Geol Environ 73:209–263.

Costa, J.E. (1984), Physical geomorphology of debris flows. In Costa, J.e. and Fleisher, P.J. (Editors), Developments and Applications in Geomorphology: Springer Verlag, pp.268-317.

Crosta, G.B., Frattini, P. (2001), Rainfall thresholds for triggering soil slips and debris flow, in: Proceedings of the 2nd EGS Plinius Conference on Mediterranean Storms, edited by: Mugnai, A., Guzzetti, F., and Roth, G., Siena, Italy, 463–487.

Dahal, R.K. and Hasegawa, S. (2008), Representative rainfall thresholds for landslides in the Nepal Himalaya. Geomorphology Vol. 100, No.3-4, pp. 429-443.

Dhakal, A.S., Amada, T., and Aniya, M. (1997), A GIS approach to landslide susceptibility mapping: A case study from the Kulekhani watershed, Nepal. In: Proceeding from 18th Asian Conference on Remote Sensing, Kuala Lumpur, Malaysia. Pp JS-6-1 to JS-6-6.

Dhakal, A.S., Amada, T., Aniya, M. (1999). Landslide hazard mapping and the application of GIS in the Kulekhani watershed Nepal. Mt Res Dev, 19(1): 3–16.

Dhakal, A.S., Amada, T., Aniya, M. (2000), landslide hazard mapping and its evaluation using GIS: An investigation of sampling scheme for grid-cell based quantitative method. Photogrammetric Engineering and Remote Sensing 66, 981-989.

Deoja, B.B., Dhital, M.R., Thapa, B., Wagner, A. (1991), Mountain risk engineering handbook, International Centre for Integrated Mountain Development (ICIMOD), Kathmandu, Nepal, pp 875.

Dhital, M.R. (2005), Landslide investigation and mitigation in Himalayas: focus on Nepal. In: Proceedings of International Symposium Landslide Hazard in Orogenic Zone from the Himalaya to Island Arc in Asia, Kathmandu, Nepal, 1–1.

Dhital, M.R. (2000), An overview of landslide hazard mapping and rating systems in Nepal. *J Nepal Geol Soc*, 22: 533–538

Dhital, M.R., Khanal, N., Thapa, K.B. (1993), The role of extreme weather events, mass movements, and land use changes in increasing natural hazards, A Report of the preliminary field assessment and workshop on causes of recent damage incurred in southcentral Nepal, July 19-20 1993. ICIMOD, Kathmandu, 123 pp.

Dhital, M.R. (2003), Causes and consequences of the (1993), debris flows and landslides in the Kulekhani watershed, central Nepal, Debris-flow Hazards Mitigation:Mechanics, Prediction and assessment, Rickenmann &Chen (eds) pp 1931-1943.

Enrico, C., Antonello, T. (2012), Simplified approach for the analysis of rainfall-induced shallow landslides, Journal of Geotechnical and Geoenvironmental Engineering 138, pp 398-406.

Fall, M. (2009), A GIS-based mapping of historical coastal cliff recession. Bulletin of Engineering Geology and Environment 68(4): 473-482.

Fall, M., (2009), Lecture notes hazard assessment, University of Ottawa, Ottawa, Canada

Fall, M., Azzam, R., Noubactep, C. (2006), A multi-method approach to study the stability of natural slopes and landslide susceptibility mapping, Engineering Geology 82 (2006) 241– 263.

Freeze, A., Cherry, J.A. (1979), Groundwater. Prentice Hall Inc.

Fell, R., (1994), Landslide risk assessment and acceptable risk. Canadian Geotechnical Journal 31, 261– 272.

Fell, R., Ho, K.K.S., Lacasse, S., Leroi, E. (2005), A framework for landslide risk assessment and management. In: Hungr O, Fell R, Couture R, Eberhardt E (eds) Landslide risk management. *Taylor and Francis*, London, pp 3–26

Fell, R., Corominas, J., Bonnard, C.H., Cascini, L., Leroi, E., Savage, W.Z. (2008), (on behalf of the JTC-1 Joint Technical Committee on Landslides and Engineered Slopes), Guidelines for landslide susceptibility, hazard and risk zoning for land use planning. Eng Geol 102:85–98.

Fredlund, D.G., Morgenstern, N.R., Widger, R.A. (1978), Shear strength of unsaturated soils, *Can. Geotech. J* 15, 313–321.

Fredlund, D.G., Xing, A.E. (1994), Equation for the soil-water characteristic curve, *Can. Geotech. J* 31:521-532.

Fredlund, D.G., Xing A., Fredlund M.D., Barbour, S.L. (1996), The relation of the unsaturated soil shear strength to the soil-water characteristics curve. *Canadian Geotechnical Journal* 33, 440-448.

Fredlund, D.G., Rahardjo, H. (1993), Soil Mechanics for unsaturated Soils, John Wiley and Sons, Canada.

Fredlund, D.G., Rahardjo, H., Can, J.K. M. (1987), Nonlinearity of strength envelope for unsaturated soils. Proceedings of the 6th International Conference on Expansive Soils, New Delhi, India, pp. 49-54.

Fannin, R.J., Wise, M.P. (2001), An empirical-statistical model for debris flow travel distance, Canadian Geotechnical Journal, 38, 982-994.

Finlay, P.J., Mostyn, G.R., fell, R. (1999), Landslide risk assessment prediction of travel distance Canadian Geotechnical Journal 36, 556-562.

Garven, E., Vanapalli, S.K. (2006), Evaluation of empirical procedures for predicting the shear strength of unsaturated soils. American Society of Civil Engineers Geotechnical Special Publication No. 147, Vol. 2, pp. 2570-2581.

Gamma, P. (2000), dfwalk – Ein Murgang-Simulationsprogramm zur Gefahrenzonierung, Geographisches Institut der Universität Bern, (in German).

Green, W.H., Ampt C.A. (1911), Studies on soil physics: flow of air and water through soils. Journal of Agricultural Science 4: 1–24.

Guzzetti, F., Carrara, A., Cardinali, M., Reichenbach, P. (1999) Landslide hazard evaluation: an aid to a sustainable development. Geomorphology, 31: 181-216.

Guzzetti, F., Peruccacci, S., Rossi, M., Stark, C.P. (2008), The rainfall intensity–duration control of shallow landslides and debris flows: an update Landslides, Volume 5, Issue 1, pp 3-17

Guzzetti, F., Reichenbach, P., Ardizzone, F., Cardinali, M., Galli, M. (2006), Estimating the quality of landslide susceptibility models. Geomorphology 81, 166–184.

Guzzetti, F., Ardizzone, F., Cardinali, M., Galli, M., Reichenbach, P. (2008), Distribution of landslides in the Upper Tiber River basin, central Italy. Geomorphology 96, 105–122

Guzzetti, F. (2005), Landslide Hazard and Risk Assessment PhD Dissertation Rheinischen Friedrich-Wilhelms Univestitat Bonn.

Holmgren, P. (1994), Multiple flow direction algorithms for runoff modelling in grid based elevation models: An empirical evaluation, Hydrol. Process., 8, 327–334.

Horton, P., Jaboyedoff, M., Rudaz, B., Zimmermann, M. (2013), Flow-R, a model for susceptibility mapping of debris flows and other gravitational hazards at a regional scale, Nat. Hazards Earth Syst. Sci.,13, pp 869-885.

Horton, P., Jaboyedoff, M., Bardou, E. (2008), Debris flow susceptibility mapping at a regional scale, in: Proceedings of the 4th Canadian Conference on Geohazards, edited by: Locat, J., Perret, D., Turmel, D., Demers, D., and Leroueil, S., Qu´ebec, Canada, 20–24 May pp 339–406.

Horton, P., Loye, A., Jaboyedoff, M. (2009), Debris flows and avalanches susceptibility hazard mapping for Pakistan – modelling of the two pilot districts Muzaffarabad and Manshera, Technical Report, Faculty of Geosciences and Environment, Institute of Geomatics and Risk Analysis, University of Lausanne, Switzerland.

Hsu, S.M, Ni, C.F., Hung, P.E. (2002), Assessment of three infiltration formulas based on model fitting on Richard's equation, Journal of Hydrologic Engineering 7, (5) 373-379.

Hsu, K. (1975), On sturzstroms—catastrophic debris streams generated by rockfalls, GSA Bull., 86, 129 – 140.

Hungr, O. (1995), A model for the runout analysis of rapid flow slides, debris flows, and avalanches, Canadian Geotechnical journal, Vol. 32, pp610-623.

Hungr, O., Morgenstern, N.R. (1984), Experiments on the flow behavior of granular materials at high velocity in an open channel, Geotechnique, 34, 3 405-413

Hunter, G., Fell, R. (2003), Travel distance angle for 'rapid' landslides in constructed and natural soil slopes. Canadian Geotechnical Journal, 40(6): 1123–1141.

Hurlimann, M. Rickenmann D., Medina, V. Medina, V., Beteman, A. (2008), Evaluation of approach to calculate debris-flow parameters for hazard assessment Engineering Geology 102, pp 152-163.

Hutter, K., Svendsen, B., Rickenmann, D. (1996), Debris flow modeling: A review, Continuum Mech. Thermodyn. 8 1-35 @ Springer-Verlag 1996.

Iverson, R.M. (2000), Landslide triggering by rain infiltration, Water Resources Research Vol 36, 7 1897-1910.

Iverson, R.M. (1997), The physics of debris flow, Reviews of Geophysics, Vol. 35(3) pp245-296.

Iverson, R.M., Reid, M.E., La Husen, R.G. (1997), Debris flow mobilization from landslides, Annual Review Earth Planet Science Volume 25 pp85-138.

Jaiswal, P., Van Westen, C.J., Jetten, V. (2011), Quantitative estimation of landslide risk from rapid debris slides on natural slopes in the Nilgiri hills, India. Nat Hazards Earth Syst Sci 11:1723–1743.

Johnson, A.M., Rodine, J.R. (1984), Debris Flow, Brundsden, D., and Prior, D.B., eds., Slope Instability, John Wiley & Sons. p. 257-361.

Kim, D., Im, S., Lee, S.H., Hong, Y., Cha, K.S. (2010), Predicting the Rainfall-Triggered Landslides in a Forested Mountain Region Using TRIGRS Model, J. Mt. Sci., 7, pp 83–91.

Khallili, N., Khabbaz, M.H. (1998), A unique relationship for the determination of the shear strength of unsaturated soils. Geotechnique, 48(5), 681-687.

K.C., S. (2013), Community Vulnerability to Floods and Landslides in Nepal Ecology and Society 18(1): 8.http://dx.doi.org/10.5751/ES-05095-180108.

Kayastha, P., Dhital, M.R., Smedt, F.D. (2013), Evaluation and comparison of GIS based landslide susceptibility mapping procedures in Kulekhani watershhed, Nepal. Jurnal of Gelogical Society of India, v 81, 219-231.

Kayastha, P., Dhital, M.R., Smedt, F.D. (2012), Landslide Susceptibility mapping using the weight of evidence method in the Tinau Watershed, Nepal. Nat Hazards 63:479-498.

Kayastha, P., De Smedt, F., Dhital, M.R. (2010), GIS based landslide susceptibility assessment in Nepal Himalaya: a comparison of heuristic and statistical bivariate analysis. In: Malet J P, Glade T, Casagli N, eds. Mountain Risks: Bringing Science to Society. CERG Editions, 121–128.

Kayastha, P., De Smedt, F. (2009), Regional slope instability zonation using GIS technique in Dhading, Central Nepal. In: Malet J P, Remaître A, Boggard T, eds. Landslide Processes: From Geomorphologic Mapping to Dynamic Modelling, CERG, France, 303–309.

Lamichhanne, S.P. (2000), Engineering geological watershed management studies in the Kulekhani watershed, M,Sc. Thesis, Tribhuvan, University, Nepal.

Lumb, P. (1962), Effect of rainstorm on slope stability. In: Proceeding of the symposium on Hong Kong Soils, Hong Kong, pp 73–87

Legros, F. (2002), The mobility of long-runout landslide. Eng Geol 63:301–331.

Ministry of Home (2011, 2012, 2013, 2015), Disaster Report (http://neoc.gov.np/en/)

Mein, R.G., Larson, C.L. (1973), Modeling infiltration during a steady rain. Water Resour Res 9(2):384–393 Green WH, Ampt CA (1911) Studies on soil physics, I. flow of air and water through soils. J Agric Sci 4:1–24

Meyer, N.K., Dyrrdal, A.V., Frauenfelder, R., Etzelmuller, B., Nadim, F. (2012), Hydrometeorological threshold conditions for debris flow initiation in Norway, Nat. Hazards Earth Syst. Sci., 12, 3059–3073, 2012.

Muntohar, A.S., Liao, H.J. (2009), Analysis of rainfall-induced infinite slope failure during typhoon using a hydrological–geotechnical model, Environ Geol (2009) 56:1145–1159.

NHMRC (Nepal Hydrological and Meteorological Research Center and Consultancy P. Ltd). (2015), Study of Climate and climatic variation over Nepal(http://www.dhm.gov.np/uploads/climatic/47171194Climate%20and%20Climatic%20variability%20of%20Nepal-2015.pdf)

O'Brien, J. S. (2003), FLO-D Users Manual, version 2003, FLO-2D Software Inc.

Pierson, T.C. (2005), Hyper-concentrated flow - transitional process between water flow and debris flow. In Debris-flow Hazards and Related Phenomena. Praxis Publishing Ltd, Chichester, pp. 159-202.

Paudel, B., Fall, M., Danesfar B. (2018b), GIS-based assessment of debris flow runout in Kulekhani Watershed, Nepal (submitted).

Perla, R., Cheng, T.T., McClung, D.M. (1980), A two-parameter model of snow-avalanche motion, J. Glaciol., 26, 197–207.

Park, D.W., Nikhil, N.V., Lee, S.R. (2013), Landslide and debris flow susceptibility zonation using TRIGRS for the 2011 Seoul landslide, Nat. Hazards Earth Syst. Sci., 13, 2833–2849.Poudyal, C. P., Chang, C., Oh, H., Lee, S. (2010), Landslide susceptibility maps comparing frequency ratio and artificial neural networks: a case study from the Nepal Himalaya. Environ Earth Sci, 61(5), 1049–1064.

Rahardjo, H., Ong, T.H., Rezaur, R.B., and Leong, E.C. (2007), Factors controlling instability of homogeneous soil slopes under rainfall, J. Geotech. Geoenviron. Eng., v 133, n12, 1532–1543.

Reid, L.M., Page M.J. (2003), Magnitude and frequency of landsliding in a large New Zealand catchment Geomorphology Volume 49, Issues 1–2, 1 January 2003, Pages 71–88Rickenmann, D. (1999), Empirical relationships for debris flows, Nat. Hazards, 19, 47–77.

Remondo, J., Bonachea, J., Cendrero, A. (2008), A statistical approach to landslide risk modelling at basin scale; from landslide sus-ceptibility to quantitative risk assessment, Geomorphology 94 (2008) 496–507.

Rickenmann, D. (1999), Empirical relationships for debris flows. Natural Hazards 19: 47-77.

Salciarini, D., Godt, J.W., Savage, W.Z., Baum, R.L., Conversini, P. (2008), Modeling landslide recurrence in Seattle, Washington, USA, Engineering Geology 102 (2008) 227–237.

Salciarini, D., Godt, J.W., Savage, W.Z., Conversini, P., Baum, R.L., Michael, J.A. (2006), Modeling regional initiation of rainfall-induced shallow landslides in the eastern Umbria Region of Central Italy, Landslide (2006) 3 181-194.

Saito, H., Nakayama, D., Matsuyama, H. (2010), Relationship between the initiation of a shallow landslide and rainfall intensity duration thresholds in Japan, Geomorphology, 118, 167–175.

Scheidegger, A.E. (1973), On the prediction of the reach and velocity of catastrophic landslide, Rock Mechanics, 5 231-236.

Savage, W., Baum, R. (2005), Instability of steep slopes. In Debris-flow Hazards and Related Phenomena. Praxis Publishing Ltd, Chichester, pp. 53-79.

Savage, S.B., and Hutter, K. (1989), The motion of a finite mass of granular material down a rough incline. Journal of Fluid Mechanics, 199: 177-215.

Sassa, K., Wang, G. (2005), Mechanism of landslide-triggered debris flows: Liquefaction phenomena due to the undrained loading of torrent deposits. In Debris-flow Hazards and Related Phenomena. Praxis Publishing Ltd, Chichester, pp. 81-104.

Sassa, K. (2000), Mechanism of flows in granular soils. In GeoEng 2000: An International Conference on Geotechnical and Geological Engineering.

Sun, H.W., Wong, H.N. and Ho K.K.S. (1998), Analysis of infiltration in unsaturated ground. In Slope Engineering in Hong Kong (Li, KS, Kay JN and Ho KKS (eds)). Balkema, Rotterdam, the Netherlands, pp. 101–109.

Takahashi, T., Nakagawa, H., Tarada, T., Yamashike, Y. (1992), Routing debris flows with particle segregation. Journal of Hydraulic Engineering, 118(11):1490-1507.

Takahashi, T. (1978), Mechanical characteristics of debris flow. Journal of the Hydraulics Division, Proceedings of the American Society of Civil Engineers, 104(HY8): 1153-1169.

Takahashi, T. (1980), Debris flow on prismatic open channel. Journal of the Hydraulics Division, Proceedings of the American Society of Civil Engineers, 106(HY3): 381-396.

Tsai, T.L., Yang, J.C. (2006), Modeling of rainfall-triggered shallow landslide Environ Geol(2006) 50: 525–534.

Tsai, T.L. and Chiang, S.J. (2013), Modeling of layered infinite slope failure triggered by rainfall, Environmental Earth Sciences, Vol. 68, No. 5, pp 1429-1434.

Tomlinson, A.I. (1980), the frequency of high intensity rainfallin New Zealand, Water and Soil Tech.publ. no 19, Ministry of Work and Development, Wellington, New Zealand.

Torres, G.H. (2011), Estimating the soil-water characteristics curve using grain-size analysis and plasticity index, M.Sc. Thesis, Arizona State University, Tempe, AZ.

Vanapalli, S.K., Fredlund, D.G. (1999), Empirical Procedures to predict the shear strength of unsaturated soils. Eleventh Asian Regional Conference on Soil Mechanics and Geotechnical Engineering, Hong et al. (eds) @Balkema, Rotterdam, ISBN 90 58090531.

Vanapalli, S.K., Fredlund, D.G. Pafahl, D.E., Clifton, A.W. (1996), Model for the prediction of shear strength with respect to soil suction, Canadian, Geotechnical, Journal 33 379-392.

Vanapalli, S.K., Fredlund, D.G. (2000), Comparison of different procedures to predict the shear strength of unsaturated soils uses the soil-water characteristic curve. Geo-Denver 2000, American Society of Civil Engineers, Special Publication, No. 99, pp. 195-209.

Varnes, D.J. (1978), Slope movement types and processes, in Schuster, R.L. and R.J. Krizek (ed.), Landslides Analysis and Control: National Academy of Sciences Transportation Research Board Special Report No. 176, p. 12-33.

Varnes, D.J., IAEG Commission on Landslides and other Mass-Movements (1984), Landslide hazard zonation: a review of principles and practice. The UNESCO Press, Paris, p 63.

Wang, C., Li, S., Esak, T. (2008), Natural Hazards and Earth System Sciences GIS-based two-dimensional numerical simulation of rainfall-induced debris flow Nat. Hazards Earth Syst. Sci., 8, 47–58, 2008 www.nat-hazards-earth-syst.

Wieczorek, G.F. (1987), Effect of rainfall intensity and duration on debris flows in central Santa Cruz Mountains, California, in: Debris Flows/Avalanches: Processes, Recognition and Mitigation, edited by: Costa, J. E. and Wieczorek, G. F., Reviews in Engineering Geology, Geological Society of America, 7, 23–104.

Wieczorek, G.F., Naeser, N.D. (2000), Proceedings of the Second International Conference on Debris-Flow Hazards Mitigation: Mechanics, Prediction, and Assessment. A.A. Balkema, Rotterdam.212

Zapata, C.E. (1999), Uncertainity in Soil-Water Characteristic Curve and Impacts on unsaturated shear strength Prediction. Ph.D. Dissertation, Arizona State University, Tempe, United States.

Zezere, J.L., Trigo, R.M., Trigo, I.F. (2005), Shallow and deep landslides induced by rainfall in the Lisbon region (Portugal): assessment of relationships with the North Atlantic Oscillation, Nat. Hazards Earth Syst. Sci., 5, 331–344, 2005.

Zhang, L.L, Zang, J., Zang, L.M., Tang, W.H. (2011), Stability of analysis of rainfall induced slope failure: a review, Geotechnical Engineering Volume 164 Issue GE5, Institute of Civil Engineers Geotechnical Engineering 164 October 2011 Issue GE5.

Chapter 7: Synthesis and integration of all the results

The landslide initiation threshold rainfall intensity and duration identified for all Nepalese mountains (Dahal Hasegawa 2008) is tested for the study watershed. The threshold rainfall combinations are: (1) 12 mm rainfall for 10 hours, (2) 2 mm rainfall per hour for 100 hours, and (3) 144 mm rainfall in 24 hours. The minimum Factor of Safety (FoS) observed from the model for the first combination within the watershed was 1.02. The result shows that there is no landslide from (1) within the study watershed. Similarly, the threshold rainfall intensity and duration for the second and third combinations were tested and found. The intensity of 2 mm rainfall per hour for 100 hours, or 6 mm rainfall per hour for 24 hours is considered to be the rainfall thresholds. These longer-duration and low-intensity rainfall conditions are analyzed, and the developed model shows instability in the watershed. For 2 mm rainfall per hour for 100 hours, about 0.017% of the watershed area was unstable. For this intensity and duration of rainfall, the lowest FoS observed was 0.90 for 0.017% of the watershed area, and FoS of less than 1.5 for 0.026% of the watershed. Similarly, for 6 mm rainfall per hour for 24 hours, or 144 mm for 24 hours, the observed minimum FoS was 0.97. For this rainfall intensity, the area of watershed found to be unstable for FoS 0.97 and 1.50 are 0.015 and 0.022% of the watershed, respectively. As these thresholds are identified by other researchers based on landslides and rainfall all over Nepal, they may not necessarily be truly representative of the study watershed.

Two landslides were identified for debris flow model (Flow-R) validation. The debris flow analysis was first conducted for these landslides, one located in the north east and another in the north west. The landslide located in the north east, Jure, is about 72 km from the study watershed, and another landslide chosen was located to the north west at Taprang, 130 km away. Both landslides were in the Mahabharat Range and in similar geographical and geological settings to the study area. Various models available in Flow-R were applied and compared with the field results. After applying the available algorithms in the model, Holmgren (1984) appropriately matched debris flow spreading

with field information for both landsides. Algorithm D8 found no spreading; D∞ (D infinity) algorithm was also used for analysis of observed debris flow, but spreading was small. The stochastic method Rho8 algorithm was unable to capture the observed debris flow location. The result of the Quinn et al. (1991) proposed multiple flow direction model provided satisfactory results. The Freeman (1991) model result found slight spreading. Modified Holmgren (1984) algorithms provided a little bit more spreading than was observed. For the study watershed, modified Holmgren (1984) algorithms with low travel angle and low velocity were considered for debris flow analysis in this research.

The selected algorithms were used for assessment of debris flow spreading in the study watershed. Three combinations of rainfall-induced landslide locations identified were applied as a debris flow source. The results of the landslide source for 144 mm rainfall in 24 hours were applied in the model for debris flow spreading. The initial landslide source was 0.0012% of the watershed area, and the unstable area was 0.16 hectare (1600 m^2). The spreading area for this rainfall intensity and duration was 0.44 hectare (4400 m^2). The second combination of rainfall and duration applied in the model was 2 mm rainfall per hour for 24 hours. The source area of this combination was identified as 0.017% of the watershed area, or 2.16 hectare. The debris flow observed for this rainfall source was 12.40 hectare.

The model was also applied for a known rainfall and landslide event in the watershed of 540 mm rainfall within a 24-hour period. Dhar and Dhital (2004) showed that 2.35 km^2 of the watershed was area covered with sliding soil mass during the extreme rainfall (this is 1.9% of the total watershed). The predicted total unstable area from the model is 0.02% of the total watershed, and covers 0.023 km^2 of the watershed. This difference is explained by the following two factors. First, the areas affected by previous landslides not only include the initiation zones of the landslides (scrap of the landslide), but also the areas covered by the slide mass during its downhill travel (depends on the runout behavior). Second, one recorded rainfall event (540 mm rainfall in 24 hours) was

considered in the simulated landslide-susceptible areas. However, the maps of the previous landslides included landslides triggered by all rainfall events that occurred in the study areas. Therefore, the area observed in the landslide is almost 100 times more than the area that was unstable at the time. The area beyond the unstable area can be modeled as a debris flow.
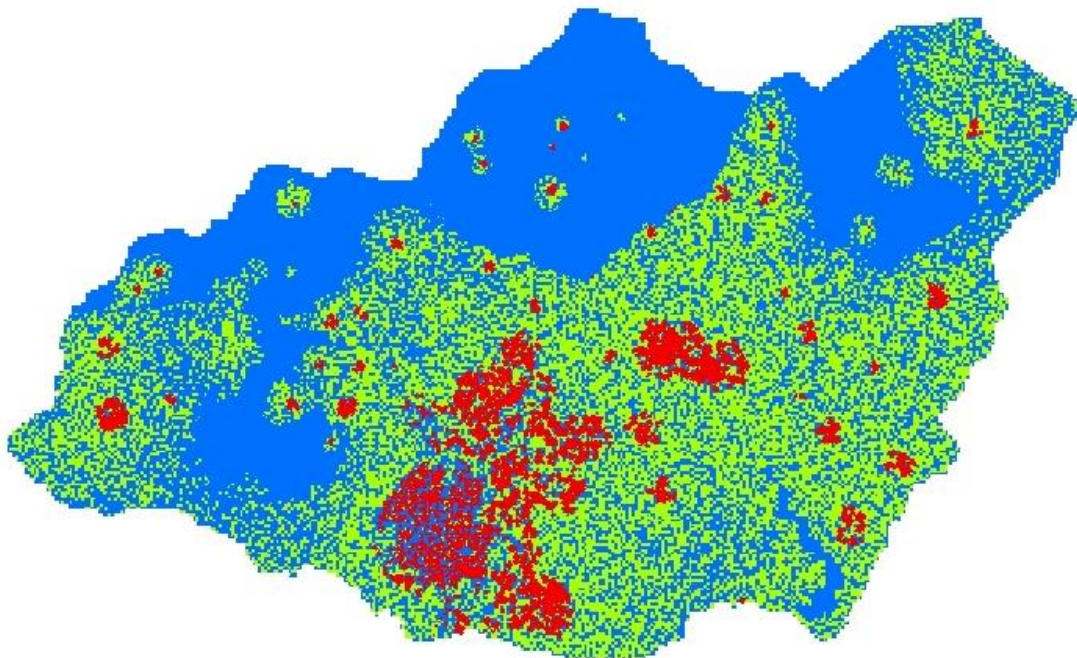
The unstable area for the extreme rainfall conditions of 540 mm in 24 hours was also modeled in this study. The unstable location in the watershed was 0.02% (0.023 km^2) of the total area. The debris flow spreading in this area is 2.68% of the total watershed (3.325 km^2) or 332.53 hectare.

Debris flow hazard maps are developed by combining landslide initiation, debris flow runout areas and their buffer with 10 m outlines. The watershed area beyond the hazard area is also categorized as medium and low landslide susceptible areas based on the higher FoS of the stability of the initial slope. For the watershed area which has an FoS, 1 to 2 is considered as a medium susceptibility, and more than 2 as low susceptibility. The medium susceptibility area is the map area for FoS less than 2, minus the hazard areas. The low susceptibility zone has a FoS of more than 2, minus the hazard area and medium susceptibility areas. This analysis was carried out for seven-day rainfall and one-day rainfall only, and is summarized in Table 7.1. The hazard area for the watershed for seven-day rainfall with a 1 in 200 years return period is shown in Figure 7.1.

Table 7.1 Hazard area for 1 in 200 years return rainfall at Chisapani Ghadi rain gauge station.

Return Period (Years)	Annual Probability	Days of Rainfall	Total Watershed Area (Ha)	Hazard Area (Ha)	Medium Susceptibility Area (Ha)	Low Susceptibility Area (Ha)
25	0.04	1	12400	13	1387	11001
50	0.02	1	12400	18	2624	9740
100	0.01	1	12400	24	4998	7802
200	0.005	1	12400	36	5009	7355
25	0.04	7	12400	77	3960	8364
50	0.02	7	12400	154	4365	8035
100	0.01	7	12400	284	4706	7409
200	0.005	7	12400	418	8403	7384

Figure 7.1: Hazard area for seven days rainfall in 200 years return period.

Chapter 8: Summary, application, conclusions, and recommendations

8.1   Summary

Rainfall-induced landslides can change into debris flows and devastate large areas in mountainous Nepal. Initial landslide and debris flow inundation in both locations are important to consider for landslide hazard analysis. Debris flow runout analysis is a complex physical process and needs lots of information and computational processing. A simple model with reasonable results from minimum resources and accessible computing tools is used for this research.

Details of soil water characteristics, grain size, initial moisture content, specific gravity, unit weight, in situ infiltration capacity, shear strength parameters, index properties, and rainfall in the study area are obtained and then used in the unsaturated slope stability model to develop a landslide susceptibility map. Previously identified rainfall thresholds for landslide initiation were tested for model validity. Some of the recommended rainfall thresholds (rainfall intensity and duration for landslide initiation) in the region are applied to the study watershed. The spatial distribution of landslides in those rainfall conditions is identified. The expected maximum rainfall and its implication for slope stability is understood.

The Flow-R model is an empirical method requiring minimal data for susceptibility and runout analysis. The model is also capable of simulating runout from user-defined debris flow sources. The Flow-R model was applied for two recent landslides, which changed into debris flow. Various algorithms available in Flow-R were applied to simulate runout analysis, and compared with the observed travelled area of the debris flow. The model showed that it can predict debris flow from rainfall-induced initial landslides using its selected algorithms for Nepal's mountains.

The appropriate algorithms obtained in Flow-R from two recent landslides were applied in the study watershed. The debris flow source was a landslide-susceptible area identified initially in this research. The results show that the debris-flow-spread from the model for the study watershed was 2.68% of the total area for an extreme rainfall event in the region in 1993. The modelling results match the debris observed by Kayastha et al. (2013), Dhital et al. (1993), Nippon Koei Co. (1996), and Dhital (2003). The modelled debris flow spreading from landside sources shows that the minor landslide event has more source-to-spreading-area ratio than the extreme events in the selected algorithms.

Landslide hazard assessment was carried out from the annual rainfall-induced landslide probability. The daily rainfall record for the 34-year-period from 1980 to 2013 was available for rainfall probability assessment. One-day to seven-day annual maximum rainfalls were derived for 34 years for probability of one-day to seven-day extreme maximum rainfall. The rainfall-associated landslide events were modeled to identify landslide susceptibility for the study watershed. These susceptible areas were used as a source for analysis of debris flow inundation area using Flow-R model. A setback distance was added in the susceptibility area and debris flow inundation area for the total debris flow zone for the study watershed. The areas covered from the debris flow with a given probability were considered to be landslide hazard. The probability of 0.04, 0.02, 0.01 and 0.005 (return period 25, 50, 100 and 200 years) debris hazard zones were identified and a landslide (debris flow) hazard map of the study watershed was developed. This debris flow hazard map is valuable for reducing or mitigating debris flow risks as well as for making developments in policy and saving lives and property in the study area and Nepalese montains.

8.2   Application of the methodology

The methodology applied in this research is equally applicable to other regions of the world. Landcover, land use patterns and geography of the Nepal mountains are given in

Appendix 1. The slope stability model used in this research is a single soil layered slope stability model. Because rainfall-induced landslides are shallow landslides, their failure surfaces mostly develop within a single soil layer slope region. If this slope is in more than one soil layer system, some modification of this methodology is required to avoid missing any failure in the surface depth above the bottom impervious layer. Two-soil-layer infinite slope failure was studied by Tsai and Chiang (2013), who concluded that there will be chances of slope failure with two-soil-layer interfaces. If a multiple-soil-layer system is encountered, it is necessary to develop susceptibility of each sampled location. Using factors of safety of the sampled locations, the IDW method will be employed to find landslide susceptibility for the entire watershed.

The frequency of the landslide susceptibility, its run-out, and hazard is directly related to the frequency of the rainfall duration and intensity. The duration and intensity of extreme rainfall changes annually because of climate change. The changing pattern of rainfall intensity and duration with climate change also need to be incorporated periodically for frequency analysis for future hazard areas forecasting in a given return period.

8.3 Conclusions

The required steps necessary for landslide hazard analysis were carried out in the GIS environment. A slope stability model, proposed for unsaturated soil conditions, was applied for stability-of-slope analysis, to find landslide-susceptible locations and develop landslide susceptibility or debris flow initiation map for the stuy area. The Flow-R model was used for debris-flow-spreading analysis. The relation of the rainfall return period and landslide events were derived using these methods.

The recorded rainfall and physical changes in mountain slopes were modeled to predict instability in mountain slopes in the study watershed. Annual rainfall probability or respective returns periods were applied to assess the probability of rainfall-induced landslide. Rainfall records for 34 years (from 1980 to 2013) were used to identify annual

one-day to seven-day maximum rainfall. Information about maximum annual cumulative rainfall during the above-recorded period was used for the annual rainfall probability and return period. The one-day and the seven-day maximum cumulative rainfall from the analysis was 443 and 1033 mm, respectively. The annual probability of rainfall computed for 1.01 to 200 years' return period has an annual probability 0.990099 to 0.005. The rainfall for a return period of 200 years and annual probability of 0.005 of one-day duration is 458 mm, while for seven days it is 1051 mm. For landslide probability analysis, only four return periods 25, 50, 100, and 200 years (annual probability 0.04 to 0.005) were selected to find a trend of landslide susceptibility with an annual probability or return period in the watershed. The area of potential landslide increases for the higher return period rainfall and number of days.

Slope areas were categorized as having high, medium, or low landslide susceptibility based on FoS of less than 1, 1 to 2, and more than 2, respectively. The watershed area is 124 km^2, and the unstable portion is up to 400 hectares for seven-day rainfall with an annual probability of 0.005 (recurrence period 200 years). The landslide-susceptible area is 3.25% of the total watershed area. The longer-duration and higher-intensity rainfalls are triggering factors for rainfall-induced landslides.

The area of the watershed with FoS less than 1 is considered as a source of landslide for debris flow analysis. The Flow-R model was applied for debris flow runout and inundation area computation. An algorithm modified from Holmgren (1994) and developed by Horton et al. (2013), was found to be approptiate and was used for debris flow spreading. For the initial algorithm, weights were chosen. The weights algorithm has three sub algorithms, the default (proportional) algorithm, Gamma (2000), and Cosinus. Any of these algorithms can provide appropriate debris flow spreading in this region; however, the default was chosen for the analysis. This algorithm uses the proportional method of spreading to adjacent cells. Friction loss function and energy limitation algorithms are available and were used in energy calculation. The low travel

angle and low velocity were appropriate for debris flow runout analysis for this watershed, and these were chosen for the friction loss function and energy limitation.

The debris flow area and landslide initiation area from the susceptibility analysis were combined in a single map to develop debris flow hazard maps. These combined total areas were transformed into polygons. Landslide hazard areas require a setback distance, which depends on various factors including the type of soil, proximity of a river or water body, and topography. Analysis of the setback distance of individual polygons is beyond the scope of this research, but, briefly, a 10-m setback distance was chosen for all polygons, and used to buffer them from the outer side. The final area within the buffered area is termed the hazard area. For return periods of 25, 50, 100, and 200 years, one-day and seven-day duration rainfall intensities were used for these analyses. For a 25-year return period and one-day duration rainfall, the computed hazard area is 13 hectares (ha), while for a 200-year return period it is 36 ha. This area drastically changed for seven-day rainfall, as it is 77 ha for a 25-year return period, and 418 ha for a 200-year return period. Large return periods with high intensity rainfall are hazardous in the study watershed.

The landslide hazard areas for different return periods were developed for the study watershed. The annual rainfall probability (recurrence period) and hazard location in any watershed is important for policy makers. For instance, if an area is hazardous for a 1 in 10-year return period, it should be avoided for hospitals, school buildings, or any such community services facilities. It may or may not be suitable for residential development, depending on other factors and the decision of the local authority. Hazard maps have been developed which will be useful for policy makers, and for future risk analysis of landslide-induced debris flow in the study region.

8.4   Recommendations for future works

It is recommended that more detailed geotechnical information be collected for use in this model. In this research, only 73 locations were used for, especially SWCC and infiltration depth. Like these data, soil strength parameters for different locations and types of soil can provide more representative results and may provide detailed type of surface and subsurface layer information for hazard analysis.

For the application of this research, live rainfall recording systems may help to develop landslide warnings based on the rainfall intensity and duration. Rainfall records are available only once per 24 hours in Nepal. A live rainfall recording system collecting data every 15 minutes, and up to 24 hours cumulative rainfall, may be required for identifying rainfall conditions conducive to landsides. This data will indicate whether or not there will be any landslides in areas prone to them. A pilot watershed could be chosen to gather detailed information and apply models for hazard assessment. Annual monitoring of new landslides and rainfall records could help to improve the effectiveness of this model, and provide more realistic results to save lives and property.

The iteration process was carried out using a spreadsheet in this research for computation of saturation depth, and nonlinear regression analysis to develop SWCC from grainsize method to Fredlund and Xing's (1994) equation. Software developed for both processes could expedite data processing in the future use.

A debris flow risk assessment of the study should be performed in the future.
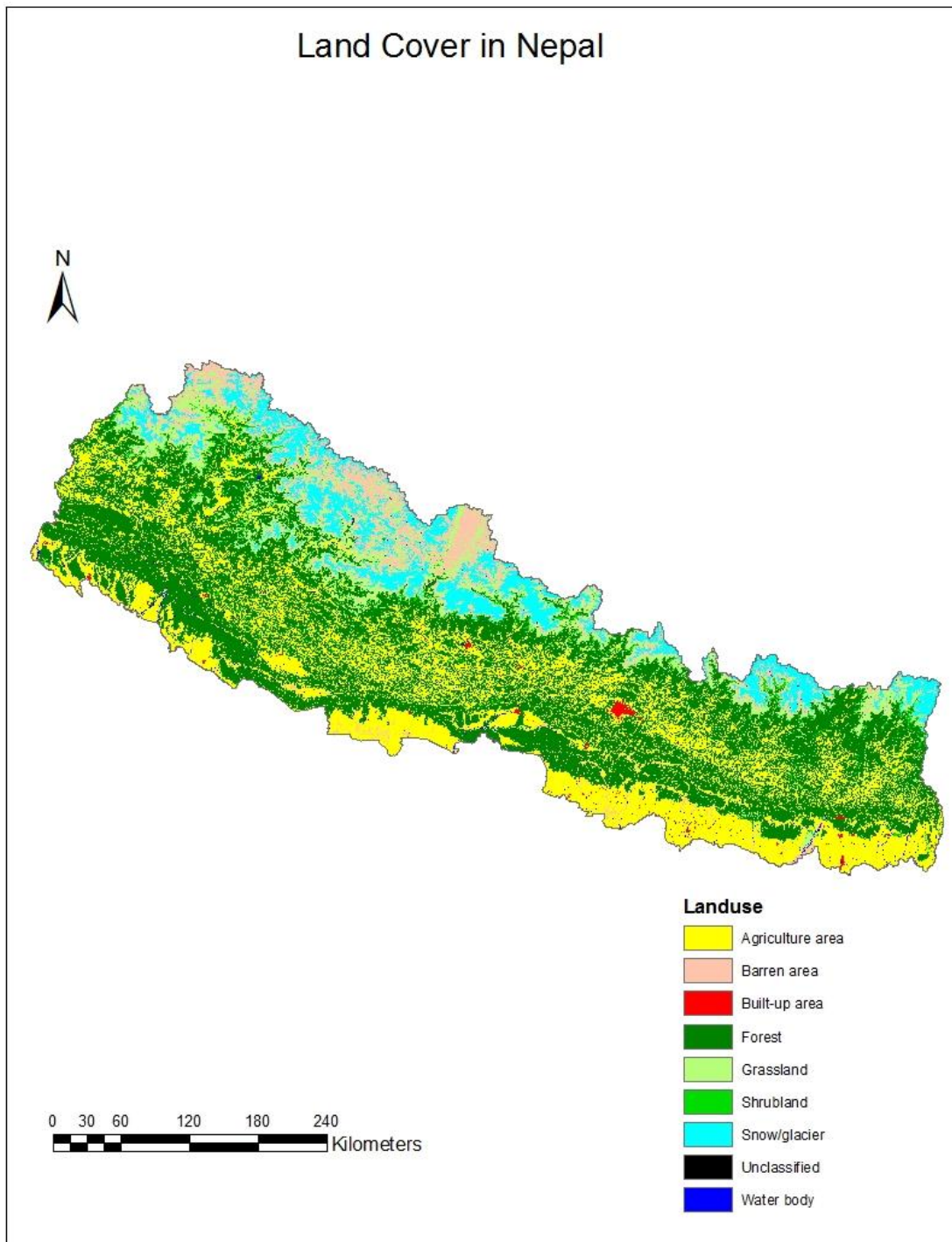
Appendix A

Figure A.1: Land use map of Nepal (Source: ICIMOD data portal)
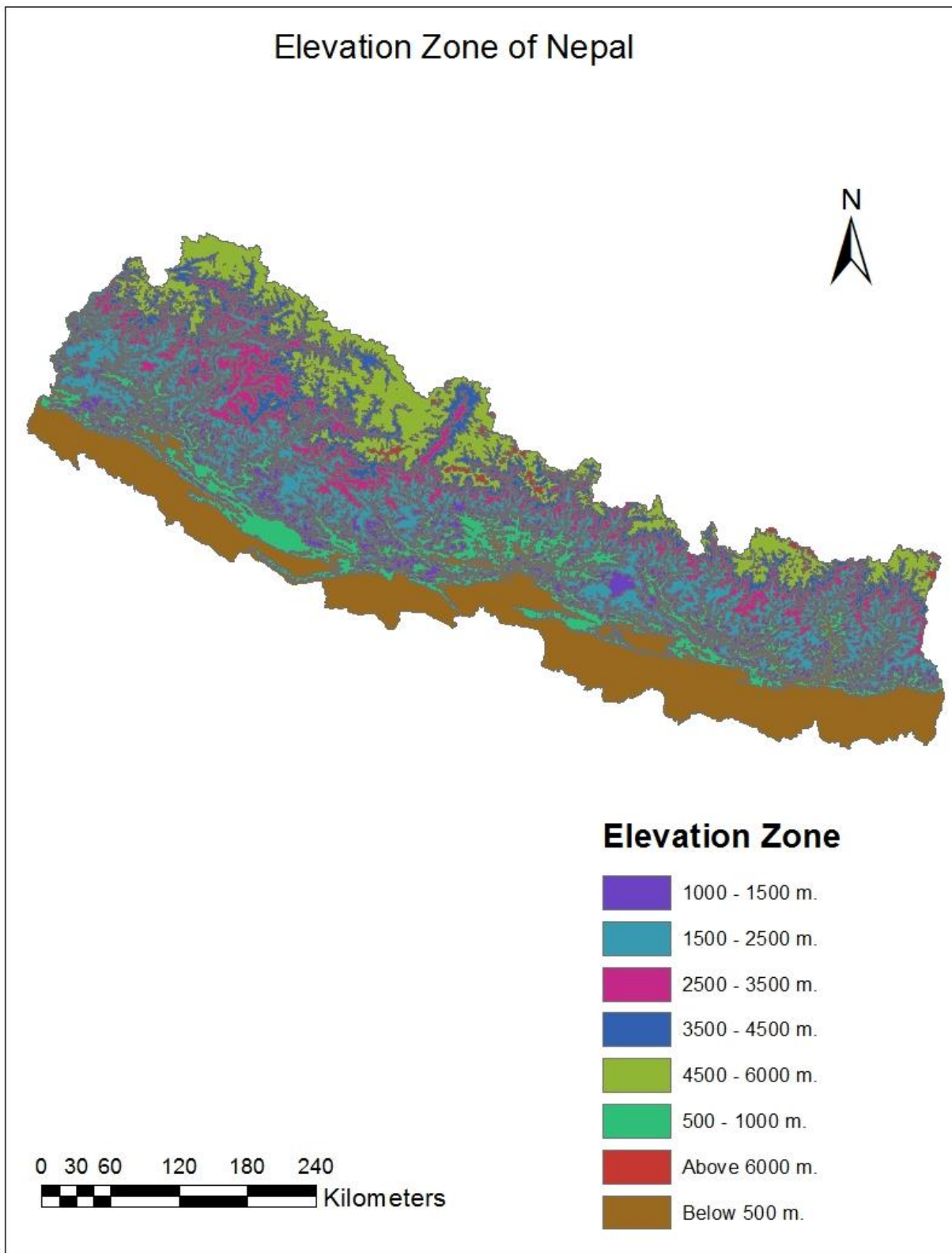
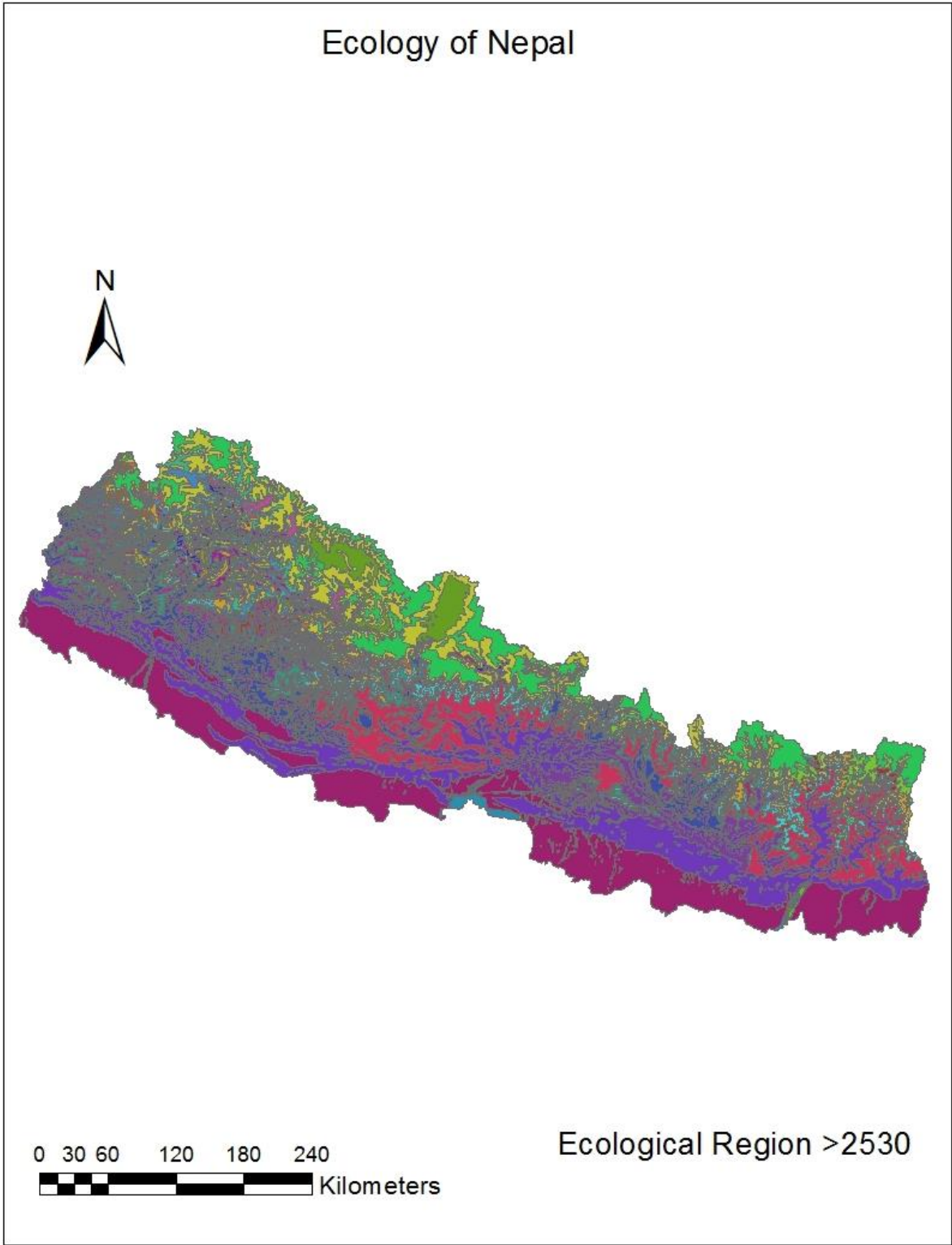Figure A.2: Elevation zone of Nepal (Source: ICIMOD data portal)

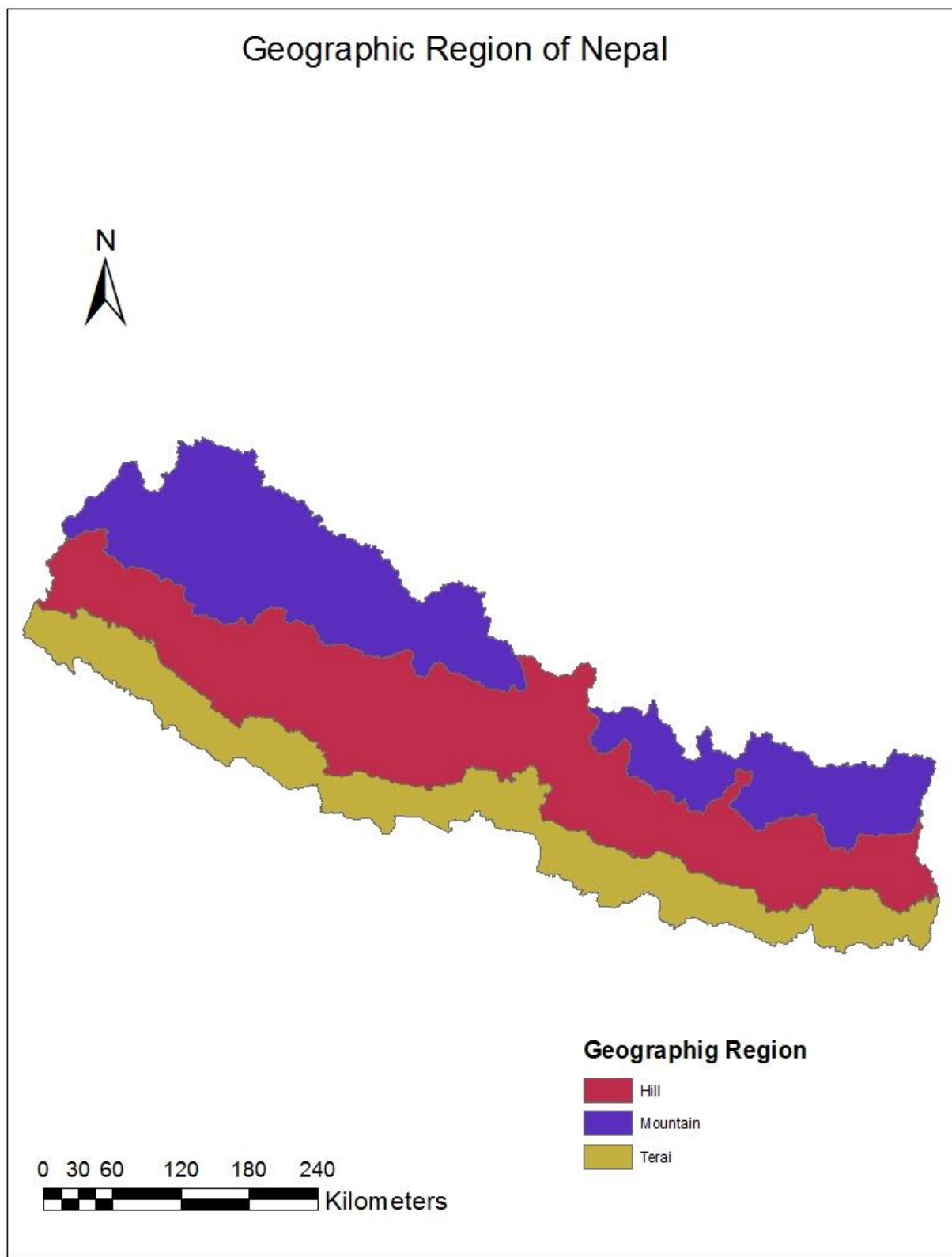Figure A.3: Ecological Regions of Nepal (Source: ICIMOD data portal)

Figure A.4: Ecological Regions of Nepal (Source: ICIMOD data portal)